

MP FILE COPY

2

AD-A202 375

AFOSK - PK



SCIENTIFIC RESEARCH (AFSC)
DTIC
... and is
... 190-12.
... unlimited.
MATTHEW J. KERPER
Chief, Technical Information Division

Approved for public
release

Final Report
Contract No. F49620-86-C-0038

Maximum Entropy/Optimal Projection Design Synthesis for Decentralized Control of Large Space Structures

DTIC
ELECTE
DEC 09 1988
S D
H

HARRIS CORPORATION GOVERNMENT AEROSPACE SYSTEMS DIVISION
PO. BOX 94000, MELBOURNE, FLORIDA 32902 (407) 727-5115

Final Report
Contract No. F49620-86-C-0038

Maximum Entropy/Optimal Projection Design Synthesis for Decentralized Control of Large Space Structures

By
David C. Hyland
Dennis S. Bernstein
Emmanuel G. Collins, Jr.

For
Air Force Office of Scientific Research
Bolling Air Force Base
Washington, DC 20337

This data, furnished in connection with Contract Number F49620-86-C-0038, shall not be disclosed outside the Government and shall not be duplicated, used, or disclosed in whole or in part for any purpose other than to evaluate the document, provided that if a contract is awarded to this offeror as a result of or in connection with the submission of this data, the Government shall have the right to duplicate, use, or disclose the data to the extent provided in the contract. This restriction does not limit the Government's right to use information contained in the data if it is obtained from another source without restriction. The data subject to this restriction is contained in sheets ALL. (1966 DEC).

List of Figures

2.0-1	Large-Scale Input-Output Formulation	2-2
2.0-2	Block-Norm Matrices	2-4
2.0-3	Matrix Majorants and Minorants	2-5
2.0-4	Example of Bound Derivation	2-7
2.0-5	Hierarchy of L_p Output Bounds	2-8
2.0-6	Solution of M -Matrix Equations	2-9
2.0-7	Subsystem Interaction Model	2-11
2.0-8	Kronecker Matrix Algebra	2-12
2.0-9	Block-Kronecker Algebra	2-13
2.0-10	Identities for the Block Kronecker Algebra	2-15
2.0-11	A Hierarchy of Majorant Bounds for the Second-Moment Matrix	2-16
2.0-12	Majorant Lyapunov Equation	2-17
2.0-13	Robustness Due to Weak Subsystem Interaction	2-18
2.0-14	Numerical Solution of the Majorant Lyapunov Equation	2-20
2.0-15	Second Member of the Majorant Hierarchy	2-21
2.0-16	Majorant Hierarchy and Stratonovich Models: the Link Between Analysis and Synthesis	2-22
2.1-1	Time-Domain Robustness Analysis Problem	2-25
2.1-2	Time-Domain Majorant Bound	2-26
2.1-3	Spacecraft Tracking Example	2-28
2.1-4a	Time-Domain Majorant Bounds for Spacecraft Tracking Example	2-29
2.1-4b	Additional Results for Spacecraft Tracking Example	2-30
3.1-1	Scope of MEOP	3-2
3.2.2-1	General Multiechelon Hierarchical Control Structure	3-4
3.2.2-2a	Multiechelon Hierarchical Control	3-6
3.2.2-2b	Detail of the j th Dynamic Compensator of the i th Level	3-7
3.2.2-3	Strategy for Solving the Optimal Multiechelon Hierarchical Control Design Problem	3-8
3.2.2-4	Derivation of First-Order Necessary Conditions for Compensator (i, j)	3-10
3.2.2-5a	First-Order Necessary Conditions Pertaining to (i, j) th Compensator	3-11
3.2.2-5b	First-Order Necessary Conditions (cont'd)	3-12
4.1-1	Homotopy Paths	4-2
4.1-2	Solution of the Optimal Reduced-Order Compensator Design Problems (Bernstein, Hyland, Richter)	4-5
4.3-1	Interconnected Beam Example for Decentralized Control	4-9
4.3-2	Deployable Truss Structure Configuration	4-11
4.3-3	Modal Data for the Deployable Truss Structure	4-12
4.3-4	Deployable Truss Structure Mode Shapes	4-13
4.3-5	Deployable Truss Structure Mode Shapes (cont'd)	4-14
4.3-6	Deployable Truss Structure Mode Shapes (cont'd)	4-15
4.3-7	Control Systems Instrumentation for the Deployable Truss Structure	4-17
4.3-8	Sequential Decentralized Design Procedure for Deployable Truss Structure	4-18

UNCLASSIFIED

SECURITY CLASSIFICATION OF THIS PAGE

REPORT DOCUMENTATION PAGE

1a. REPORT SECURITY CLASSIFICATION Unclassified		1b. RESTRICTIVE MARKINGS	
2a. SECURITY CLASSIFICATION AUTHORITY		3. DISTRIBUTION/AVAILABILITY OF REPORT Approved for public release, distribution unlimited	
2b. DECLASSIFICATION/DOWNGRADING SCHEDULE		4. PERFORMING ORGANIZATION REPORT NUMBER(S)	
4. PERFORMING ORGANIZATION REPORT NUMBER(S)		5. MONITORING ORGANIZATION REPORT NUMBER(S) AFOSR-TR-88-203 AFOSR-TR-88-203	
6a. NAME OF PERFORMING ORGANIZATION Harris Corporation Government Aerospace Div.	6b. OFFICE SYMBOL (If applicable)	7a. NAME OF MONITORING ORGANIZATION AFOSR	
6c. ADDRESS (City, State and ZIP Code) MS 22/4848 Melbourne, FL 32901		7b. ADDRESS (City, State and ZIP Code) AFOSR, NA, Bldg 410 Bolling AFB, DC 20332-6448	
8a. NAME OF FUNDING/SPONSORING ORGANIZATION Air Force Office of Scientific Research	8b. OFFICE SYMBOL (If applicable) NA	9. PROCUREMENT INSTRUMENT IDENTIFICATION NUMBER F49620-86-C-0038	
8c. ADDRESS (City, State and ZIP Code) Building 410 Bolling AFB Washington, DC 20322 - 6448		10. SOURCE OF FUNDING NOS.	
		PROGRAM ELEMENT NO. 61102+	PROJECT NO. 2302
		TASK NO. B1	WORK UNIT NO.
11. TITLE (Include Security Classification) "Maximum Entropy/Optimal Projection Design Synthesis for Decentralized Control of Large Space Structures"			
12. PERSONAL AUTHOR(S) Hyland, David, Charles Bernstein, Dennis, S. Collins, Emmanuel, G., Jr.			
13a. TYPE OF REPORT Final	13b. TIME COVERED FROM 10/86 TO 5/88	14. DATE OF REPORT (Yr., Mo., Day) 1988, May	15. PAGE COUNT
16. SUPPLEMENTARY NOTATION			
17. COSATI CODES		18. SUBJECT TERMS (Continue on reverse if necessary and identify by block number)	
FIELD	GROUP	SUB. GR.	Robust control design, Decentralized controller, majorant robustness analysis
22	02		
12	01		
19. ABSTRACT (Continue on reverse if necessary and identify by block number)			
<p>The Maximum Entropy/Optimal Projection (MEOP) methodology is a novel approach to designing implementable vibration-suppression controllers for large space systems. Two issues, in particular, have been addressed, namely, controller order (i.e., complexity) and system robustness (i.e., sensitivity to plant variations). Extensions developed herein include generalizations to decentralized controller architectures and a new robustness analysis technique known as Majorant Robustness Analysis.</p> <p>This final report also encompasses extensions to hierarchical control as well as the development of numerical algorithms for solving the control design equations.</p>			
20. DISTRIBUTION/AVAILABILITY OF ABSTRACT UNCLASSIFIED/UNLIMITED <input checked="" type="checkbox"/> SAME AS RPT. <input checked="" type="checkbox"/> DTIC USERS <input checked="" type="checkbox"/>		21. ABSTRACT SECURITY CLASSIFICATION UNCLASSIFIED	
22a. NAME OF RESPONSIBLE INDIVIDUAL DR. HARMONY K. AMOS		22b. TELEPHONE NUMBER (Include Area Code) (202) 767-4937	22c. OFFICE SYMBOL NA

SECTION 1.0

Introduction and Study Overview

1.0 Introduction and Study Overview

As its name suggests, the Maximum Entropy/Optimal Projection (MEOP) theory of control design for large space systems represents the synthesis of two distinct and novel ideas: (1) minimum information stochastic modeling of parameter uncertainties (to characterize the inevitable tradeoff between robustness and performance) and (2) optimal reduced-order compensator design for a given high-order plant (to optimally quantify the tradeoff between controller complexity and performance). A previous AFOSR-funded study (contract no. F49620-84-C-0015) consolidated MEOP theory developments and successfully demonstrated the theory on a variety of flexible space structure models.

It is now possible to extend the basic MEOP theory and design capability to handle an even larger class of structural concepts. In particular, the sheer size, or dimensionality, of proposed flight structures (such as Space Station) necessitates what may be called *decentralized analysis and design*. In brief, this terminology refers to procedures which treat portions of the system individually and then combine the results. Often the need for such analysis arises from such basic constraints as computer capacity, i.e., the model may simply be too large to be manipulated by the computer at one time.

Our thinking concerning decentralized analysis and design is closely related to the current literature on large scale systems. Our goal is thus to go beyond previous work by using the MEOP theory to quantify uncertain interactions among subsystems, thus providing an *informational system partitioning*. A major goal in this regard is to utilize our theory to extend the applicability of the concept of *connective stability* to complex, multibody spacecraft.

In practice, a direct consequence of the physical size and physical complexity of proposed spacecraft imposes severe constraints on the communication links between sensors, processors and actuators. Relevant issues include cabling mass and RF shielding problems along with reliability concerns. This leads to consideration of multiple sensor/processor/actuator subcontrollers or substations on the spacecraft without real-time intercommunication. Although the processors do not directly exchange data, preflight design of their software must, of course, account for complex operational interactions among subcontrollers via the structural response.

The design of such a *decentralized architecture* or *implementation* is clearly a nontrivial task and can be thought of as involving two interrelated steps:

1. Determination of the control-system architecture including the number of substations and the assignments of sensors and actuators to particular substations; and
2. For a given architecture, design of the processor software for each subcontroller.

The aims of the present study are to extend MEOP to address both of the above items. Indeed, because maximum entropy modeling quantifies uncertainty (i.e., lack of knowledge) it is possible to directly include informational aspects in the system model. One goal is to quantify the degree of suboptimality resulting from interaction uncertainties and alternative controller architectures. Once a particular architecture is selected, the design of each subcontroller often requires iterative solution of high-dimensional design synthesis equations. A second major goal is thus to evolve efficient approaches to the solution of the MEOP design equations for optimal, decentralized control.

1.1 Objectives

The specific tasks required to accomplish the goals of this project are discussed in detail within the original technical proposal and are summarized as follows:

Task 1:

Undertake rigorous extensions of the MEOP design equations to the case of distributed (decentralized) controller architecture in a variety of settings. These developments include:

- 1.1 Extension of the continuous-time MEOP equations to the decentralized case.
- 1.2 Derivation of the MEOP design equations for decentralized discrete-time control of discrete-time systems.
- 1.3 Extension of the MEOP design equations to a hierarchical controller architecture.

Task 2:

Develop methods for determining performance degradation due to uncertainty so as to evaluate the performance of different decentralized architectures with controllers obtained via the design equations derived in Task 1. In particular:

- 2.1 Derive methods for bounding the degree of suboptimality resulting from decentralized design and decentralized implementation.
- 2.2 Evolve effective methods for deriving uncertainty bounds which imply connective stability

for the overall system.

Task 3:

Verify the analysis carried out in Task 2 and develop solution techniques for the decentralized form of the MEOP design equations. The following sequence of developments was carried out:

- 3.1 Develop more efficient techniques for solving the MEOP *centralized* control design equations. In particular, apply topological degree theory to elucidate the solution set and establish the globally optimal solution. Then develop homotopy methods for highly efficient numerical solution of the centralized design equations.
- 3.2 Exploit the developments of 3.1 to analyze the existence, uniqueness, and global optimality of solutions to the decentralized MEOP design equations derived in Task 1. Utilize the homotopy algorithms derived in 3.1 to establish a convergent solution procedure for the decentralized design equations.

Task 4:

Apply the various decentralized extensions of MEOP to realistic design problems. For each of the selected design examples the following subtasks encompass the desired goals:

- 4.1 Generate detailed state-space model, define uncertainties, define sensor/actuator number, type and placement, and assign disturbance spectrum. Use system model to perform *centralized* control-tradeoff studies. Such designs may utilize decentralized design techniques.
- 4.2 Using the centralized tradeoff studies as baseline, determine decentralized/hierarchical implementation architectures based upon uncertainty patterns, physical constraints and processing requirements. For each design assess the degree of suboptimality resulting from the loss of centralization.

1.2 Outline of Program Accomplishments

In this section, we briefly summarize the results obtained under the tasks listed above. Further details are given in Sections 2.0 through 5.0 and the Appendices.

Since developments under Task 2 are not only of fundamental significance to MEOP design but also represent the discovery of entirely new design analysis tools, these accomplishments are discussed first in this report.

The essential problem to be addressed in subtasks 2.1 and 2.2 is the determination of non-conservative bounds on system performance degradation due to uncertainties and/or subsystem interactions. Note that once performance degradation (e.g., line-of-sight error, surface shape errors) is characterized, so is robust stability. Thus both 2.2 and 2.3 are handled by developing a suitable performance robustness analysis. This has been accomplished by the development of a new robustness analysis tool, namely, Majorant Robustness Analysis (MRA). Based upon the work of Ostrowski and Dahlquist on matrix majorants, MRA determines bounds on the degradation of system performance due to unstructured or parametrically structured uncertainties and bounded subsystem dynamics. Since the basic development is carried out in a general operator setting, MRA can be applied within both frequency-domain/input-output and time-domain/state-space descriptions. In the frequency domain/input-output setting MRA generalizes previous robustness results (e.g., singular-value analysis), while in the state-space setting it is fully compatible with MEOP design synthesis. MRA thus provides a design *analysis* tool which nicely complements our design *synthesis* theory. Moreover, MRA reveals a direct link between the MEOP *stochastic* modeling and design formulation and a *deterministic* bound for robust performance, thereby immensely strengthening the foundations of the Maximum Entropy modeling approach. Section 2.0 outlines the theory of MRA and illustrates its application to statistical response, frequency domain analysis, and, finally, time-domain analysis of system transient response.

With the development of MRA as a rigorous design analysis tool, one is in position to formulate the problem of robust decentralized control as a well-posed optimization problem. The robust optimization problem reduces to the optimization of controller gains for fixed-structure controllers under a Maximum Entropy stochastic system model (or, equivalently, under a MRA model). The application of optimization theory to the theoretical solution of these fixed-structure optimization problems (i.e., the derivation of optimality conditions) is the essence of Task 1 and has been fully carried out. More details on the resulting MEOP design synthesis equations for decentralized and hierarchical controllers is given in Section 3.0.

The MEOP design equations derived under Task 1 show that the optimality conditions for robust decentralized/hierarchical controllers can be decomposed into a sequence of design equations involving four nonlinear matrix equations for each control substation or coordinator. Each set of four equations has the same fundamental structure as the four MEOP design equations for *centralized* control design. This surprising decomposition of the structure of the decentralized hierarchical MEOP equations immediately suggests an iterative solution procedure which reduces

the overall problem to the sequential solution of standard MEOP design equations pertaining to each subcontroller and/or coordinator.

The above observations have greatly simplified the development of efficient solution algorithms under Task 3. Since, however, each subcontroller problem may be of high dimension and the number of subsystems may often be considerable, it was recognized that an order of magnitude improvement was needed for the efficiency of the MEOP solution algorithm. Thus, we proceeded in two stages: Develop greatly improved solution techniques for the MEOP centralized control design (Task 3.1), then exploit the results for solving the decentralized/hierarchical design equations (Task 3.2).

Under Task 3.1, S. Richter has developed and successfully tested a homotopic continuation algorithm for solving the basic MEOP design equations. In place of solving four $(n \times n)$ ($n =$ dimension of the plant) nonlinear matrix equations as in previously developed algorithms, Richter's method reduces the problem to solving four $n_c \times n$ ($n_c =$ dimension of compensator) linear equations for a modest number of continuations steps. The algorithm converges to machine accuracy, and for n_c small actually entails *less* computation than is required for the standard Riccati solutions involved in the full-order compensator. Moreover, using the continuation approach together with topological degree theory, Richter has succeeded in resolving many heretofore intractable issues connected with multiplicity of solutions and convergence to the global minimum. These results essentially complete the theoretical foundation of the optimal projection theory of fixed-order dynamic compensator design. It should also be noted that in a broader context, these results illustrate a new general approach to nonconvex optimization problems. Further details on the iterative approach to decentralized design and on Richter's algorithm are given in Section 4.0.

Finally, both dynamic modeling and determination of baseline centralized control designs have been completed for a variety of realistic example problems thus completing Task 4. These are discussed in numerous publications and are highlighted in the body of this report.

SECTION 2.0

**Performance Degradation
Due to Uncertainties and Subsystem Interactions
Via Majorant Analysis**

2.0 Performance Degradation Due to Uncertainties and Subsystem Interactions Via Majorant Analysis

The problem addressed here is the determination of bounds on the degradation of system performance due to uncertainties and/or unforeseen and imperfectly modeled subsystem interactions. Such bounding techniques represent a fundamental systems analysis tool that is indispensable for further elucidation of decentralized controller architectures and robust design.

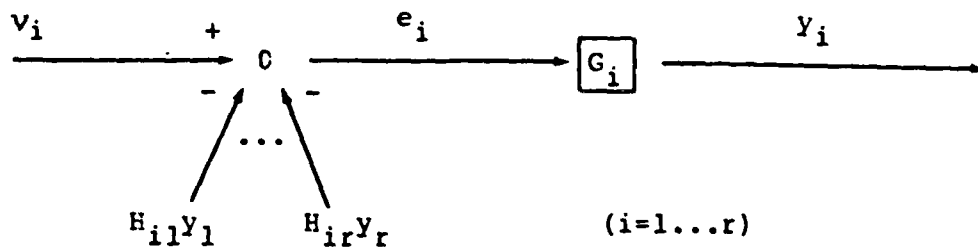
Extensive work has been carried out in the area of frequency-domain analysis of robust stability giving rise to the H -infinity theory of robustness characterization and robust design [2.1-2.5]. However, although the H -infinity world-view is a beautiful and compelling theory within its proper province, its fundamental assumptions render it inapplicable to structural vibration control which involves parametric and often nondestabilizing open-loop uncertainties. A principal difficulty is the *conservatism* of H -infinity robustness characterizations. A stability robustness analysis technique is called *conservative* if the *predicted* set of nondestabilizing perturbations is a proper subset of the *actual* set of nondestabilizing perturbations. Note that conservatism jointly depends upon both the definition of admissible perturbation classes *and* the robustness analysis technique.

The well-known conservatism of H -infinity theory does *not* arise because it operates in the frequency domain, per se, or because the infinity norm is employed, but rather because of the crudeness of H -infinity bounds. What is the fundamental source of this crudeness? Possibly this arises because the fundamental intent of H -infinity development was the *extension of classical control design concepts to the multivariable case per se rather than specifically for the problem at hand*.

For example, in keeping with classical ideas, there has been widespread insistence upon couching all questions of performance and uncertainty in terms of simplistic (albeit traditional) unity gain feedback diagrams. Thus, singular value developments have lumped uncertainty in a single block thereby obscuring the often complex structure of modeling error. Moreover, this feedback paradigm is maintained even for structured uncertainty approaches [2.6].

To achieve a less confining point of view, the first step is to represent uncertain systems by means of a large-scale system input-output formulation as depicted in Figure 2.0-1.

Referring to Figure 2.0-1, the overall system is represented by interconnected subsystems undergoing interactions. The subsystems, characterized by the operators G_k ($k = 1, \dots, r$), represent



(i=1...r)

$$(I + GH)y = y_0$$

$$y_0 \triangleq Gv$$

$G = \text{block-diag } \{G_k\}; \quad G_k \text{ known}$
 $k=1...r$

$$H = \begin{bmatrix} 0 & H_{12} & H_{13} & \dots \\ H_{21} & 0 & H_{23} & \\ H_{31} & H_{32} & 0 & \\ \vdots & & & \end{bmatrix} \in \mathcal{H}, \text{ some compact, arcwise connected set with off-diagonal block structure}$$

uncertain subsystem interactions or parametric uncertainties

 \mathcal{H} specifies uncertainty about H

Problem: Bound output y or deviation from nominal, $y - y_0$,
 for all $H \in \mathcal{H}$

Figure 2.0-1. Large-Scale Input-Output Formulation

the known dynamics of the system while the subsystem interactions, given by the operators H_{kj} , correspond to uncertainties. Note that the partitioned off-block-diagonal operator H is stipulated to belong to some compact arcwise connected set \mathcal{X} . The set \mathcal{X} specifies both the character and extent of dynamical uncertainties.

The motivation for the above input-output formulation within the context of large-scale systems is obvious. But in addition, thanks to the Dynamic Inclusion Principle and related ideas elaborated by Siljak and his co-workers [2.7,2.8] the representation of Figure 2.0-1 is also suitable for parametric perturbations in monolithic systems, i.e., systems without explicit interconnections.

The problem now addressed is how to bound the degradation of the system output vector y or the prediction $y - y_0$ in the presence of the uncertainties. To give this problem mathematical form, we must use the block-matrix results of Ostrowski [2.9] and define the *block- L_p norm matrix* of a partitioned operator \tilde{M} and the block-norm matrix of a partitioned matrix M as in the top half of Figure 2.0-2. With these definitions, the principal problem is to bound the block-norm vector of the system output y over all variations of the uncertain perturbations, i.e., $|y|_L$ as H varies over the whole set \mathcal{X} . Bounding off-nominal prediction errors is handled similarly and so will not be given separate treatment here.

Referring again to Figure 2.0-2, it is evident that a suitable bound for $|y|_L$ takes the form of a *nonnegative matrix* (i.e., a matrix whose elements are nonnegative) \hat{L} multiplied by the block-norm vector of the nominal output. Note that the double inequality sign relating two matrices indicates element-by-element inequality. The "gain matrix" \hat{L} is just a nonnegative bound on the *worst-case* value of the block- L_p norm matrix of the *output gain operator* \mathcal{L} . Note that, in essence, \hat{L} maps the nominal output into the actual output as corrupted by uncertain interactions. In the following, we focus on bounding the gain operator. Note (from the bottom of Figure 2.0-2) that this formulation gives rise to a clear definition of conservatism. Note also that the existence of a finite bound $\hat{L}(\mathcal{X})$ implies input-output stability (see [2.10]). Thus robust stability and performance degradation can be handled by one and the same theoretical apparatus.

Now, the above articulation of uncertainties into numerous interactions permits more *finely articulated* methods of computing bounds beyond singular value analysis, namely, methods associated with the *majorant analysis* of Dahlquist [2.11]. Following Dahlquist, we define the *majorant* and *minorant* matrices of a partitioned matrix or operator as in the top portion of Figure 2.0-3. The inequalities shown in the center of the figure follow directly from the definitions and indicate

Block- L_p norm matrix of \tilde{M} :

$$|\tilde{M}|_{L_p} = \begin{bmatrix} \|\tilde{M}_{11}\|_{L_p} & \|\tilde{M}_{12}\|_{L_p} & \dots \\ \|\tilde{M}_{21}\|_{L_p} & \|\tilde{M}_{22}\|_{L_p} & \dots \\ \vdots & \vdots & \ddots \end{bmatrix} \in R_+^{r \times r}$$

Block-norm matrix of M :

$$|M|_p = \begin{bmatrix} \|M_{11}\|_p & \|M_{12}\|_p & \dots \\ \|M_{21}\|_p & \|M_{22}\|_p & \dots \\ \vdots & \vdots & \ddots \end{bmatrix} \in R_+^{r \times r}$$

Output bound:

$$\|y\|_L \leq \hat{y} = \hat{\mathcal{L}}y_0$$

where $\hat{\mathcal{L}} \in R_+^{r \times r}$ and

$$\hat{\mathcal{L}}(\mathcal{H}) \geq \sup_{H \in \mathcal{H}} \|k\|_L = \mathcal{L}^*(\mathcal{H})$$

where:

$$(I + GH)\mathcal{L} = \mathcal{L} ; \|k\|_L = I$$

Conservative bound: $\hat{\mathcal{L}} \geq \mathcal{L}^* ; \hat{\mathcal{L}} * \mathcal{L}^*$

Nonconservative bound: $\hat{\mathcal{L}} = \mathcal{L}^*$

Finite $\hat{\mathcal{L}}(\mathcal{H})$ exists \implies Input-Output L_p stability

Figure 2.0-2. Block-Norm Matrices

that the majorant and minorant are matrix generalizations of the maximum and minimum singular values, respectively. Moreover, these inequalities can be very efficiently used to bound the block- L_p norm matrix of the output gain operator. In fact, what we seek is merely some *majorant* of the gain operator.

Figure 2.0-4 shows a simple example of how the inequalities of Figure 2.0-3 can be used to derive such a majorant for the gain operator, starting from the defining relation

$$(I + GH)\mathcal{L} = I$$

for \mathcal{L} given in Figure 2.0-2. The result obtained in Figure 2.0-4, namely:

$$|\mathcal{L}|_{\mathcal{L}} \leq \hat{\mathcal{L}}$$

$$(I - GH)\mathcal{L} = I_r$$

is, in fact, the crudest possible majorant bound and is equivalent to the small gain theorem for L_p input-output stability of a large scale-system [2.10]. When there is only one system block, this further reduces the singular-value bound as a particular special case.

But the uncertain subsystem interaction format (introduced in Figure 2.0-1) in conjunction with majorant analysis gives an almost unlimited potential for formulating sharper bounds. Using a process of operator iteration, one can obtain the results displayed in the top half of Figure 2.0-5. Here we have a *hierarchy* of output bounds, where each successive member of the hierarchy requires more and more information but is less and less conservative (with respect to the set \mathcal{X}). For the results shown in Figure 2.0-5, the sequence of bounds approaches the least upper bound under a norm-bounded uncertainty set, i.e., for this set \mathcal{X} the hierarchy is nonconservative in the limit! Note also that, because we work in an operator setting, distinctions between the time and frequency domains are blurred. It is parochial to assert that *only* frequency-domain or time-domain methods must be used. What's needed is easy and fluent translation between the frequency and time domains as provided here. Furthermore, the computational advantage of this kind of hierarchy is that each bound requires only the inversion of an M -matrix. This is quite straightforward and nicely tractable, even for many subsystems, since it involves computing a monotonically increasing sequence where each iteration involves an addition and a multiplication of low-order matrices. Figure 2.0-6 summarizes the relevant facts on the solution of majorant equations. One has only to contrast the simplicity of these results with the difficulties of the μ -function computation [2.12]

$$\begin{aligned}
\|z\|_L &= \|(I + GH)^{-1}z\|_L \\
&\leq \widehat{\|(I+GH)^{-1}z\|} \\
&\leq \widehat{\|(I+GH)^{-1}\|} \hat{z} \\
&\leq \widehat{\|(I+GH)\|}^{-1} \quad (\|z\|_L = I) \\
&\leq \widehat{\|(I-\hat{G}\hat{H})\|}^{-1} \\
&\leq \widehat{\|(I-\hat{\tilde{G}}\hat{\tilde{H}})\|}^{-1} \\
&\Downarrow \\
\|z\|_L &\leq \hat{z} \\
(I-\hat{\tilde{G}}\hat{\tilde{H}})\hat{z} &= I_r
\end{aligned}$$

- * Bounding $\|z\|_L$ means: Find a majorant of $z \forall H \in \mathcal{H}$
- * This is the crudest possible bound,
 $r = 1 \Rightarrow$ singular value inequality
- * There are much more refined bounds
- obtained by iteration of operators...

Figure 2.0-4. Example of Bound Derivation

n.th ($m = 0, 1, \dots$) member:

$$|\mathcal{L}|_L \leq L^{(m)} \quad \forall H \in \mathcal{H}$$

$$(I - \mathcal{G}^{(m)})_L^{(m)} = \mathcal{M}^{(m)}$$

$$G^{(m)} \triangleq \sup_{H \in \mathcal{H}} |(GH)^{2^m}|_L \in \mathbb{R}_+^{r \times r}$$

$$\mathcal{M}^{(m)} \triangleq \sup_{H \in \mathcal{H}} \left| \prod_{r=0}^{m-1} (I + (-GH)^{2^r}) \right|_L \in \mathbb{R}_+^{r \times r}$$

* Each member of the hierarchy requires more information and is sharper and sharper:

$$L^{(0)} \gg L^{(1)} \gg L^{(2)} \gg \dots$$

* Lowest member: $L^{(0)} = (I - \widehat{GH})^{-1}$

* If $\mathcal{H} \triangleq \{H: |H|_L \leq \bar{H} \in \mathbb{R}_+^{r \times r}; \bar{H}_{kk} = 0\}$, then:

$$\lim_{m \rightarrow \infty} L^{(m)} = \mathcal{L}^*(\mathcal{H})$$

- i.e. $L^{(m)}$ is nonconservative in the limit

* Input data can be given in time-domain or frequency domain
- as appropriate

* Each member of the hierarchy requires only inversion of an $r \times r$ M-matrix

Figure 2.0-5. Hierarchy of L_p Output Bounds

All majorant bounds involve equations of the form:

$$(I - B)L = C$$

$$C, B \in R_+^{r \times r}$$

* $L \in R_+^{r \times r}$ exists iff $(I-B)$ is a nonsingular M-matrix

* $L \in R_+^{r \times r}$ exists iff the sequence:

$$L_0 = 0$$

$$(I - \{B\})L_{n+1} = \langle B \rangle L_n + C$$

$$\{B\} \triangleq \text{diagonal part of } B$$

$$\langle B \rangle \triangleq B - \{B\}$$

converges. If so, $L = \lim_{n \rightarrow \infty} L_n$

* $L \in R_+^{r \times r}$ exists iff the sequence:

$$\Lambda_0 = (I - \{B\})^{-1} \langle B \rangle, S_0 = I + \Lambda_0$$

$$k \geq 0: \Lambda_{k+1} = \Lambda_k^2; S_{k+1} = S_k (I + \Lambda_{k+1})$$

converges. If so:

$$L = \lim_{k \rightarrow \infty} S_k (I - \{B\})^{-1} C$$

(nth iterate = 2^n simple iterations)

Figure 2.0-6. Solution of M-Matrix Equations

to appreciate the power of the "uncertain subsystem" representation of Figure 2.0-1 and its allied bounding technique, majorant analysis.

The above discussion has set forth the general development of majorant robustness analysis within an operator setting which employs L_p norms to describe the "size" of subsystem outputs. For systems with stochastic inputs and time independent parameter uncertainties, the main lines of development are analogous. However, in this case one needs to work with the Lyapunov equation for the steady-state second-moment matrix of response and then derive majorant bounds for the block-norm matrix of the second moment. The general setup for undertaking majorant analysis for the parametrically uncertain stochastic systems is shown in Figure 2.0-7. Here, the block-diagonal matrix A represents the known subsystem or nominal system dynamics while the off-block-diagonal matrix G represents uncertain subsystem interactions or parametric uncertainties. Generally, G is stipulated to be some element of a compact, arcwise connected set \mathcal{G} which describes the geometry and severity of uncertainties. The simplest prescription, for example, is that \mathcal{G} contains all off-diagonal block matrices such that the norm of each off-diagonal block is bounded by a stipulated number.

Note that the disturbance intensity matrix V and the second-moment matrix Q are partitioned conformably with A and G . We bound performance degradation due to uncertain interactions G ranging over the admissible set \mathcal{G} by bounding the block-norm matrix of Q . To do this, however, requires additional algebraic tools, such as the *Kronecker algebra* which centers on the VEC operator, Kronecker product, and Kronecker sum. These operations, which are defined by the relations shown in Figure 2.0-8, are critical to the development. The reader is encouraged to consult the review paper by Brewer [2.13] for a thorough discussion of the Kronecker algebra. Because of the algebraic complexity of deriving majorants for the second-moment matrix, the Kronecker algebra is far more than a mere notational convenience.

For our development, the standard Kronecker algebra is a completely adequate tool only when each subsystem (with dynamics A_k , $k = 1, \dots, r$) is one-dimensional. However, we are concerned with systems composed of many high-dimensional subsystems. To handle the algebraic work, one needs a generalization of the Kronecker algebra, namely, the *block-Kronecker algebra*. The underlying operations of the VECb operator are the *block* Kronecker product and sum which are displayed in Figure 2.0-9. Note that while the VEC operator stacks the columns of a matrix into a vector, the VECb operator stacks the VEC's of the columns of subblocks in a partitioned matrix.

$$\dot{x} = (A + G)x + w$$

$$O = (A + G)Q + Q(A + G)^T + V$$

$$A = \begin{bmatrix} A_1 & 0 & \text{---} \\ 0 & A_2 & \\ \vdots & & \diagdown \\ \vdots & & \end{bmatrix}$$

Known Subsystem Dynamics

$$G = \begin{bmatrix} G_{11} & G_{12} & \text{---} \\ G_{21} & G_{22} & \\ \vdots & & \diagdown \\ \vdots & & \end{bmatrix}$$

Uncertain Subsystem Interaction
and Nominal Dynamics

$$V = \begin{bmatrix} V_{11} & V_{12} & \text{---} \\ V_{21} & V_{22} & \\ \vdots & & \diagdown \\ \vdots & & \end{bmatrix}$$

Noise Intensity

$$Q = \begin{bmatrix} Q_{11} & Q_{12} & \text{---} \\ Q_{21} & Q_{22} & \\ \vdots & & \diagdown \\ \vdots & & \end{bmatrix}$$

State Covariance

Figure 2.0-7. Subsystem Interaction Model

~ Definitions ~

(J. W. Brewer, IEEE Trans. Circ. Sys., Vol. CAS-25, pp. 772-781, 1978.)

$$(M, A, I \in R^{n \times n})$$

VEC operator, $\text{vec}(M)$:

$$\text{vec}(M) \triangleq \begin{pmatrix} M_{11} \\ M_{21} \\ \vdots \\ M_{n1} \\ \text{---} \\ M_{12} \\ M_{22} \\ \vdots \\ M_{n2} \\ \text{---} \\ \vdots \end{pmatrix}$$

Kronecker Product, \otimes

$$A \otimes B \triangleq \begin{bmatrix} a_{11}B & a_{12}B & \dots & a_{1n}B \\ a_{12}B & a_{22}B & \dots & a_{2n}B \\ \vdots & \vdots & & \vdots \\ a_{n1}B & a_{n2}B & \dots & a_{nn}B \end{bmatrix}$$

Kronecker Sum, \oplus

$$A \oplus B \triangleq A \otimes I_n + I_n \otimes B$$

Figure 2.0-8. Kronecker Matrix Algebra

- Definitions -

1. Block vec operator, vecb(M).

$$\text{If } M = \begin{bmatrix} M_{11} & M_{12} & \dots \\ & & \\ M_{21} & M_{22} & \\ \vdots & & \end{bmatrix}, \text{ then:}$$

$$\text{vecb } M \hat{=} \begin{pmatrix} \text{vec } M_{11} \\ \text{vec } M_{21} \\ \vdots \\ \text{vec } M_{r1} \\ \text{-----} \\ \text{vec } M_{12} \\ \vdots \\ \text{vec } M_{r2} \\ \text{-----} \\ \vdots \end{pmatrix}$$

2. Block Kronecker Product, \otimes

$$A \otimes B \hat{=} \begin{bmatrix} A_{11} \otimes B & A_{12} \otimes B & \dots & A_{1r} \otimes B \\ A_{21} \otimes B & A_{22} \otimes B & \dots & A_{2r} \otimes B \\ \vdots & \vdots & & \vdots \\ A_{r1} \otimes B & A_{r2} \otimes B & \dots & A_{rr} \otimes B \end{bmatrix}$$

where:

$$M \otimes A \hat{=} \begin{bmatrix} M \otimes A_{11} & M \otimes A_{12} & \dots & M \otimes A_{1r} \\ M \otimes A_{21} & M \otimes A_{22} & \dots & M \otimes A_{2r} \\ \vdots & \vdots & & \vdots \\ M \otimes A_{r1} & M \otimes A_{r2} & \dots & M \otimes A_{rr} \end{bmatrix}$$

3. Block Kronecker Sum, \oplus

$$A \oplus B \hat{=} A \otimes I + I \otimes B$$

4. {·}, <·> and vecb:

$$\{M\} \hat{=} \text{bl-diag } \{M_{kk}\}, \quad \langle M \rangle \hat{=} M - \{M\}$$

$$\text{vecb } M \hat{=} \begin{pmatrix} \text{vec } M_{11} \\ \text{vec } M_{22} \\ \vdots \\ \text{vec } M_{rr} \end{pmatrix}$$

Figure 2.0-9. Block-Kronecker Algebra

If the subblocks of the partitioned matrix M are all one-dimensional, the block-Kronecker algebra definitions given in Figure 2.0-9 revert to those given in Figure 2.0-8. Moreover, the block-Kronecker algebra is endowed with the same battery of identities as in the standard Kronecker algebra. These identities, shown in Figure 2.0-10, are invaluable in effecting the required algebraic manipulations to obtain the results discussed below.

In particular, using the block-Kronecker algebra, one can first reduce the second-moment Lyapunov equation into a rather compact equation determining the diagonal subblocks (the individual subsystem second-moment matrices) *alone*. This equation is the second from the top in Figure 2.0-11. With this as the starting point, one then applies majorant analysis to obtain a hierarchy of majorant bounds as shown in the bottom half of Figure 2.0-11. As in the L_p bound analysis, each successive member of the hierarchy offers *less and less conservative bounds*.

Note that having obtained the expressions shown in Figure 2.0-11, we do *not* calculate the block-Kronecker sums and products explicitly. Rather, in each case, we reverse the VECb operator to reduce each member of the hierarchy of bounds to a low-order modified Lyapunov equation for the matrix majorant of the second-moment matrix.

We now consider in more detail the first two members of the majorant hierarchy in order to illustrate the specific forms of the modified Lyapunov equations that are obtained. For example, Figure 2.0-12 shows the first member of the second-moment majorant hierarchy. This gives the majorant Q as the solution of a simple nonnegative matrix equation, where $*$ denotes the Hadamard (element-by-element) product and the dimension of the equation is the number of subsystems. For the norm-bounded uncertainty set shown in Figure 2.0-12, the existence of a nonnegative solution implies a bound for the block-norm matrix of the second moment in addition to robust stability, i.e., $A + G$ is stable for all perturbations G in the norm-bounded set.

One particular advantage of the first member of the hierarchy is that it correctly shows the effect of wide frequency separation of subsystems on performance degradation and robust stability. This effect is illustrated in Figure 2.0-13. Here we have two subsystems whose poles are indicated by the crosses in the complex plane, with ν_1 and ν_2 denoting the damping of the subsystems and $\omega_1 - \omega_2$ the separation in frequencies. The majorant equation in Figure 2.0-12 gives the expression shown in Figure 2.0-13 for the square of the tolerable interaction strength under which stability is preserved. Thus, if the frequency separation ($\omega_1 - \omega_2$) is large, then even very large uncertain interactions can be tolerated. In contrast, the vector Lyapunov function theory of [2.7,2.8] would

Identities

$$I.1 \quad (A+B) \bar{\otimes} C = A \bar{\otimes} C + B \bar{\otimes} C$$

$$I.2 \quad A \bar{\otimes} (B+C) = A \bar{\otimes} B + A \bar{\otimes} C$$

$$I.3 \quad (A \bar{\otimes} B)^T = A^T \bar{\otimes} B^T$$

$$I.4 \quad (A \bar{\otimes} E)(C \bar{\otimes} D) = (AC) \bar{\otimes} (ED)$$

$$I.5 \quad (A \bar{\otimes} E)^{-1} = A^{-1} \bar{\otimes} E^{-1}$$

$$I.6 \quad \text{vecb}(AYB) = (B^T \bar{\otimes} A) \text{vecb} Y$$

$$I.7 \quad \text{vecb}(AX + XB) = (B^T \bar{\oplus} A) \text{vecb} X$$

$$I.8 \quad \text{vecb}(\{M\}) = \mathcal{E} \text{vecb}(M)$$

$$\mathcal{E} \triangleq \sum_{k=1}^r \hat{e}^{(k,k)} \bar{\otimes} E^{(k,k)}$$

$$\hat{e}^{(k,k)} \triangleq \text{diag} \{ \delta_{km} \}_{m=1..r}$$

$$E^{(k,k)} \triangleq \text{bl}_{m}^{-\text{diag}} \{ I_{n_k} \delta_{km} \}$$

$$I.9 \quad \text{vecb}(\langle M \rangle) = \mathcal{E}_1 \text{vecb}(M); \quad \mathcal{E}_1 \triangleq I_{n^2} - \mathcal{E}$$

$$I.10 \quad \text{vecb}(\{M\}) = \hat{\mathcal{E}} \text{vecb} \bar{a}(M)$$

$$\hat{\mathcal{E}} \triangleq \sum_{k=1}^r e^{(k,k)} \bar{\otimes} E^{(k,k)}; \quad e_n^{(k,k)} = \delta_{nk}$$

$$I.11 \quad \hat{\mathcal{E}}^T \hat{\mathcal{E}} = I_n$$

$$I.12 \quad \hat{\mathcal{E}}^T \hat{\mathcal{E}} = \hat{\mathcal{E}}^T$$

Figure 2.0-10. Identities for the Block Kronecker Algebra

$$0 = (A+G)Q + Q(A+G)^T + V$$

$$[v + p] \begin{pmatrix} \text{vec } Q_{11} \\ \text{vec } Q_{22} \\ \vdots \\ \text{vec } Q_{rr} \end{pmatrix} = \begin{pmatrix} \text{vec } V_{11} \\ \text{vec } V_{22} \\ \vdots \\ \text{vec } V_{rr} \end{pmatrix}$$

$$v \hat{=} - \text{block-diag } (A_k \oplus A_k)_{k=1 \dots r}$$

$$p \hat{=} \hat{E}^T (G \oplus G) \mathcal{E}_1 [A \oplus A + G \oplus G]^{-1} \mathcal{E}_1 (G \oplus G) \hat{E}$$

Letting $\mathcal{Q} \hat{=} (\hat{Q}_{11}, \hat{Q}_{22}, \dots, \hat{Q}_{rr})$; $\gamma \hat{=} (\hat{V}_{11}, \hat{V}_{22}, \dots, \hat{V}_{rr})$ apply majorant analysis to get a hierarchy of bounds for the majorant of vecbd Q:

1st member:

$$[\hat{V} - \hat{E}^T (\hat{G} \oplus \hat{G}) \mathcal{E}_1 [A \oplus A - \hat{G} \oplus \hat{G}]^{-1} \mathcal{E}_1 (\hat{G} \oplus \hat{G}) \hat{E}] \mathcal{Q} = \gamma$$

2nd member:

$$[\hat{V}_2 - \hat{P}_2] \mathcal{Q} = \gamma$$

$$v_2 \hat{=} v + \hat{E}^T (G \oplus G) (A \oplus A)^{-1} (G \oplus G) \hat{E}$$

$$p_2 \hat{=} \hat{E}^T (G \oplus G) (A \oplus A)^{-1} \mathcal{E}_1 G \oplus G [A \oplus A + G \oplus G]^{-1} \mathcal{E}_1 (G \oplus G) \hat{E}$$

\vdots
etc.

Figure 2.0-11. A Hierarchy of Majorant Bounds for the Second-Moment Matrix

$$A * \hat{Q} = G\hat{Q} + \hat{Q}G^T + \mathcal{V}$$

$$\bar{\sigma}(G_{ij}) \leq G_{ij}$$



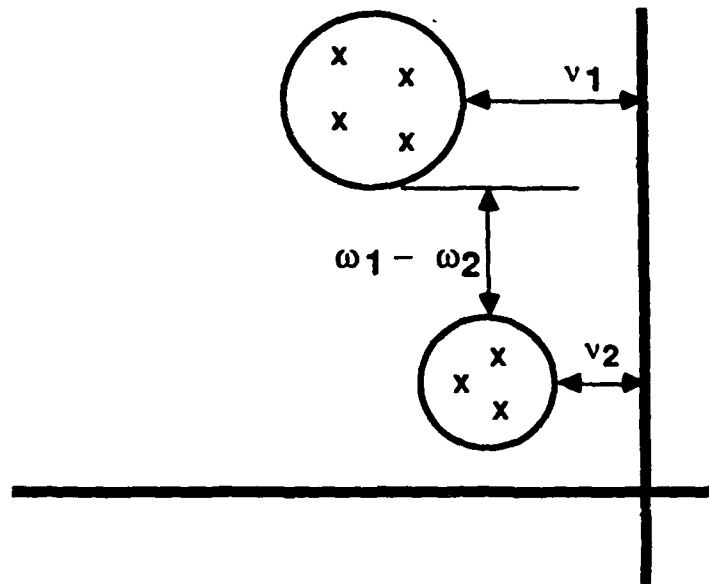
$$Q \leq \hat{Q}$$



- Robust Stability
- Robust Performance

Figure 2.0-12. Majorant Lyapunov Equation

ROBUSTNESS DUE TO WEAK SUBSYSTEM INTERACTION



MAJORANT LYAPUNOV EQUATION BOUND $\sim \sqrt{(v_1 + v_2)^2 + (\omega_1 - \omega_2)^2}$

Figure 2.0-13. Robustness Due to Weak Subsystem Interaction

give $\nu_1 + \nu_2$ which is a much more conservative result for lightly damped systems. Thus, the majorant equation will correctly predict that as frequency separation becomes sufficiently large, subsystems become effectively decoupled. Such predictions cannot be made by either the small gain theorem for large-scale systems or by vector Lyapunov theory. Thus, even the first member of the majorant hierarchy offers greatly reduced conservatism compared to previous results.

Moreover, note that thanks to the properties of M -matrices, the first (and all higher) members of the hierarchy of majorant bounds require only a simple iterative sequence for their computation. The relevant facts are summarized in Figure 2.0-14. The sequence is monotonically nondecreasing, and each iteration requires only two matrix additions, two multiplications and a Hadamard product for its computation. Convergence of the sequence implies robust stability while the degradation of a quadratic performance index J from its nominal (zero interaction) value J_0 is given in terms of Q by the simple expression at the bottom of Figure 2.0-14.

Furthermore, the second member of the second-moment majorant hierarchy, shown in Figure 2.0-15, gives even tighter bounds and can even predict the *nondestabilizing* effect of certain kinds of perturbations. The form of the majorant equation (top of Figure 2.0-15) is similar to the first member of the hierarchy except that the operator $\mathcal{N}[Q]$ appears. This operator is precisely what would arise in the equation for the second-moment matrix for a system with Stratonovich multiplicative noise parameters! So far, we have discussed a design *analysis* tool for predicting performance degradation due to uncertainty. This crucial observation brings us to consideration of the link between majorant robustness analysis and MEOP design synthesis theory.

Figure 2.0-16 illustrates this link and the accompanying sequence of logical developments. Overall, one may regard the MEOP design synthesis theory as arising from a particular robustness analysis tool. Although any member of the second-moment majorant hierarchy might be chosen as the basis of a design synthesis theory, we choose the second member of the hierarchy (see the lower right block in Figure 2.0-16) to serve as the point of departure since it is the simplest bound that also handles nondestabilizing uncertainties. Referring to the lower left block of Figure 2.0-16, it is seen that the second-moment equation of a multiplicative Stratonovich noise model essentially gives an approximation to the majorant equation *and* a smooth optimization problem. The Stratonovich second moment equation then leads to an auxiliary optimization problem (upper left block in Figure 2.0-16), namely, choose dynamic compensator gains to minimize the quadratic performance of a system having *multiplicative stochastic* parameters. Because of the Stratonovich modifications to

MLE has a unique solution iff $\{\hat{Q}_K, K=0, 1, \dots, \infty\}$ where:

$$\hat{Q}_0 = 0$$

$$\hat{Q}_{K+1} = AHI * (S \hat{Q}_K + \hat{Q}_K S^T + v)$$

$$(AHI)_{mn} \triangleq A^{-1}mn$$

converges. If so, then:

$$\hat{Q} = \lim_{K \rightarrow \infty} \hat{Q}_K$$

$$J - J_0 \leq 2 \sum_{K=1}^r (\text{tr } \hat{P}_K) (S \hat{Q})_{KK}$$

$$(0 = A_K^T \hat{P}_K + \hat{P}_K A_K + R_K)$$

Figure 2.0-14. Numerical Solution of the Majorant Lyapunov Equation

Second member of the hierarchy:

$$A * \hat{Q} + \hat{H}[\hat{Q}] = \mathcal{G} \langle \hat{Q} \rangle + \langle \hat{Q} \rangle \mathcal{G}^T + v$$

$$J - \text{tr}[\hat{Q}R] \leq 2 \sum_{K=1}^r (\text{tr } \hat{P}_K) (\mathcal{G} \langle \hat{Q} \rangle)_{KK}$$

$$0 = A\hat{Q} + \hat{Q}A^T + H[\hat{Q}] + V$$

$$0 = A^T\hat{P} + \hat{P}A + H^*[\hat{P}] + R$$

where:

$$\langle \hat{Q} \rangle \triangleq \text{off-diagonal part of } \hat{Q}$$

$$H[.] = \text{Stratonovich model operator}$$

- Tighter bound—incorporates more information on A and G
- Predicts stability when $(A + A^T)$ stable, $G = -G^T$
- "Nominal" performance, $\text{tr}[\hat{Q}R]$, given by Stratonovich model

Figure 2.0-15. Second Member of the Majorant Hierarchy

Auxilliary Optimization Problem

$$0 = A \bar{Q} + \bar{Q}A^T + \mathcal{H}[\bar{Q}] + V$$

$$\bar{J} = \text{tr}[\bar{Q}R]$$

$$A = \begin{bmatrix} A & -EK \\ FC & A_c \end{bmatrix}$$

Find K, F, A_c to minimize \bar{J}

OPME Design Equations

$$0 = A_1 Q - Q A_1^T - A_0^T V_1 - (A_1 R_{21}^{-1} Q_1 + R_{21}^{-1} Q_1^T V_1 - V_1^T R_{21}^{-1} Q_1 - V_1^T R_{21}^{-1} V_1)$$

$$0 = A_1^T P - P A_1 - A_1^T V_1 - (A_1 R_{21}^{-1} Q_1 + R_{21}^{-1} Q_1^T V_1 - V_1^T R_{21}^{-1} Q_1 - V_1^T R_{21}^{-1} V_1)$$

$$0 = (A_1 - B_1 R_{21}^{-1} Q_1) Q - Q (A_1 - B_1 R_{21}^{-1} Q_1)^T - V_1^T R_{21}^{-1} V_1 - V_1^T R_{21}^{-1} V_1$$

$$0 = (A_1 - B_1 R_{21}^{-1} Q_1)^T P - P (A_1 - B_1 R_{21}^{-1} Q_1) + V_1^T R_{21}^{-1} V_1 - V_1^T R_{21}^{-1} V_1$$



Stochastic Design Model

Stratonovich 2nd Moment Equation

$$0 = A \bar{Q} + \bar{Q}A^T + \mathcal{H}[\bar{Q}] + V$$

$$\{\bar{Q}\} \leq \{|\bar{Q}|\}$$

$$J(\bar{Q}) - J_0 \leq J(\hat{Q}) - J_0$$

Majorant Hierarchy

$$0\text{th: } (\hat{P} - \mathcal{L}) \hat{Q} + \hat{Q} (\hat{P} - \mathcal{L})^T + \gamma = 0$$

$$1\text{st: } A^* \hat{Q} = \mathcal{L} \hat{Q} + \hat{Q} \mathcal{L}^T + \gamma$$

$$2\text{nd: } A^* \hat{C} + \hat{\mathcal{H}}_2[\hat{Q}] = \mathcal{L} \langle \hat{Q} \rangle + \langle \hat{Q} \rangle \mathcal{L}^T + \gamma$$

$$3\text{rd: } A^* \hat{C} + \hat{\mathcal{H}}_3[\hat{Q}] = \dots$$

Figure 2.0-16. Majorant Hierarchy and Stratonovich Models: the Link Between Analysis and Synthesis

the standard form of the Lyapunov equation that appear in the equation for \bar{Q} , the robust stability condition implied by the majorant equation is still enforced since the optimization problem imposes a robust performance constraint.

The optimization of an *apparently* stochastic system actually approximates the majorant bound which was derived purely deterministically and leads to the rather elegant MEOP optimality conditions given in the upper right block in Figure 2.0-16.

Of course, the use of Stratonovich stochastic models was earlier indicated by maximum entropy principles and stochastic approximation theory, and this line of development still stands. But the import of the more recent majorant analysis developments is that there is a *direct link* between maximum entropy stochastic modeling and deterministic performance bounds. This link strengthens the foundations of MEOP synthesis theory and, most importantly, tends to blur the distinctions between stochastic and deterministic points of view. This is just as well since the task confronting the systems and control theory community is *not* to resolve the stochastic versus deterministic debate one way or the other, but rather to *rise above it*. As the work described here suggests, there is a plane upon which the points of view are *numerically indistinguishable*.

2.1 Additional Extensions of Majorant Analysis to Frequency-domain Analysis and to Time-domain Transient Response

The previous section outlined the general majorant theory in an operator setting, discussed its application to the bounding of uncertainty effects on statistical response, and noted the connections between second-moment majorant analysis and MEOP design synthesis theory. Here we discuss additional developments of majorant theory which go beyond considerations of any particular design synthesis approach to provide new and more powerful tools for system robustness analysis.

The first of these applications concerns the use of majorants for frequency-domain robustness analysis. Here, we specialize to linear, time-invariant systems and assume L_2 system inputs and outputs. Referring to the notation of Figure 2.0-2, let $p = 2$, and

$$\|\mathcal{L}\|_{L_2} = \sup_{\omega \in \mathbb{R}} \|\mathcal{L}(i\omega)\|_2, \quad (2.1-1)$$

where $\mathcal{L}(s)$ is a partitioned matrix of transfer function blocks and $\|\cdot\|_2$ denotes the block-norm matrix associated with the matrix 2-norm. Instead of dealing with $\hat{\mathcal{L}}(\mathcal{X})$ and $\mathcal{L}^*(\mathcal{X})$ directly, we seek $\hat{\mathcal{L}}(\mathcal{X}, \omega)$ such that

$$\hat{\mathcal{L}}(\mathcal{X}, \omega) \geq \sup_{H \in \mathcal{X}} \|\mathcal{L}(i\omega)\|_2 = \mathcal{L}^*(\mathcal{X}, \omega).$$

In other words, we determine frequency-dependent bounds on subsystem transfer function blocks so that the block- L_2 norm bounds are then easily obtained via relation (2.1-1). This approach permits considerable insight into the impact of subsystem frequency response and generalizes singular-value analysis.

Reference [112] specialized the majorant hierarchy of Figure 2.0-5 to the above setting to produce a frequency domain majorant analysis which can nonconservatively address highly structured uncertainties. Numerical results given in [112] illustrate convergence of the frequency domain majorant hierarchy to nonconservative bounds which are clearly superior to singular-value analysis and previously developed large-scale system methods.

A further extension of majorant analysis is concerned with analyzing the impact of uncertainties on system transient response in the time domain. In essence, we specialize the formulation of Figure 2.0-2 to L_∞ input and output spaces. In other words, system inputs and outputs are characterized as functions which are pointwise bounded in time. The general majorant hierarchy has been specialized to this case both for continuous-time and discrete-time systems. Because of its direct applicability to numerous current spacecraft pointing design problems, its utility in establishing system identification requirements, and its potential for extension to nonlinear control system analysis, we discuss the discrete-time system majorant analysis results in more detail below.

Figure 2.1-1 depicts the basic formulation and motivation of the discrete-time majorant analysis. Here, as before, we use a subsystem decomposition representation where the actual system differs from the nominal system model via an uncertain interaction matrix G . Typically, we suppose that the block-norm of G is bounded by some nonnegative matrix \hat{G} so that \hat{G} describes the magnitude of the modeling uncertainties. More highly structured sets for G have also been considered. The principal goal of the discrete-time majorant analysis is to determine a worst case bound on the off-nominal prediction error, $E(k) \triangleq x(k) - \bar{x}(k)$ as a function of the discrete-time index when G ranges over the set of uncertainties (i.e., $|G| \leq \hat{G}$). To do this, the general majorant hierarchy of Figure 2.0-5 has been specialized to this setting. Figure 2.1-2 explicitly shows that the 0th order majorant is essentially a vector Lyapunov bound and the 1st member can be shown to be always less conservative than the 0th order bound. Note that all these majorants represent upper bounds for the exact worst case off-nominal prediction error $E^*(k)$, where $E^*(k)$ is defined as

$$E^*(k) \triangleq \sup_{G \in \mathcal{G}} |x(k) - \bar{x}(k)|.$$

Beginning with the first-order majorant, there is an associated lower bound for $E^*(k)$. In other

TIME DOMAIN MAJORANT

$$\text{ACTUAL SYSTEM } \begin{cases} x_{k+1} = Ax_k + Gz_k + v_k; & x_0 = 0 \\ A = \text{diag } \{A_k\}; & A_k \text{ stable} \\ G = (G); & |G| \leq \hat{G} \in \mathbb{R}_+^{n \times n} \end{cases}$$

$$\text{NOMINAL SYSTEM } \begin{cases} \bar{x}_{k+1} = A\bar{x}_k + v_k, & \bar{x}_0 = 0 \end{cases}$$

GIVEN THAT $|G| \leq \hat{G}$, WHAT IS THE WORST CASE BOUND ON $x_k - \bar{x}_k \equiv E_k$?

MORE SPECIFICALLY, FIND A NOT-TOO-CONSERVATIVE $\hat{E}_l(k) \in \mathbb{R}_+^n$ SUCH THAT:

$$|x_l(k) - \bar{x}_l(k)| \leq \hat{E}_l(k)$$

$$\forall G : |G| \leq \hat{G}$$

Figure 2.1-1. Time-Domain Robustness Analysis Problem

TIME DOMAIN MAJORANT

ZEROth ORDER BOUND: $\hat{E}(k)$

OBTAINED BY DIRECTLY MAJORIZING THE ERROR PROPORATION EQUATION

$$\hat{E}(k) = \sum_{\ell=0}^{k-1} \hat{G}[\hat{E}(\ell) + |\bar{z}(\ell)|]$$

HIGHER ORDER BOUND: $\hat{E}(k)$ (UPPER)

GIVEN

$$\begin{aligned} \hat{E}_n(k) = & \sum_{\ell=0}^{k-1} \sum_{m=1}^n \hat{G}_{nm} |P_{nm}(k-\ell-1)| \hat{G}_{mr} \hat{E}_r(\ell) \\ & + \sum_{r=1}^n \hat{G}_{nr} \hat{F}(k-1) + \sum_{m=1}^n \hat{G}_{nm} \hat{G}_{mr} \hat{g}_{nmr}(k-1) \end{aligned}$$

WHERE

$$P_{nm}(\ell) \triangleq \begin{cases} \frac{\lambda_n^\ell - \lambda_m^\ell}{\lambda_n - \lambda_m} & n \neq m \\ \ell \lambda_n^{\ell-1} & n = m \end{cases}$$

Figure 2.1-2. Time-Domain Majorant Bound

words, the first-order and higher order majorant bounds produce two nonnegative matrix functions of time $\hat{E}(k)$ and $\check{E}(k)$ such that

$$\check{E}(k) \leq E^*(k) \leq \hat{E}(k).$$

Thus, the theory provides not only an upper bound on prediction error but also a measure of conservatism of the bound, i.e., $\hat{E}(k) - \check{E}(k)$.

To illustrate the capabilities of the time-domain majorants, we discuss an example given in [91]. This example, depicted in Figure 2.1-3, considers a tracking problem where a flexible spacecraft with a rigidly mounted antenna must track a target through an encounter which takes 5.0 seconds and covers 180 degrees. To illustrate the system analysis aspect of majorants, we suppose that the tracker control loop was designed taking into account only the rigid body dynamics and that all that is known about the dynamics is that there are modes above 20 Hz with specified bounds on the elastic modal coefficients associated with the tracker sensor and thrusters. Given this rather crude knowledge of the elastic modes, it is required to determine how much the actual closed-loop tracking performance can deviate from the predictions of the nominal, rigid-body model. Thus, we illustrate not only the effects of uncertainty but also the utility of majorants in ascertaining the impact of unmodeled dynamics. An additional objective is to indicate how majorant bounds can be used to determine the quality of system identification necessary to support system certification for flight.

Details of the problem formulation and the analytical setup are given in [91]. Figures 2.1-4a,b show final results for various cases in which the first-order majorant bound has been applied. In each of these graphs, we show five curves. The central curve is the trajectory predicted by the nominal model which includes only the rigid body dynamics; in addition we plot the nominal trajectory plus or minus the upper bound $\hat{E}(k)$ on the exact worst-case prediction error; finally, we also show the nominal plus or minus the lower bound $\check{E}(k)$ on the exact worst case error $E^*(k)$. Note that despite the uncertain elastic mode effects, the actual system trajectory is certain to lie between the outermost curves. Thus, majorants predict not merely a single trajectory, but rather a "tube" or band wherein the actual trajectory must lie. Furthermore, note that in all cases the curves representing nominal $\pm \hat{E}(k)$ and nominal $\pm \check{E}(k)$ are relatively close thereby indicating that the upper bound on the prediction error entails very little conservatism. In particular, in cases 1, 3 and 4, the curve corresponding to upper and lower bounds are so close together that they cannot be distinguished.

- ENCOUNTER DURATION : 5.0 SECONDS
- 180 DEGREES USING THRUSTERS.
- DYNAMIC MODEL: RIGID BODY MODES AND TWO ELASTIC MODES AT 20.0 AND 40.0 HZ
- CONTROLLER SAMPLE RATE: 50.0 HZ

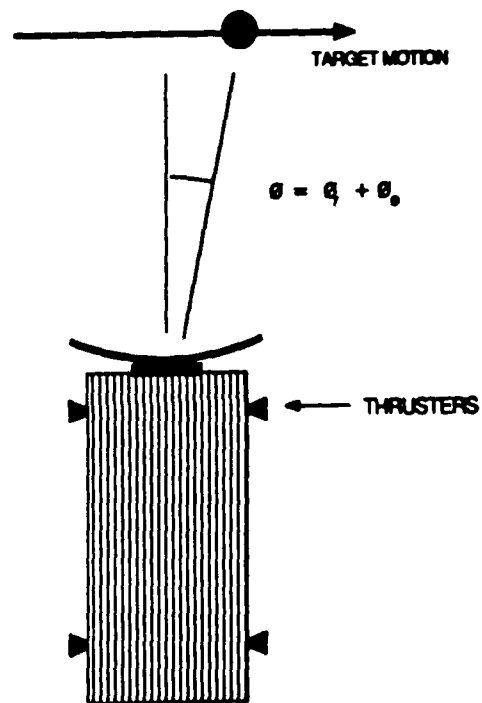
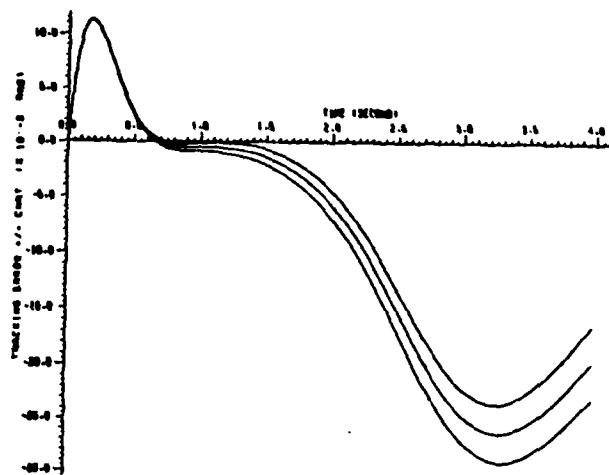
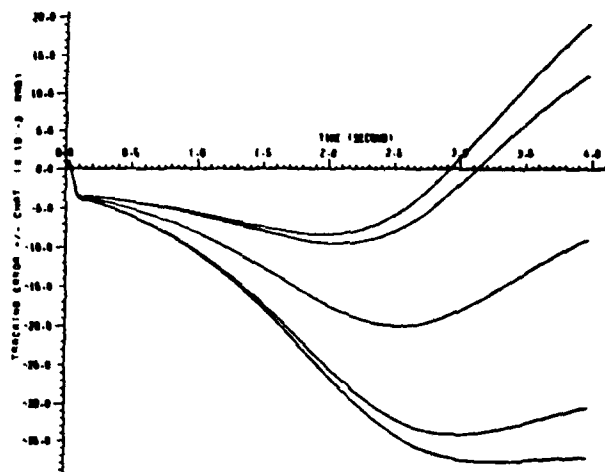


Figure 2.1-3. Spacecraft Tracking Example

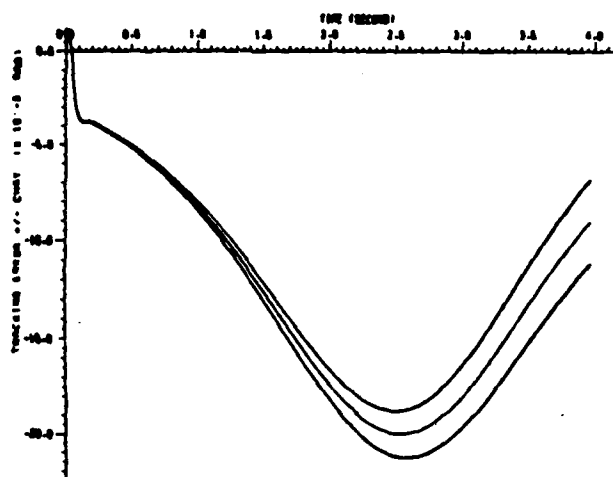


CASE 1: $f_c=1.0$ Hz, NOMINAL UNCERT.

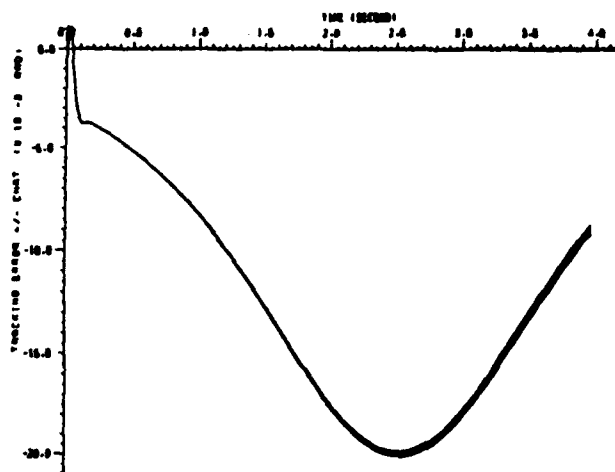


CASE 2: $f_c=5.0$ Hz, NOMINAL UNCERT.

Figure 2.1-4a. Time-Domain Majorant Bounds for Spacecraft Tracking Example



CASE 3: $f_c=5.0$ Hz, 0.1 X UNCERT.



CASE 4: $f_c=5.0$ Hz, 0.01 X UNCERT.

Figure 2.1-4b. Additional Results for Spacecraft Tracking Example

Referring to Figure 2.1-4a, in particular, cases 1 and 2 show how increasing the controller bandwidth (from 1.0 Hz to 5.0 Hz) reduces the nominal target tracking error but increases the prediction error for a given amount of elastic mode uncertainty. This illustrates the use of majorant analysis to help determine controller bandwidths appropriate for the precision of modeling information. Cases 2 through 4 show how decreasing the elastic mode uncertainty decreases the performance bounds. In going from case 2 (Figure 2.1-4a) to case 4 (Figure 2.1-4b) the uncertainty is reduced by an order of magnitude each time. This shows the capability of majorant analysis to ascertain the precision of system identification that is required to attain a given level of guaranteed performance. In the present example, it is seen that a 20 multi-radian tracking specification would require a system ID test that reduces model uncertainty by an order of magnitude.

2.2 References

- [2.1] J. C. Doyle and G. Stein, "Multivariable Feedback Design: Concepts for a Classical/Modern Synthesis," *IEEE Trans. Autom. Contr.*, Vol. AC-26, pp. 4-16, 1981.
- [2.2] G. Zames, "Feedback and Optimal Sensitivity: Model Reference Transformations, Multiplicative Seminorms, and Approximate Inverses," *IEEE Trans. Autom. Contr.*, Vol. AC-26, pp. 301-320, 1981.
- [2.3] G. Zames and B. A. Francis, "Feedback, Minimax Sensitivity, and Optimal Robustness," *IEEE Trans. Autom. Contr.*, Vol. AC-28, pp. 585-601, 1983.
- [2.4] G. Stein and M. Athans, "The LQG/LTR Procedure for Multivariable Feedback Control Design," *IEEE Trans. Autom. Contr.*, Vol. AC-32, pp. 105-114, 1987.
- [2.5] B. A. Francis, *A Course in H_∞ Control Theory*, Springer-Verlag, New York, NY, 1987.
- [2.6] J. C. Doyle, "Analysis of Feedback Systems with Structured Uncertainties," *IEE Proc.*, Vol. 129, pp. 242-250, 1982.
- [2.7] D. D. Siljak, *Large-Scale Dynamic Systems*, Elsevier/North-Holland, 1978.
- [2.8] M. Ikeda and D. D. Siljak, "Generalized Decomposition of Dynamic Systems and Vector Lyapunov Functions," *IEEE Trans. Autom. Contr.*, Vol. AC-26, pp. 1118-1125, 1981.
- [2.9] A. M. Ostrowski, "On Some Metrical Properties of Operator Matrices and Matrices Partitioned Into Blocks," *J. Math. Anal. Appl.*, Vol. 2, pp. 161-209, 1961.
- [2.10] M. Vidyasagar, "New Directions of Research in Nonlinear System Theory," *Proc. IEEE*, Vol. 74, pp. 1060-1091, 1986.
- [2.11] G. Dahlquist, "On Matrix Majorants and Minorants, With Applications to Differential Equations," *Lin. Alg. Appl.*, Vol. 52/53, pp. 199-216, 1983.

- [2.12] M. K. H. Fan and A. L. Tits, "Characterization and Efficient Computation of the Structured Singular Value," *IEEE Trans. Autom. Contr.*, Vol. AC-31, pp. 734-743, 1986.
- [2.13] J. W. Brewer, "Kronecker Products and Matrix Calculus in System Theory," *IEEE Trans. Circ. Sys.*, Vol. CAS-25, pp. 772-781, 1978.

SECTION 3.0

**MEOP Design Synthesis Extensions to
Decentralized/Hierarchical Control**

3.0 MEOP Design Synthesis Extensions to Decentralized/Hierarchical Control

3.1 Review of Centralized Theory

Optimal projection control-design theory has undergone considerable development over the past several years. As shown in Figure 3.1-1, optimal projection theory now encompasses problems in reduced-order, robust modeling, estimation and control in both continuous-time and discrete-time settings. A comprehensive reference list appears in Section 5.0.

For control-design purposes optimal projection theory provides new machinery for synthesizing multivariable feedback controllers. This machinery consists of a system of algebraic design equations which characterize optimal feedback controllers while accounting for both controller order and parameter uncertainties. The design equations consist of a system of two algebraic Riccati equations and two algebraic Lyapunov equations coupled by both an oblique projection and uncertainty terms. The Riccati equations are directly related to the pair of separated Riccati equations arising in LQG theory. Indeed, when the controller order is set equal to the order of the plant and all uncertainties are absent, then the design equations specialize immediately to the standard LQG equations.

3.2 Extensions to Decentralized Controllers

In keeping with the optimal projection philosophy, our approach to decentralized control design is based upon fixed-structure optimization. That is, we assume that the structure of the controller is determined by implementation constraints and/or subsystem analysis. Once the controller architecture is fixed, the feedback gains can be chosen to optimize the performance functional for the closed-loop system. This approach can be used to determine preferable controller architectures by varying the decentralized information structure and optimizing the performance of each configuration.

The fixed structure approach is distinct from methods which are based upon subsystem decomposition with centralized design procedures applied to the individual subsystems. For such methods there remains the problem of determining conditions under which the reassembled closed-loop system has acceptable behavior. An additional drawback of decomposition methods is that the decentralized controller architecture specified by implementation constraints may be completely unrelated to desirable architectures arising from dynamical considerations. For example, physical implementation constraints may impose a particular decentralized architecture which does not correspond to any discernible dynamical decomposition. Furthermore, subsystem decomposition as a

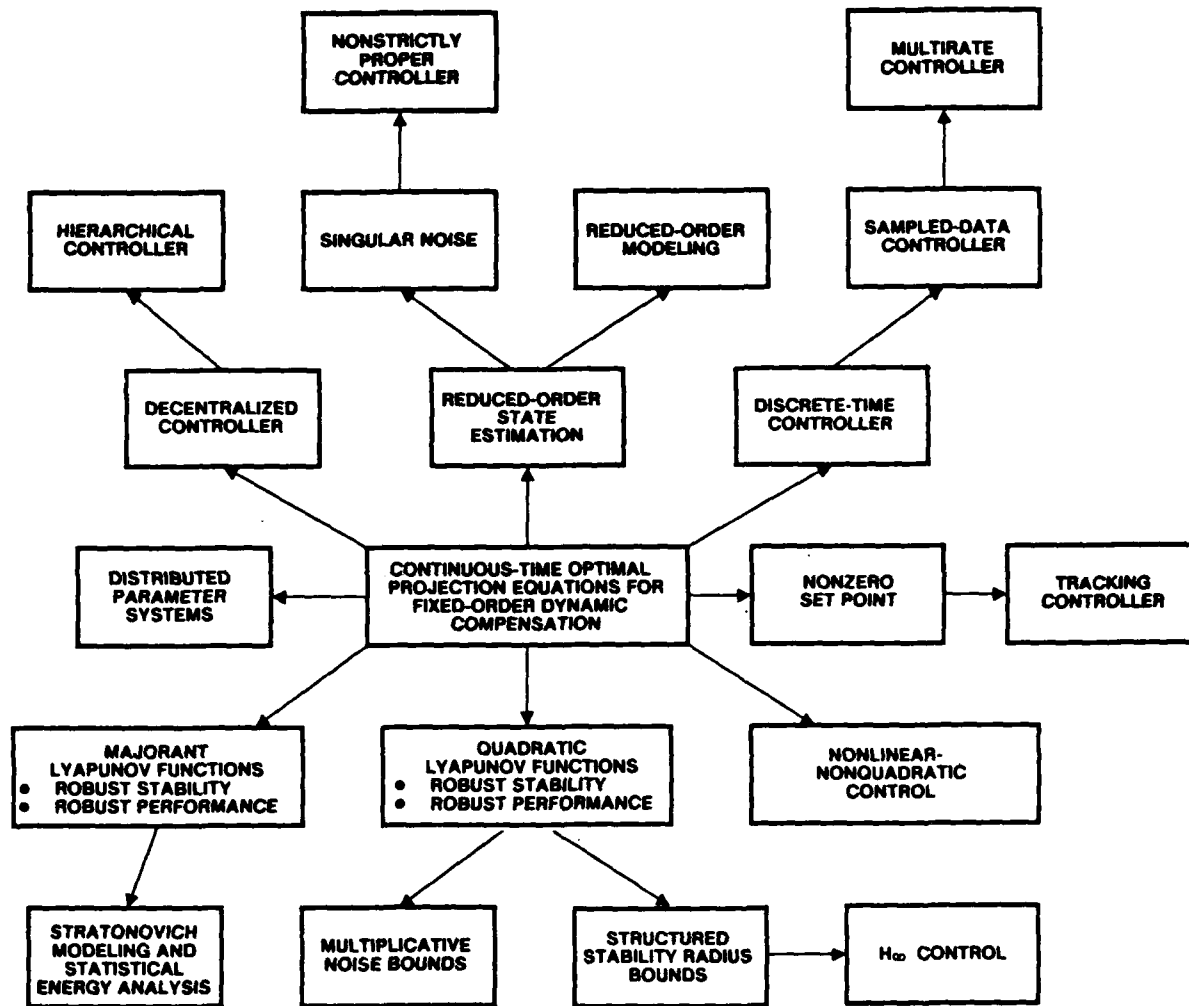


Figure 3.1-1. Scope of MEOP

design tool may constrain the class of attainable designs at the expense of achievable performance.

Of course, in many cases, such as the presence of high dimensionality, subsystem decomposition is absolutely essential for making progress in designing decentralized controllers. However, only by developing methods which avoid unnecessary constraints on the design space can the efficiency of decomposition methods be assessed. Furthermore, methods which retain the full system dynamics may provide a useful starting point for applying existing decomposition techniques as well as the means for developing new methods.

Our overall approach is thus to regard the fixed-structure approach as *complementary* to subsystem decomposition techniques. To this end, majorant robustness analysis has been developed (see Section 2.0) to account for subsystem interactions arising, for example, from system uncertainties. In addition, majorant robustness analysis is closely related to MEOP synthesis particularly with regard to nondestabilizing uncertainties.

3.2.1 Decentralized Controller Design for Static Controllers

We first consider the problem in which each subcontroller is assumed to be static, i.e., a fixed gain multiplying the measurements. For realism, of course, only the physical measurements are assumed to be available for feedback. Earlier versions of this problem were considered in [3.1,3.2]. The most general treatment of this problem obtained thus far can be found in [122]. The development in [122] includes, in particular, noisy and nonnoisy measurements, weighted and unweighted controls, and parameter uncertainties in the A , B , and C matrices. The optimality conditions for this problem are given in the form of a pair of modified Riccati equations coupled by a pair of oblique projections corresponding, respectively, to singular measurement noise and singular control weighting. By utilizing a Lyapunov function to guarantee robust stability, these optimality conditions serve as sufficient conditions for robust stability and performance over a specified range of parametric uncertainty.

3.2.2 Decentralized/Hierarchical Controller Design for Dynamic Controllers

A more complex situation arises when the decentralized subcontrollers are allowed to be fixed-order dynamic controllers. As an additional element of complexity, we assume the various decentralized dynamic controllers are combined within a general *multiechelon hierarchical control* (MHC) structure, illustrated conceptually in Figure 3.2.2-1 which is given in [3.4]. This is the most general arrangement of decentralized control elements and consists of a number of subsystems situated in

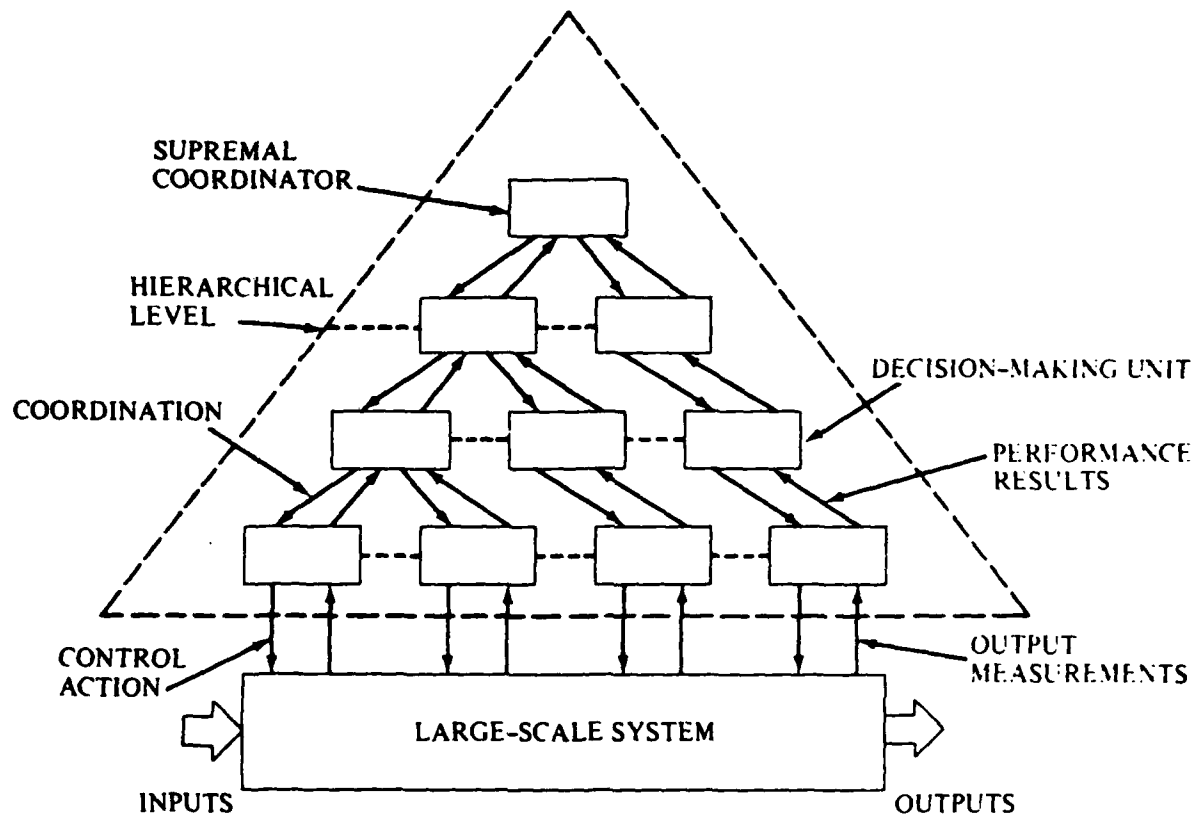


Figure 3.2.2-1. General Multiechelon Hierarchical Control Structure

levels such that each one can coordinate lower-level units and be coordinated by a higher-level one. Previous work, described above, which considers a purely decentralized (but nonhierarchical) architecture, represents the special case of Figure 3.2.2-1 in which only the first hierarchical level is present.

Specific realization of an MHC system within the context of linear dynamic compensation is illustrated by the typical configuration shown in Figure 3.2.2-2a. Here compensators on the first level interact directly with the large scale structure to be controlled. Compensators on higher levels receive linear combinations (defined by the matrices $D_j^{(i)}$) of the direct sensor measurements ($y_j^{(i)}$) and the dynamic states ($q_j^{(i)}$) of the lower-level compensators as inputs and produce output control signals ($u_j^{(i)}$), which serve to coordinate and reconcile the (sometimes competing) actions of the lower-level compensators. The disposition of control inputs, measurements and the matrices $D_j^{(i)}$, $E_j^{(i)}$ defining each coordination level are defined by practical implementation and communication constraints. The important motivations for the MHC arrangement are to reduce processor cost and complexity by breaking up the processing task into relatively small pieces and to decompose the fast and slow control functions. Typically, the lower levels involve relatively simple compensation but relatively high bandwidth, while the upper levels may utilize more nearly centralized and higher-order compensation with relatively low bandwidth. To reduce individual processing burden, it is essential that for each subcontroller, the number of inputs ($y_j^{(i)}$), outputs ($u_j^{(i)}$) and the dimension of the compensator be relatively small.

Figure 3.2.2-2b defines the problem further by defining the generic arrangement of the j th dynamic compensator on the i th hierarchical level. It is seen that each compensator is of the form of an output feedback dynamic compensator whose dimension $n_c^{(i,j)}$ is a fixed number determined by implementation constraints. We address the quadratically optimal multiechelon hierarchical, fixed-order control design problem, i.e., choose the gain matrices $A_{c_j}^{(i)}$, $B_{c_j}^{(i)}$, $C_{c_j}^{(i)}$, for $i = 1, \dots, M$ and $j = 1, \dots, N_i$ for all the dynamic compensators to minimize a steady-state quadratic performance index subject to the selected MHC configuration and the compensator dimension constraints.

This optimization problem is nonconvex and displays multiple local extrema. Figure 3.2.2-3 illustrates the general difficulties and indicates our overall strategy for solving such nonconvex optimization problems. The two-state strategy consists in (1) computing all extremalizing designs, i.e., control gains for which $\frac{\partial J}{\partial A_{c_j}^{(i)}} = \frac{\partial J}{\partial B_{c_j}^{(i)}} = \frac{\partial J}{\partial C_{c_j}^{(i)}} = 0$, by solving the first-order necessary conditions (FONC) for the optimization problem and then (2) selecting the design which is determined to have

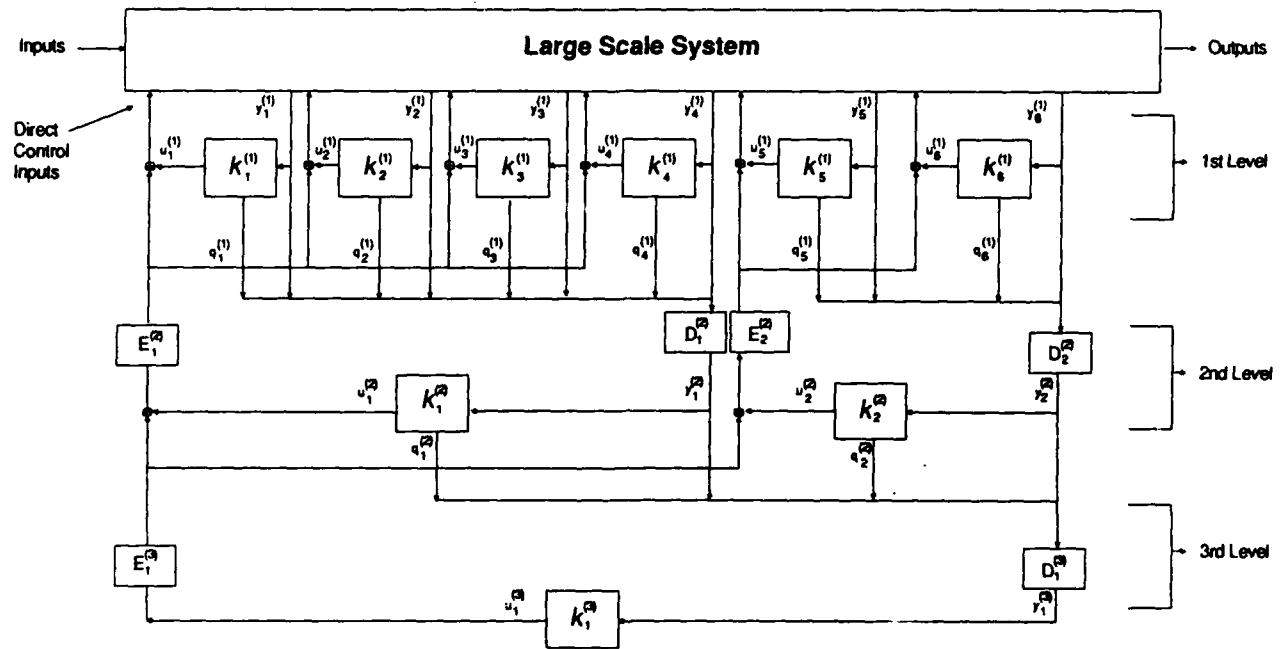


Figure 3.2.2-2a. Multiechelon Hierarchical Control

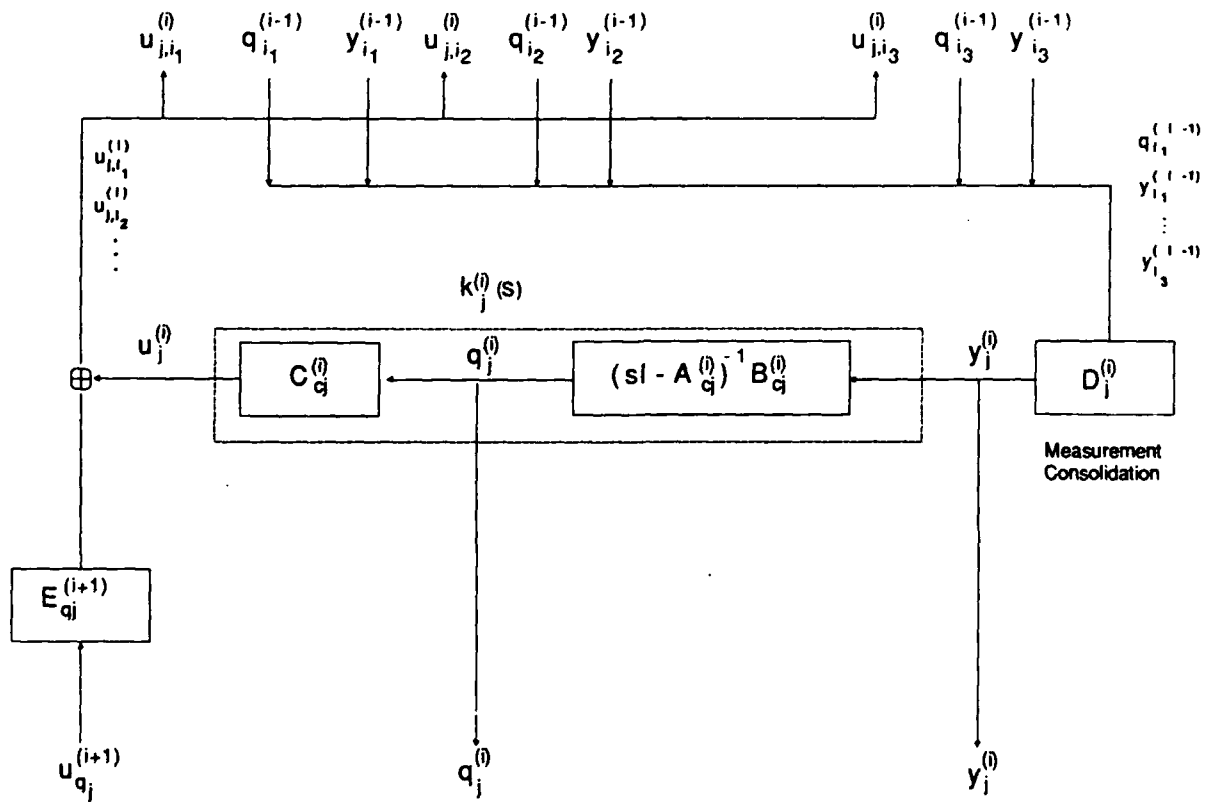
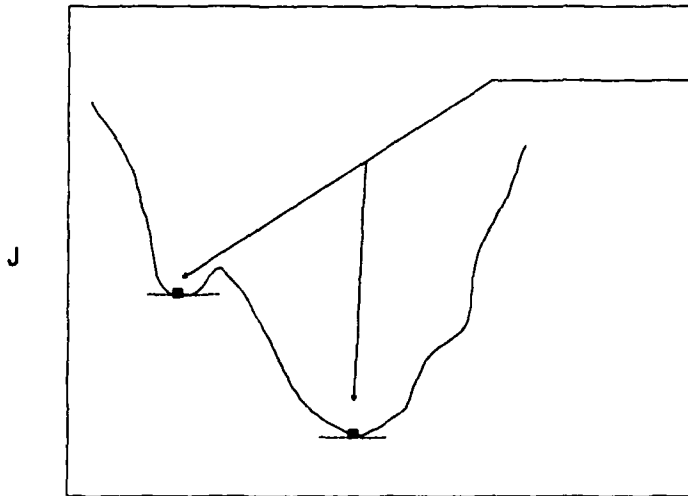


Figure 3.2.2-2b. Detail of the j th Dynamic Compensator of the i th Level



1. Compute All Extremal Designs By Solving The First-Order Necessary Conditions for the Optimization Problem.

* How many solutions are there?

* How can the solutions be computed?

2. For All Design in Step 1, Compute the Performance J and Select the Design with the Best Performance.

$$\left(\begin{array}{ccc} A_{Cj}^{(i)} & B_{Cj}^{(i)} & C_{Cj}^{(i)} \\ i=1, \dots, M \\ j=1, \dots, N_j \end{array} \right)$$

* Gradient Search Methods Can Converge To High-Cost Local Minima and Cannot Assure Global Optimality

* Above Strategy Avoids These Pitfalls, but Feasibility Requires Satisfactory Answers to Questions About Multiplicity of Solutions and Effective Solution Algorithms

Figure 3.2.2-3. Strategy for Solving the Optimal Multiechelon Hierarchical Control Design Problem

the smallest quadratic cost. Although this approach avoids the pitfalls of gradient search methods and can guarantee global optimality, its *feasibility* requires that the number of FONC solutions be relatively small (no more than one, ideally) and that there exist effective algorithms for computing the FONC solutions.

Immediately below we discuss results on the derived forms of the FONC and then address questions about multiplicity of solutions and effective solution algorithms in the remainder of this section and in the following section.

First, the overall FONC comprise the set of all first-order necessary conditions for each subcontroller individually. Figure 3.2.2-4 shows that the formulation of the FONC corresponding to compensator (i, j) (j th controller on the i th hierarchical level) is *exactly identical* to the formulation of first-order necessary conditions for a *single* centralized, fixed-order compensator for an "equivalent plant" which comprises the dynamics of the original plant and *all the other subcontrollers*. The necessary conditions for this "equivalent" centralized design problem are well known by virtue of the earlier MEOP development. Thus, we immediately obtain for the (i, j) th compensator the FONC shown in Figure 3.2.2-5a,b.

Thus, the first-order necessary conditions of the quadratically optimal MHC design problem decompose into sets of four nonlinear matrix equations (Figure 3.2.2-5b) involving one set of four equations for each of the subcontrollers in the multiechelon hierarchical system. Each set of four equations has a form identical to the four MEOP design equations for centralized design, namely, two modified Riccati and two modified Lyapunov equations, all coupled by an oblique projection $\tau^{(i,j)}$ which characterizes the geometric structure of the (i, j) th fixed-order compensator. These results directly generalize earlier results for the purely decentralized problem in [76].

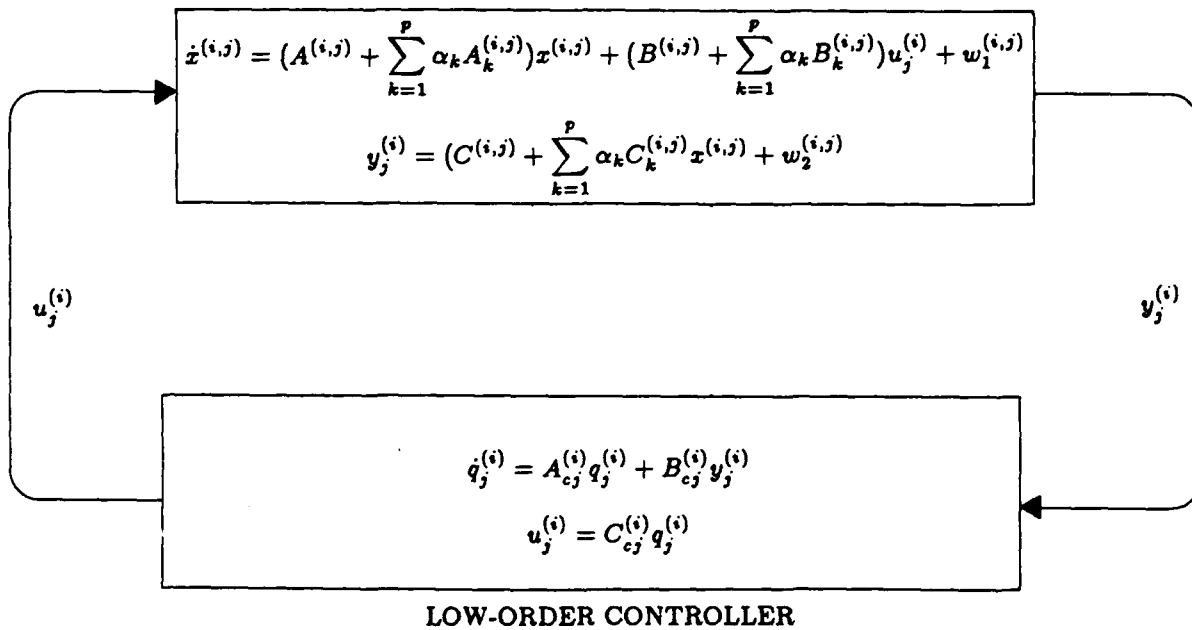
Clearly, the overall FONC will display multiple solutions (since this is the case for fixed-order, centralized design) corresponding to the various local extrema. The decomposition of the FONC noted above shows that the key to establishing the number of solutions is to determine the number of solutions to the *MEOP design equations for centralized fixed-order compensation*. Specifically, the next section discusses new results which establish a generic upper bound on the number of solutions to the MEOP centralized control design equations. Using these results, one can determine an upper bound $\mathcal{N}^{(i,j)}$ on the number of solutions to the matrix equations (Figure 3.2.2-5b) corresponding to the (i, j) th compensator, where $\mathcal{N}^{(i,j)}$ is independent of the other subcontrollers. Then, considering

CONDITIONS

$$\frac{\partial J}{\partial A_{c_j^{(i)}}} = 0, \quad \frac{\partial J}{\partial B_{c_j^{(i)}}} = 0, \quad \frac{\partial J}{\partial C_{c_j^{(i)}}} = 0$$

ARE THE SAME AS FONC FOR THE "(i,j)th EQUIVALENT OPTIMIZATION PROBLEM":

"EQUIVALENT PLANT" FOR (i,j) COMPENSATOR



PERFORMANCE CRITERION

$$J = \lim_{t \rightarrow \infty} \mathbb{E} [x^{(i,j)T} R_1^{(i,j)} x^{(i,j)} + 2x^{(i,j)T} R_{12}^{(i,j)} u_j^{(i)} + u_j^{(i)T} R_2^{(i,j)} u_j^{(i)}]$$

WHERE $A^{(i,j)}, A_k^{(i,j)}, B^{(i,j)}, B_k^{(i,j)}, C^{(i,j)}, C_k^{(i,j)}, w_1^{(i,j)}, w_2^{(i,j)}$ ARE INDEPENDENT OF $A_{c_j^{(i)}}, B_{c_j^{(i)}}, C_{c_j^{(i)}}$ AND $\dim(q_j^{(i)}) = n_c^{(i,j)}$

Figure 3.2.2-4. Derivation of First-Order Necessary Conditions for Compensator (i,j)

GAIN EXPRESSIONS:

$$\begin{aligned} A_{c_j}^{(i)} &= \Gamma^{(i,j)}(A_s - B_s R_{2_s}^{-1} P_s - Q_s V_{2_s}^{-1} C_s) G^{(i,j)T} \\ B_{c_j}^{(i)} &= \Gamma^{(i,j)} Q_s V_{2_s}^{-1} \\ C_{c_j}^{(i)} &= -R_{2_s}^{-1} P_s G^{(i,j)T} \end{aligned}$$

NOTATION

$$\hat{Q}^{(i,j)} \hat{P}^{(i,j)} = G^{(i,j)T} M^{(i,j)} \Gamma^{(i,j)}, \quad \Gamma^{(i,j)} G^{(i,j)T} = I_{n_s} (\Rightarrow \tau^{(i,j)} = G^{(i,j)T} \Gamma^{(i,j)} = \tau^{(i,j)2})$$

$$A Q^{(i,j)} A^T = \sum_{k=1}^P A_k^{(i,j)} Q^{(i,j)} A_k^{(i,j)T}, \quad A Q^{(i,j)} B = \sum_{k=1}^P A_k^{(i,j)} Q^{(i,j)} B_k^{(i,j)}, \text{ etc.}$$

$$A_s = A^{(i,j)} + \frac{1}{2} A^2 \quad B_s = B^{(i,j)} + \frac{1}{2} A B \quad C_s = C^{(i,j)} + \frac{1}{2} C A$$

$$R_{2_s} = R_2^{(i,j)} + B^T (P^{(i,j)} + \hat{P}^{(i,j)}) B$$

$$V_{2_s} = V_2^{(i,j)} + C (Q^{(i,j)} + \hat{Q}^{(i,j)}) C^T$$

$$Q_s = Q^{(i,j)} C_s^T + V_{12}^{(i,j)} + A (Q^{(i,j)} + \hat{Q}^{(i,j)}) C^T$$

$$P_s = B_s^T P^{(i,j)} + R_{12}^{(i,j)T} + B^T (P^{(i,j)} + \hat{P}^{(i,j)}) A$$

Figure 3.2.2-5a. First-Order Necessary Conditions Pertaining to (i,j)th Compensator

SOLVE FOR NONNEGATIVE-DEFINITE $Q^{(i,j)}$, $P^{(i,j)}$, $\hat{Q}^{(i,j)}$, $\hat{P}^{(i,j)}$

$$0 = A_s Q^{(i,j)} + Q^{(i,j)} A_s^T + A Q^{(i,j)} A^T + V_1^{(i,j)} + (A - B R_{2s}^{-1} P_s) \hat{Q}^{(i,j)} (A - B R_{2s}^{-1} P_s)^T \\ - Q_s V_{2s}^{-1} Q_s^T + \tau_{\perp}^{(i,j)} Q_s V_{2s}^{-1} Q_s^T \tau_{\perp}^{(i,j)T}$$

$$0 = A_s^T P^{(i,j)} + P^{(i,j)} A_s + A^T P^{(i,j)} A + R_1^{(i,j)} + (A - Q_s V_{2s}^{-1} C)^T \hat{P}^{(i,j)} (A - Q_s V_{2s}^{-1} C) \\ - P_s^T R_{2s}^{-1} P_s + \tau_{\perp}^{(i,j)T} P_s^T R_{2s}^{-1} P_s \tau_{\perp}^{(i,j)}$$

$$0 = (A_s - B_s R_{2s}^{-1} P_s) \hat{Q}^{(i,j)} + \hat{Q}^{(i,j)} (A_s - B_s R_{2s}^{-1} P_s)^T + Q_s V_{2s}^{-1} Q_s^T - \tau_{\perp}^{(i,j)} Q_s V_{2s}^{-1} Q_s^T \tau_{\perp}^{(i,j)T}$$

$$0 = (A_s - Q_s V_{2s}^{-1} C_s)^T \hat{P}^{(i,j)} + \hat{P}^{(i,j)} (A_s - Q_s V_{2s}^{-1} C_s) + P_s^T R_{2s}^{-1} P_s - \tau_{\perp}^{(i,j)T} P_s^T R_{2s}^{-1} P_s \tau_{\perp}^{(i,j)}$$

$$\text{RANK } \hat{Q}^{(i,j)} = \text{RANK } \hat{P}^{(i,j)} = \text{RANK } \hat{Q}^{(i,j)} \hat{P}^{(i,j)} = n_c^{(i,j)}$$

$$\tau^{(i,j)} = \hat{Q}^{(i,j)} \hat{P}^{(i,j)} (\hat{Q}^{(i,j)} \hat{P}^{(i,j)})^{\#} \quad \tau_{\perp}^{(i,j)} = I_n - \tau^{(i,j)}$$

\Rightarrow GROUP GENERALIZED INVERSE

Figure 3.2.2-5b. First-Order Necessary Conditions (cont'd)

all the first order necessary conditions, it follows that

$$\left(\begin{array}{l} \text{Number of admissible solutions} \\ \text{to the FONC for the} \\ \text{MHC design problem} \end{array} \right) < \prod_{i=1}^M \prod_{j=1}^{N_i} \mathcal{N}^{(i,j)}$$

We shall see that in many practical situations the above number is quite small (indeed, unity in most instances) so that the solution strategy of Figure 3.2.2-3 is feasible and can effectively produce the globally optimal solution.

Also, the structure of the first-order necessary conditions for the MHC problem suggests a solution algorithm consisting of the sequential solution of centralized, fixed-order design equations for each subcontroller in turn. We have developed an effective MHC solution algorithm by first constructing efficient homotopy solution algorithms for the centralized design problem and then applying the results to the more general MHC problem. These matters are discussed in the next section.

3.3 References

- [3.1] J. Medanic, "On Stabilization and Optimization by Output Feedback," *Proc. Twelfth Asilomar Conf. Circ. Sys. Comp.*, pp. 412-416, 1978.
- [3.2] S. Renjen and D. P. Looze, "Synthesis of Decentralized Output State Regulators," *Proc. Amer. Contr. Conf.*, Arlington, VA, pp. 758-762, 1982.
- [3.3] Y. Liu and B. D. O. Anderson, "Controller Reduction Via Stable Factorization and Balancing," *Int. J. Contr.*, Vol. 44, pp. 507-531, 1986.
- [3.4] M. Jamshidi, *Large-Scale Systems*, North-Holland, Amsterdam, 1983.

SECTION 4.0

**Analysis and Solution of the
MEOP Multiechelon Hierarchical Control (MEOP-MHC)
Design Equations**

4.0 Analysis and Solution of the MEOP Multiechelon Hierarchical Control (MEOP-MHC) Design Equations

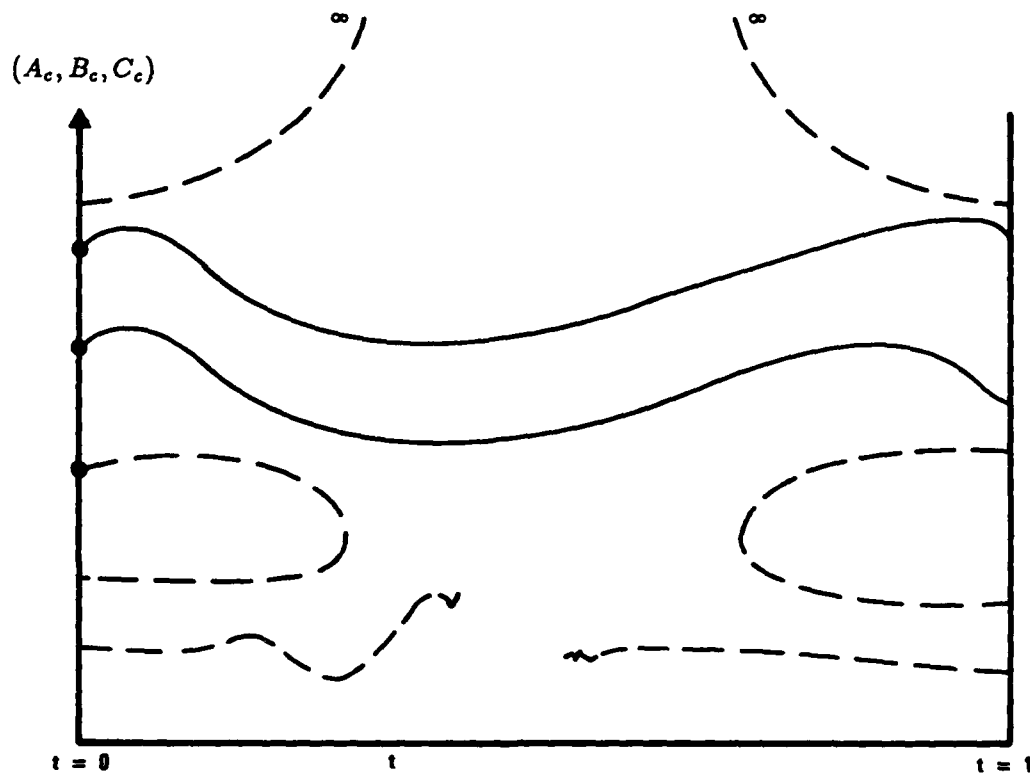
In Section 3.2.2, we described (see Figure 3.2.2-3) how the quadratically optimal, fixed-order multiechelon hierarchical control problem can be reduced to (1) determination of all admissible solutions of the MEOP-MHC design equations (Figure 3.2.2-5b) and (2) selection of the solution for which the quadratic cost is minimal. As noted, the feasibility of this approach depends on satisfactory answers to questions concerning multiplicity of solutions as well as the existence of effective solution algorithms. However, from the structure of the MEOP-MHC design equations noted above we have discovered that optimal MHC dynamic compensator design can be viewed as a collection of subcontroller designs obtained for an augmented system. Essentially, each subcontroller is viewed as a reduced-order controller for the plant augmented by all other subcontrollers. This problem is thus a direct application of centralized MEOP design theory.

In Section 4.1 we review results for the MEOP centralized design theory wherein effective solution algorithms are developed and then show, in Section 4.2, how these centralized design results are applied to resolve residual issues in the MHC design problem.

4.1 Homotopic Continuation and Degree Theory for Optimal Fixed-Order, Centralized Control

Here we return to consideration of the optimal fixed-order dynamic compensator design problem, approached via solution of the MEOP centralized design equations. Note that this is also a nonconvex optimization problem with multiple extrema. Thus the number of solutions, their stability properties, and determination of the global minimum are important issues. It seems clear that any attempt to address these issues must utilize mathematical methods which are global in nature. To this end, we have applied topological degree theory and associated homotopy methods (see [4.1-4.3]) to analyze the solutions of the MEOP centralized design equations and to construct convergent solution algorithms. In essence, a homotopic continuation method involves first solving an "easy" problem, then continuously deforming the easy problem into the original problem, and finally following the path of solutions as the easy problem is deformed into the original problem. This is shown conceptually in Figure 4.1-1 where the dashed lines also indicate several pathologies that can occur. Here t is the continuation parameter, $t = 0$ represents the easy problem, and $t = 1$ corresponds to the original problem to be solved.

In [63,68], Richter formulated a homotopy method and then applied topological degree theory



Topological degree theory \Rightarrow The dashed paths do not exist
 If $n_c \geq \min(\ell, m, n) - n_u$ there is only *one* solution (\Rightarrow global minimum)

Figure 4.1-1. Homotopy Paths

to develop a homotopy method for solving the MEOP equations for which the dashed lines in Figure 4.1-1 cannot occur. That is, the only solutions to the MEOP design equations at $t = 0$ (or for $0 \leq t \leq 1$) are those which are continuously derived from the solutions at $t = 0$. Furthermore, the MEOP equations possess at most

$$\begin{cases} \binom{\min(n, m, \ell) - n_u}{n_c - n_u}, & n_c \leq \min(n, m, \ell), \\ 1, & \text{otherwise,} \end{cases}$$

stabilizing solutions where $\binom{a}{b}$ is the standard combinatoric notation, n_u denotes the dimension of the unstable subspace of the plant, n is the plant dimension, m the number of control inputs, ℓ the number of sensor outputs, and n_c is the desired dimension of the compensator. Moreover, each such solution is reachable via a homotopic path. Finally, if the plant is stabilizable by means of an n_c -th-order dynamic compensator, then there exists at least one solution to the design equations.

Note that if n_c is larger than the number of inputs or outputs, then there is only one solution to the MEOP equations and this solution corresponds to the global minimum of the quadratic performance index. Also note that Richter's homotopy algorithm permits the *a priori* selection of a starting solution (all starting solutions being known in closed form) leading to an admissible, final solution. Hence, even when $n_c \leq \min(n, m, \ell)$, one can compute all solutions, then pick the solution corresponding to the smallest quadratic cost.

An additional benefit of the homotopy algorithm is the ability to exploit the structure of the design equations to an even greater extent than the iterative algorithm. Specifically, Richter has shown that the computational burden using the homotopy methods involves solving four equations of order $n_c \times n$. Hence, the computational requirements *decrease* as n_c decreases. This is, of course, quite pleasing since low-order controllers ought to be easier to design than high-order controllers. For MHC design this property is particularly advantageous since it will generally be true that $n_c \ll \tilde{n}$ where \tilde{n} is the plant dimension augmented by all other subcontrollers.

Since the computational burden of the iterative algorithm tends to increase as n_c decreases, the advantages of the homotopy algorithm over previously developed iterative algorithms are obvious. Computational savings have been at least an order of magnitude and final convergence has been greatly improved. Moreover, the example considered in [4.4] and [94] was reconsidered using the homotopy algorithm in [63,68]. The main result was the ability to produce controllers as low as second order at control authorities which were three orders of magnitude beyond the cases considered in [4.4] and [94]. In each case the performance of the reduced-order controller was

within 20 percent of the full-order design.

In summary, the homotopy and degree theory results render feasible the solution strategy for optimal fixed-order compensation shown in Figure 4.1-2. This directly parallels Figure 3.2.2-3. Here, we compute all extremal designs by solving the FONC in the form of the MEOP design equations. Degree theory shows that the number of solutions is typically small and homotopy algorithms provide efficient methods for computing the solutions. Thus, effective methods exist to carry out step 1 in Figure 4.1-2. Step 2 is relatively straightforward and its completion yields the globally optimal solution to the nonconvex optimization problem.

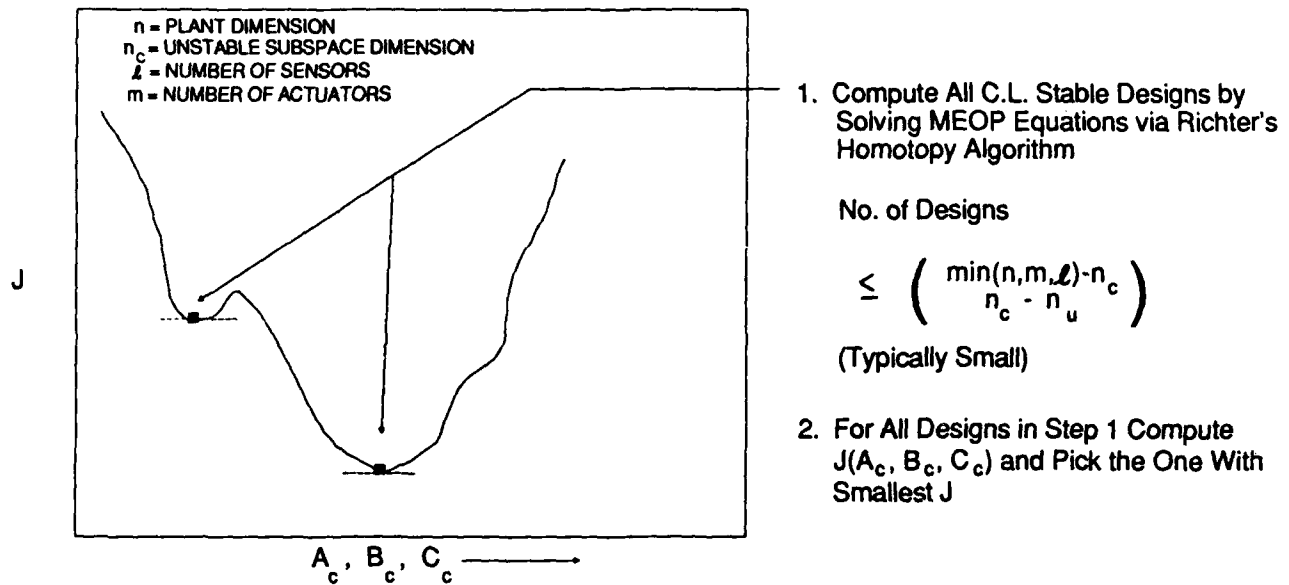
It is evident that the homotopy results for fixed-order centralized control represent a powerful vehicle for successfully addressing the optimal, fixed-order multiechelon hierarchical control problem. The manner in which these results have been adapted to the MHC problem is described in the next section.

4.2 Application of Homotopy and Degree Theory to Optimal Multiechelon Hierarchical Control Design

We now return to the questions raised in connection with the strategy for solving the optimal MHC design problem depicted in Figure 3.2.2-3. We first examine how many solutions exist to the MEOP/MHC design equations shown in Figure 3.2.2-5b.

Clearly, the first-order necessary conditions for the (i, j) th subcontrollers are identical to the MEOP design equations for a single fixed-order controller in the presence of an augmented plant consisting of the original plant and all other subcontrollers. Thus the degree theory results on the centralized design problem can be applied to this case. For the (i, j) th subcontroller, let $m^{(i,j)}$ denote the dimension of $u_j^{(i)}$ and $\ell^{(i,j)}$ the dimension of $y_j^{(i)}$ (see Figure 3.2.2-2b). To simplify this outline of results, we assume an open-loop stable plant and suppose that the dimension of the augmented "equivalent plant" for the (i, j) th compensator is larger than either $m^{(i,j)}$ or $\ell^{(i,j)}$. Then under these rather typical conditions, the degree theory results described in the last section can be utilized to show:

$$\left(\begin{array}{l} \text{Number of admissible solutions} \\ \text{to the MEOP-MHC design} \\ \text{equations (equivalent to the} \\ \text{FONC for the MHC design problem)} \end{array} \right) < \prod_{i=1}^M \prod_{n=1}^{N_m} \mathcal{N}^{(i,j)} \quad (4.2-1)$$



- * Only Method Simultaneously Guaranteeing Parametric Robustness and Order-Reduction
- * Only Known Method Guaranteeing Global Optimality
- * Extended to Infinite-Dimensional Systems and H_∞ Design Constraints (Bernstein, Haddad)

Figure 4.1-2. Solution of the Optimal Reduced-Order Compensator Design Problem (Bernstein, Hyland, Richter)

$$\mathcal{N}^{(i,j)} = \begin{cases} \binom{\min(m^{(i,j)}, \ell^{(i,j)})}{n_{c_j}^{(i)}}, & n_{c_j}^{(i)} \leq \min(m^{(i,j)}, \ell^{(i,j)}) \\ 1, & \text{otherwise,} \end{cases}$$

When it is recalled that the design of simple subcontrollers requiring little on-line computation necessitates a decentralized control structure in which the number of subcontrollers inputs and outputs is small, it is seen that $\mathcal{N}^{(i,j)}$ is typically a small number. Also, if either $m^{(i,j)}$ or $\ell^{(i,j)}$ is small (say < 4) for all i and j then one can choose

$$n_{c_j}^{(i)} \geq \min(m^{(i,j)}, \ell^{(i,j)}) \quad (4.2-2)$$

and still have compensators of acceptably small dimension.

If the above choices can be made for the dimensions of all the subcontrollers, then $\mathcal{N}^{(i,j)}$ is unity for all i, j and the MEOP-MHC design equations have, at most, one solution. Moreover, one solution always exists since for a stable plant, a stabilizing MHC design exists and there is at least one extremalizing design. Since the MEOP-MHC equations are the first-order necessary conditions, they have at least one solution under a stabilizability assumption. Thus, under the conditions postulated, the MEOP-MHC design equations have a unique solution and this corresponds to the global minimum of the performance index.

The above results render step 1 in Figure 3.2.2-3 feasible. Even if $\mathcal{N}^{(i,j)} > 1$, practical constraints on $m^{(i,j)}$ and $\ell^{(i,j)}$ will tend to keep the total number of admissible solutions to within a manageable level.

Next, retaining assumption (4.2-2) we consider the application of the centralized design homotopy algorithm discussed in the previous section to MHC design. The structure of the MEOP-MHC equations immediately suggests sequential design as in [4.5-4.7] whereby the equivalent centralized design problem is solved for each individual subcontroller in turn. Specifically, let each (i, j) correspond, one to one, to an integer k , where $k = 1, \dots, N_T$, where

$$N_T \triangleq \sum_{i=1}^M N_i$$

is the total number of subcontrollers. With this re-indexing of the subcontrollers, consider the following algorithm:

Start: Choose any set of stabilizing gains (in the present case, it suffices to choose $A_{c_j}^{(i)} = B_{c_j}^{(i)} = C_{c_j}^{(i)} = 0$, for all (i, j)) and let $k = 1$ and $L = 1$.

- 1.A Apply the homotopy algorithm to solve the MEOP-MHC equations for the k th subcontroller, i.e., solve the equations shown in Figure 3.2.2-5b (with (4.4-2), the solution is unique).
 - B Update the gains for the k th subcontroller using the expressions in Figure 3.2.2-5a and incorporate these within the closed-loop system model.
 - C Compute the overall closed-loop cost J .
2. If $k < N_T$, increment k by unity and go to step 1. Otherwise, increment L by unity and go to 1.

The above establishes an infinite sequence of redesigns and a corresponding sequence of closed-loop costs $\{J(k, L); k = 1, \dots, N_T, L = 1, \dots, \infty\}$. It is easily seen that $J(k, L)$ is monotonically nonincreasing. This occurs because step 1.A is the solution of a centralized, fixed order optimization problem and the value of J cannot increase following a redesign. Since $\{J(k, L)\}$ is a monotonic nonincreasing sequence which is also inherently nonnegative, it converges to a nonnegative value. This implies also that the sequence of subcontroller gains converge and, by virtue of step 1.A, the values to which they converge satisfy the full MEOP-MHC design equations. This solution can be shown to be unique and corresponds to the globally optimal design. Thus, under the conditions postulated, the above general algorithm involving sequential redesign and directly using the homotopy algorithm for centralized MEOP design is seen to converge monotonically to the globally optimal design. The questions raised in Figure 3.2.2-3 are answered quite satisfactorily and the overall solution (which now parallels Figure 4.1-2 for centralized design) is seen to be practically feasible and (thanks to the homotopy algorithm) effective and efficient.

The above results also follow for open-loop unstable systems if, in the above algorithm, one starts by first designing the highest level controller (the supremal coordinator) to stabilize the system. The general case $n_{c_j}^{(i)} < \min(m^{(i,j)}, \ell^{(i,j)})$ has not been extensively investigated and must remain the object of further research.

Also, note that the sequential redesign algorithm does not presuppose any particular *order* in which the subcontroller redesigns are to be carried out. There are many possibilities. One could, for example cycle through all subcontrollers in some order within a given iteration. Alternatively, in what might be called the "echelon scheme," one might iterate only the compensator designs in a given hierarchical level (keeping designs in other levels fixed) until there is convergence for that

level and then move on to another hierarchical level. How each such ordering and iteration scheme affects the *rate* of convergence is just beginning to be appreciated. Only limited design experience has been acquired to-date and much remains to be done to establish the ordering of the sequential redesign steps which will, for any given problem, *promote the most rapid convergence*.

4.3 Decentralized/Hierarchical Design Examples

To illustrate the ideas developed in the previous sections, we have carried out detailed numerical calculations for two design problems. The first example involves a pair of interconnected flexible beams while the second involves a deployable truss structure. For each problem a decentralized controller was designed using the sequential design algorithm developed in the previous sections. Although only single echelon designs were considered, the extension to multiechelon controllers is straightforward.

The first example involves a pair of simply supported Euler-Bernoulli flexible beams interconnected by a spring and constrained to vibrate in one spatial dimension (see Figure 4.3-1 and [76]). Each beam possesses one rate sensor and one force actuator which are noncolocated. No special requirements were imposed on the locations of the sensors, actuators, and spring attachment points except to avoid nodes of the beam mode shapes. Two vibrational modes were retained in each beam so that the interconnected system possesses eight poles. The interconnection spring was chosen to be sufficiently stiff so that high authority local decentralized designs designed with the spring absent suffered significant degradation when the spring was reinserted. To obtain high authority designs we chose quadratic weights so that the closed-loop performance of the centralized controller yielded an order of magnitude performance improvement over the open-loop system.

To design a decentralized controller we began by designing local 4th-order decentralized controllers for each beam individually. Reinsertion of the spring resulted (as noted above) in significant performance degradation. Each subcontroller was then redesigned alternatively yielding the results given in the following table:

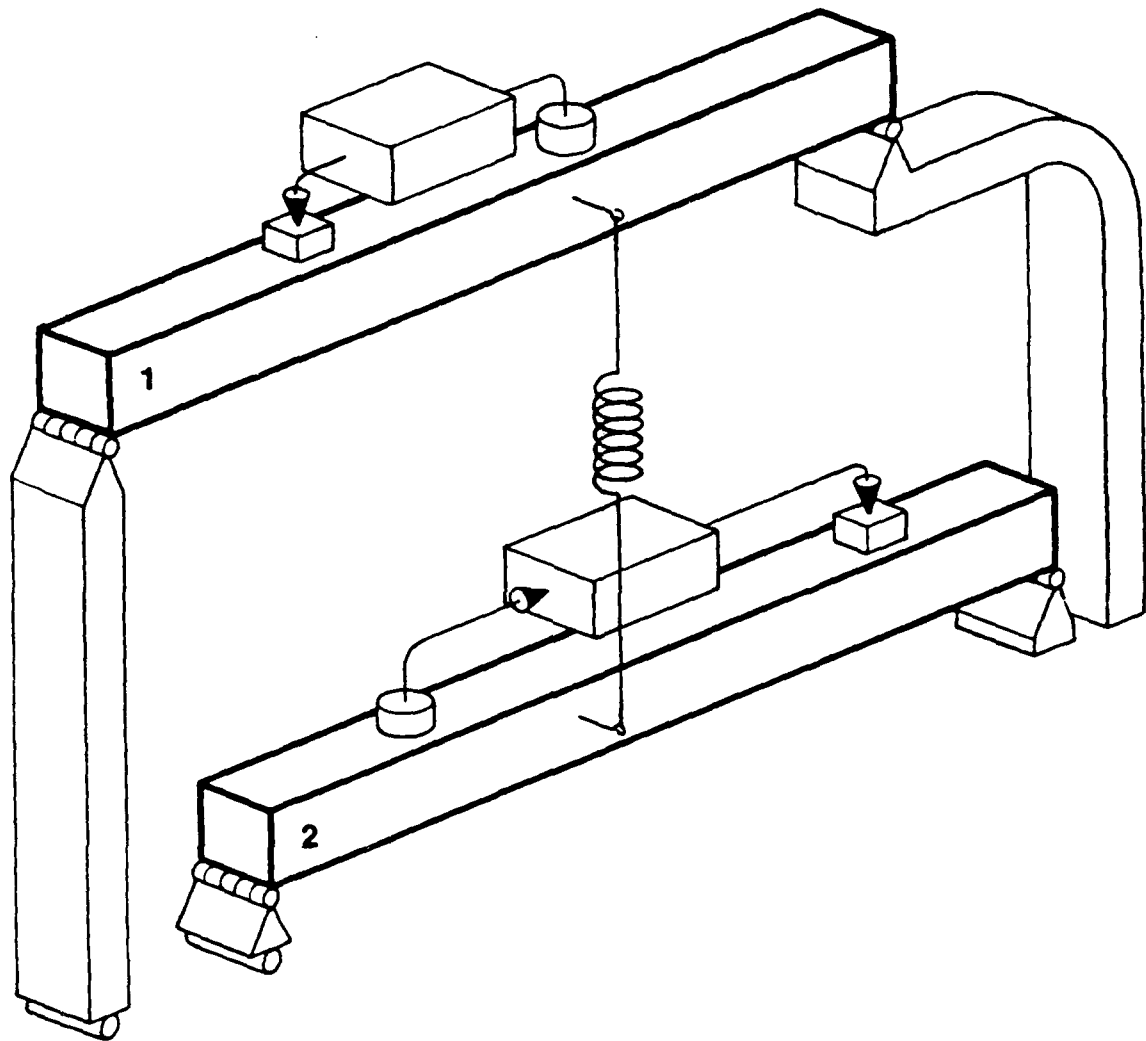


Figure 4.3-1. Interconnected Beam Example for Decentralized Control

Design	Cost
Open loop	163.5
Centralized LQG $n_c = 8$	19.99
Suboptimal decentralized $n_{c1} = n_{c2} = 4$	59.43
Redesign subcontroller 2	28.19
Redesign subcontroller 1	23.29
Redesign subcontroller 2	23.04
Redesign subcontroller 1	22.25
Redesign subcontroller 2	21.94
Redesign subcontroller 1	21.86
Redesign subcontroller 2	21.81
Redesign subcontroller 1	21.79

It is immediately evident that each redesign step resulted in improved performance of the decentralized closed-loop system. As noted previously, this monotonic improvement is a direct result of the fact that at each redesign stage a suboptimal subcontroller is being replaced by a subcontroller which is optimal with respect to the augmented plant consisting of the actual plant and remaining subcontroller. Finally, note that since each subcontroller involves one sensor and one actuator, there exists at most one solution to the design equations at each redesign step. Thus the sequence converges to the global minimum of the decentralized design problem.

As a second and more realistic example we consider the decentralized control of a deployable truss structure (Figure 4.3-2). Unlike the previous example this structure does not involve physically identifiable subsystems. Rather, the motivation for a decentralized architecture arises from the desire to minimize real-time communication among sensors and actuators located at different points (bays) along the structure. Hence we consider a decentralized feedback architecture in which each subcontroller involves only sensors and actuators located within a single bay. Although subcontrollers do not communicate with one another by exchanging data, they do interact via the dynamics of the structure. Modal data for the first 10 modes of the structure are given in Figure 4.3-3 while mode shapes are shown in Figures 4.3-4, 4.3-5 and 4.3-6.

In designing a decentralized feedback architecture we considered control instrumentation at bays 23, 46 and 54 (tip). Specifically, for control we considered rate sensors and force actuators at bays 28, 46 and 54 along the x and y axes and at bay 54 about the z axis. Furthermore,

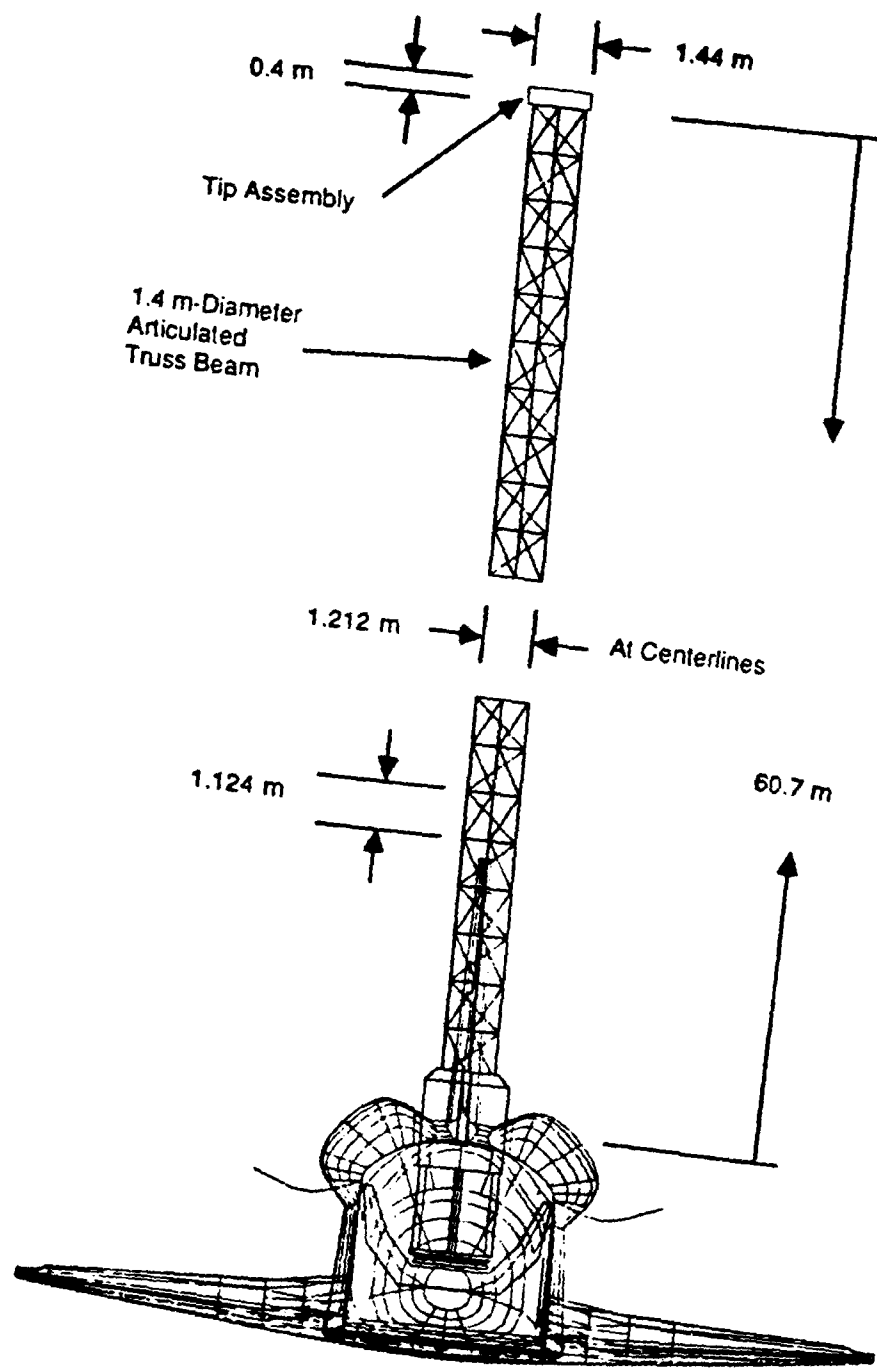


Figure 4.3-2. Deployable Truss Structure Configuration

Mode	Mode Frequency ω	Modal Damping ν	Mode Shape Description
1	0.179	0.002	1st $x-z$ Bending
2	0.236	0.002	1st $y-z$ Bending
3	1.270	0.003	2nd $y-z$ Bending
4	1.320	0.003	2nd $x-z$ Bending
5	1.460	0.005	1st Torsion
6	3.640	0.005	3rd $y-z$ Bending
7	3.800	0.005	3rd $x-z$ Bending
8	5.180	0.005	2nd Torsion
9	6.200	0.005	4th $y-z$ Bending
10	6.410	0.005	4th $x-z$ Bending

Figure 4.3-3. Modal Data for the Deployable Truss Structure

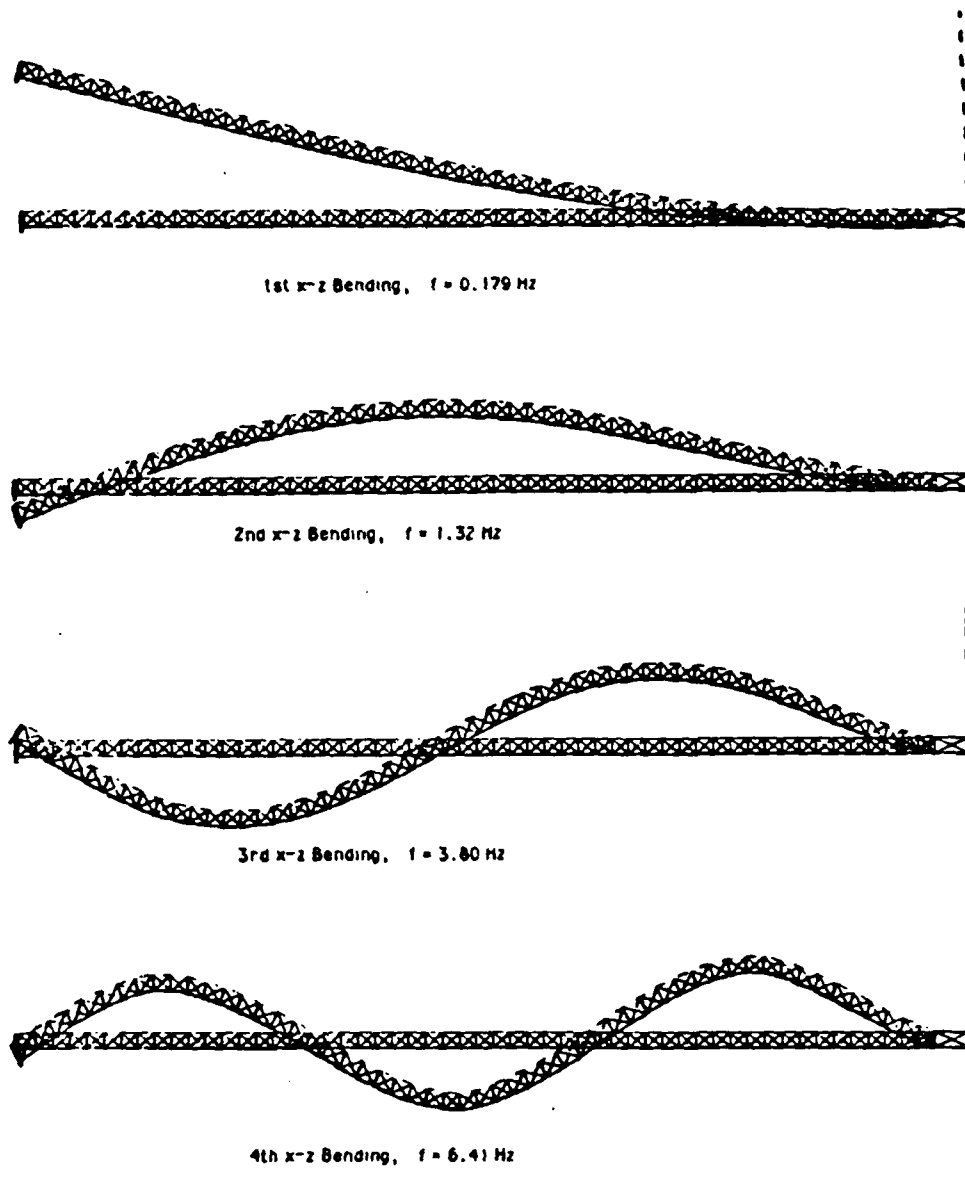


Figure 4.3-4. Deployable Truss Structure Mode Shapes

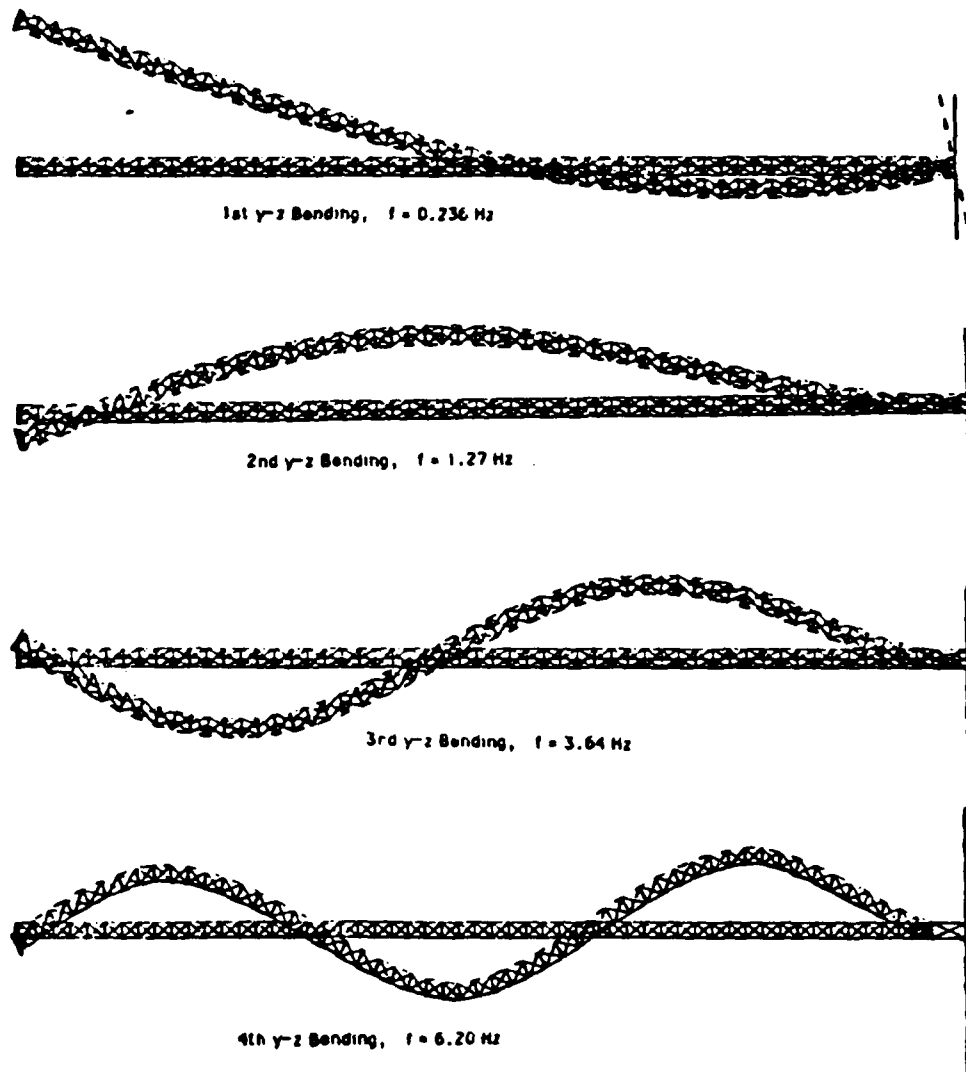


Figure 4.3-5. Deployable Truss Structure Mode Shapes (cont'd)

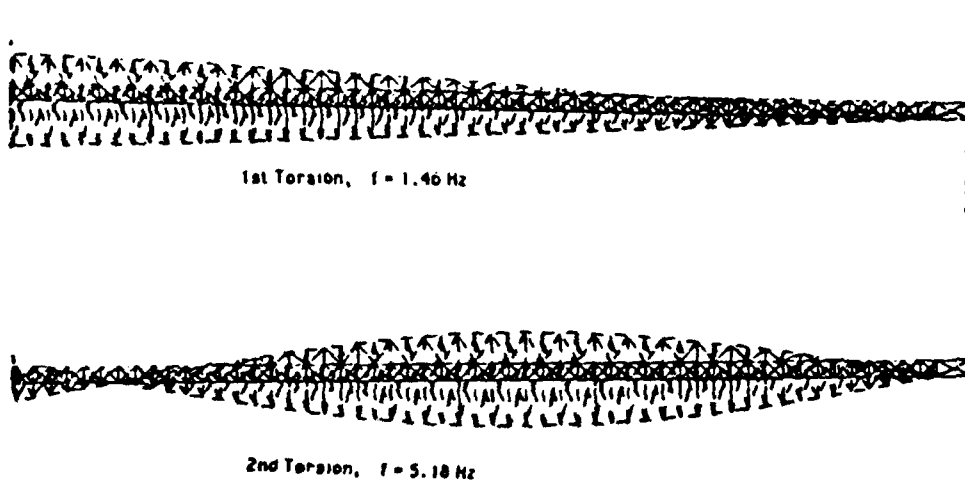


Figure 4.3-6. Deployable Truss Structure Mode Shapes (cont'd)

disturbances were assumed to be generated by actuators at bay 10 (along the x and y axes), bay 28 (about the z axis), and bay 54 (along the x and y axes and about the z axis). As a measure of performance we considered the motion of the tip along the x and y axes and about the x , y and z axes. Sensor noise levels and control signal weighting matrices were chosen so that a centralized LQG controller reduced mean-squared variation to 1% of their open-loop levels. Note that such an LQG controller is of 20th order and involves feedback loops between all sensors and actuators.

To produce a decentralized controller we constrained the architecture to involve three subcontrollers involving sensors and actuators at bays 28, 46 and 54 (see Figure 4-3.7). Each subcontroller was constrained to be a 4th-order compensator. The sequence of evaluations and refinements is shown in Figure 4.3-8. The final controller consisting of three 4th-order local subcontrollers represented only an 8% cost degradation compared to the significantly more complex 20th-order centralized LQG design.

4.4 References

- [4.1] S. Richter and R. DeCarlo, "Continuation Methods: Theory and Applications," *IEEE Trans. Autom. Contr.*, Vol. 28, pp. 660-665, 1983.
- [4.2] S. Richter and R. DeCarlo, "A Homotopy Method for Eigenvalue Assignment Using Decentralized State Feedback," *IEEE Trans. Autom. Contr.*, Vol. AC-29, pp. 148-155, 1984.
- [4.3] S. Lefebvre, S. Richter and R. DeCarlo, "A Continuation Algorithm for Eigenvalue Assignment by Decentralized Constant-Output Feedback," *Int. J. Contr.*, Vol. 41, pp. 1273-1292, 1985.
- [4.4] Y. Liu and B. D. O. Anderson, "Controller Reduction Via Stable Factorization and Balancing," *Int. J. Contr.*, Vol. 44, No. 2, pp. 507-531, 1986.
- [4.5] E. J. Davison and W. Gesing, "Sequential Stability and Optimization of Large Scale Decentralized Systems," *Automatica*, Vol. 15, pp. 307-324, 1979.
- [4.6] Z. Uskokovic and J. Medanic, "Sequential Design of Decentralized Low-Order Dynamic Regulators," *Proc. IEEE Conf. Dec. Contr.*, pp. 387-842, Fort Lauderdale, FL, December 1985.
- [4.7] N. Viswanadham and J. H. Taylor, "Sequential Design of Decentralized Control Systems," *Int. J. Contr.*, Vol. 47, pp. 257-279, 1988.

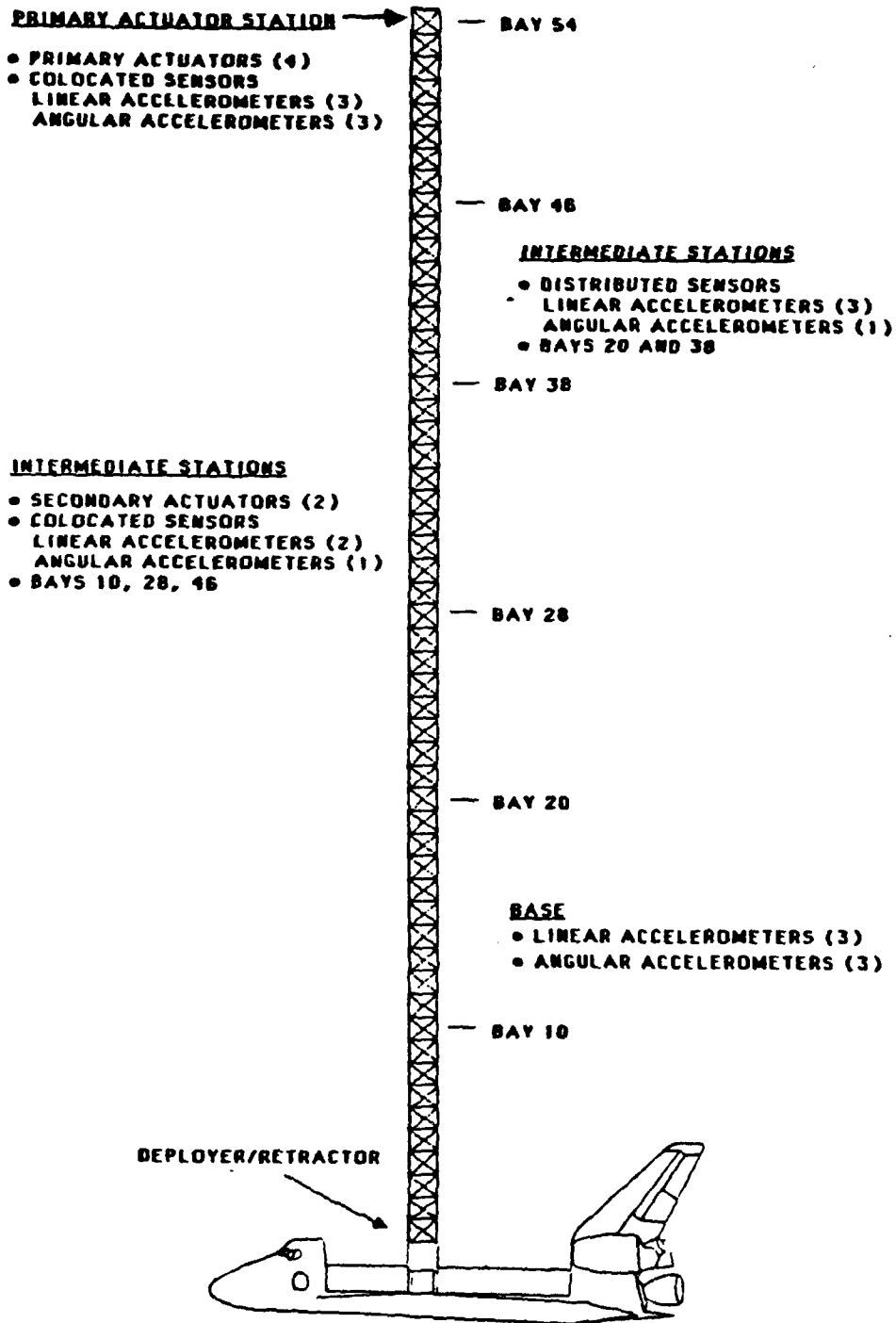


Figure 4.3-7. Control System Instrumentation for the Deployable Truss Structure

Procedure	State Cost	Control Cost	Total
Evaluate Open Loop Cost	429	0	429
Design LQG Centralized Controller ($n = 20$)	2.97	1.28	4.25
Design LQG Single Channel Controller ($n_c = 20$) with Bay 54 Instrumentation Only	3.08	1.42	4.50
(I) Design OP Single Channel Controller ($n_c = 4$) with Bay 54 Instrumentation Only	5.94	1.34	7.28
Design LQG Single Channel Controller ($n_c = 20$) with Bay 46 Instrumentation Only	10.2	1.83	12.0
(II) Design OP Single Channel Controller ($n_c = 4$) with Bay 46 Instrumentation Only	10.2	1.97	12.2
Design LQG Single Channel Controller ($n_c = 20$) with Bay 28 Instrumentation Only	23.2	6.26	29.4
(III) Design OP Single Channel Controller ($n_c = 20$) with Bay 28 Instrumentation Only	23.3	7.04	30.3
Evaluate Performance of I + II + III	N/A	N/A	10.9
Evaluate Performance of I + II	N/A	N/A	7.72
Redesign II (I + II')	6.86	1.80	7.04
Redesign I (I' + II')	3.42	1.36	4.78
Evaluate (I' + II' + III)	N/A	N/A	7.97
Redesign III (I' + II' + III')	4.63	.034	4.66
Redesign I (I'' + II' + III')	3.26	1.31	4.57

Figure 4.3-8. Sequential Decentralized Design Procedure for Deployable Truss Structure

SECTION 5.0

MEOP References

1. D. C. Hyland, "The Modal Coordinate/Radiative Transfer Formulation of Structural Dynamics--Implications for Vibration Suppression in Large Space Platforms," MIT Lincoln Laboratory, TR-27, 14 March 1979.
2. D. C. Hyland, "Optimal Regulation of Structural Systems With Uncertain Parameters," MIT Lincoln Laboratory, TR-551, 2 February 1981, DDC# ADA-099111/7.
3. D. C. Hyland, "Active Control of Large Flexible Spacecraft: A New Design Approach Based on Minimum Information Modelling of Parameter Uncertainties," Proc. Third VPI&SU/AIAA Symposium, pp. 631-646, Blacksburg, VA, June 1981.
4. D. C. Hyland, "Optimal Regulator Design Using Minimum Information Modelling of Parameter Uncertainties: Ramifications of the New Design Approach," Proc. Third VPI&SU/AIAA Symposium, pp. 701-716, Blacksburg, VA, June 1981.
5. D. C. Hyland and A. N. Madiwale, "Minimum Information Approach to Regulator Design: Numerical Methods and Illustrative Results," Proc. Third VPI&SU/AIAA Symposium, pp. 101-118, Blacksburg, VA, June 1981.
6. D. C. Hyland and A. N. Madiwale, "A Stochastic Design Approach for Full-Order Compensation of Structural Systems with Uncertain Parameters," Proc. AIAA Guid. Contr. Conf., pp. 324-332, Albuquerque, NM, August 1981.
7. D. C. Hyland, "Optimality Conditions for Fixed-Order Dynamic Compensation of Flexible Spacecraft with Uncertain Parameters," AIAA 20th Aerospace Sciences Meeting, paper 82-0312, Orlando, FL, January 1982.
8. D. C. Hyland, "Structural Modeling and Control Design Under Incomplete Parameter Information: The Maximum Entropy Approach," AFOSR/NASA Workshop on Modeling, Analysis and Optimization Issues for Large Space Structures, Williamsburg, VA, May 1982.
9. D. C. Hyland, "Minimum Information Stochastic Modelling of Linear Systems with a Class of Parameter Uncertainties," Proc. Amer. Contr. Conf., pp. 620-627, Arlington, VA, June 1982.
10. D. C. Hyland, "Maximum Entropy Stochastic Approach to Control Design for Uncertain Structural Systems," Proc. Amer. Contr. Conf., pp. 680-688, Arlington, VA, June 1982.
11. D. C. Hyland, "Minimum Information Modeling of Structural Systems with Uncertain Parameters," Proceedings of the Workshop on Applications of Distributed System Theory to the Control of Large Space Structures, G. Rodriguez, ed., pp. 71-88, JPL, Pasadena, CA, July 1982.

12. D. C. Hyland and A. N. Madiwale, "Fixed-Order Dynamic Compensation Through Optimal Projection," Proceedings of the Workshop on Applications of Distributed System Theory to the Control of Large Space Structures, G. Rodriguez, ed., pp. 409-427, JPL, Pasadena, CA, July 1982.
13. D. C. Hyland, "Mean-Square Optimal Fixed-Order Compensation--Beyond Spillover Suppression," paper 1403, AIAA Astrodynamics Conference, San Diego, CA, August 1982.
14. D. C. Hyland, "Robust Spacecraft Control Design in the Presence of Sensor/Actuator Placement Errors," AIAA Astrodynamics Conference, San Diego, CA, August 1982.
15. D. C. Hyland, "The Optimal Projection Approach to Fixed-Order Compensation: Numerical Methods and Illustrative Results," AIAA 21st Aerospace Sciences Meeting, paper 83-0303, Reno, NV, January 1983.
16. D. C. Hyland, "Mean-Square Optimal, Full-Order Compensation of Structural Systems with Uncertain Parameters," MIT Lincoln Laboratory, TR-626, 1 June 1983.
17. D. S. Bernstein and D. C. Hyland, "Explicit Optimality Conditions for Finite-Dimensional Fixed-Order Dynamic Compensation of Infinite-Dimensional Systems," presented at SIAM Fall Meeting, Norfolk, VA, November 1983.
18. D. C. Hyland and D. S. Bernstein, "Explicit Optimality Conditions for Fixed-Order Dynamic Compensation," Proc. 22nd IEEE Conf. Dec. Contr., pp. 161-165, San Antonio, TX, December 1983.
19. F. M. Ham, J. W. Shipley and D. C. Hyland, "Design of a Large Space Structure Vibration Control Experiment," Proc. 2nd Int. Modal Anal. Conf., pp. 550-558, Orlando, FL, February 1984.
20. D. C. Hyland, "Comparison of Various Controller-Reduction Methods: Suboptimal Versus Optimal Projection," Proc. AIAA Dynamics Specialists Conf., pp. 381-389, Palm Springs, CA, May 1984.
21. D. S. Bernstein and D. C. Hyland, "The Optimal Projection Equations for Fixed-Order Dynamic Compensation of Distributed Parameter Systems," Proc. AIAA Dynamics Specialists Conf., pp. 396-400, Palm Springs, CA, May 1984.
22. F. M. Ham and D. C. Hyland, "Vibration Control Experiment Design for the 15-M Hoop/Column Antenna," Proceedings of the Workshop on the Identification and Control of Flexible Space Structures, pp. 229-252, San Diego, CA, June 1984.
23. D. S. Bernstein and D. C. Hyland, "Numerical Solution of the Optimal Model Reduction Equations," Proc. AIAA Guid. Contr. Conf., pp. 560-562, Seattle, WA, August 1984.

24. D. C. Hyland and D. S. Bernstein, "The Optimal Projection Equations for Fixed-Order Dynamic Compensation," IEEE Trans. Autom. Contr., Vol. AC-29, pp. 1034-1037, 1984.
25. D. C. Hyland, "Application of the Maximum Entropy/Optimal Projection Control Design Approach for Large Space Structures," Proc. Large Space Antenna Systems Technology Conference, pp. 617-654, NASA Langley, December 1984.
26. D. C. Hyland and D. S. Bernstein, "The Optimal Projection Approach to Model Reduction and the Relationship Between the Methods of Wilson and Moore," Proc. 23rd IEEE Conf. Dec. Contr., pp. 120-126, Las Vegas, NV, December 1984.
27. D. S. Bernstein and D. C. Hyland, "The Optimal Projection Approach to Designing Optimal Finite-Dimensional Controllers for Distributed Parameter Systems," Proc. 23rd IEEE Conf. Dec. Contr., pp. 556-560, Las Vegas, NV, December 1984.
28. L. D. Davis, D. C. Hyland and D. S. Bernstein, "Application of the Maximum Entropy Design Approach to the Spacecraft Control Laboratory Experiment (SCOLE)," Final Report, NASA Langley, January 1985.
29. D. S. Bernstein and D. C. Hyland, "The Optimal Projection Equations for Reduced-Order State Estimation," IEEE Trans. Autom. Contr., Vol. AC-30, pp. 583-585, 1985.
30. D. S. Bernstein and D. C. Hyland, "The Optimal Projection Equations for Reduced-Order State Estimation," Proc. Amer. Contr. Conf., pp. 164-167, Boston, MA, June 1985.
31. D. S. Bernstein and D. C. Hyland, "Optimal Projection/Maximum Entropy Stochastic Modelling and Reduced-Order Design Synthesis," Proc. IFAC Workshop on Model Error Concepts and Compensation, Boston, MA, June 1985, R. E. Skelton and D. H. Owens, Eds., pp. 47-54, Pergamon Press, Oxford, 1986.
32. D. C. Hyland and D. S. Bernstein, "The Optimal Projection Equations for Model Reduction and the Relationships Among the Methods of Wilson, Skelton and Moore," IEEE Trans. Autom. Contr., Vol. AC-30, pp. 1201-1211, 1985.
33. D. S. Bernstein, "The Optimal Projection Equations for Fixed-Structure Decentralized Dynamic Compensation," Proc. 24th IEEE Conf. Dec. Contr., pp. 104-107, Fort Lauderdale, FL, December 1985.
34. D. S. Bernstein, L. D. Davis, S. W. Greeley and D. C. Hyland, "The Optimal Projection Equations for Reduced-Order, Discrete-Time Modelling, Estimation and Control," Proc. 24th IEEE Conf. Dec. Contr., pp. 573-578, Fort Lauderdale, FL, December 1985.

35. D. S. Bernstein and D. C. Hyland, "The Optimal Projection/Maximum Entropy Approach to Designing Low-Order, Robust Controllers for Flexible Structures," Proc. 24th IEEE Conf. Dec. Contr., pp. 745-752, Fort Lauderdale, FL, December 1985.
36. D. S. Bernstein, L. D. Davis, S. W. Greeley and D. C. Hyland, "Numerical Solution of the Optimal Projection/Maximum Entropy Design Equations for Low-Order, Robust Controller Design," Proc. 24th IEEE Conf. Dec. Contr., pp. 1795-1798, Fort Lauderdale, FL, December 1985.
37. D. S. Bernstein and D. C. Hyland, "The Optimal Projection Equations for Finite-Dimensional Fixed-Order Dynamic Compensation of Infinite-Dimensional Systems," SIAM J. Contr. Optim., Vol. 24, pp. 122-151, 1986.
38. J. W. Shipley and D. C. Hyland, "The Mast Flight System Dynamic Characteristics and Actuator/Sensor Selection and Location," Proc. 9th Annual AAS Guid. Contr. Conf., Keystone, CO, February 1986, R. D. Culp and J. C. Durrett, Eds., pp. 31-49, American Astronautical Society, San Diego, CA, 1986.
39. D. S. Bernstein and S. W. Greeley, "Robust Controller Synthesis Using the Maximum Entropy Design Equations," IEEE Trans. Autom. Contr., Vol. AC-31, pp. 362-364, 1986.
40. D. C. Hyland, D. S. Bernstein, L. D. Davis, S. W. Greeley and S. Richter, "MEOP: Maximum Entropy/Optimal Projection Stochastic Modelling and Reduced-Order Design Synthesis," Final Report, Air Force Office of Scientific Research, Bolling AFB, Washington, DC, April 1986.
41. D. S. Bernstein, L. D. Davis and D. C. Hyland, "The Optimal Projection Equations for Reduced-Order, Discrete-Time Modelling, Estimation and Control," AIAA J. Guid. Contr. Dyn., Vol. 9, pp. 288-293, 1986.
42. D. S. Bernstein, L. D. Davis and S. W. Greeley, "The Optimal Projection Equations for Fixed-Order, Sampled-Data Dynamic Compensation with Computation Delay," Proc. Amer. Contr. Conf., pp. 1590-1597, Seattle, WA, June 1986.
43. D. S. Bernstein and S. W. Greeley, "Robust Output-Feedback Stabilization: Deterministic and Stochastic Perspectives," Proc. Amer. Contr. Conf., pp. 1818-1826, Seattle, WA, June 1986.
44. D. S. Bernstein, L. D. Davis and S. W. Greeley, "The Optimal Projection Equations for Fixed-Order, Sampled-Data Dynamic Compensation with Computation Delay," IEEE Trans. Autom. Contr., Vol. AC-31, pp. 859-862, 1986.
45. D. S. Bernstein, "Optimal Projection/Guaranteed Cost Control Design Synthesis: Robust Performance via Fixed-Order Dynamic Compensation," presented at SIAM Conference on Linear Algebra in Signals, Systems and Control, Boston, MA, August 1986.

46. D. C. Hyland, "Control Design Under Stratonovich Models: Robust Stability Guarantees via Lyapunov Matrix Functions," presented at SIAM Conference on Linear Algebra in Signals, Systems and Control, Boston, MA, August 1986.
47. D. S. Bernstein, "OFUS: Optimal Projection for Uncertain Systems," Annual Report, Air Force Office of Scientific Research, Bolling AFB, Washington, DC, October 1986.
48. B. J. Boan and D. C. Hyland, "The Role of Metal Matrix Composites for Vibration Suppression in Large Space Structures," Proc. MMC Spacecraft Survivability Tech. Conf., MMCIAC Kaman Tempo Publ., Stanford Research Institute, Palo Alto, CA, October 1986.
49. L. D. Davis, T. Otten, F. M. Ham and D. C. Hyland, "Mast Flight System Dynamic Performance," presented at 1st NASA/DOD CSI Technology Conference, Norfolk, VA, November 1986.
50. D. C. Hyland, "An Experimental Testbed for Validation of Control Methodologies in Large Space Optical Structures," in Structural Mechanics of Optical Systems II, pp. 146-155, A. E. Hatheway, ed., Proceedings of SPIE, Vol. 748, Optoelectronics and Laser Applications Conference, Los Angeles, CA, January 1987.
51. J. W. Shipley, L. D. Davis, W. T. Burton and F. M. Ham, "Development of the Mast Flight System Linear DC Motor Inertial Actuator," Proc. 10th Annual AAS Guid. Contr. Conf., Keystone, CO, February 1987, R. D. Culp and T. J. Kelley, Eds., pp. 237-255, American Astronautical Society, San Diego, CA, 1987.
52. W. M. Haddad, Robust Optimal Projection Control-System Synthesis, Ph.D. Dissertation, Department of Mechanical Engineering, Florida Institute of Technology, Melbourne, FL, March 1987.
53. A. W. Daubendiek and R. G. Brown, "A Robust Kalman Filter Design," Report ISU-ERI-Ames-87226, College of Engineering, Iowa State University, Ames, IA, March 1987.
54. W. M. Haddad and D. S. Bernstein, "The Optimal Projection Equations for Discrete-Time Reduced-Order State Estimation for Linear Systems with Multiplicative White Noise," Sys. Contr. Lett., Vol. 8, pp. 381-388, 1987.
55. D. C. Hyland and D. S. Bernstein, "MBOP Control Design Synthesis: Optimal Quantification of the Major Design Tradeoffs," in Structural Dynamics and Control Interaction of Flexible Structures, Part 2, pp. 1033-1070, NASA Conf. Publ. 2467, 1987.
56. F. M. Ham and S. W. Greeley, "Active Damping Control Design for the Mast Flight System," Proc. Amer. Contr. Conf., pp. 355-367, Minneapolis, MN, June 1987.

57. D. C. Hyland and D. S. Bernstein, "Uncertainty Characterization Schemes: Relationships to Robustness Analysis and Design," presented at Amer. Contr. Conf., Minneapolis, MN, June 1987.
58. W. M. Haddad and D. S. Bernstein, "The Optimal Projection Equations for Reduced-Order State Estimation: The Singular Measurement Noise Case," Proc. Amer. Contr. Conf., pp. 779-785, Minneapolis, MN, June 1987.
59. D. C. Hyland and D. S. Bernstein, "The Majorant Lyapunov Equation: A Nonnegative Matrix Equation for Robust Stability and Performance of Large Scale Systems," Proc. Amer. Contr. Conf., pp. 910-917, Minneapolis, MN, June 1987.
60. D. S. Bernstein, "Sequential Design of Decentralized Dynamic Compensators Using the Optimal Projection Equations: An Illustrative Example Involving Interconnected Flexible Beams," Proc. Amer. Contr. Conf., pp. 986-989, Minneapolis, MN, June 1987.
61. L. D. Davis, "Issues in Sampled-Data Control: Discretization Cost and Aliasing," presented at Amer. Contr. Conf., Minneapolis, MN, June 1987.
62. D. C. Hyland, "Majorant Bounds, Stratonovich Models, and Statistical Energy Analysis," presented at Amer. Contr. Conf., Minneapolis, MN, June 1987.
63. S. Richter, "A Homotopy Algorithm for Solving the Optimal Projection Equations for Fixed-Order Dynamic Compensation: Existence, Convergence and Global Optimality," Proc. Amer. Contr. Conf., pp. 1527-1531, Minneapolis, MN, June 1987.
64. D. S. Bernstein, "The Optimal Projection Equations For Nonstrictly Proper Fixed-Order Dynamic Compensation," Proc. Amer. Contr. Conf., pp. 1991-1996, Minneapolis, MN, June 1987.
65. D. S. Bernstein and W. M. Haddad, "Optimal Output Feedback for Nonzero Set Point Regulation," Proc. Amer. Contr. Conf., pp. 1997-2003, Minneapolis, MN, June 1987.
66. D. S. Bernstein and S. Richter, "A Homotopy Algorithm for Solving the Optimal Projection Equations for Fixed-Order Dynamic Compensation," presented at Int. Symp. Math. Thy. Net. Sys., Phoenix, AZ, June 1987.
67. D. S. Bernstein and W. M. Haddad, "Optimal Output Feedback for Nonzero Set Point Regulation," IEEE Trans. Autom. Contr., Vol. AC-32, pp. 641-645, 1987.
68. S. Richter, "Reduced-Order Control Design via the Optimal Projection Approach: A Homotopy Algorithm for Global Optimality," Proc. Sixth VPI&SU Symp. Dyn. Contr. Large Str., L. Meirovitch, Ed., pp. 17-30, Blacksburg, VA, June 1987.
69. D. S. Bernstein and W. M. Haddad, "Optimal Projection Equations for Discrete-Time Fixed-Order Dynamic Compensation of Linear Systems with Multiplicative White Noise," Int. J. Contr., Vol. 46, pp. 65-73, 1987.

70. F. M. Ham, B. L. Henniges and S. W. Greeley, "Active Damping Control Design for the COFS Mast Flight System," Proc. AIAA Conf. Guid. Nav. Contr., pp. 354-360, Monterey, CA, August 1987.
71. S. W. Greeley and D. C. Hyland, "Reduced-Order Compensation: LQG Reduction Versus Optimal Projection," Proc. AIAA Conf. Guid. Nav. Contr., pp. 605-616, Monterey, CA, August 1987.
72. D. S. Bernstein, "Decentralized Control of Large Space Structures via Fixed-Order Dynamic Compensation," presented at IEEE CSS Workshop on Current Issues in Decentralized and Distributed Control, Columbus, OH, September 1987.
73. D. S. Bernstein, "OPUS: Optimal Projection for Uncertain Systems," Annual Report, Air Force Office of Scientific Research, Bolling AFB, Washington, DC, October 1987.
74. R. C. Talcott, J. W. Shipley, T. Kimball and S. W. Greeley, "Mast Flight System Engineering Development and System Integration," presented at 2nd NASA/DOD CSI Technology Conference, Colorado Springs, CO, November 1987.
75. D. C. Hyland and D. S. Bernstein, "The Majorant Lyapunov Equation: A Nonnegative Matrix Equation for Guaranteed Robust Stability and Performance of Large Scale Systems," IEEE Trans. Autom. Contr., Vol. AC-32, pp. 1005-1013, 1987.
76. D. S. Bernstein, "Sequential Design of Decentralized Dynamic Compensators Using the Optimal Projection Equations," Int. J. Contr., Vol. 46, pp. 1569-1577, 1987.
77. D. S. Bernstein, "Robust Static and Dynamic Output-Feedback Stabilization: Deterministic and Stochastic Perspectives," IEEE Trans. Autom. Contr., Vol. AC-32, pp. 1076-1084, 1987.
78. W. M. Haddad and D. S. Bernstein, "The Optimal Projection Equations for Reduced-Order State Estimation: The Singular Measurement Noise Case," IEEE Trans. Autom. Contr., Vol. AC-32, pp. 1135-1139, 1987.
79. D. S. Bernstein, "The Optimal Projection Equations for Static and Dynamic Output Feedback: The Singular Case," IEEE Trans. Autom. Contr., Vol. AC-32, pp. 1139-1143, 1987.
80. W. M. Haddad and D. S. Bernstein, "The Unified Optimal Projection Equations for Simultaneous Reduced-Order, Robust Modeling, Estimation and Control," Proc. IEEE Conf. Dec. Contr., pp. 449-454, Los Angeles, CA, December 1987.
81. S. W. Greeley and D. C. Hyland, "Reduced-Order Compensation: LQG Reduction Versus Optimal Projection Using a Homotopic Continuation Method," Proc. IEEE Conf. Dec. Contr., pp. 742-747, Los Angeles, CA, December 1987.

82. D. S. Bernstein and W. M. Haddad, "The Optimal Projection Equations with Petersen-Hollot Bounds: Robust Controller Synthesis with Guaranteed Structured Stability Radius," Proc. IEEE Conf. Dec. Contr., pp. 1308-1318, Los Angeles, CA, December 1987.
83. W. M. Haddad and D. S. Bernstein, "Robust, Reduced-Order, Nonstrictly Proper State Estimation via the Optimal Projection Equations with Petersen-Hollot Bounds," Sys. Contr. Lett., Vol. 9, pp. 423-431, 1987.
84. D. C. Hyland, "Experimental Investigations in Active Vibration Control for Application to Large Space Systems," in Space Structures, Power, and Power Conditioning, R. F. Askew, Ed., Proc. SPIE, Vol. 871, pp. 242-253, 1988.
85. D. C. Hyland and D. J. Phillips, "Development of the Linear Precision Actuator," 11th Annual AAS Guid. Contr. Conf., Keystone, CO, January 1988.
86. W. M. Haddad and D. S. Bernstein, "Optimal Output Feedback for Nonzero Set Point Regulation: The Discrete-Time Case," Int. J. Contr., Vol. 47, pp. 529-536, 1988.
87. D. S. Bernstein, "Commuting Matrix Exponentials," Problem 88-1, SIAM Review, Vol. 30, p. 123, 1988.
88. D. S. Bernstein and D. C. Hyland, "Optimal Projection for Uncertain Systems (OPUS): A Unified Theory of Reduced-Order, Robust Control Design," in Large Space Structures: Dynamics and Control, S. N. Atluri and A. K. Amos, Eds., pp. 263-302, Springer-Verlag, New York, 1988.
89. W. M. Haddad and D. S. Bernstein, "The Unified Optimal Projection Equations for Simultaneous Reduced-Order, Robust Modeling, Estimation and Control," Int. J. Contr., Vol. 47, pp. 1117-1132, 1988.
90. D. C. Hyland, "Homotopic Continuation Methods for the Design of Optimal Fixed-Form Dynamic Controllers," in Computational Mechanics '85, Proc. Int. Conf. Comp. Eng. Sci., S. N. Atluri and G. Yagawa, Eds., Vol. 2, pp. 44.i.1-4, 1988.
91. D. C. Hyland and J. W. Shipley, "A Unified Process for Systems Identification Based on Performance Assessment," presented at USAF/NASA Workshop on Model Determination for Large Space Systems, Pasadena, CA, March 1988.
92. D. S. Bernstein, "Inequalities for the Trace of Matrix Exponentials," SIAM J. Matrix Anal. Appl., Vol. 9, pp. 156-158, 1988.
93. D. C. Hyland, D. S. Bernstein, and E. G. Collins, Jr., "Maximum Entropy/Optimal Projection Design Synthesis for Decentralized Control of Large Space Structures," Final Report, Air Force Office of Scientific Research, Bolling AFB, Washington, DC, May 1988.

To Appear

94. S. W. Greeley and D. C. Hyland, "Reduced-Order Compensation: IQG Reduction Versus Optimal Projection," AIAA J. Guid. Contr. Dyn., 1988, to appear.
95. D. S. Bernstein and W. M. Haddad, "The Optimal Projection Equations with Petersen-Hollot Bounds: Robust Stability and Performance via Fixed-Order Dynamic Compensation for Systems with Structured Real-Valued Parameter Uncertainty," IEEE Trans. Autom. Contr., Vol. AC-33, pp. 578-582, 1988 to appear.
96. W. M. Haddad and D. S. Bernstein, "Robust, Reduced-Order, Nonstrictly Proper State Estimation via the Optimal Projection Equations with Guaranteed Cost Bounds," IEEE Trans. Autom. Contr., Vol. AC-33, pp. 591-595, 1988, to appear.
97. D. S. Bernstein and W. M. Haddad, "IQG Control with an H_{∞} Performance Bound: A Riccati Equation Approach," Amer. Contr. Conf., Atlanta, GA, June 1988.
98. S. W. Greeley, D. J. Phillips and D. C. Hyland, "Experimental Demonstration of Maximum Entropy, Optimal Projection Design Theory for Active Vibration Control," Amer. Contr. Conf., Atlanta, GA, June 1988.
99. D. C. Hyland and E. G. Collins, Jr., "A Robust Control Experiment Using an Optical Structure Prototype," Amer. Contr. Conf., Atlanta, GA, June 1988.
100. D. S. Bernstein and W. M. Haddad, "Robust Stability and Performance for Fixed-Order Dynamic Compensation via the Optimal Projection Equations with Guaranteed Cost Bounds," Amer. Contr. Conf., Atlanta, GA, June 1988.
101. S. Richter, "Recent Advances in the Application of Homotopic Continuation Methods to Control Problems," Amer. Contr. Conf., Atlanta, GA, June 1988.
102. W. M. Haddad and D. S. Bernstein, "Robust, Reduced-Order Modeling via the Optimal Projection Equations with Petersen-Hollot Bounds," IEEE Trans. Autom. Contr., Vol. AC-33, 1988, to appear.
103. W. M. Haddad and D. S. Bernstein, "Optimal Nonzero Set Point Regulation via Fixed-Order Dynamic Compensation," IEEE Trans. Autom. Contr., Vol. AC-33, 1988, to appear.
104. D. S. Bernstein and D. C. Hyland, "The Optimal Projection Equations for Reduced-Order Modelling, Estimation and Control of Linear Systems with Multiplicative White Noise," J. Optim. Thy. Appl., Vol. 58, 1988, to appear.
105. D. C. Hyland and E. G. Collins, Jr., "Block Kronecker Products and Block-Norm Matrices in Large Scale Systems Analysis," SIAM J. Matrix Anal. Appl., to appear.
106. W. M. Haddad and D. S. Bernstein, "Combined L_2/H_{∞} Model Reduction," Int. J. Contr., to appear.

Submitted

107. D. S. Bernstein and W. M. Haddad, "LQG Control With An H_{∞} Performance Bound: A Riccati Equation Approach," submitted to IEEE Trans. Autom. Contr.
108. D. S. Bernstein and W. M. Haddad, "Robust Stability and Performance for Fixed-Order Dynamic Compensation via the Optimal Projection Equations with Guaranteed Cost Bounds," submitted to Math. Contr. Sig. Sys.
109. D. S. Bernstein and W. M. Haddad, "Robust Stability and Performance Analysis for Linear Dynamic Systems," submitted to IEEE Trans. Autom. Contr.
110. E. G. Collins, Jr., and D. C. Hyland, "Improved Robust Performance Bounds in Covariance Majorant Analysis," submitted to Int. J. Contr.
111. D. S. Bernstein, "Robust Stability and Performance via Fixed-Order Dynamic Compensation," submitted to SIAM J. Contr. Optim.
112. D. C. Hyland and E. G. Collins, Jr., "An M-Matrix and Majorant Approach to Robust Stability and Performance Analysis for Systems with Structured Uncertainty," submitted to IEEE Trans. Autom. Contr.
113. D. S. Bernstein and W. M. Haddad, "Robust Decentralized Optimal Output Feedback: The Static Controller Case," submitted to Proc. IEEE Conf. Dec. Contr., Austin, TX, December 1988.
114. D. S. Bernstein and W. M. Haddad, "Optimal Reduced-Order State Estimation for Unstable Plants," submitted to Proc. IEEE Conf. Dec. Contr., Austin, TX, December 1988.
115. D. S. Bernstein and W. M. Haddad, "LQG Control with An H_{∞} Performance Bound," submitted to Proc. IEEE Conf. Dec. Contr., Austin, TX, December 1988.
116. D. S. Bernstein and W. M. Haddad, "Robust Stability and Performance Analysis for Linear Dynamic Systems with Structured Uncertainty via Quadratic Lyapunov Bounds," submitted to Proc. IEEE Conf. Dec. Contr., Austin, TX, December 1988.
117. W. M. Haddad and D. S. Bernstein, "Combined L_2/H_{∞} Model Reduction," submitted to Proc. IEEE Conf. Dec. Contr., Austin, TX, December 1988.
118. D. S. Bernstein and I. G. Rosen, "An Approximation Technique for Computing Optimal Fixed-Order Controllers for Infinite-Dimensional Systems," submitted to Proc. IEEE Conf. Dec. Contr., Austin, TX, December 1988.
119. E. G. Collins, Jr., and D. C. Hyland, "Improved Robust Performance Bounds in Covariance Majorant Analysis," submitted to Proc. IEEE Conf. Dec. Contr., Austin, TX, December 1988.

120. D. C. Hyland and E. G. Collins, Jr., "An M-Matrix and Majorant Approach to Robust Stability and Performance Analysis for Systems with Structured Uncertainty," submitted to Proc. IEEE Conf. Dec. Contr., Austin, TX, December 1988.
121. D. C. Hyland, D. J. Phillips, B. L. Henniges and E. G. Collins, Jr., "Application of Robust Design and Analysis to an Optical Structure Vibration Experiment," abstract submitted to Proc. IEEE Conf. Dec. Contr., Austin, TX, December 1988.
122. D. S. Bernstein and W. M. Haddad, "Robust Decentralized Optimal Output Feedback: The Static Controller Case," submitted to Sys. Contr. Lett.
123. D. S. Bernstein and W. M. Haddad, "Steady-State Kalman Filtering with an H_{∞} Error Bound," submitted to Sys. Contr. Lett.
124. D. S. Bernstein and I. G. Rosen, "Finite-Dimensional Approximation for Optimal Fixed-Order Compensation of Distributed Parameter Systems," submitted to Opt. Contr. Appl. Meth.

In Preparation

125. D. S. Bernstein and W. M. Haddad, "Robust Stability and Performance Analysis for State Space Systems via Quadratic Lyapunov Bounds," in preparation for SIAM J. Matrix Anal. Appl.
126. W. M. Haddad and D. S. Bernstein, "Optimal Reduced-Order Observer-Estimator Design With a Frequency-Domain Error Bound," in preparation for Advances in Control and Dynamic Systems, Vol. 31.
127. D. S. Bernstein and C. V. Hollot, "Robust Stability of Sampled-Data Systems," in preparation for IEEE Trans. Autom. Contr.
128. W. M. Haddad and D. S. Bernstein, "Robust Stability and Performance of Linear Dynamic Systems via Quadratic Lyapunov Bounds: Nonstrictly Proper Controller Synthesis," in preparation for Int. J. Contr.
129. D. C. Hyland and E. G. Collins, Jr., "A Majorant Approach to Robust Stability and Time-Domain Performance for Discrete-Time Systems," in preparation for Math. Contr. Sig. Sys.
130. W. M. Haddad and D. S. Bernstein, "Robust IQG/ H_{∞} Control Design with Structured Real-Valued Parameter Variations," in preparation for Int. J. Contr.
131. D. S. Bernstein and W. M. Haddad, Linear-Quadratic Feedback Control: Analysis and Design, in preparation for Lecture Notes in Control and Information Sciences, Springer-Verlag.

APPENDIX A

**Optimal Projection for Uncertain Systems (OPUS):
A Unified Theory of Reduced-Order, Robust Control
Design**

Optimal Projection for Uncertain Systems (OPUS): A Unified Theory of Reduced-Order, Robust Control Design

Dennis S. Bernstein and David C. Hyland
Harris Corporation
Government Aerospace Systems Division
Melbourne, Florida 32902

This research was supported in part by the Air Force Office of Scientific Research under contracts F49620-86-C-0002 and F49620-86-C-0038.

Abstract

OPUS (Optimal Projection for Uncertain Systems) provides new machinery for designing active controllers for suppressing vibration in flexible structures. The purpose of this paper is to review this machinery and demonstrate its practical value in addressing the structural control problem.

1. Introduction

For many years it has been widely recognized that the desire to orbit large, lightweight space structures possessing high-performance capabilities would require active feedback control techniques. More generally, the need for such techniques may arise due to the combinations of either 1) moderate performance requirements for highly flexible structures with low-frequency modes or 2) stringent performance requirements for semi-rigid structures with relatively high-frequency modes (Figure 1). Applications include pointing, slewing, and aperture shape control for optical and RF systems.

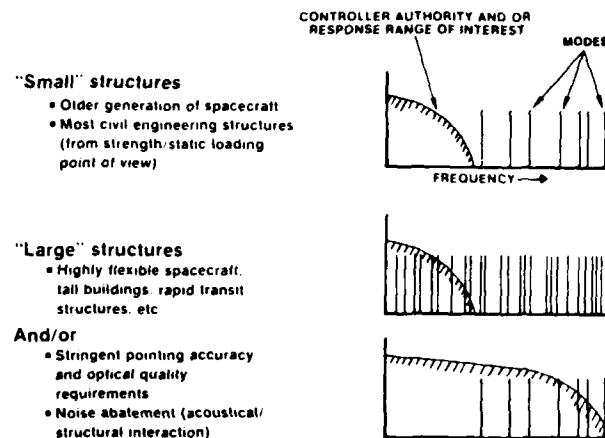


Figure 1. The Need for Active Structural Control Arises From Stringent Performance Requirements or Low-Frequency Modes

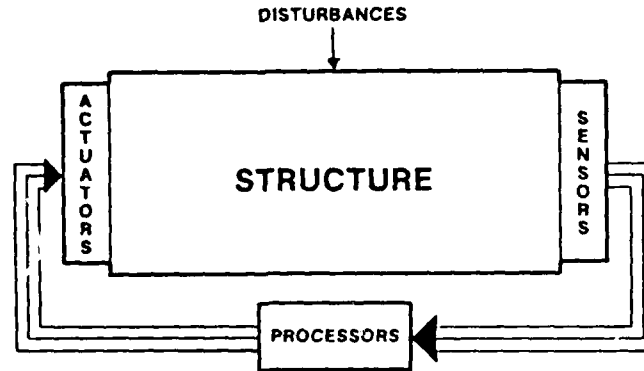


Figure 2. Vibration Control Systems Utilize Sensors, Processors and Actuators to Suppress Disturbances

The problem of active vibration suppression (Figure 2) entails the following considerations:

1. Multiple, highly coupled feedback loops. The potentially large number of sensors and actuators leads to a fully coupled multi-input, multi-output feedback control system.
2. Limited actuator power. The control authority available from on-board actuators is limited by weight, size, cost and power considerations.
3. High-dimensional models. Large structures subjected to broadband disturbances are typically represented by high-order finite element models.
4. Limited processor capacity. Reliability and cost considerations limit the processor capacity available for on-board real-time implementation of the control system.
5. Highly uncertain models with structured uncertainty. Finite element models often exhibit significant error particularly as modal frequency increases. Although modal testing and related identification methods may be used to improve modeling accuracy, residual uncertainty always remains and unpredictable on-orbit changes due to aging, thermal effects, etc., must be tolerated.

6. Stringent performance requirements. Since active space structure control is most relevant in precision applications, it can readily be expected that performance specifications will be particularly stringent.
7. Design efficiency. Because of implementation complexity due to the presence of multiple loops, high dimension, and high levels of uncertainty, the control design approach should efficiently utilize both synthesis and analysis techniques (Figure 3).

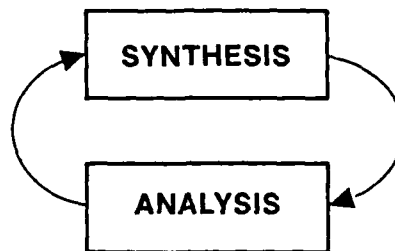
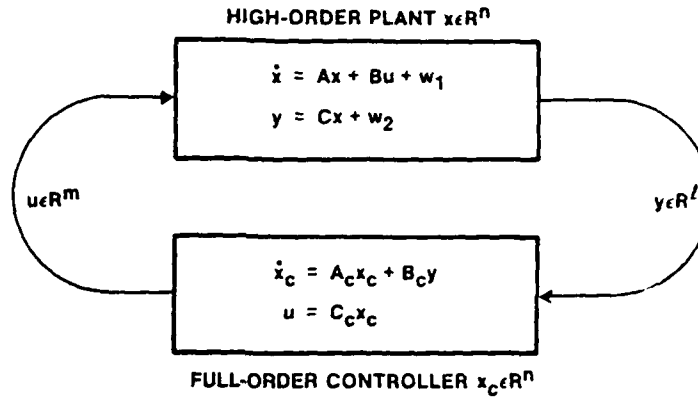


Figure 3. Control-System Design Must Efficiently Utilize Both Synthesis and Analysis Techniques

These considerations pose a considerable challenge to the state-of-the-art in control-design methodologies. For example, the presence of multiple, coupled feedback paths essentially precludes the effectiveness of single-loop design techniques. The sheer number of loops, their interaction, and the need to address a host of other issues render such methods inefficient and unwieldy.

In addition to the presence of multiple loops, the high dimensionality of dynamic models places a severe burden on control-design methodologies. For example, although LQG (linear-quadratic-Gaussian) design is applicable to multi-loop problems, such controllers are of the same order as the structural model (Figures 4 and 5). Thus LQG and similar high-order controllers can be expected to place an unacceptable computational burden on the real-time processing capability. Hence it is not surprising that a variety of techniques have been proposed to reduce the order of LQG controllers. A comparison of several such methods is given in [1].

All of the above difficulties are severely exacerbated by the fact that the dynamic (i.e., finite element) model upon which the control design is predicated may be highly inaccurate in spite of extensive modal identification. Hence, applicable control-design methodologies must account for modeling uncertainties by providing robust (i.e., insensitive) controllers. Furthermore, because of stringent



STEADY-STATE PERFORMANCE CRITERION

$$J(A_c, B_c, C_c) = \lim_{t \rightarrow \infty} E[x^T R_1 x + u^T R_2 u]$$

Figure 4. LQG Theory Addresses the Problem of Designing a Quadratically Optimal, Full-Order Dynamic Compensator

FULL-ORDER CONTROLLER GAINS

$$A_c = A - Q\bar{\Sigma} - \Sigma P$$

$$B_c = Q C^T V_2^{-1}$$

$$C_c = -R_2^{-1} B^T P$$

SEPARATED RICCATI EQUATIONS

$$0 = A Q + Q A^T + V_1 - Q \bar{\Sigma} Q \quad (\text{Kalman Filter})$$

$$0 = A^T P + P A + R_1 - P \Sigma P \quad (\text{Regulator})$$

$$\bar{\Sigma} \equiv B R_2^{-1} B^T \quad \bar{\Sigma} \equiv C^T V_2^{-1} C$$

Figure 5. The Optimal Full-Order (LQG) Controller Is Determined by a Pair of Separated Riccati Equations

performance requirements, robust control design must avoid conservatism with respect to modeling uncertainty which may unnecessarily degrade performance. A salient example of conservatism is illustrated in Figure 6. If uncertainty in the modal frequency is complexified in a transfer function setting, then the resulting pole location uncertainty has the form of a disk. This disk, however, intersects the right half plane in violation of energy dissipation. Hence one source of conservatism is the inability to differentiate between physically distinct parameters such as modal frequency and modal damping.

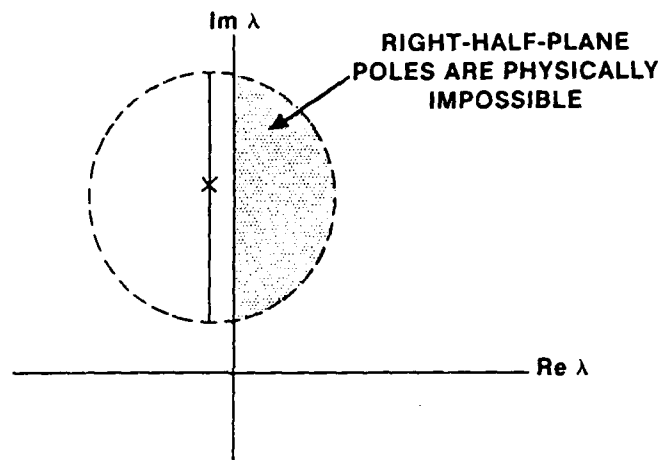


Figure 6. Complexification of Real Parameters May Lead to Robustness Conservatism

Although classical methods are inappropriate for vibration control, a wide variety of modern techniques are available. These include both multi-loop frequency-domain methods and time-domain techniques. A comprehensive review of such methods will not be attempted here. Rather, we shall merely point out aspects of several methods which motivate the philosophy of OPUS development.

As is well known, dynamic models can be transformed (at least in theory) between the frequency and time domains. Significant differences arise, however, in attempting to represent modeling errors. Specifically, model-error characterization of a particular type, which is natural and tractable in one domain, may become extremely cumbersome when transformed into the other domain. For example, consider a state space model with parameter uncertainties arising in the system matrices (A,B,C). Upon transforming to a frequency domain model $G(s) = C(sI-A)^{-1}B$ the parametric uncertainties may perturb the transfer function coefficients in a

complicated manner. A more natural measure of uncertainty for transfer functions has been developed in [2] where system uncertainty in the frequency domain is modeled by means of normed neighborhoods in the H-infinity topology. There are limitations with this approach, however, in designing controllers for vibration suppression. For example, as shown in Figure 6, complexification of real-parameter uncertainties such as modal frequencies may yield unnecessary conservatism, while norm bounds often fail to preserve the physical structure of parameter variations. A case in point is the lightly damped oscillator. As shown in [42], norm bounds predict stability over a frequency range on the order of the damping while in fact the oscillator is unconditionally stable. Furthermore, with regard to processor throughput tradeoffs, modern frequency-domain methods typically yield high-order controllers.

Although LQG addresses performance/actuator and performance/sensor tradeoffs in a multi-loop setting, it fails to incorporate modeling uncertainty. Thus it is not surprising, as shown in [3], that LQG designs fail to possess guaranteed gain margin. Since LQG designs lack such margins, attempts have been made to apply frequency-domain techniques to improve their characteristics. One such method, known as LQG/LTR ([4,5]) seeks to recover the gain margin of full-state-feedback controllers. Specifically, full-state-feedback LQR controllers are guaranteed to remain stable in the face of perturbations of the input matrix B of the form αB where $\alpha \in [1/2, \infty)$. As shown in [6,7], however, the full-state-feedback gain margin fails to provide robustness with respect to perturbations which are not of this form. For instance, the example given in [6] with $B = [0 \ 1]^T$ can be destabilized for suitable performance weightings with perturbation $B(E) = [E \ 1]^T$ for arbitrarily small E in spite of the 6 dB margin. Furthermore, since LQG/LTR loop shaping is based upon singular value norm bounds, treatment of physically meaningful real parameter variations may lead to unnecessary conservatism. Several approaches have been proposed for circumventing these difficulties (see, e.g., [8]).

The importance of addressing the problem of structured uncertainty in finite element models cannot be overemphasized. Structural characteristics such as modal frequencies, damping ratios, and mode shapes appear explicitly in (A,B,C) state-space models as physically meaningful parameters. Uncertainty in mode shapes, for example, which appear as columns of the B matrix, cannot in general be expected to be of a multiplicative form in accordance with traditional gain-margin specifications. This is precisely the problem illustrated by the example of [6] discussed above. Furthermore, uncertainties in modal frequencies and damping ratios must be carefully differentiated since, roughly speaking, modal frequency uncertainties affect only the imaginary part of the pole location while damping uncertainty affects the real part. Although these and related observations

concerning uncertainty in the dynamic characteristics of lightly damped structures may be self evident, they have remained largely unexploited in standard control-design methods.

2. OPUS: New Machinery for Control-System Design

In view of the ability of LQG theory to synthesize dynamic controllers for multi-input, multi-output controllers, it is not surprising that LQG forms the basis for a variety of structural control methods. However, as discussed previously, LQG lacks the ability to address performance/processor and performance/robustness tradeoffs. This situation has thus motivated the development of numerous variants of LQG which entail additional procedures which attempt to remedy these defects. OPUS, however, is distinctly different. Rather than append additional procedures to LQG design, OPUS extends LQG theory itself by generalizing the basic underlying machinery.

As shown in Figure 5, the basic machinery of LQG consists of a pair of separated Riccati equations whose solutions serve to directly and explicitly synthesize the gains of an optimal dynamic compensator. The contribution of OPUS is to directly expand this machinery. The overall approach is illustrated in Figure 7 which portrays two distinct generalizations of the basic LQG machinery. As Figure 7 illustrates, these generalizations can be developed individually when either low-order or robust controllers are desired. The appealing aspect of OPUS, however, is the ability to extend LQG to address both problems simultaneously in a unified manner.

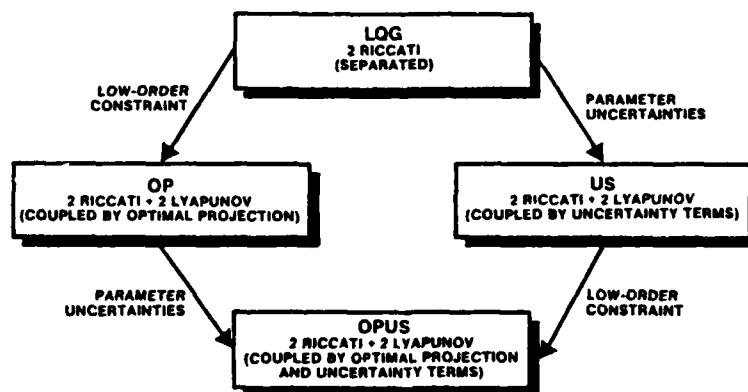


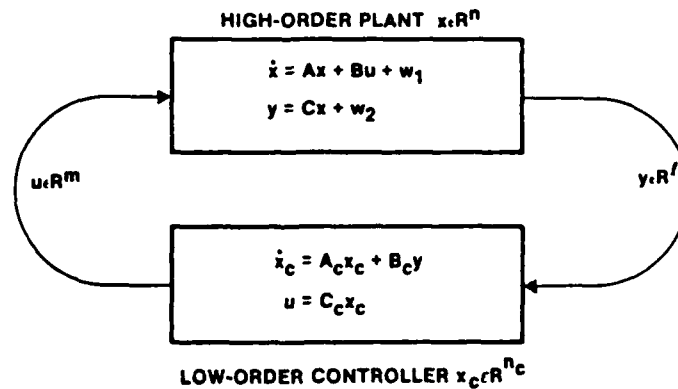
Figure 7. The Standard LQG Result Is Generalized by Both the Fixed-Order Constraint and Modeling of Parameter Uncertainties

In the following sections the generalizations depicted in Figure 7 will be reviewed following the left branch. That is, the optimal projection approach to reduced-order controller design will first be discussed in Section 3 without introducing plant uncertainties. In Section 4 the reduced-order constraint will be retained while considering, in addition, uncertainties in the system model. In each case the discussion will focus on the underlying ideas with a minimum of technical detail.

Clearly, in order for a novel design methodology to be of practical value it must be computationally tractable. Hence Section 5 will present an overview of the current state of algorithm development for solving the OPUS design equations. Finally, Section 6 will briefly summarize further OPUS generalizations of LQG theory which are relevant to structural control.

3. Extensions of LQG to Reduced-Order Dynamic Compensation

The simplest, most direct way to obtain optimal reduced-order controllers is to redevelop the standard LQG result in the presence of a constraint on controller dimension (Figure 8). The mathematical technique required to do this is remarkably straightforward. Specifically, the structure and order of the controller are fixed and the performance is optimized with respect to the controller gains. The resulting necessary conditions obtained using Lagrange multipliers thus characterize the optimal gains.



STEADY-STATE PERFORMANCE CRITERION

$$J(A_c, B_c, C_c) = \lim_{t \rightarrow \infty} E[x^T R_1 x + u^T R_2 u]$$

Figure 8. In Accordance With On-Board Processor Requirements, a Reduced-Order Constraint Is Imposed on the Dimension of the Dynamic Compensator

This parameter optimization approach as such is not new and was investigated extensively in the 1970's. Typically, however, the optimality conditions were found to be complex and unwieldy while offering little insight and requiring gradient search methods for numerical solution.

One curious aspect of the parameter optimization literature is that no attempt was made to actually use this direct method to rederive the LQG result itself. Such an exercise, it may be surmised, might reveal hidden structure within the optimality conditions which would shed light on the reduced-order case. Indeed, such an approach led to the realization that an oblique projection (idempotent matrix) is the key to unlocking the unwieldy optimality conditions ([A7,A17]). Although the result is mathematically straightforward, it is by no means obvious since in the full-order (LQG) case the projection is the identity and hence not readily apparent.

By exploiting the presence of the projection, the necessary conditions can be transformed into a coupled system of four algebraic matrix equations consisting of a pair of modified Riccati equations and a pair of modified Lyapunov equations (Figure 9). The coupling is via the oblique projection τ which appears in all four equations and which is determined by the solutions \hat{Q} and \hat{P} of the modified Lyapunov equations. A satisfying feature of the optimality conditions is that in the full-order case the projection becomes the identity, the modified Lyapunov equations drop out, and, since $\tau_1 = 0$, the modified Riccati equations specialize to the usual separated Riccati equations of LQG theory. Since, furthermore, $G = \Gamma = n \times n$ identity, the standard LQG gain expressions are recovered.

Although the modified Riccati equations specialize to the standard Riccati equations in the full-order case, the modified Lyapunov equations have no counterpart in the standard theory. The role of these equations can be understood by considering the problem of optimal model reduction alone. For this problem the optimal reduced-order model is characterized by a pair of coupled modified Lyapunov equations (see [A22]). Thus the modified Lyapunov equations arising in the reduced-order dynamic-compensation problem are directly analogous to the modified Lyapunov equations arising in model reduction alone. The modified Lyapunov equations arising in the control problem, however, are intimately coupled with the modified Riccati equations. Hence it cannot be expected that reduced-order control-design techniques based upon LQG will generally yield optimal fixed-order controllers (Figure 10). It is interesting to note that several such methods discussed in [1] are based upon balancing which was shown in [A22] to be suboptimal with respect to the quadratic (least squares) optimality criterion.

REDUCED-ORDER CONTROLLER GAINS

$$A_c = I'(A-Q\bar{\Sigma}-\Sigma P)G^T$$

$$B_c = I'QCTV_2^{-1}$$

$$C_c = -R_2^{-1}B^T P G^T$$

COUPLED RICCATI/LYAPUNOV EQUATIONS

$$0 = A\hat{Q} + \hat{Q}A^T + V_1 - Q\bar{\Sigma}Q + \gamma_1 Q\bar{\Sigma}Q^T \gamma_1$$

$$0 = A^T \hat{P} + \hat{P}A + R_1 - P\Sigma P + \gamma_1^T P\Sigma P \gamma_1$$

$$0 = (A-\Sigma P)\hat{Q} + \hat{Q}(A-\Sigma P)^T + Q\bar{\Sigma}Q - \gamma_1 Q\bar{\Sigma}Q^T \gamma_1$$

$$0 = (A-Q\bar{\Sigma})^T \hat{P} + \hat{P}(A-Q\bar{\Sigma}) + P\Sigma P - \gamma_1^T P\Sigma P \gamma_1$$

$$\text{rank } \hat{Q} = \text{rank } \hat{P} = \text{rank } \hat{Q}\hat{P} = n_c$$

$$\hat{Q}\hat{P} = G^T M I' \quad I'G^T = I_{n_c}$$

$$\gamma = G^T I' = \hat{Q}\hat{P}(\hat{Q}\hat{P})^\# \quad \gamma_1 = I_{n_c} - \gamma$$

$$\Sigma = BR_2^{-1}B^T \quad \bar{\Sigma} = CTV_2^{-1}C$$

Figure 9. The Optimal Reduced-Order Compensator Is Determined by a Pair of Modified Riccati Equations and a Pair of Modified Lyapunov Equations Coupled by the Oblique Projection γ

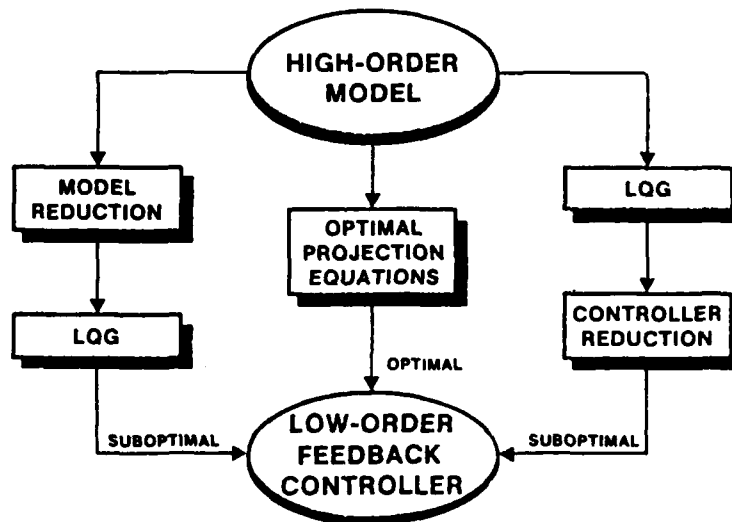


Figure 10. The Optimal Projection Equations Provide a Direct Path to Optimal Reduced-Order Dynamic Compensators

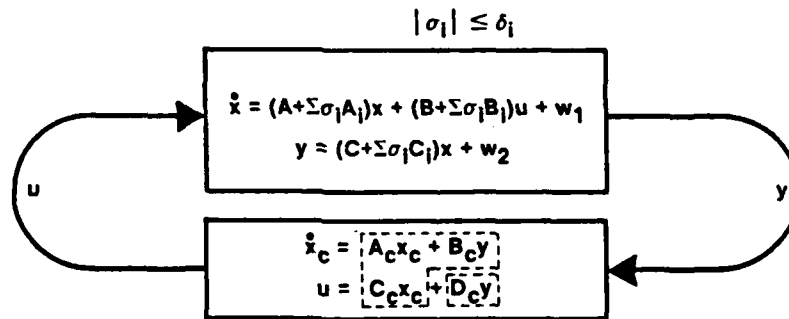
In summary, the optimal projection equations for reduced-order dynamic compensation comprise a direct extension of the basic LQG machinery to the reduced-order control problem. The design equations, which reduce to the standard LQG result in the full-order case, provide direct synthesis of optimal reduced-order controllers in accordance with implementation constraints.

4. Extensions of LQG to Uncertain Modeling

Two fundamental sources of error in modeling flexible structures are truncated modes and parameter uncertainties. Since the optimal projection approach permits the utilization of the full dynamics model, modal truncation can be largely avoided. There remains, however, a tendency to truncate poorly known modes and thus it is essential to incorporate a model of parameter uncertainty in both well-known and poorly known components of the system. Hence the problem formulation of Figure 8 is now generalized in Figure 11 to include uncertain parameters σ_j appearing in the A, B and C matrices. The parameter σ_j is assumed to lie within the interval $[-\delta_j, \delta_j]$ in accordance with identification accuracy. Clearly, when uncertainty is absent, i.e., when $A_j, B_j, C_j = 0$, the reduced-order design problem of Figure 8 is recovered.

HIGH-ORDER, UNCERTAIN PLANT

- Stochastic disturbance model
- Deterministic parameter uncertainty model



LOW-ORDER CONTROLLER

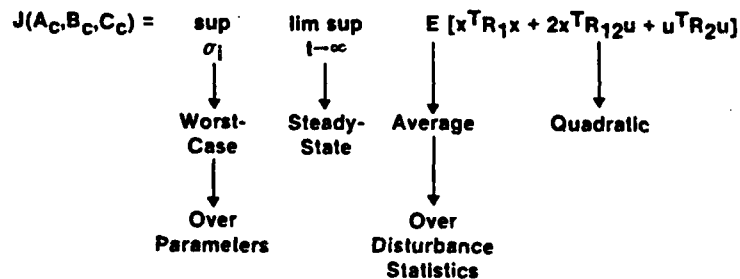
- Dynamic (strictly proper)
- Static (constant gain)
- Dynamic/static (nonstrictly proper)

Figure 11. Robust Optimal Projection Design Is Based Upon a Hybrid Uncertainty Model Involving a Deterministic Parameter Uncertainty Model and a Stochastic Disturbance Model

A salient feature of the design model is that uncertainty is modeled in two distinctly different ways. External uncertainty appearing as additive white noise is modeled stochastically. Such a model appears appropriate for disturbances such as coolant flow for which only power spectral data are available. On the other hand, internal uncertainty appearing as parameter variations is modeled deterministically. Such a model appears appropriate for uncertainty arising from directly measurable quantities such as mass and stiffness. Thus the overall uncertainty model is hybrid in the sense that it utilizes both deterministic and stochastic characterizations of uncertainty.

A natural performance measure which accounts for both types of uncertainty characterization involves the usual LQG quadratic criterion averaged over the disturbance statistics and then maximized over the uncertain parameters (Figure 12). Hence this performance measure incorporates on the average and worst case aspects in accordance with physical considerations.

PERFORMANCE CRITERION



ROBUST PERFORMANCE PROBLEM

Minimize $J(A_c, B_c, C_c)$ over the class of robustly stabilizing controllers (A_c, B_c, C_c)

Figure 12. Performance Is Defined To Be Worst Case Over the Uncertain Parameters and Average Over the Disturbance Statistics

The resulting Robust Performance Problem thus involves determining the gains (A_c, B_c, C_c) to minimize the performance J . The static gain D_c can also be included but will not be discussed here. Despite the apparent complexity of the problem, remarkably simple techniques can be used. Specifically, first note that after taking the expected value the performance J has the form

$$J(A_c, B_c, C_c) = \sup_{\sigma_i} \limsup_{t \rightarrow \infty} \text{tr } \bar{Q}(t) \bar{R}, \quad (4.1)$$

where "tr" denotes trace of a matrix, $\bar{Q}(t)$ is the covariance of the closed-loop system, and \bar{R} is an augmented weighting matrix composed of R_1 , R_{12} and R_2 . The covariance $\bar{Q}(t)$ satisfies the standard Lyapunov differential equation

$$\dot{\bar{Q}} = (\bar{A} + \sum \sigma_i \bar{A}_i) \bar{Q} + \bar{Q} (\bar{A} + \sum \sigma_i \bar{A}_i)^T + \bar{V}, \quad (4.2)$$

where \bar{A} is the closed-loop dynamics, \bar{A}_i is composed of A_i , B_i and C_i , and \bar{V} is the intensity of external disturbances for the closed-loop system including the plant and measurement noise.

Two distinct approaches to this problem will be considered. The first involves bounding the performance over the class of parameter uncertainties and then choosing the gains to minimize the bound. Since bounding precedes control design this approach is known as robust design via a priori performance bounds. The second approach involves exploiting the nondestabilizing nature of structural systems via weak subsystem interaction.

4.1 Robust Design Via A Priori Performance Bounds

The key step in bounding the performance (4.1) is to replace (4.2) by a modified Lyapunov differential equation of the form

$$\dot{\bar{Q}} = \bar{A}\bar{Q} + \bar{Q}\bar{A}^T + \Psi(\bar{Q}) + \bar{V}, \quad (4.3)$$

where the bound Ψ satisfies the inequality

$$\sum \sigma_i (\bar{A}_i \bar{Q} + \bar{Q} \bar{A}_i^T) \leq \Psi(\bar{Q}) \quad (4.4)$$

over the range of uncertain parameters σ_i and for all candidate feedback gains. Note that the inequality (4.4) is defined in the sense of nonnegative-definite matrices. Now rewrite (4.3) by appropriate addition and subtraction as

$$\dot{\bar{Q}} = (\bar{A} + \sum \sigma_i \bar{A}_i) \bar{Q} + \bar{Q} (\bar{A} + \sum \sigma_i \bar{A}_i)^T + \Psi(\bar{Q}) - \sum \sigma_i (\bar{A}_i \bar{Q} + \bar{Q} \bar{A}_i^T) + \bar{V}. \quad (4.5)$$

Now subtract (4.2) from (4.5) to obtain

$$\dot{\bar{Q}} - \dot{\bar{Q}} = (\bar{A} + \sum \sigma_i \bar{A}_i) (\bar{Q} - \bar{Q}) + (\bar{Q} - \bar{Q}) (\bar{A} + \sum \sigma_i \bar{A}_i)^T + \Psi(\bar{Q}) - \sum \sigma_i (\bar{A}_i \bar{Q} + \bar{Q} \bar{A}_i^T). \quad (4.6)$$

Since by (4.4) the term

$$\Psi(\bar{Q}) = \sum \sigma_i (\bar{A}_i \bar{Q} + \bar{Q} \bar{A}_i^T) \quad (4.7)$$

is nonnegative definite, it follows immediately that

$$\bar{Q} \leq \bar{Q} \quad (4.8)$$

over the class of uncertain parameters. Thus the performance (4.1) can be bounded by

$$J(A_c, B_c, C_c) \leq \underline{J}(A_c, B_c, C_c) \triangleq \lim_{t \rightarrow \infty} \text{tr } \bar{Q} R. \quad (4.9)$$

The auxiliary cost \underline{J} is thus guaranteed to bound the actual cost J . This leads to the Auxiliary Minimization Problem: Minimize the auxiliary cost \underline{J} over the controller gains. The advantage of this approach is that necessary conditions for the Auxiliary Minimization Problem effectively serve as sufficient conditions for robust performance in the original problem. Since the bounding step precedes the optimization procedure, this approach is referred to as robust design via a priori performance bounds. This procedure is philosophically similar to guaranteed cost control ([9,10]). Note that since bounding precedes optimization, the bound (4.4) must hold for all gains since the optimal gains are yet to be determined.

To obtain sufficient conditions for robust stability, the bounding function Ψ must be specified. Since the ordering of nonnegative-definite matrices appearing in (4.4) is not a total ordering, a unique lowest bound should not be expected. Furthermore, each differentiable bound leads to a fundamental extension of the optimal projection equations and thus of the basic LQG machinery. In work thus far, two bounds have been extensively investigated. Only one bound, the right shift/multiplicative white noise bound, will be discussed here. The structured stability radius bound introduced in [11,12] is discussed in [A43].

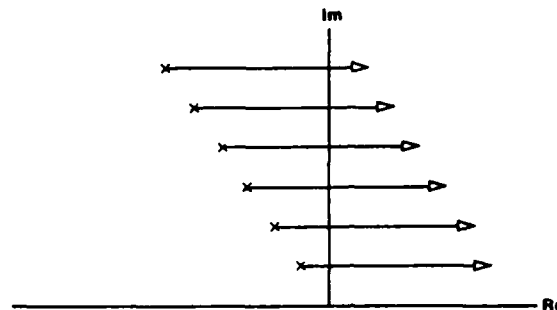
The right shift/multiplicative white noise bound investigated in [A29,A41] is given by

$$\Psi(\bar{Q}) = \sum \delta_j (\alpha_j \bar{Q} + \alpha_j^{-1} \bar{A}_j \bar{Q} \bar{A}_j^T), \quad (4.10)$$

where $\alpha_j > 0$ are arbitrary scalars. Note that this bound consists of two distinct parts which must appear in an appropriate ratio. The first term $\alpha_j \bar{Q}$ arises naturally when an exponential time weighting $e^{\alpha_j t}$ is included in the performance measure. As is well known ([13]) this leads to a prescribed uniform stability margin for the

closed-loop system (Figure 13). A uniform stability margin, no matter how large, however, does not guarantee robustness with respect to arbitrary parameter variations. The complementary second term $\alpha_i^{-1} \bar{A}_i \bar{Q}_i \bar{A}_i^T$ is crucial in this regard.

$$\dot{x} = Ax \rightarrow \dot{x} = (A + \alpha I)x, \alpha > 0$$



APPLY CONTROL-DESIGN TECHNIQUES
TO RIGHT-SHIFTED OPEN-LOOP SYSTEM
⇔ UNIFORM STABILITY MARGIN
(Anderson and Moore, 1969)

Figure 13. Open-Loop Right-Shifted Dynamics Arising From Exponential Cost Weighting Lead to a Uniform Closed-Loop Stability Margin

Although terms of the form $\bar{A}_i \bar{Q}_i \bar{A}_i^T$ are unfamiliar in robust control design, they arise naturally in stochastic differential equations with multiplicative white noise. That is, if the uncertain parameters σ_i are replaced by white noise processes entering multiplicatively rather than additively, then the covariance equation for \bar{Q} automatically includes terms of the form $\bar{A}_i \bar{Q}_i \bar{A}_i^T$. The literature on systems with multiplicative white noise is quite extensive; see [A38] for references. It should be stressed, however, that for our purposes the multiplicative white noise model is not interpreted literally as having physical significance. Rather, multiplicative white noise can be thought of as a useful design model which correctly captures the impact of uncertainty on the performance functional via the state covariance. Furthermore, just as the right shift term alone does not guarantee robustness, neither does the multiplicative white noise term. Both terms must appear simultaneously. Roughly speaking, since multiplicative white noise disturbs the plant through uncertain parameters, the closed-loop system is automatically desensitized to actual parameter variations.

After incorporating the right shift/multiplicative white noise bound (4.10) into (4.3) to obtain a bound \underline{J} for the performance, the optimal projection equations can be rederived following exactly the same parameter optimization procedure discussed in Section 3. Again, the mathematics required is but a straightforward application of Lagrange multipliers. The additional bounding terms are carried through the derivation to yield a direct generalization of the optimal projection equations shown in Figure 14 with gains given in Figure 15.

$$0 = A_s Q + Q A_s^T + \lambda Q A^T + V_1 + (A_s B_s R_{2s}^{-1} P_s) \hat{Q} (A_s B_s R_{2s}^{-1} P_s)^T - Q_s V_{2s}^{-1} Q_s^T + r_1^T Q_s V_{2s}^{-1} Q_s^T r_1$$

$$0 = A_s^T P + P A_s + \lambda^T P A + R_1 + (A_s - Q_s V_{2s}^{-1} C_s)^T \hat{P} (A_s - Q_s V_{2s}^{-1} C_s) - P_s^T R_{2s}^{-1} P_s + r_1^T P_s^T R_{2s}^{-1} P_s r_1$$

$$0 = (A_s - B_s R_{2s}^{-1} P_s) \hat{Q} + \hat{Q} (A_s - B_s R_{2s}^{-1} P_s)^T + Q_s V_{2s}^{-1} Q_s^T - r_1^T Q_s V_{2s}^{-1} Q_s^T r_1$$

$$0 = (A_s - Q_s V_{2s}^{-1} C_s)^T \hat{P} + \hat{P} (A_s - Q_s V_{2s}^{-1} C_s) + P_s^T R_{2s}^{-1} P_s - r_1^T P_s^T R_{2s}^{-1} P_s r_1$$

Figure 14. The Robustified Optimal Projection Design Equations Account for Both Reduced-Order Dynamic Compensation and Parametric Uncertainty

GAINS

$$A_c = (A_s - B_s R_{2s}^{-1} P_s - Q_s V_{2s}^{-1} C_s) G^T$$

$$B_c = Q_s V_{2s}^{-1}$$

$$C_c = -R_{2s}^{-1} P_s G^T$$

NOTATION

$$\hat{Q} \hat{P} = G^T M \Gamma, \quad \Gamma G^T = I_{n_c} \quad (\Rightarrow r = G^T \Gamma = r^2)$$

$$\lambda Q A^T = \sum_{i=1}^p \lambda_i Q A_i^T, \quad \lambda Q B = \sum_{i=1}^p \lambda_i Q B_i, \text{ etc.}$$

$$R_{2s} = R_2 + B^T (P + \hat{P}) B \quad V_{2s} = V_2 + C(Q + \hat{Q})C^T$$

$$Q_s = Q C_s^T + V_{12} + \lambda(Q + \hat{Q})C^T \quad P_s = B_s^T P + R_{12}^T + B^T (P + \hat{P}) \lambda$$

Figure 15. The OPUS Controller Gains Are Explicitly Characterized as a Direct Generalization of the Classical LQG Gains

The robustified optimal projection equations comprise a system of four matrix equations coupled by both the optimal projection and uncertainty terms. When the uncertainty terms are absent, the optimal projection equations of Figure 9 are immediately recovered. On the other hand, if the order of the controller is set equal to the order of the plant, then all terms involving τ_1 can be deleted. However, in this case the modified Lyapunov equations do not drop out since \bar{Q} and \bar{P} still appear in the modified Riccati equations. Hence the basic machinery of LQC is again extended to include a pair of Lyapunov equations coupled to a generalization of the standard LQC equations. It is interesting to note that a related result in the context of multiplicative noise also appeared in the Soviet literature ([14]). It should also be pointed out that although the modified Lyapunov equations arising in the reduced-order control-design problem have analogues in model reduction, the modified Lyapunov equations appearing in the full-order robustified equations represent new machinery not anticipated in robustness theories. Hence using straightforward mathematical techniques, the basic LQC machinery has again been extended in novel directions.

Solving the design equations shown in Figures 14 and 15 yields controllers with guaranteed levels of robustness. The actual robustness levels may, however, be larger than specified by a priori bounds. Thus, to achieve desired robustification levels for the uncertainty structure specified by the a priori bounds, the design procedure may be utilized within an iterative synthesis/analysis procedure (Figure 16).

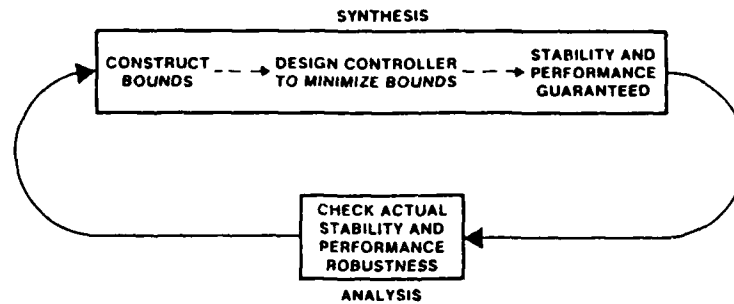


Figure 16. Optimal Projection/Guaranteed Cost Control Provides Direct Synthesis of Robust Dynamic Compensators

4.2 Robust Design Via Weak Subsystem Interaction

The mechanism by which LQC was robustified in Section 4.1 involved bounding the performance over the class of parameter uncertainties and then determining optimal controller gains for the performance bound. As discussed in Section 2,

however, flexible structures possess special properties which may, in addition, be exploited to achieve robustness. Specifically, aside from rigid-body modes, energy dissipation implies that mechanical structures are open-loop stable regardless of the level of uncertainty. That is, flexible structures possess only nondestabilizing uncertainties. Hence, in the closed loop, a given controller may or may not render a particular uncertainty destabilizing. A priori bounds on controller performance must, however, be valid for all gains since bounding precedes optimization. Hence, a priori bounding may in certain cases fail to exploit nondestabilizing uncertainties.

A familiar example of a nondestabilizing uncertainty involves uncertain modal frequencies. Such an uncertainty will not, of course, destabilize an uncontrolled (open-loop) structure. If particular modal frequencies are poorly known then it is clearly advisable to avoid applying high authority control. Hence, rather than the right-shift approach of Figure 13, it appears advantageous (although, at first, counterintuitive) to utilize just the opposite, namely, a left shift (Figure 17). Furthermore, in view of the fact that uncertainty usually increases with modal frequency (Figure 18), a variable left shift appears to be more appropriate than a uniform left shift. By left-shifting high-frequency poorly known modes, the control-system design procedure applies correspondingly reduced authority to modes "perceived" as highly damped. Hence the variable left shift can be roughly thought of as a device for achieving suitable authority rolloff. As will be seen, however, the underlying robustification mechanism, namely, weak subsystem interaction, is far more subtle than the approach of classical rolloff techniques. It is also interesting to note that the weak subsystem interaction approach to robustness is entirely distinct from classical robustness approaches which utilize high loop gain to reduce sensitivity.

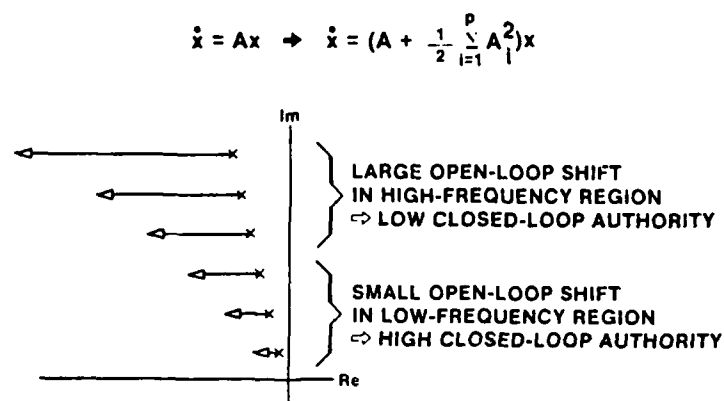


Figure 17. A Variable Left Shift Exploits Open-Loop Nondestabilizing Uncertainties

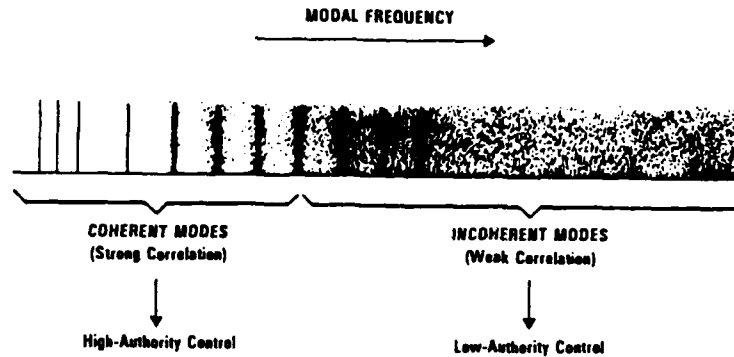


Figure 18. Modal Uncertainty Generally Increases With Frequency

A variable left shift can readily be introduced into the robustified optimal projection design equations by replacing A by

$$A_g = A + \frac{1}{2} \sum A_i^2 \quad (4.11)$$

where A_i denotes the structure of modal frequency uncertainty (Figure 19). Most interestingly, such a modification of the dynamics matrix arises naturally from a multiplicative white noise model defined not in the usual Ito sense but rather in the sense of Stratonovich. Thus, as in the a priori bounding approach, a stochastic

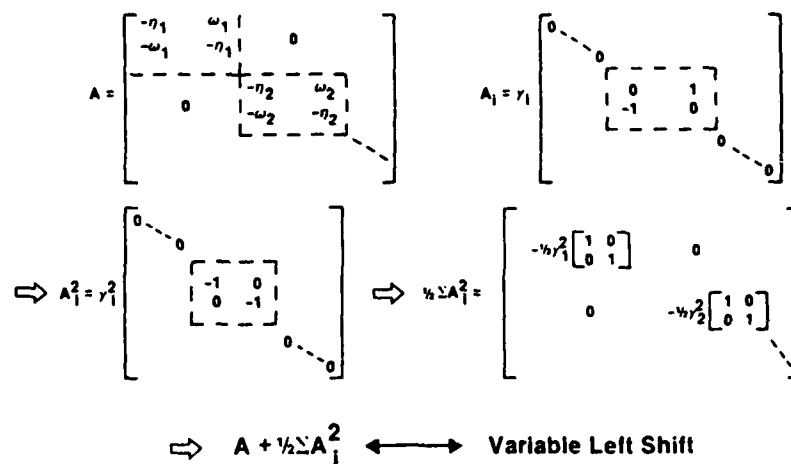


Figure 19. For Modal Systems With Frequency Uncertainty the Stratonovich Correction Corresponds to a Variable Left Shift

model serves to suggest a mechanism for robustification (Figure 20). Again it is important to stress that the multiplicative white noise model is not interpreted literally as having physical significance, but rather can be thought of as a useful design model which correctly captures the impact of uncertainty on the performance functional via the state covariance.

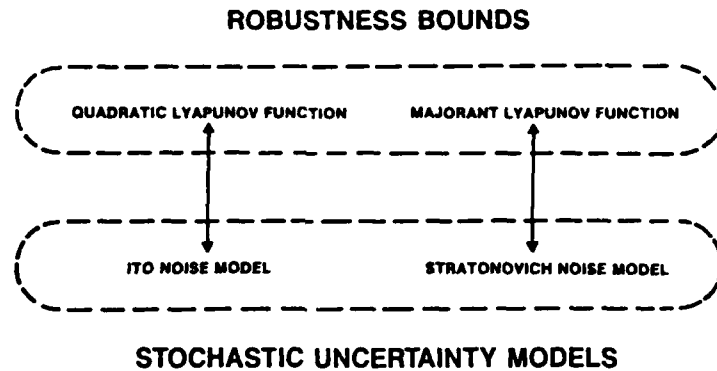


Figure 20. Stochastic Models and Robustness Bounds Are Fundamentally Related

In earlier work the Stratonovich dynamics model was justified by means of the minimum information/maximum entropy approach ([A1-A15]). A central result of the maximum entropy approach is that the high authority/low authority transition of a vibration control system from well-known low-frequency modes to poorly known high-frequency modes (Figure 18) is directly reflected in the structure of the state covariance matrix (Figure 21). A full-state feedback design applied to a simply

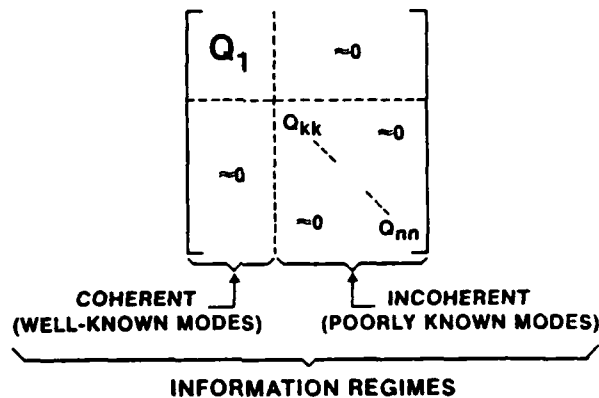


Figure 21. Frequency Uncertainties in the Stratonovich Model Lead to Suppressed Cross Correlation in the Steady-State Covariance

supported beam illustrates this point (Figure 22). By assuming that uncertainty in modal frequencies increases linearly with frequency, the structure of the covariance matrix leads directly to the control gains illustrated in Figure 23. Note that in the high-frequency region the position gains are essentially zero and thus the control law approaches positive-real energy dissipative rate feedback. This, of course, is precisely the type of structural controller expected in the presence of poor modeling information. Of course, any effective control-design theory for active vibration suppression in flexible structures should produce energy dissipative controllers when structural modeling information is highly uncertain.

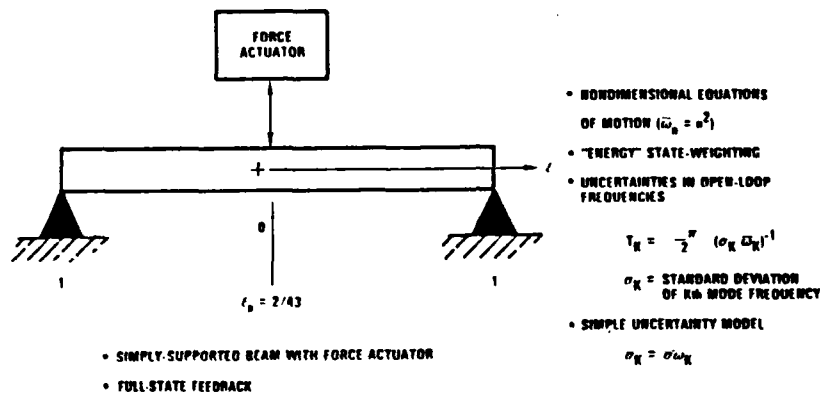


Figure 22. The Effects of Frequency Uncertainties Can Be Illustrated for a One-Dimensional Beam With Idealized Full-State Feedback

To carry out robustified optimal projection design in the presence of left-shifted open-loop dynamics, it is only necessary to utilize the left-shifted dynamics matrix (4.11) in place of the right-shifted matrix. All of the robustified optimal projection machinery, including gain expressions, can be utilized directly. It is also important to stress that the left shift must be used in conjunction with terms of the form $\tilde{A}_i Q A_i^T$.

One explanation for the mechanism by which robustification is achieved is illustrated in Figure 24. By left shifting the open-loop dynamics within the design process, the compensator poles are similarly left-shifted. Thus the compensator poles are effectively moved further into the left half plane away from the actual plant poles. Since the interaction between compensator and plant poles is weakened, the closed-loop system is correspondingly robustified with respect to uncertainties in the plant pole locations. A sensitivity analysis of this mechanism utilizing a uniform left shift in the context of LQG design is given in [15].

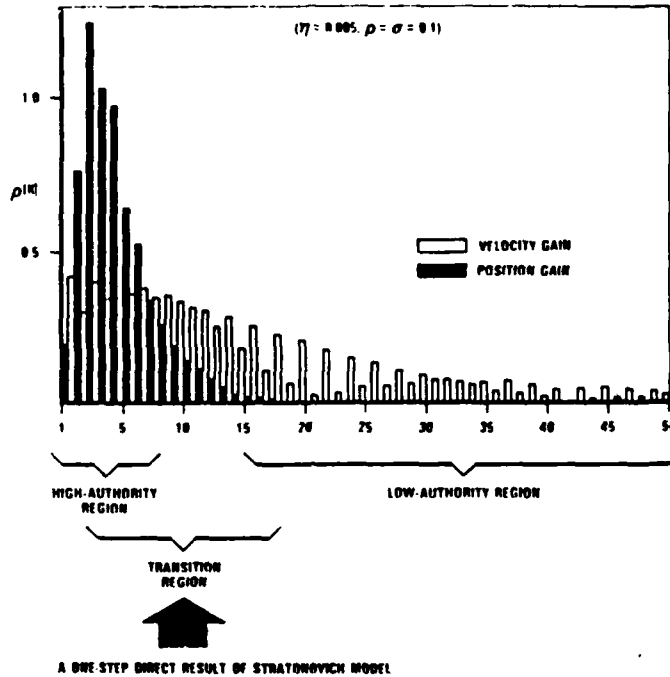


Figure 23. The Maximum Entropy Controller Approaches Rate Feedback in the Limit of Poor Modeling Information (High Uncertainty)

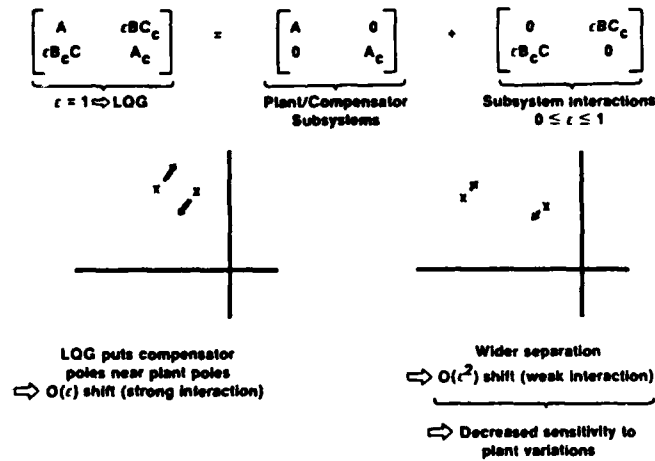


Figure 24. The Stratonovich Variable Left-Shift Model Effectively Places the Compensator Poles Further Into the Left Half Plane Where Plant/Compensator Interaction Is Weakened

As discussed above, the left-shift approach exploits open-loop nondestabilizing uncertainties and thus cannot operate through a priori bounding. Thus the actual level of robustification achieved from the robustified optimal projection equations for a given level of uncertainty modeling cannot be predicted a priori, i.e., in advance of control design. Indeed, this situation is to be expected when nondestabilizing uncertainties are exploited in a nonconservative design theory. Thus a suitable robust analysis technique is required for nonconservatively determining the robustification of the closed-loop system with respect to open-loop nondestabilizing uncertainties.

A suitable robustness analysis technique, known as majorant Lyapunov analysis, has indeed been developed ([A42]). Essentially, this technique employs a new type of Lyapunov function for assessing robustness due to weak subsystem interaction. The underlying machinery consists of the block-norm matrix which is a nonnegative matrix each of whose elements is the norm of a block of a suitably partitioned matrix (Figure 25). A matrix which bounds the block-norm matrix in the sense of nonnegative matrices, i.e., element by element, is known as a majorant. Majorants were introduced in [16] and were applied to stability analysis of integration algorithms for ODE's in [17].

(Ostrowski, 1961; Dahlquist, 1983)

$$M = \begin{bmatrix} M_1 & M_{12} & \dots \\ M_{21} & M_2 & \dots \\ \vdots & & \ddots \end{bmatrix}$$

$$m = \begin{bmatrix} \|M_1\| & \|M_{12}\| & \dots \\ \|M_{21}\| & \|M_2\| & \dots \\ \vdots & & \ddots \end{bmatrix}$$

NONNEGATIVE CONE ORDERING

$$m \leq \hat{m}$$

Figure 25. The Matrix Majorant Is a Bound for the Matrix Block Norm, i.e., the Nonnegative Matrix Each of Whose Elements Is the Norm of the Corresponding Block of a Given Matrix

To apply majorants to dynamical systems, the model is written in the form shown in Figure 26. The matrix A is block diagonal and consists of subsystem dynamics. The subsystem interactions represented by the partitioned matrix G are assumed to be uncertain. By suitable manipulation, uncertainties in the diagonal blocks of A can also be captured by G. By assuming that the spectral norm (largest singular value) of the blocks of G satisfy given bounds, the covariance block-norm inequality is obtained (Figure 27). This inequality is interpreted in the sense of nonnegative matrices, i.e., element-by-element, and * denotes the Hadamard (element-by-element) product.

$$\dot{x} = (A + G)x + w \quad \dot{Q} = (A + G)Q + Q(A + G)^T + V$$

$$A = \begin{bmatrix} A_1 & 0 & \dots \\ 0 & A_2 & \dots \\ \vdots & & \ddots \end{bmatrix}$$

Known Subsystem Dynamics

$$G = \begin{bmatrix} 0 & G_{12} & \dots \\ G_{21} & 0 & \dots \\ \vdots & & \ddots \end{bmatrix}$$

Uncertain Subsystem Interactions

$$V = \begin{bmatrix} V_1 & V_{12} & \dots \\ V_{21} & V_2 & \dots \\ \vdots & & \ddots \end{bmatrix}$$

Noise Intensity

$$Q = \begin{bmatrix} Q_1 & Q_{12} & \dots \\ Q_{21} & Q_2 & \dots \\ \vdots & & \ddots \end{bmatrix}$$

State Covariance

Figure 26. The Large-Scale System Model Involves Known Local Dynamics and Uncertain Interactions

$$\dot{x} = (A + G)x + w \quad J = E[x^T R x] = \text{tr } QR$$

$$\dot{Q} = (A + G)Q + Q(A + G)^T + V \quad J = |g(A_i \otimes A_i)|$$

$$V = \begin{bmatrix} \|V_1\|_F & \|V_{12}\|_F & \dots \\ \|V_{21}\|_F & \|V_2\|_F & \dots \\ \vdots & & \ddots \end{bmatrix}$$

$$Q = \begin{bmatrix} \|Q_1\|_F & \|Q_{12}\|_F & \dots \\ \|Q_{21}\|_F & \|Q_2\|_F & \dots \\ \vdots & & \ddots \end{bmatrix}$$

$$\begin{bmatrix} 0 & \bar{\sigma}(G_{12}) & \dots \\ \bar{\sigma}(G_{21}) & 0 & \dots \\ \vdots & & \ddots \end{bmatrix} \leq \leq G$$

↓

$$A * Q \leq \leq GQ + QG^T + V$$

Figure 27. The Block-Norm Matrix of the State Covariance Satisfies a Lyapunov-Type Inequality Involving Nonnegative Matrices

To achieve robustness, the covariance block-norm inequality is replaced by the majorant Lyapunov equation (Figure 28). The solution of the majorant Lyapunov equation provides a bound (majorant) for the block norm of the covariance thereby guaranteeing both robust stability and performance.

MAJORANT LYAPUNOV EQUATION

$$A \cdot \hat{Q} = S\hat{Q} + \hat{Q}S^T + V$$

$$\sigma(G_{ij}) \leq S_{ij}$$



$$Q \leq \hat{Q}$$



■ Robust Stability

■ Robust Performance

Figure 28. The Corresponding Nonnegative Matrix Equation Yields a Majorant for the State Covariance and Hence Robust Stability and Performance

It is interesting to note that numerical solution of the majorant Lyapunov equation requires no new techniques. Utilizing properties of M matrices, the solution can be obtained monotonically by means of a straightforward iterative technique (Figure 29).

MLE has a unique solution iff $\{\hat{Q}_K, K=0, 1, \dots, \infty\}$ where:

$$\hat{Q}_0 = 0$$

$$\hat{Q}_{K+1} = (I - S) \cdot (\hat{Q}_K + \hat{Q}_K S^T + V)$$

$$(I)_{mn} \triangleq I^{-1}_{mn}$$

converges. If so, then:

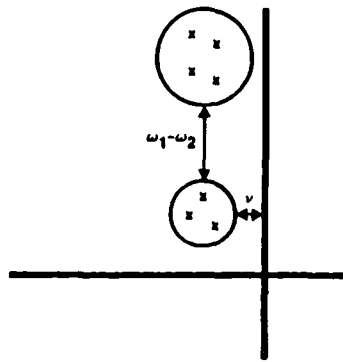
$$\hat{Q} = \lim_{K \rightarrow \infty} \hat{Q}_K$$

$$J - J_0 \leq 2 \sum_{K=1}^r (\text{tr } \hat{P}_K) (\hat{Q})_{KK}$$

$$(0 = A_K^T \hat{P}_K + \hat{P}_K A_K + R_K)$$

Figure 29. By Exploiting the Properties of M-Matrices, the Majorant Lyapunov Equation Can Be Solved Monotonically by Means of a Simple Iterative Technique

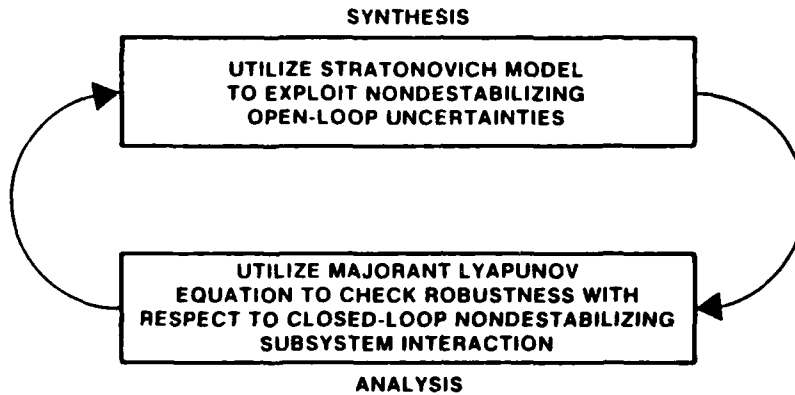
An illustrative application of the majorant Lyapunov equation involves lightly damped subsystems (Figure 30). As shown in [A42] (and expected intuitively), robustness with respect to uncertain subsystem interaction is proportional to the frequency separation between the subsystems. The ability to capture this robustification mechanism is a unique feature of the majorant Lyapunov function not available from quadratic (i.e., scalar) Lyapunov functions or vector Lyapunov functions ([18,19]).



$$\text{Majorant Lyapunov Equation Bound} \sim \nu \sqrt{(2\nu)^2 + (\omega_1 - \omega_2)^2}$$

Figure 30. Robustness Bounds for Uncertain Coupling in Modal Systems Are Proportional to the Frequency Separation Between Subsystems

The next step in the majorant development involves a hierarchy of finer and finer robustness bounds which account for higher order subsystem interactions, e.g., the interaction between the *i*th and *j*th subsystems via the *k*th subsystem. The second member of the hierarchy (Figure 31) provides robustness guarantees with respect to frequency uncertainties. The interesting aspect of this robustness test is the fact that the performance bound is characterized precisely by a Stratonovich model. Hence the Stratonovich model can be viewed as an approximation to a robustness bound, while exploiting the Stratonovich/majorant relationship leads to a natural synthesis/analysis scheme (Figure 32) which nonconservatively exploits open-loop nondestabilizing uncertainties.



Stratonovich synthesis = approximation to majorant analysis

Figure 31. The Stratonovich Synthesis Model Provides a First Approximation to the Majorant Analysis Bounds

Second member of the hierarchy:

$$n \cdot \hat{Q} + \hat{H}[\hat{Q}] = \mathcal{G}\langle\hat{Q}\rangle + \langle\hat{Q}\rangle\mathcal{G}^T + \mathcal{V}$$

$$J - \text{tr}[\hat{Q}R] \leq 2 \sum_{K=1}^r (\text{tr } \hat{P}_K) (\mathcal{G}\langle\hat{Q}\rangle)_K K$$

$$0 = A\hat{Q} + \hat{Q}A^T + \hat{H}[\hat{Q}] + \mathcal{V}$$

$$0 = A^T\hat{P} + \hat{P}A + \hat{H}[\hat{P}] + R$$

where:

$$\langle\hat{Q}\rangle \triangleq \text{off-diagonal part of } \hat{Q}$$

$$\hat{H}[\cdot] = \text{Stratonovich model operator}$$

- Tighter bound—incorporates more information on A and G
- Predicts stability when $(A + A^T)$ stable, $G = -G^T$
- "Nominal" performance, $\text{tr}[\hat{Q}R]$, given by Stratonovich model

Figure 32. The Refined Majorant Bound Incorporates a Stratonovich Covariance Model

5. Numerical Algorithms and Examples

Practical design of controllers is only possible when efficient, reliable algorithms are available. Indeed, the optimal projection equations are readily solvable and have been applied to a wide variety of examples. Numerical results appear in [A3-A6, A8, A11, A12, A14-A16, A18, A19, A21-A24, A26-A28, A30-A33, A39, A42, A44, A46]. Two distinctly different algorithms have been developed thus far, namely, an iterative method and a homotopy algorithm.

The iterative method, developed in [A14, A16, A44] and further studied in [20, 21], is outlined in Figure 33. The nice feature of this approach is that only a standard LQG software package is required for its implementation. The basic motivation for the method is the observation that the main source of coupling is via the terms involving τ_1 . The coupling is absent, of course, when τ is the identity, i.e., LQG. Note also that the terms involving τ_1 are small when R_2 and V_2 are large, i.e., when control cost is high and the measurement noise is significant. This case, which yields low-authority controllers, is approximately characterized by decoupled control-design and controller-reduction operations. Thus it is not surprising that LQG reduction techniques are most successful when controller authority is low.

Since the τ_1 terms occasion the greatest difficulty, it appears advantageous to bring them into play gradually. This can be accomplished by fixing τ after each iteration to yield updated values of Q , P , \hat{Q} and \hat{P} . Furthermore, τ is introduced gradually by means of α to reduce its rank.

The crucial step of the algorithm concerns the construction of the projection τ from the pseudogramians \hat{Q} and \hat{P} . Specifically, τ can be characterized (see [A22]) as the sum of eigenprojections of $\hat{Q}\hat{P}$, where each choice of eigenprojections may correspond to a local extremal. However, the necessary conditions do not specify which eigenprojections are to be selected for obtaining a particular local solution. Nevertheless, there do exist useful methods for constructing τ . For example, component-cost decomposition methods ([22]) when applied within the optimal projection framework often permit efficient identification of the global optimum.

Although the iterative method is convenient to use because it utilizes readily available software, it is suboptimal in the sense that it does not fully exploit the structure of the equations. Specifically, while the iterative method addresses a system of four $n \times n$ matrix equations, careful analysis reveals that because of the rank deficiency of the projection the problem can be recast as four $n_c \times n$ equations. Hence, when n_c is much smaller than n , which is clearly the most

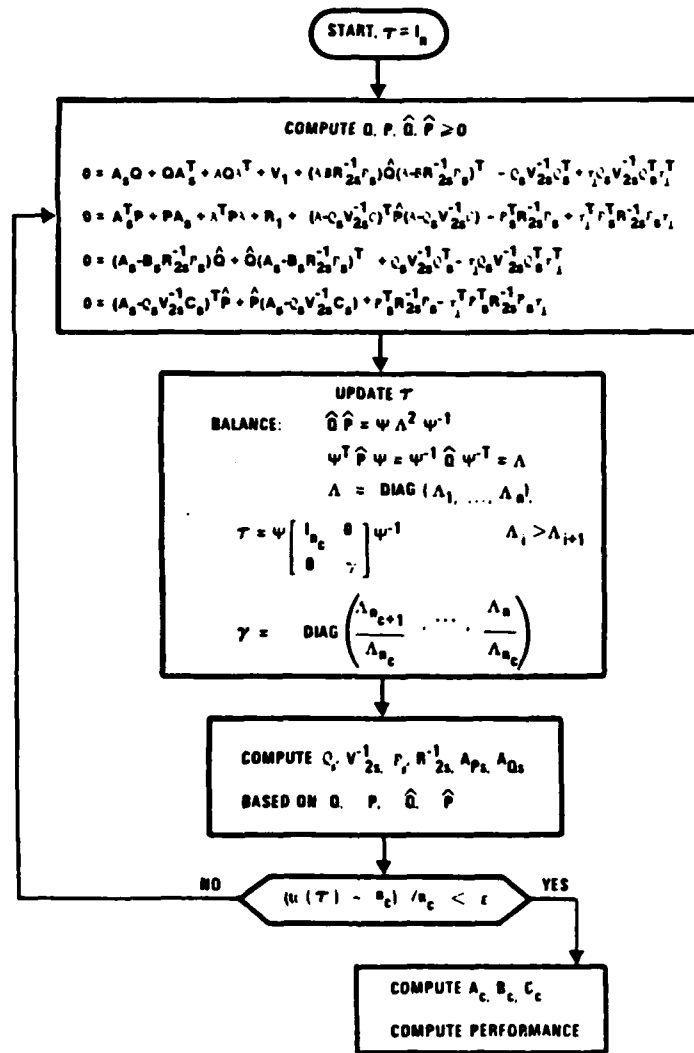


Figure 33. The Iterative Method for Solving the Robustified OPUS Design Equations Requires Only an LQG Software Package and Involves Refinement of the Optimal Projection τ

desirable case for practical implementation, there exists considerable opportunity for increased computational efficiency. Furthermore, and most satisfying, the computational complexity decreases with n_c as is intuitively expected below that required by LQG design. Hence the optimal projection approach has computational complexity less than LQG reduction methods for which LQG is but the first step.

S. Richter ([23,A46]) has developed a homotopy algorithm which fully exploits this crucial structure. Numerical experiments thus far have shown that considerable computational savings can be achieved over the iterative method. Furthermore, by applying topological degree theory to investigate the branches and character of the local extremals, it can be shown that the maximum number of possible extremals is

$$\binom{\min(n,m,l)}{n_c}$$

if $n_c \leq \min(n,m,l)$ or 1 otherwise. Hence in most practical cases the equations support a relatively small number of solutions.

Both the iterative method and the homotopy algorithm have been applied to a design problem involving an 8th-order flexible structure originally due to D. Enns and considered in [1]. Specifically, a variety of LQG reduction methods are compared in [1] for a range of controller authorities. These methods include:

1. Enns: This method is a frequency-weighted, balanced realization technique applicable to either model or controller reduction.
2. Glover: This method utilizes the theory of Hankel norm optimal approximation for controller reduction.
3. Davis and Skelton: This is a modification of compensator reduction via balancing which addresses the case of unstable controllers.
4. Yousuff and Skelton: This is a further modification of balancing for handling stable or unstable controllers.
5. Liu and Anderson: In place of using a balanced approximation of the compensator transfer function directly, this method approximates the component parts of a fractional representation of the compensator.

All of the above methods proceed by first obtaining the full-order LQG compensator design for a high-order state-space model and then reducing the dimension of the resulting LQG compensator.

Figure 34 summarizes the results reported in [1] for the above LQG reduction methods along with results obtained using the iterative method for solving the optimal projection equations. Here q_2 is a scale factor for the plant disturbance noise affecting controller authority. Clearly, LQG reduction methods experience increasing difficulty as authority increases, i.e., as the τ_1 terms become increasingly more important in coupling the control and reduction operations. For the low authority cases, the optimal projection calculations, which were performed on a Harris H800 minicomputer, appeared to incur roughly the same computational burden as the LQG reduction methods. Although the optimal projection computational burden increases with authority, comparison with the LQG reduction methods is not meaningful because of the difficulty experienced by these methods in achieving closed-loop stability. See [A44] for further details and for comparisons involving transient response.

The homotopy algorithm was also applied to the example considered in [1]. One of the main goals of the development effort was to extend the range of disturbance intensity or, equivalently, observer bandwidth, out beyond $q_2 = 2000$. To this end, second-order ($n_c = 2$) controllers were obtained with relatively little computation for $q_2 = 10,000, 100,000$ and $1,000,000$. In addition, the performance of each reduced-order controller was within 25% of LQG. These cases can surely be expected to present a nontrivial challenge to both the LQG reduction methods and the iterative optimal projection method.

Numerical solution of the robustified optimal projection equations has been carried out for several examples. For illustrative purposes a 2x2 example was considered in [A26] and the results illustrated in Figure 35 indicate performance/robustness tradeoffs possible. The variable left-shift technique was applied in [A19] to the NASA SCOLE problem with frequency uncertainties. The robustness of LQG and two robustified designs is shown in Figure 36. The plots illustrate the degradation in performance due to simultaneous perturbation of all modal frequencies. Note that LQG is rendered unstable by +5% frequency perturbation while a high-authority robustified design improves this region to +8%. The low-authority design increases this region significantly while sacrificing 6% nominal performance.

Method	$\frac{q_2}{n_c}$	0.01	0.1	1	10	100	1000	2000
Enns	7	S	S	S	S	S	S	S
	6	S	S	S	S	S	S	S
	5	S	S	S	S	S	S	S
	4	S	S	S	S	S	S	U
	3	S	S	S	S	S	S	S
	2	S	S	S	S	S	U	U
Glover	7	S	S	S	S	S	U	S
	6	S	S	S	S	U	U	U
	5	S	S	S	S	U	U	U
	4	S	S	S	S	U	U	U
	3	S	S	U	S	U	U	U
	2	S	U	S	U	S	U	U
Davis & Skelton	7	S	U	U	S	S	S	S
	6	S	S	S	S	S	S	S
	5	S	U	S	S	S	U	U
	4	S	S	U	S	S	U	U
	3	U	U	U	U	U	U	U
	2	S	U	S	U	U	U	U
Yousuff & Skelton	7	S	S	S	S	U	U	U
	6	S	S	S	S	U	U	U
	5	S	S	S	U	U	U	U
	4	S	S	S	U	U	U	U
	3	S	U	U	U	U	U	U
	2	S	S	S	U	U	U	U
Liu & Anderson	7	S	S	S	S	S	S	U
	6	S	S	S	S	S	S	S
	5	S	S	S	S	S	S	S
	4	S	S	S	S	S	S	S
	3	S	S	S	S	S	U	U
	2	S	S	S	S	S	S	S
Optimal Projection	7	S	S	S	S	S	S	S
	6	S	S	S	S	S	S	S
	5	S	S	S	S	S	S	S
	4	S	S	S	S	S	S	S
	3	S	S	S	S	S	S	S
	2	S	S	S	S	S	S	S

S - The closed-loop system is stable
 U - The closed-loop system is unstable

Figure 34. The Optimal Projection Approach Was Compared to Several LQG Reduction Techniques Over a Range of Controller Authorities for an Example of Enns

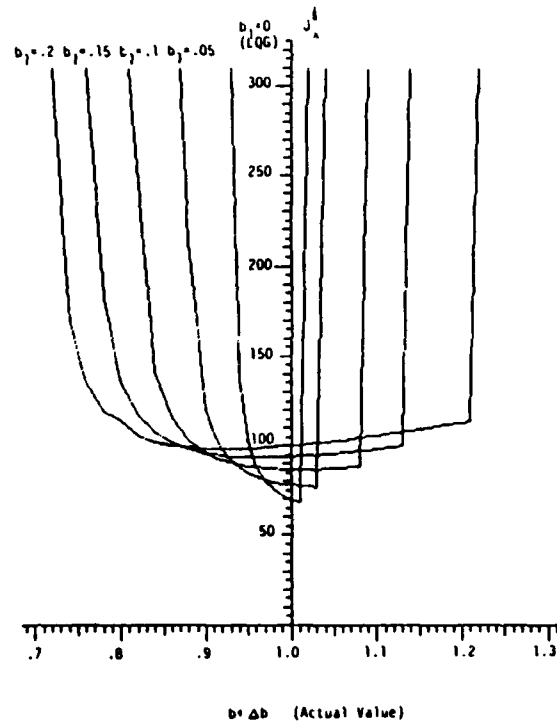


Figure 35. The Robustified Optimal Projection Equations Provide Robustness/Performance Tradeoffs for a Highly Sensitive Nominal LQG Design.

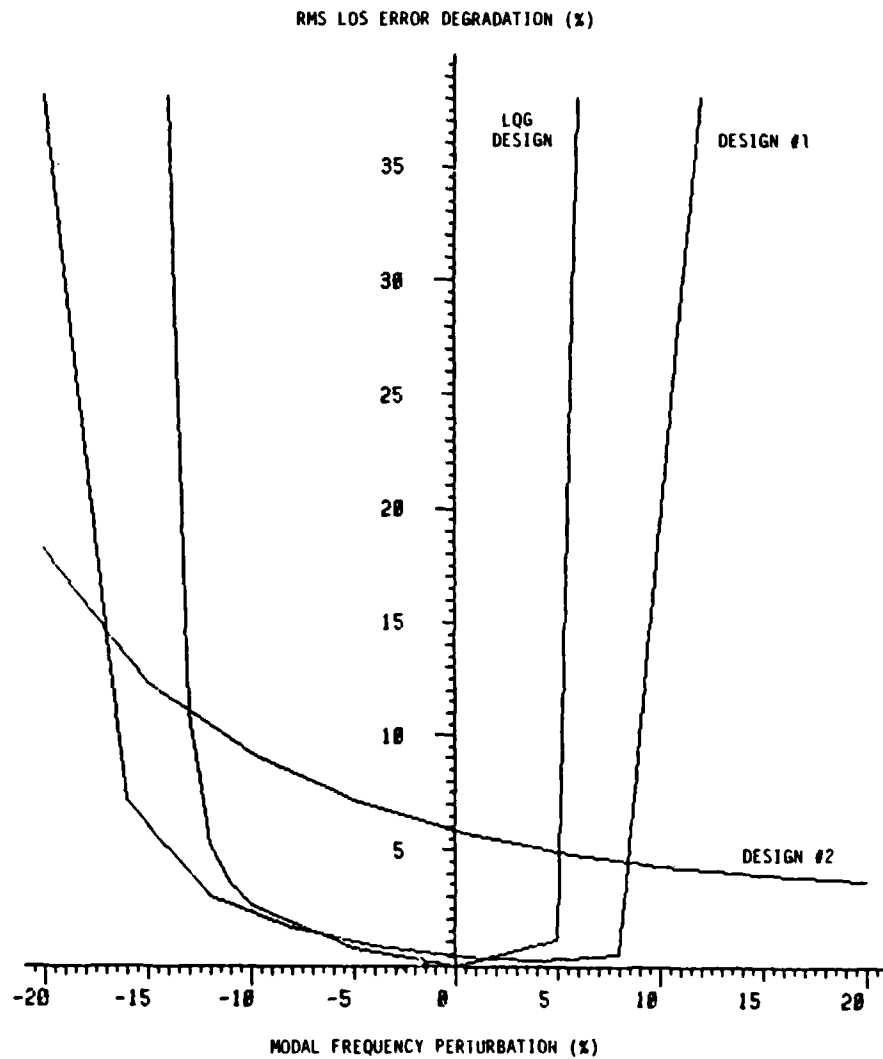


Figure 36. The Stratonovich Model Robustifies the LQG Design for the NASA SCOLE Model with Uncertain Modal Frequencies

6. Additional Extensions

The robustified optimal projection design machinery has been further extended to encompass a larger number of design cases arising in practical application. Here we merely list the extensions:

1. Discrete-time and sampled-data controllers ([A28,A30,A34,A35]).
2. Decentralized controllers ([A39]).
3. Nonstrictly proper controllers ([A37]).
4. Distributed parameter systems ([A25]).

7. Concluding Remarks

The machinery provided by OPUS for designing active controllers for flexible structures has been reviewed. The basic machinery is a system of coupled Riccati and Lyapunov equations which directly generalize the classical LQG result to include both a constraint on controller order and a model of parameter uncertainty. The overall approach thus encompasses all major design tradeoffs arising in vibration-suppression applications. Substantial numerical experience has been gained through an iterative method requiring only an LQG software package and, more recently, by means of a highly efficient homotopy algorithm developed by S. Richter. The overall approach opens the door for effective design of implementable controllers for large precision space structures.

Acknowledgment. We wish to thank Ms. Jill M. Straehle for the excellent preparation of this paper.

General References

1. Y. Liu and B. D. O. Anderson, "Controller Reduction Via Stable Factorization and Balancing," Int. J. Contr., Vol. 44, pp. 507-531, 1986.
2. G. Zames, "Feedback and Optimal Sensitivity: Model Reference Transformations, Multiplicative Seminorms, and Approximate Inverses," IEEE Trans. Autom. Contr., Vol. AC-26, pp. 301-320, 1981.
3. J. C. Doyle, "Guaranteed Margins for LQG Regulators," IEEE Trans. Autom. Contr., Vol. AC-23, pp. 756-757, 1978.
4. J. C. Doyle and G. Stein, "Multivariable Feedback Design: Concepts for a Classical/Modern Synthesis," IEEE Trans. Autom. Contr., Vol. AC-26, pp. 4-16, 1981.
5. G. Stein and M. Athans, "The LQG/LTR Procedure for Multivariable Feedback Control Design," IEEE Trans. Autom. Contr., Vol. AC-32, pp. 105-114, 1987.
6. E. Soroka and U. Shaked, "On the Robustness of LQ Regulators," IEEE Trans. Autom. Contr., Vol. AC-29, pp. 664-665, 1984.
7. U. Shaked and E. Soroka, "On the Stability Robustness of the Continuous-Time LQG Optimal Control," IEEE Trans. Autom. Contr., Vol. AC-30, 1039-1043.
8. J. C. Doyle, "Analysis of Feedback Systems with Structured Uncertainties," IEE Proc., Vol. 129, pp. 242-250, 1982.
9. S. S. L. Chang and T. K. C. Peng, "Adaptive Guaranteed Cost Control of Systems with Uncertain Parameters," IEEE Trans. Autom. Contr., Vol. AC-17, pp. 474-483, 1972.
10. A. Vinkler and L. J. Wood, "Multistep Guaranteed Cost Control of Linear Systems with Uncertain Parameters," J. Guid. Contr., Vol. 2, pp. 449-456, 1979.
11. I. R. Petersen and C. V. Hollot, "A Riccati Equation Approach to the Stabilization of Uncertain Systems," Automatica, Vol. 22, pp. 433-448, 1986.
12. D. Hinrichsen and A. J. Pritchard, "Stability Radius for Structured Perturbations and the Algebraic Riccati Equation," Sys. Contr. Lett., Vol. 8, pp. 105-113, 1986.
13. B. D. O. Anderson and J. B. Moore, Linear Optimal Control, Prentice-Hall, Englewood Cliffs, NJ, 1970.
14. G. N. Milstein, "Design of Stabilizing Controller with Incomplete State Data for Linear Stochastic System with Multiplicative Noise," Autom. Remote Contr., Vol. 43, pp. 653-659, 1982.
15. G. A. Adamian and J. S. Gibson, "Sensitivity of Closed-Loop Eigenvalues and Robustness," preprint.
16. A. M. Ostrowski, "On Some Metrical Properties of Operator Matrices and Matrices Partitioned into Blocks," J. Math. Anal. Appl., Vol. 2, pp. 161-209, 1961.
17. G. Dahlquist, "On Matrix Majorants and Minorants, with Applications to Differential Equations," Lin. Alg. Appl., Vol. 52/53, pp. 199-216, 1983.

18. D. D. Siljak, Large-Scale Dynamic Systems, Elsevier/North-Holland, 1978.
19. M. Ikeda and D. D. Siljak, "Generalized Decompositions of Dynamic Systems and Vector Lyapunov Functions," IEEE Trans. Autom. Contr., Vol. AC-26, pp. 1118-1125, 1981.
20. A. Gruzzen, "Robust Reduced Order Control of Flexible Structures," C. S. Draper Laboratory Report #CSDL-T-900, April 1986.
21. A. Gruzzen and W. E. Vander Velde, "Robust Reduced-Order Control of Flexible Structures Using the Optimal Projection/Maximum Entropy Design Methodology," AIAA Guid. Nav. Contr. Conf., Williamsburg, VA, August 1986.
22. A. Yousuff and R. E. Skelton, "Controller Reduction by Component Cost Analysis," IEEE Trans. Autom. Contr., Vol. AC-24, pp. 520-530, 1984.
23. S. Richter and R. DeCarlo, "Continuation Methods: Theory and Applications," IEEE Trans. Autom. Contr., Vol. 28, pp. 660-665, 1983.

OPUS References

- A1. D. C. Hyland, "The Modal Coordinate/Radiative Transfer Formulation of Structural Dynamics--Implications for Vibration Suppression in Large Space Platforms," MIT Lincoln Laboratory, TR-27, 14 March 1979.
- A2. D. C. Hyland, "Optimal Regulation of Structural Systems With Uncertain Parameters," MIT Lincoln Laboratory, TR-551, 2 February 1981, DDC# AD-A099111/7.
- A3. D. C. Hyland, "Active Control of Large Flexible Spacecraft: A New Design Approach Based on Minimum Information Modelling of Parameter Uncertainties," Proc. Third VPI&SU/AIAA Symposium, pp. 631-646, Blacksburg, VA, June 1981.
- A4. D. C. Hyland, "Optimal Regulator Design Using Minimum Information Modelling of Parameter Uncertainties: Ramifications of the New Design Approach," Proc. Third VPI&SU/AIAA Symposium, pp. 701-716, Blacksburg, VA, June 1981.
- A5. D. C. Hyland and A. N. Madiwale, "Minimum Information Approach to Regulator Design: Numerical Methods and Illustrative Results," Proc. Third VPI&SU/AIAA Symposium, pp. 101-118, Blacksburg, VA, June 1981.
- A6. D. C. Hyland and A. N. Madiwale, "A Stochastic Design Approach for Full-Order Compensation of Structural Systems with Uncertain Parameters," Proc. AIAA Guid. Contr. Conf., pp. 324-332, Albuquerque, NM, August 1981.
- A7. D. C. Hyland, "Optimality Conditions for Fixed-Order Dynamic Compensation of Flexible Spacecraft with Uncertain Parameters," AIAA 20th Aerospace Sciences Meeting, paper 82-0312, Orlando, FL, January 1982.
- A8. D. C. Hyland, "Structural Modeling and Control Design Under Incomplete Parameter Information: The Maximum Entropy Approach," AFOSR/NASA Workshop in Modeling, Analysis and Optimization Issues for Large Space Structures, Williamsburg, VA, May 1982.
- A9. D. C. Hyland, "Minimum Information Stochastic Modelling of Linear Systems with a Class of Parameter Uncertainties," Proc. Amer. Contr. Conf., pp. 620-627, Arlington, VA, June 1982.

- A10. D. C. Hyland, "Maximum Entropy Stochastic Approach to Control Design for Uncertain Structural Systems," Proc. Amer. Contr. Conf., pp. 680-688, Arlington, VA, June 1982.
- A11. D. C. Hyland, "Minimum Information Modeling of Structural Systems with Uncertain Parameters," Proceedings of the Workshop on Applications of Distributed System Theory to the Control of Large Space Structures, G. Rodriguez, ed., pp. 71-88, JPL, Pasadena, CA, July 1982.
- A12. D. C. Hyland and A. N. Madiwale, "Fixed-Order Dynamic Compensation Through Optimal Projection," Proceedings of the Workshop on Applications of Distributed System Theory to the Control of Large Space Structures, G. Rodriguez, ed., pp. 409-427, JPL, Pasadena, CA, July 1982.
- A13. D. C. Hyland, "Mean-Square Optimal Fixed-Order Compensation--Beyond Spillover Suppression," paper 1403, AIAA Astrodynamics Conference, San Diego, CA, August 1982.
- A14. D. C. Hyland, "The Optimal Projection Approach to Fixed-Order Compensation: Numerical Methods and Illustrative Results," AIAA 21st Aerospace Sciences Meeting, paper 83-0303, Reno, NV, January 1983.
- A15. D. C. Hyland, "Mean-Square Optimal, Full-Order Compensation of Structural Systems with Uncertain Parameters," MIT Lincoln Laboratory, TR-626, 1 June 1983.
- A16. D. C. Hyland, "Comparison of Various Controller-Reduction Methods: Suboptimal Versus Optimal Projection," Proc. AIAA Dynamics Specialists Conf., pp. 381-389, Palm Springs, CA, May 1984.
- A17. D. C. Hyland and D. S. Bernstein, "The Optimal Projection Equations for Fixed-Order Dynamic Compensation," IEEE Trans. Autom. Contr., Vol. AC-29, pp. 1034-1037, 1984.
- A18. D. C. Hyland, "Application of the Maximum Entropy/Optimal Projection Control Design Approach for Large Space Structures," Proc. Large Space Antenna Systems Technology Conference, pp. 617-654, NASA Langley, December 1984.
- A19. L. D. Davis, D. C. Hyland and D. S. Bernstein, "Application of the Maximum Entropy Design Approach to the Spacecraft Control Laboratory Experiment (SCOLE)," Final Report, NASA Langley, January 1985.
- A20. D. S. Bernstein and D. C. Hyland, "The Optimal Projection Equations for Reduced-Order State Estimation," IEEE Trans. Autom. Contr., Vol. AC-30, pp. 583-585, 1985.
- A21. D. S. Bernstein and D. C. Hyland, "Optimal Projection/Maximum Entropy Stochastic Modelling and Reduced-Order Design Synthesis," Proc. IFAC Workshop on Model Error Concepts and Compensation, Boston, MA, June 1985, pp. 47-54, R. E. Skelton and D. H. Owens, eds., Pergamon Press, Oxford, 1986.
- A22. D. C. Hyland and D. S. Bernstein, "The Optimal Projection Equations for Model Reduction and the Relationships Among the Methods of Wilson, Skelton and Moore," IEEE Trans. Autom. Contr., Vol. AC-30, pp. 1201-1211, 1985.
- A23. D. S. Bernstein and D. C. Hyland, "The Optimal Projection/Maximum Entropy Approach to Designing Low-Order, Robust Controllers for Flexible Structures," Proc. 24th IEEE Conf. Dec. Contr., pp. 745-752, Fort Lauderdale, FL, December 1985.

- A24. D. S. Bernstein, L. D. Davis, S. W. Greeley and D. C. Hyland, "Numerical Solution of the Optimal Projection/Maximum Entropy Design Equations for Low-Order, Robust Controller Design," Proc. 24th IEEE Conf. Dec. Contr., pp. 1795-1798, Fort Lauderdale, FL, December 1985.
- A25. D. S. Bernstein and D. C. Hyland, "The Optimal Projection Equations for Finite-Dimensional Fixed-Order Dynamic Compensation of Infinite-Dimensional Systems," SIAM J. Contr. Optim., Vol. 24, pp. 122-151, 1986.
- A26. D. S. Bernstein and S. W. Greeley, "Robust Controller Synthesis Using the Maximum Entropy Design Equations," IEEE Trans. Autom. Contr., Vol. AC-31, pp. 362-364, 1986.
- A27. D. C. Hyland, D. S. Bernstein, L. D. Davis, S. W. Greeley and S. Richter, "MEOP: Maximum Entropy/Optimal Projection Stochastic Modelling and Reduced-Order Design Synthesis," Final Report, Air Force Office of Scientific Research, Bolling AFB, Washington, DC, April 1986.
- A28. D. S. Bernstein, L. D. Davis and D. C. Hyland, "The Optimal Projection Equations for Reduced-Order, Discrete-Time Modelling, Estimation and Control," J. Guid. Contr. Dyn., Vol. 9, pp. 288-293, 1986.
- A29. D. S. Bernstein and S. W. Greeley, "Robust Output-Feedback Stabilization: Deterministic and Stochastic Perspectives," Proc. Amer. Contr. Conf., pp. 1818-1826, Seattle, WA, June 1986.
- A30. D. S. Bernstein, L. D. Davis and S. W. Greeley, "The Optimal Projection Equations for Fixed-Order, Sampled-Data Dynamic Compensation with Computation Delay," IEEE Trans. Autom. Contr., Vol. AC-31, pp. 859-862, 1986.
- A31. D. S. Bernstein, "OPUS: Optimal Projection for Uncertain Systems," Annual Report, Air Force Office of Scientific Research, Bolling AFB, Washington, DC, October 1986.
- A32. B. J. Boan and D. C. Hyland, "The Role of Metal Matrix Composites for Vibration Suppression in Large Space Structures," Proc. MMC Spacecraft Survivability Tech. Conf., NMCIAAC Kaman Tempo Publ., Stanford Research Institute, Palo Alto, CA, October 1986.
- A33. D. C. Hyland, "An Experimental Testbed for Validation of Control Methodologies in Large Space Optical Structures," SPIE Optoelectronics and Laser Applications Conference, Los Angeles, CA, January 1987.
- A34. W. M. Haddad and D. S. Bernstein, "The Optimal Projection Equations for Discrete-Time Reduced-Order State Estimation for Linear Systems with Multiplicative White Noise," Sys. Contr. Lett., 1987.
- A35. D. S. Bernstein and W. M. Haddad, "The Optimal Projection Equations for Discrete-Time Fixed-Order Dynamic Compensation of Linear Systems with Multiplicative White Noise," Int. J. Contr., 1987.
- A36. W. M. Haddad and D. S. Bernstein, "The Optimal Projection Equations for Reduced-Order State Estimation: The Singular Measurement Noise Case," IEEE Trans. Autom. Contr., 1987.
- A37. D. S. Bernstein, "The Optimal Projection Equations for Static and Dynamic Output Feedback: The Singular Case," IEEE Trans. Autom. Contr., 1987.

- A38. D. S. Bernstein and D. C. Hyland, "The Optimal Projection Equations for Reduced-Order Modelling, Estimation and Control of Linear Systems with Multiplicative White Noise," J. Optim. Thy. Appl., 1987.
- A39. D. S. Bernstein, "Sequential Design of Decentralized Dynamic Compensators Using the Optimal Projection Equations," Int. J. Contr., 1987.
- A40. D. S. Bernstein and W. M. Haddad, "Optimal Output Feedback for Nonzero Set Point Regulation," Proc. Amer. Contr. Conf., Minneapolis, MN, June 1987.
- A41. D. S. Bernstein, "Robust Static and Dynamic Output-Feedback Stabilization: Deterministic and Stochastic Perspectives," IEEE Trans. Autom. Contr., 1987.
- A42. D. C. Hyland and D. S. Bernstein, "The Majorant Lyapunov Equation: A Nonnegative Matrix Equation for Guaranteed Robust Stability and Performance of Large Scale Systems," IEEE Trans. Autom. Contr., 1987.
- A43. D. S. Bernstein and W. M. Haddad, "The Optimal Projection Equations with Petersen-Hollot Bounds: Robust Controller Synthesis with Guaranteed Structured Stability Radius," submitted.
- A44. S. W. Greeley and D. C. Hyland, "Reduced-Order Compensation: LQG Reduction Versus Optimal Projection," submitted.
- A45. W. M. Haddad, Robust Optimal Projection Control-System Synthesis, Ph.D. Dissertation, Department of Mechanical Engineering, Florida Institute of Technology, Melbourne, FL, March 1987.
- A46. S. Richter, "A Homotopy Algorithm for Solving the Optimal Projection Equations for Fixed-Order Dynamic Compensation: Existence, Convergence and Global Optimality," Proc. Amer. Contr. Conf., Minneapolis, MN, June 1987.

APPENDIX B

**The Majorant Lyapunov Equation: A Nonnegative
Matrix Equation for Robust Stability and
Performance of Large Scale Systems**

The Majorant Lyapunov Equation: A Nonnegative Matrix Equation for Robust Stability and Performance of Large Scale Systems

DAVID C. HYLAND AND DENNIS S. BERNSTEIN, MEMBER, IEEE

Abstract—A new robust stability and performance analysis technique is developed. The approach involves replacing the state covariance by its block-norm matrix, i.e., the nonnegative matrix whose elements are the norms of subblocks of the covariance matrix partitioned according to subsystem dynamics. A bound (i.e., majorant) for the block-norm matrix is given by the majorant Lyapunov equation, a Lyapunov-type nonnegative matrix equation. Existence, uniqueness, and computational tractability of solutions to the majorant Lyapunov equation are shown to be completely characterized in terms of M matrices. Two examples are considered. For a damped simple harmonic oscillator with uncertain but constant natural frequency, the majorant Lyapunov equation predicts unconditional stability. And, for a pair of nominally uncoupled oscillators with uncertain coupling, the majorant Lyapunov equation shows that the range of nondestabilizing couplings is proportional to the frequency separation between the oscillators, a result not predictable from quadratic or vector Lyapunov functions.

I. INTRODUCTION

THE importance of robustness in control-system analysis and design cannot be overemphasized. The past ten years' literature reflects considerable frequency-domain development [1]–[11], while recent publications indicate increasing time-domain activity [12]–[19]. Wide variations in underlying assumptions, mathematical settings, and problem data render it difficult, if not impossible, to clearly delineate the relative effectiveness of different methods. Our own philosophical outlook has thus been guided by two general criteria:

- 1) effectiveness for simple examples;
- 2) efficiency when applied to large scale problems.

The first criterion involves applying robustness techniques to simple, perhaps trivially obvious, examples to serve as "acid tests." A given method's effectiveness on a collection of such examples can possibly reveal inherent shortcomings. As an illustration of this criterion, consider a damped harmonic oscillator with constant but uncertain natural frequency. Using the notation of [6], stability is guaranteed so long as

$$\sigma_{\max}[R(j\omega)(I + G(j\omega)K(j\omega))^{-1}G(j\omega)L^{-1}(j\omega)] < 1, \quad \omega \geq 0 \quad (1.1)$$

where, for $\nu > 0$,

$$G(s) = (s^2 + 2\nu s + \omega_n^2)^{-1}$$

Manuscript received August 8, 1986; revised May 6, 1987. Paper recommended by Associate Editor, M. G. Safonov. This work was supported in part by the Air Force Office of Scientific Research under Contracts F49620-86-C-0002 and F49620-86-C-0038.

The authors are with the Government Aerospace Systems Division, Harris Corporation, Melbourne, FL 32902.
IEEE Log Number 8716541.

and uncertainty in the nominal natural frequency ω_n is modeled by

$$\Delta(s) = L^{-1}(s)\theta(s)R(s) = \delta\omega_n^2,$$

$$L(s) = 1/\alpha, \quad \theta(s) = \delta/\alpha, \quad R(s) = \omega_n^2, \quad K(s) = 0,$$

$$\delta \in [-\min(1, \alpha), \alpha], \quad \alpha > 0.$$

Note that

$$\sigma_{\max}[\theta(j\omega)] \leq 1, \quad \omega \geq 0$$

as required in [6]. The perturbation $\Delta(s)$ (modeled as a feedback gain) effectively replaces ω_n^2 in $G(s)$ by $(1 + \delta)\omega_n^2$. Hence, for a given $\alpha > 0$ this uncertainty model permits perturbed natural frequencies in the range $[0, (1 + \alpha)^{1/2}\omega_n]$. Evaluating (1.1) yields the upper bound

$$\alpha < [(\omega_n^2 - \omega^2)^2 + 4\nu^2\omega^2]^{1/2}/\omega_n^2, \quad \omega \geq 0 \quad (1.2)$$

or, equivalently,

$$\alpha < 2\xi(1 - \xi^2)^{1/2} \quad (1.3)$$

where $\xi \equiv \nu/\omega_n$. The conservatism of (1.3) is obviously most pronounced when the damping ratio ξ is small. In all cases, however, the conservatism is infinite.

The second criterion is obviously subjective and depends upon a variety of factors such as problem structure, designer experience, and computational resources. This criterion is, in our opinion, most important since the need for robustness techniques becomes increasingly critical as system complexity grows. Indeed, the ultimate test of a given approach is to scale it up to larger and larger problems to reveal inherent limitations. Obviously, such tests are not only difficult, but may entail a significant commitment of human and financial resources. Nevertheless, crude predictions are sometimes available, and a case in point is the "curse of dimensionality" encountered in the approach of [9]. Another example involves computational difficulties in obtaining bounds for the μ -function with more than three blocks [10].

The contribution of the present paper is a new robustness analysis method developed specifically for large scale systems. The basic idea, motivated by the work of Siljak [30] on connective stability, is as follows. The system is assumed to be in the form of a collection of subsystems with uncertain local dynamics and uncertain interactions. Parameter uncertainties are modeled as either structured or unstructured constant variations contained in prescribed sets. The state covariance, partitioned conformably with the subsystem dynamics, is replaced by its *block-norm matrix*, i.e., the nonnegative matrix each of whose elements is the norm of the corresponding subblock of the original matrix. This nonnegative matrix satisfies a novel inequality designated the

¹ Uncertainties in a single subsystem can also be regarded as interaction uncertainties. To see this, write $x = (A + G)x$ twice so that the uncertainty G is represented by $\begin{bmatrix} 0 & G \\ G & 0 \end{bmatrix}$.

\mathbb{E}	expected value
$\mathbb{R}, \mathbb{R}^{p \times q}, \mathbb{R}^p$	real numbers, $p \times q$ real matrices, $\mathbb{R}^{p \times 1}$
$I_p, O_{p \times q}, O_p$	$p \times p$ identity matrix, $p \times q$ zero matrix, $O_{p \times p}$
\bullet, \otimes	Kronecker sum, Kronecker product [24]-[27]
*	Hadamard product [27], [28]
col, (Z)	i th column of matrix Z
vec (Z)	$\begin{bmatrix} \text{col}_1(Z) \\ \vdots \\ \text{col}_q(Z) \end{bmatrix} \in \mathbb{R}^{pq}, Z \in \mathbb{R}^{p \times q}$
$Z_{(i,j)}$	(i, j) element of matrix Z
Z^T	transpose of vector or matrix Z
$(Z^T)^{-1}$ or $(Z^{-1})^T$	
tr Z	trace of matrix Z
diag (Z_1, \dots, Z_p)	diagonal matrix with listed diagonal elements
block-diag (Z_1, \dots, Z_p)	block-diagonal matrix with listed diagonal blocks
$\rho(Z)$	spectral radius of Z
asymptotically stable matrix	matrix with eigenvalues in open left-half plane
nonnegative-definite matrix	symmetric matrix with nonnegative eigenvalues ($Z \geq 0$)
positive-definite matrix	symmetric matrix with positive eigenvalues ($Z > 0$)
$Z_1 \geq Z_2$	$Z_1 - Z_2 \geq 0, Z_1, Z_2$ symmetric
$Z_1 > Z_2$	$Z_1 - Z_2 > 0, Z_1, Z_2$ symmetric
nonnegative matrix	matrix with nonnegative elements ($Z \geq 0$) [29], [30]
positive matrix	matrix with positive elements ($Z \gg 0$)
$Z_1 \geq Z_2$	$Z_1 - Z_2 \geq 0$
$Z_1 \gg Z_2$	$Z_1 - Z_2 \gg 0$
Z^{HI}	Hadamard inverse, $(Z^{HI})_{(i,j)} \triangleq [Z_{(i,j)}]^{-1}, Z \gg 0$
block-norm matrix	nonnegative matrix each of whose elements is the norm of a corresponding subblock of a given partitioned matrix
majorant	nonnegative matrix each of whose elements bounds the corresponding element of a block-norm matrix
$\ Z\ _2$	Euclidean norm of vector Z
$\sigma_i(Z)$	singular value of matrix Z
$\sigma_{\min}(Z), \sigma_{\max}(Z)$	smallest and largest singular values of matrix Z
$\lambda_{\max}(Z)$	largest eigenvalue of symmetric matrix Z
$\ Z\ _s$	$\sigma_{\max}(Z)$ (spectral norm induced by $\ \cdot\ _2$)
$\ Z\ _F$	$(\text{tr } ZZ^T)^{1/2} = \left[\sum_{i,j=1}^{p,q} Z_{(i,j)}^2 \right]^{1/2}$ $= \left[\sum_{i=1}^p \sigma_i^2 \right]^{1/2}$ (Frobenius norm [34]).

In subsequent sections we shall exploit the fact that the norms $\|\cdot\|_2, \|\cdot\|_s$, and $\|\cdot\|_F$ coincide for vectors. Hence, if $Z \in \mathbb{R}^p$, then by interpreting $\mathbb{R}^p = \mathbb{R}^{p \times 1}$ it follows that

$$\|Z\|_2 = \|Z\|_s = \|Z\|_F. \quad (2.1)$$

Furthermore, if $Z \in \mathbb{R}^{p \times q}$, then

$$\|Z\|_s \leq \|Z\|_F = \|\text{vec } Z\|_F = \|\text{vec } Z\|_2 = \|\text{vec } Z\|_s. \quad (2.2)$$

Lemma 2.1: If $Z \in \mathbb{R}^{p \times q}$ and $\hat{Z} \in \mathbb{R}^{q \times r}$ then

$$\sigma_{\min}(Z) \|\hat{Z}\|_F \leq \|ZZ\hat{Z}\|_F \leq \|Z\|_s \|\hat{Z}\|_F. \quad (2.3, 2.4)$$

If, furthermore, $p = q = r$, $Z \geq 0$, and \hat{Z} is symmetric, then

$$\text{tr } Z\hat{Z} \leq (\text{tr } Z) \lambda_{\max}(\hat{Z}) \leq (\text{tr } Z) \|\hat{Z}\|_s. \quad (2.5)$$

Proof: Inequality (2.4) can be found in [35, p. 263]. To prove (2.3), note that when Z is singular the result is immediate. Otherwise, if $p = q$ replace Z and \hat{Z} in (2.4) by Z^{-1} and $Z\hat{Z}$, respectively. The result now follows from $[\sigma_{\max}(Z)]^{-1} = \sigma_{\min}(Z^{-1})$. If $p \neq q$, then related arguments apply. Finally, (2.5) is given in [36]. \square

Recall [30] that a matrix $S \in \mathbb{R}^{r \times r}$ is an N matrix if $S_{(i,j)} \leq 0, i, j = 1, \dots, r, i \neq j$. If, in addition, all principal minors of S are positive, then S is an M matrix.

Lemma 2.2: Suppose $S \in \mathbb{R}^{r \times r}$ is an N matrix. Then the following are equivalent:

- i) S is an M matrix;
- ii) $\det S \neq 0$ and $S^{-1} \geq 0$;
- iii) for each $y \in \mathbb{R}^r, y \geq 0$, there exists a unique $x \in \mathbb{R}^r, x \geq 0$, such that $Sx = y$;
- iv) there exists $x \in \mathbb{R}^r, x \geq 0$, such that $Sx \gg 0$;
- v) $I, *S \gg 0$ and each diagonal matrix $D \gg I, *S$ satisfies $\rho[D^{-1}(I, *S - S)] < 1$.

Proof: The equivalence of statements i), ii), iv), and v) follows from [30, p. 396]. The implication ii) \Rightarrow iii) is immediate, and iii) \Rightarrow iv) follows by setting $y = [1 \ 1 \ \dots \ 1]^T$. \square

Lemma 2.3: Suppose $S \in \mathbb{R}^{r \times r}$ is an M matrix and let $\hat{S} \in \mathbb{R}^{r \times r}$ be an N matrix such that $\hat{S} \geq S$. Then \hat{S} is an M matrix.

Proof: See [30, p. 400]. \square

III. ROBUST STABILITY AND PERFORMANCE BOUNDS

Consider the n th-order homogeneous system²

$$\dot{x}(t) = (A(\theta) + G)x(t), \quad t \in [0, \infty), \quad (3.1)$$

$$G \in \mathfrak{G} \subset \mathbb{R}^{n \times n}, \quad (3.2)$$

$$\theta \in \Theta \subset \mathbb{R}^m, \quad (3.3)$$

where $A: \Theta \rightarrow \mathbb{R}^{n \times n}$ is continuous, $\bar{A} \triangleq A(\bar{\theta})$ denotes the known nominal dynamics for $\bar{\theta} \in \Theta$, θ denotes the unstructured parametric uncertainty in \bar{A} , G denotes the structured parametric uncertainty in \bar{A} , and $0 \in \mathfrak{G}$ is the nominal value of G . We first consider the stability of (3.1) over \mathfrak{G} and Θ .

Definition 3.1: If $A(\theta) + G$ is asymptotically stable for all $G \in \mathfrak{G}$ and $\theta \in \Theta$, then the homogeneous system (3.1) is *robustly stable* over \mathfrak{G} and Θ .

Now consider the n th-order nonhomogeneous system

$$\dot{x}(t) = (A(\theta) + G)x(t) + w(t), \quad t \in [0, \infty) \quad (3.4)$$

where $G \in \mathfrak{G}, \theta \in \Theta$, and $w(\cdot)$ is white noise with intensity $V \geq 0$. For given $G \in \mathfrak{G}$ and $\theta \in \Theta$, the steady-state average quadratic performance is defined by

$$J(G, \theta) \triangleq \limsup_{t \rightarrow \infty} \mathbb{E}[x^T(t)Rx(t)] \quad (3.5)$$

where $R = R^T \geq 0$. The system (3.4) may, for example, denote a control system in closed-loop configuration. There is no need in our development, however, to make such distinctions.

In practice, steady-state performance is only of interest when the system is robustly stable. The following result is immediate.

Proposition 3.1: Suppose the system (3.1) is robustly stable

² Upon first reading the uncertainty represented by (3.3) can be ignored since the principal contribution concerns the treatment of (3.2).

over \mathfrak{G} and Θ . Then for each $G \in \mathfrak{G}$ and $\theta \in \Theta$,

$$J(G, \theta) = \text{tr } QR \quad (3.6)$$

where $n \times n$ nonnegative-definite Q is the unique solution to

$$0 = (A(\theta) + G)Q + Q(A(\theta) + G)^T + V. \quad (3.7)$$

We shall only be concerned with the case in which \mathfrak{G} and Θ are compact. Since Q is a continuous function of G and θ , we can define the worst-case average steady-state quadratic performance

$$J_{\max} \triangleq \max_{G \in \mathfrak{G}, \theta \in \Theta} J(G, \theta). \quad (3.8)$$

Since it is difficult to determine J_{\max} explicitly, we shall seek upper bounds.

Definition 3.2: If $J_{\max} \leq \hat{\alpha}$, then $\hat{\alpha}$ is a performance bound for the nonhomogeneous system (3.4) over \mathfrak{G} and Θ .

IV. SYSTEM STRUCTURE, UNCERTAINTY CHARACTERIZATION, AND THE COVARIANCE BLOCK-NORM INEQUALITY

As discussed in Section I, (3.1) and (3.4) are assumed to be in the form of a large scale system with uncoupled local dynamics and uncertain interactions. Hence, with the subsystem partitioning

$$n = \sum_{i=1}^r n_i \quad (4.1)$$

the local system dynamics $A(\theta)$ can be decomposed into subsystem dynamics according to

$$A(\theta) = \text{block-diag} \{A_i(\theta)\}_{i=1, \dots, r} \quad (4.2)$$

where $A_i(\theta) \in \mathbb{R}^{n_i \times n_i}$, $\theta \in \Theta$. For convenience, denote

$$\bar{A} \triangleq \text{block-diag} \{\bar{A}_i\}_{i=1, \dots, r}$$

Accordingly, R is assumed to be of the form

$$R = \text{block-diag} \{R_i\}_{i=1, \dots, r} \quad (4.3)$$

where $R_i \in \mathbb{R}^{n_i \times n_i}$, $R_i \geq 0$, $i = 1, \dots, r$. The intensity V and steady-state covariance Q satisfying (3.7) are assumed to be conformably partitioned, i.e.,

$$V = \{V_{ij}\}_{i,j=1}^r, \quad V_{ij} \in \mathbb{R}^{n_i \times n_j}, \quad (4.4)$$

$$Q = \{Q_{ij}\}_{i,j=1}^r, \quad Q_{ij} \in \mathbb{R}^{n_i \times n_j}. \quad (4.5)$$

For notational simplicity define

$$V_i \triangleq V_{ii}, \quad Q_i \triangleq Q_{ii}, \quad i = 1, \dots, r. \quad (4.6)$$

Taking the Frobenius norm of each subblock of V and Q leads to the $r \times r$ symmetric nonnegative matrices \mathcal{V} and \mathcal{Q} defined by

$$\mathcal{V} \triangleq \{\|V_{ij}\|_F\}_{i,j=1}^r, \quad \mathcal{Q} \triangleq \{\|Q_{ij}\|_F\}_{i,j=1}^r. \quad (4.7)$$

Note that

$$\|\mathcal{Q}\|_F = \|Q\|_F, \quad \|\mathcal{V}\|_F = \|V\|_F. \quad (4.8)$$

A few observations concerning the nominal system, i.e., with $G = 0$ and $\theta = \bar{\theta}$, are worth noting. If \bar{A} is stable then so is \bar{A}_i , $i = 1, \dots, r$, and there exist unique, nonnegative-definite \bar{Q}_i , $\bar{\beta}_i \in \mathbb{R}^{n_i \times n_i}$, $i = 1, \dots, r$, satisfying

$$0 = \bar{A}_i \bar{Q}_i + \bar{Q}_i \bar{A}_i^T + V_i, \quad (4.9)$$

$$0 = \bar{A}_i^T \bar{\beta}_i + \bar{\beta}_i \bar{A}_i + R_i. \quad (4.10)$$

Proposition 4.1: Suppose \bar{A} is asymptotically stable. Then the nominal performance J_{nom} is given by

$$J_{\text{nom}} \triangleq J(0, \bar{\theta}) = \sum_{i=1}^r \text{tr } \bar{Q}_i R_i = \sum_{i=1}^r \text{tr } \bar{\beta}_i V_i. \quad (4.11)$$

Proof: First note that with $G = 0$ and $\theta = \bar{\theta}$ the diagonal blocks of Q satisfying (3.7) coincide with $\bar{Q}_1, \dots, \bar{Q}_r$. Thus

$$\begin{aligned} J(0, \bar{\theta}) &= \sum_{i=1}^r \text{tr } \bar{Q}_i R_i \\ &= \sum_{i=1}^r (\text{vec } \bar{Q}_i)^T \text{vec } R_i \\ &= \sum_{i=1}^r [(\bar{A}_i \oplus \bar{A}_i)^{-1} \text{vec } V_i]^T \text{vec } R_i \\ &= \sum_{i=1}^r (\text{vec } V_i)^T (\bar{A}_i^T \oplus \bar{A}_i^T)^{-1} \text{vec } R_i \\ &= \sum_{i=1}^r (\text{vec } V_i)^T \text{vec } \bar{\beta}_i \\ &= \sum_{i=1}^r \text{tr } \bar{\beta}_i V_i. \quad \square \end{aligned}$$

The matrices $G \in \mathfrak{G}$ are also conformably partitioned so that

$$G = \{G_{ij}\}_{i,j=1}^r, \quad G_{ij} \in \mathbb{R}^{n_i \times n_j} \quad (4.12)$$

and \mathfrak{G} is characterized by

$$\mathfrak{G} \triangleq \{G \in \mathbb{R}^{n \times n} : \sigma_{\max}(G_{ij}) \leq \gamma_{ij}, \quad i, j = 1, \dots, r\} \quad (4.13)$$

where $\gamma_{ij} \geq 0$, $i, j = 1, \dots, r$, are given constants. For convenience, define the $r \times r$ nonnegative matrix

$$\mathcal{G} \triangleq \{\gamma_{ij}\}_{i,j=1}^r. \quad (4.14)$$

The bound \mathcal{G} is a matrix majorant for $G \in \mathfrak{G}$ in the sense of [21]–[23].

Remark 4.1: \mathfrak{G} is compact and convex.

Finally, let symmetric, positive $\mathcal{Q} \in \mathbb{R}^{r \times r}$ satisfy

$$\mathcal{Q}_{(i,j)} \leq \min_{\theta \in \Theta} \{\sigma_{\min}(A_i(\theta) \oplus A_i(\theta))\}, \quad i, j = 1, \dots, r. \quad (4.15)$$

Proposition 4.2: Let $G \in \mathfrak{G}$ and $\theta \in \Theta$ be such that $A(\theta) + G$ is asymptotically stable and let $n \times n$ $Q \geq 0$ satisfy (3.7). Then Q defined by (4.7) satisfies

$$\mathcal{Q} * \mathcal{Q} \leq \mathcal{G} \mathcal{Q} + \mathcal{Q} \mathcal{G}^T + \mathcal{V} \quad (4.16)$$

or, equivalently,

$$\bar{\mathcal{A}} \text{vec } Q \leq \text{vec } \mathcal{V}, \quad (4.17)$$

where

$$\bar{\mathcal{A}} \triangleq [\text{diag}(\text{vec } \mathcal{Q})] - \mathcal{G} \oplus \mathcal{G}. \quad (4.18)$$

Proof: Expanding (3.7) yields

$$- [A_i(\theta) Q_{ij} + Q_{ij} A_j^T(\theta)] = \sum_{k=1}^r [G_{ik} Q_{kj} + Q_{ik} G_{jk}^T] + V_i, \quad i, j = 1, \dots, r. \quad (4.19)$$

Bounding the right-hand side of (4.19) from above using (2.4) yields for all $G \in \mathfrak{G}$

$$\left\| \sum_{k=1}^r [G_{ik} Q_{kj} + Q_{ik} G_{jk}^T] + V_{ij} \right\|_F \leq \sum_{k=1}^r [S_{(i,k)} Q_{(k,j)} + Q_{(i,k)} S_{(j,k)}] + \mathcal{V}_{(i,j)}$$

while bounding the left-hand side of (4.19) from below using (2.3) implies for all $\theta \in \Theta$

$$\begin{aligned} \|[A_i(\theta)Q_{ij} + Q_{ij}A_j^T(\theta)]\|_F &= \|\text{vec}(A_i(\theta)Q_{ij} + Q_{ij}A_j^T(\theta))\|_F \\ &= \|(A_i(\theta) \otimes A_i(\theta)) \text{vec } Q_{ij}\|_F \\ &\geq \sigma_{\min}(A_i(\theta) \otimes A_i(\theta)) \|\text{vec } Q_{ij}\|_F \\ &= \sigma_{\min}(A_i(\theta) \otimes A_i(\theta)) Q_{(i,j)} \\ &\geq \alpha_{(i,j)} Q_{(i,j)}. \end{aligned}$$

Combining the above inequalities yields (4.16). \square

Remark 4.2: Since $\mathcal{G} \geq 0$, the $r^2 \times r^2$ matrix \mathbb{A} is an N matrix [30].

V. THE MAJORANT LYAPUNOV EQUATION

In this section we interpret (4.16) as an equality rather than an inequality and consider the Lyapunov-type nonnegative matrix equation

$$\alpha * \tilde{Q} = \mathcal{G}\tilde{Q} + \tilde{Q}\mathcal{G}^T + \mathcal{V} \tag{5.1}$$

or, equivalently,

$$\mathbb{A} \text{vec } \tilde{Q} = \text{vec } \mathcal{V}. \tag{5.2}$$

Note that since α and \mathcal{V} are symmetric a unique solution of (5.1) is necessarily symmetric.

Proposition 5.1: The following are equivalent:

- i) \mathbb{A} is an M matrix;
- ii) $\det \mathbb{A} \neq 0$ and $\mathbb{A}^{-1} \geq 0$;
- iii) for each $r \times r$ symmetric $\mathcal{V} \geq 0$ there exists a unique $r \times r$ $\tilde{Q} \geq 0$ satisfying (5.1);
- iv) there exist $r \times r$ symmetric $\mathcal{V} \succ 0$ and $r \times r$ symmetric $\tilde{Q} \geq 0$ satisfying (5.1);
- v) $\text{diag}(\text{vec } \alpha) - (I_r * \mathcal{G}) \otimes (I_r * \mathcal{G}) \succ 0$ and each diagonal matrix $\mathcal{D} \geq \text{diag}(\text{vec } \alpha) - (I_r * \mathcal{G}) \otimes (I_r * \mathcal{G})$ satisfies

$$\rho(\mathcal{D}^{-1}[\mathcal{G} \otimes \mathcal{G} - (I_r * \mathcal{G}) \otimes (I_r * \mathcal{G})]) < 1; \tag{5.3}$$

vi) for each $r \times r$ symmetric $\tilde{Q}_0 \geq 0$ and $r \times r$ symmetric $\mathcal{V} \geq 0$, the sequence $\{\tilde{Q}_i\}_{i=0}^\infty$ generated by

$$\begin{aligned} \alpha * \tilde{Q}_{i+1} - (I_r * \mathcal{G})\tilde{Q}_{i+1} - \tilde{Q}_{i+1}(I_r * \mathcal{G}) \\ = (\mathcal{G} - I_r * \mathcal{G})\tilde{Q}_i + \tilde{Q}_i(\mathcal{G} - I_r * \mathcal{G})^T + \mathcal{V}, \quad i=0, 1, \dots, \end{aligned} \tag{5.4}$$

converges;

vii) for each $r \times r$ symmetric $\tilde{Q}_0 \geq 0$ there exists $r \times r$ symmetric $\mathcal{V} \succ 0$ such that the sequence $\{\tilde{Q}_i\}_{i=0}^\infty$ generated by (5.4) converges.

Proof: Statements i)-v) are equivalent to i)-v) of Lemma 2.2. Clearly, vi) implies iii), and vii) implies iv). To show v) implies vi) and vii) note that $I_{r^2} * (\mathcal{G} \otimes \mathcal{G}) = (I_r * \mathcal{G}) \otimes (I_r * \mathcal{G})$ and

$$\text{vec}(\alpha * \tilde{Q}_{i+1}) = [\text{diag}(\text{vec } \alpha)] \text{vec } \tilde{Q}_{i+1}.$$

Thus, (5.4) is equivalent to

$$\begin{aligned} \text{vec } \tilde{Q}_{i+1} &= [\text{diag}(\text{vec } \alpha) - (I_r * \mathcal{G}) \otimes (I_r * \mathcal{G})]^{-1} \\ &\quad \cdot [\mathcal{G} \otimes \mathcal{G} - I_{r^2} * (\mathcal{G} \otimes \mathcal{G})] \text{vec } \tilde{Q}_i + [\text{diag}(\text{vec } \alpha)]^{-1} \text{vec } \mathcal{V}. \end{aligned}$$

Thus, vi) and vii) follow from v) with $\mathcal{D} = \text{diag}(\text{vec } \alpha) - (I_r * \mathcal{G}) \otimes (I_r * \mathcal{G})$. \square

Since statements i)-vii) depend only upon α and \mathcal{G} we have the following definition inspired by v)-vii).

Definition 5.1: (α, \mathcal{G}) is stable if \mathbb{A} is an M matrix.

Remark 5.1: When $I_r * \mathcal{G} = 0$, i.e., when the local dynamics have no structured uncertainty, (5.4) simplifies to

$$\alpha * \tilde{Q}_{i+1} = \mathcal{G}\tilde{Q}_i + \tilde{Q}_i\mathcal{G}^T + \mathcal{V}, \quad i=0, 1, \dots, \tag{5.5}$$

or, equivalently,

$$\tilde{Q}_{i+1} = \alpha^{H^i} * (\mathcal{G}\tilde{Q}_i + \tilde{Q}_i\mathcal{G}^T + \mathcal{V}), \quad i=0, 1, \dots. \tag{5.5a}$$

The following result shows that for zero initial condition, the iterative sequence is monotonic.

Proposition 5.2: Suppose $\text{diag}(\text{vec } \alpha) - I_{r^2} * (\mathcal{G} \otimes \mathcal{G}) \succ 0$. Then the sequence $\{\tilde{Q}_i\}_{i=0}^\infty$ generated by (5.4) with $\tilde{Q}_0 = 0$ and $\mathcal{V} \geq 0$ is monotonically increasing.

Proof: To simplify notation we consider the case mentioned in Remark 5.1. Hence, assume $\alpha \succ 0$. Clearly, if $\tilde{Q}_0 = 0$, then (5.5a) implies that $\tilde{Q}_1 = \alpha^{H^1} * \mathcal{V} \geq 0$. Hence, $\tilde{Q}_1 \geq \tilde{Q}_0$. Defining $\Delta\tilde{Q}_{i+1} \triangleq \tilde{Q}_{i+1} - \tilde{Q}_i$, (5.5a) yields

$$\Delta\tilde{Q}_{i+1} = \alpha^{H^i} * (\mathcal{G}\Delta\tilde{Q}_i + \Delta\tilde{Q}_i\mathcal{G}^T).$$

Since $\Delta\tilde{Q}_1 \geq 0$, the result follows from induction. \square

Remark 5.2: Proposition 5.2 is a particularly useful result in applications and can be utilized as follows. Setting $\tilde{Q}_0 = 0$, the sequence $\{\tilde{Q}_i\}$ can be evaluated by a simple numerical procedure. As will be shown in Theorem 5.1 below, each \tilde{Q}_i corresponds to a robust performance measure $\hat{\alpha}_i$. For practical purposes the increasing sequence $\{\hat{\alpha}_i\}$ can be generated until either convergence is attained (in which case $\hat{\alpha} = \lim_{i \rightarrow \infty} \hat{\alpha}_i$ is a robust performance bound) or a maximum permissible performance level is exceeded. In the latter case the question of convergence is irrelevant since the closed-loop system is known to either be unstable for some $G \in \mathfrak{G}$ (i.e., $\hat{\alpha} = \infty$) or exceed acceptable performance specifications, thereby necessitating system redesign.

We now prove a comparison result for solutions of (5.1).

Lemma 5.1: Assume (α, \mathcal{G}) is stable, let $\hat{\alpha}, \hat{\mathcal{G}}$ be $r \times r$ nonnegative matrices where $\hat{\alpha}$ is symmetric, and assume that

$$\alpha \leq \hat{\alpha}, \quad \mathcal{G} \leq \hat{\mathcal{G}}. \tag{5.6}$$

Then $(\hat{\alpha}, \hat{\mathcal{G}})$ is stable. Furthermore, let $r \times r$ symmetric $\hat{\mathcal{V}}$ satisfy

$$\hat{\mathcal{V}} \leq \mathcal{V}, \tag{5.7}$$

let \hat{Q} be the unique, nonnegative solution to (5.1), and let \hat{Q} be the unique solution to

$$\hat{\alpha} * \hat{Q} = \hat{\mathcal{G}}\hat{Q} + \hat{Q}\hat{\mathcal{G}}^T + \hat{\mathcal{V}}. \tag{5.8}$$

Then if $\hat{Q} \geq 0$, it follows that

$$\hat{Q} \leq \tilde{Q}. \tag{5.9}$$

Proof: Since

$$\hat{\mathbb{A}} \triangleq \text{diag}(\text{vec } \hat{\alpha}) - \hat{\mathcal{G}} \otimes \hat{\mathcal{G}}$$

is an N matrix, \mathbb{A} is an M matrix, and

$$\hat{\mathbb{A}} - \mathbb{A} = \text{diag}(\text{vec } (\hat{\alpha} - \alpha)) + (\mathcal{G} - \hat{\mathcal{G}}) \otimes (\mathcal{G} - \hat{\mathcal{G}}) \geq 0$$

it follows from Lemma 2.3 that \hat{A} is an M matrix, and thus (\hat{A}, \hat{G}) is stable. Next note that (5.1) and (5.8) imply

$$\text{vec}(\hat{Q} - \tilde{Q}) = \hat{A}^{-1}(\hat{A} - \tilde{A}) \text{vec} \hat{Q} + \hat{A}^{-1} \text{vec}(\tilde{V} - \tilde{V}).$$

Since $\hat{A} - \tilde{A} \geq 0$, $\hat{A}^{-1} \geq 0$ (see Lemma 2.2), $\tilde{V} - \tilde{V} \geq 0$, and $\hat{Q} \geq 0$, it follows that (5.9) is satisfied. \square

Corollary 5.1: Suppose (α, \mathcal{G}) is stable and let \hat{Q} be the unique, nonnegative solution to (5.1). Furthermore, let $G \in \mathfrak{B}$ and $\theta \in \Theta$ be such that $A(\theta) + G$ is asymptotically stable and define Q by (4.7) for $n \times n$ $Q \geq 0$ satisfying (3.7). Then

$$Q \leq \hat{Q}. \quad (5.10)$$

Proof: By Proposition 4.2, Q satisfies the covariance block-norm inequality (4.16). In the notation of Lemma 5.1 define

$$\hat{\alpha} = \alpha, \hat{\mathcal{G}} = \mathcal{G}, \hat{V} = \alpha * Q - (\mathcal{G}Q + Q\mathcal{G}^T) \quad (5.11)$$

so that (5.6) is satisfied and (4.16) implies (5.7). Note that with the notation (5.11), equation (5.8) has the unique solution $\hat{Q} = Q \geq 0$. Hence (5.9) implies (5.10). \square

Theorem 5.1: Assume A is asymptotically stable, Θ is continuously arcwise connected, and (α, \mathcal{G}) is stable. Then the homogeneous system (3.1) is robustly stable over \mathfrak{B} and Θ , and the nonhomogeneous system (3.4) has the performance bound

$$\hat{\alpha} = \max_{\theta \in \Theta} \left\{ \sum_{i=1}^r [\text{tr}(\hat{Q}_i(\theta)R_i) + 2(\text{tr} \hat{P}_i(\theta))(\mathcal{G}\hat{Q}_i)_{(i,i)}] \right\} \quad (5.12)$$

where $n_i \times n_i$, nonnegative-definite $\hat{Q}_i(\theta)$ and $\hat{P}_i(\theta)$ satisfy

$$0 = A_i(\theta)\hat{Q}_i(\theta) + \hat{Q}_i(\theta)A_i^T(\theta) + V_i, \quad (5.13)$$

$$0 = A_i^T(\theta)\hat{P}_i(\theta) + \hat{P}_i(\theta)A_i(\theta) + R_i \quad (5.14)$$

and $r \times r$ \hat{Q} is the unique, nonnegative solution to (5.1).

Proof: First note that since robust stability is independent of the disturbances, we can set $V = I_n$ for convenience in proving the first result. Hence, suppose (3.1) is not robustly stable. Since \mathfrak{B} is convex (see Remark 4.1), A is asymptotically stable, and Θ is continuously arcwise connected, there exist $G_0 \in \mathfrak{B}$ and $\hat{\theta}: [0, 1] \rightarrow \Theta$ such that $\hat{A}(\mu) \triangleq A(\hat{\theta}(\mu)) + \mu G_0$ is asymptotically stable for all $\mu \in [0, 1]$, and $\hat{A}(1)$ is not asymptotically stable. Define

$$Q(\mu, t) \triangleq \int_0^t e^{\hat{A}(\mu)s} e^{\hat{A}^T(\mu)s} ds, \quad t \geq 0, \mu \in [0, 1]$$

which is monotonically increasing in the nonnegative-definite cone with respect to t . Clearly, the limit

$$Q(\mu) \triangleq \lim_{t \rightarrow \infty} Q(\mu, t), \quad \mu \in [0, 1]$$

exists and satisfies

$$0 = \hat{A}(\mu)Q(\mu) + Q(\mu)\hat{A}^T(\mu) + I_n, \quad \mu \in [0, 1].$$

Now define $r \times r$ nonnegative symmetric $Q(\mu)$ by

$$Q(\mu) = \{\|Q_{ij}(\mu)\|_F\}_{i,j=1}^r$$

where $Q_{ij}(\mu) \in \mathbb{R}^{n_i \times n_j}$, and $Q(\mu)$ is partitioned as in (4.5). By Corollary 5.1 with $\theta = \hat{\theta}(\mu)$, $G = \mu G_0$, $Q \triangleq Q(\mu)$, $\mu \in [0, 1]$, and $V = I_n$, it follows from (5.10) that

$$Q(\mu) \leq \hat{Q}, \quad \mu \in [0, 1]. \quad (5.15)$$

Hence, by (4.8), (5.15) implies

$$\|Q(\mu)\|_F = \|Q(\mu)\|_F \leq \|\hat{Q}\|_F, \quad \mu \in [0, 1]. \quad (5.16)$$

On the other hand, for $\mu \in [0, 1]$ it follows that

$$\begin{aligned} Q(\mu) &= Q(\mu) - Q(\mu, t) + Q(\mu, t) - Q(1, t) + Q(1, t) \\ &\geq Q(\mu, t) - Q(1, t) + Q(1, t) \end{aligned}$$

which implies, for arbitrary $x \in \mathbb{R}^n$,

$$x^T Q(\mu) x \geq x^T [Q(\mu, t) - Q(1, t)] x + x^T Q(1, t) x.$$

Thus, by continuity of $Q(\mu, t)$ in μ ,

$$\lim_{\mu \rightarrow 1} x^T Q(\mu) x \geq x^T Q(1, t) x, \quad x \in \mathbb{R}^n. \quad (5.17)$$

Now, since $\hat{A}(1)$ is not asymptotically stable and $(\hat{A}(1), I_n)$ is stabilizable, it follows from [37, Proposition 3.2, p. 67] that for some $\bar{x} \in \mathbb{R}^n$,

$$\lim_{t \rightarrow \infty} \bar{x}^T Q(1, t) \bar{x} = \infty.$$

Thus, by (5.17)

$$\lim_{\mu \rightarrow 1} \bar{x}^T Q(\mu) \bar{x} = \infty$$

and thus

$$\lim_{\mu \rightarrow 1} \|Q(\mu)\|_F = \infty. \quad (5.18)$$

However, (5.18) contradicts (5.16). Hence, (3.1) is robustly stable over \mathfrak{B} and Θ .

To derive (5.12) note that since R is block diagonal,

$$J(G, \theta) = \sum_{i=1}^r \text{tr} Q_i R_i = \sum_{i=1}^r (\text{vec} Q_i)^T \text{vec} R_i$$

where Q satisfies (3.7). Furthermore, (4.19) implies

$$\text{vec} Q_i = -[A_i(\theta) \oplus A_i(\theta)]^{-1}$$

$$\left[\text{vec} V_i + \sum_{k=1}^r \text{vec} (G_{ik} Q_{ki} + Q_{ik} G_{ik}^T) \right]$$

Hence, using Lemma 2.1,

$$\begin{aligned} J(G, \theta) &= \sum_{i=1}^r \left[\text{tr}(\hat{Q}_i(\theta)R_i) \right. \\ &\quad \left. + \sum_{k=1}^r (\text{vec} [G_{ik} Q_{ki} + Q_{ik} G_{ik}^T])^T \text{vec} \hat{P}_i(\theta) \right] \\ &= \sum_{i=1}^r \left[\text{tr}(\hat{Q}_i(\theta)R_i) + \sum_{k=1}^r \text{tr} \hat{P}_i(\theta) (G_{ik} Q_{ki} + Q_{ik} G_{ik}^T) \right] \\ &\leq \sum_{i=1}^r \left[\text{tr}(\hat{Q}_i(\theta)R_i) \right. \\ &\quad \left. + \sum_{k=1}^r (\text{tr} \hat{P}_i(\theta)) \sigma_{\max}(G_{ik} Q_{ki} + Q_{ik} G_{ik}^T) \right] \\ &\leq \sum_{i=1}^r \left[\text{tr}(\hat{Q}_i(\theta)R_i) + 2(\text{tr} \hat{P}_i(\theta)) \sum_{k=1}^r \sigma_{\max}(G_{ik}) \sigma_{\max}(Q_{ki}) \right] \\ &\leq \sum_{i=1}^r \left[\text{tr}(\hat{Q}_i(\theta)R_i) + 2(\text{tr} \hat{P}_i(\theta)) \sum_{k=1}^r \sigma_{\max}(G_{ik}) \|Q_{ki}\|_F \right] \end{aligned}$$

$$\leq \sum_{i=1}^r \left[\text{tr} (\hat{Q}_i(\theta)R_i) + 2 (\text{tr} \hat{P}_i(\theta)) \sum_{k=1}^r \mathcal{G}_{(i,k)} \hat{Q}_{(k,i)} \right]$$

$$= \sum_{i=1}^r [\text{tr} (\hat{Q}_i(\theta)R_i) + 2 (\text{tr} \hat{P}_i(\theta))(\mathcal{G}\hat{Q})_{(i,i)}]$$

which yields (5.12). \square

VI. EXAMPLES

We first confirm that the damped harmonic oscillator is asymptotically stable for all constant frequency perturbations. Hence, let

$$r=1, n=n_1=2$$

and

$$\bar{A} = \bar{A}_1 = \begin{bmatrix} -\nu & \omega \\ -\omega & -\nu \end{bmatrix}$$

where $\nu > 0$ and $\omega \in \mathbb{R}$. To represent frequency uncertainty let $\mathcal{B} = \{0\}$, $\Theta = \mathbb{R}$, $\hat{\theta} = 0$, and

$$A(\theta) = \bar{A} + \theta \begin{bmatrix} 0 & 1 \\ -1 & 0 \end{bmatrix}$$

Note that $A(\theta)$ is stable for all $\theta \in \mathbb{R}$ with poles $-\nu \pm j(\omega + \theta)$. Note that $A(\theta)$ can be diagonalized by means of the unitary transformation

$$\phi = \frac{1}{\sqrt{2}} \begin{bmatrix} 1 & 1 \\ j & -j \end{bmatrix}, \quad \phi^{-1} = \frac{1}{\sqrt{2}} \begin{bmatrix} 1 & -j \\ 1 & j \end{bmatrix}$$

so that

$$\hat{A}(\theta) \triangleq \phi^{-1}A(\theta)\phi = \begin{bmatrix} -\nu + j(\omega + \theta) & 0 \\ 0 & -\nu - j(\omega + \theta) \end{bmatrix}$$

Hence, using

$$A(\theta) \otimes A(\theta) = (\phi^{-1} \otimes \phi^{-1})(\hat{A}(\theta) \otimes \hat{A}(\theta))(\phi \otimes \phi)$$

it follows that

$$\sigma_{\min}(A(\theta) \otimes A(\theta)) = 2\nu, \quad \theta \in \mathbb{R}$$

Defining [see (4.15)]

$$\mathcal{Q} = \mathcal{Q}_{(1,1)} = 2\nu$$

and $\mathcal{G} = 0$, the scalar majorant Lyapunov equation (5.1) has the solution

$$\hat{Q} = \mathcal{V}/2\nu$$

where $\mathcal{V} = \|V\|_F$. Choosing $V = I_2$ and noting that $\mathcal{A} = \mathcal{Q} = 2\nu > 0$ is an M matrix, Theorem 5.1 guarantees robust stability for all frequency variations $\theta \in \mathbb{R}$.

The next example has been chosen to demonstrate the robustness of a pair of nominally uncoupled oscillators with respect to uncertain coupling. Hence, let

$$n=4, r=2, n_1=n_2=2$$

and

$$\bar{A}_i = \begin{bmatrix} -\nu & \omega_i \\ -\omega_i & -\nu \end{bmatrix}, \quad i=1, 2$$

where $\nu, \omega_1, \omega_2 \geq 0$. Furthermore, let $\Theta = \{\hat{\theta}\}$ and

$$\mathcal{G} = \begin{bmatrix} 0 & \gamma_{12} \\ \gamma_{21} & 0 \end{bmatrix}$$

which denotes the fact that the local subsystem (oscillator) dynamics are assumed to be known. Since

$$\sigma_{\min}(\bar{A}_j \otimes \bar{A}_i) = [4\nu^2 + (\omega_j - \omega_i)^2]^{1/2}$$

define

$$\mathcal{Q} = \begin{bmatrix} 2\nu & [4\nu^2 + (\omega_1 - \omega_2)^2]^{1/2} \\ [4\nu^2 + (\omega_1 - \omega_2)^2]^{1/2} & 2\nu \end{bmatrix}$$

Letting $V = I_4$ yields $\mathcal{V} = 2I_2$. Solving (5.1) yields

$$\hat{Q}_{(1,1)} = (2\nu^2\delta - \gamma_{12}\gamma_{21} + \gamma_{12}^2)/2\sqrt{2\nu(\nu^2\delta - \gamma_{12}\gamma_{21})},$$

$$\hat{Q}_{(1,2)} = (\gamma_{12} + \gamma_{21})/2\sqrt{2(\nu^2\delta - \gamma_{12}\gamma_{21})},$$

$$\hat{Q}_{(2,2)} = (2\nu^2\delta - \gamma_{12}\gamma_{21} + \gamma_{21}^2)/2\sqrt{2\nu(\nu^2\delta - \gamma_{12}\gamma_{21})}$$

where

$$\delta \triangleq [1 + \delta^2]^{1/2}, \quad \delta \triangleq (\omega_1 - \omega_2)/2\nu.$$

Clearly, \hat{Q} is nonnegative if and only if

$$\gamma_{12}\gamma_{21} < \nu^2\delta. \tag{6.1}$$

The bound (6.1) characterizes the magnitude of coupling uncertainty for which stability is guaranteed. Note that the parameter δ is a measure of the frequency separation of the oscillators relative to the damping. When $\delta \gg 1$, (6.1) becomes asymptotically

$$\gamma_{12}\gamma_{21} < \frac{\nu}{2} |\omega_1 - \omega_2| \tag{6.2}$$

which confirms the intuitive expectation that robust stability is proportional to damping and subsystem frequency separation. This result does not appear to be predictable from quadratic or vector Lyapunov functions.

To evaluate the conservatism inherent in the bound (6.1) we solve for the actual stability region. To render the calculation tractable we assume that G_{12} and G_{21} have the structured form

$$G_{ij} = \begin{bmatrix} \alpha_{ij} & \beta_{ij} \\ -\beta_{ij} & \alpha_{ij} \end{bmatrix} \tag{6.3}$$

By constraining (6.3) the set of coupling variations is reduced, which may or may not lead to a larger stability region. Thus, our estimate of conservatism may itself be conservative, i.e., the actual conservatism may indeed be less than the following analysis indicates. However, without (6.3) the development becomes intractable. This calculation will thus be called *semiexact*.

By considering the characteristic equation for $\bar{A} + G$, lengthy manipulation shows that $\bar{A} + G$ is stable if and only if

$$\gamma_{12}\gamma_{21} < 2\nu^2(-\epsilon + [1 + \delta^2(1 - \epsilon^2)]^{1/2})/(1 - \epsilon^2) \tag{6.4}$$

where $\epsilon \in (0, 1]$ is the smallest positive real root of

$$\epsilon = (1 + \epsilon^2)[1 + \delta^2(1 - \epsilon^2)]^{1/2}/[2 + \delta^2(1 - \epsilon^2)]. \tag{6.5}$$

The majorant bound (6.1) and semiexact bound (6.4) are illustrated in unified form in Fig. 1. For $\delta \gg 1$ note that $\epsilon = O(\delta^{-1})$ and thus (6.4) becomes asymptotically

$$\gamma_{12}\gamma_{21} < \nu |\omega_1 - \omega_2|. \tag{6.6}$$

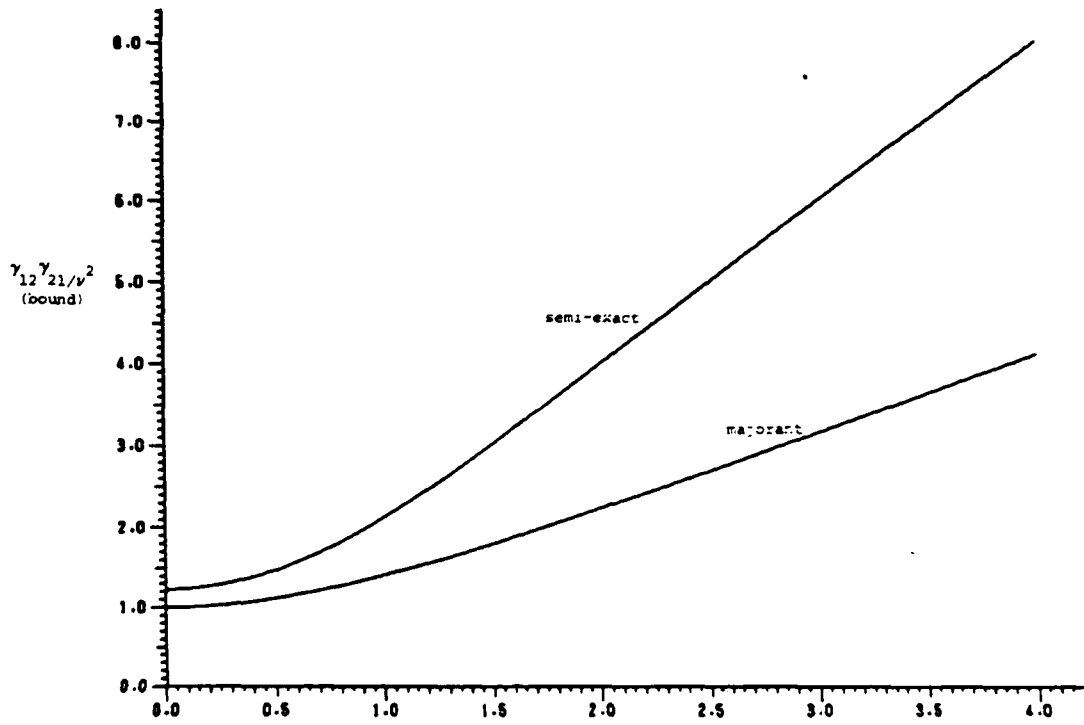


Fig. 1.

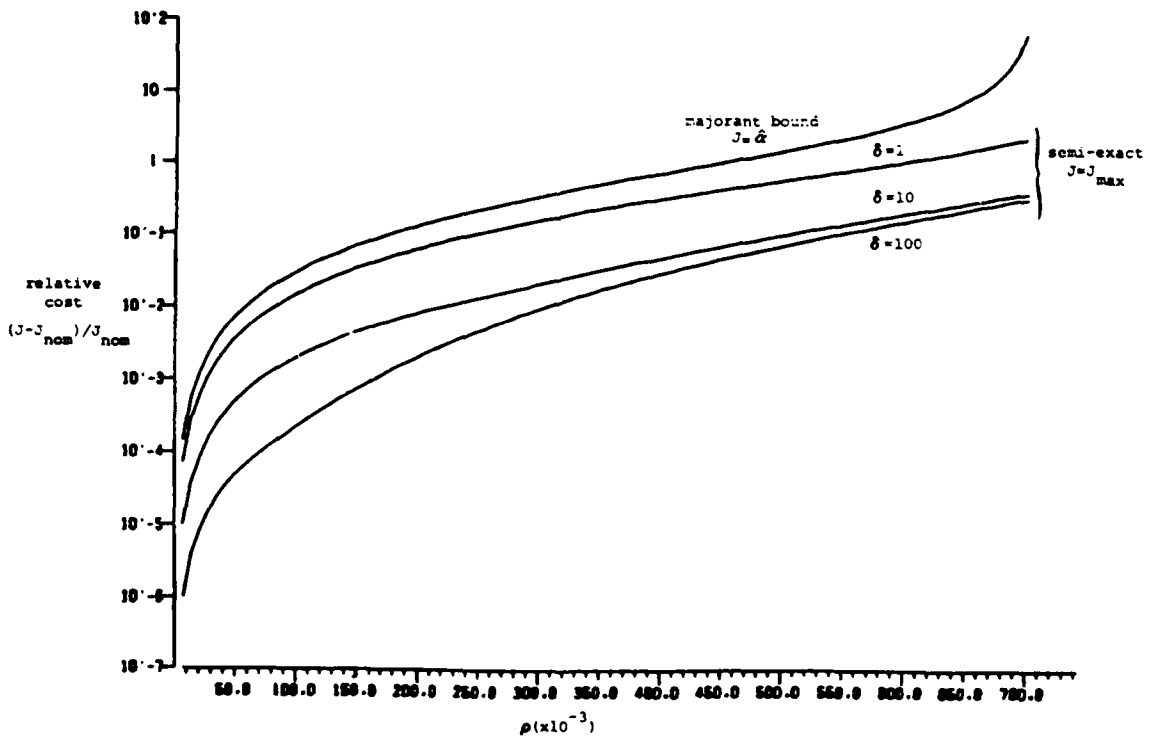


Fig. 2.

Hence, for large δ the majorant bound (6.2) is, at worst, conservative by a factor of 2 compared to the semiexact bound.

To determine the performance bound (5.12) set $R = I_4$. Hence, it can be shown that

$$J_{nom} = 2/\nu$$

and the system has the performance bound

$$\hat{\alpha} = J_{nom} + \sqrt{2(\rho_{12} + \rho_{21})^2/\nu(1 - 2\rho_{12}\rho_{21})} \quad (6.7)$$

where

$$\rho_{12} = \gamma_{12}/\sqrt{2}\delta^{1/2}, \quad \rho_{21} = \gamma_{21}/\sqrt{2}\delta^{1/2}.$$

On the other hand, the semiexact calculation yields

$$J_{\max} = \max_{\lambda \in [0,1]} \{[\rho_{12}^2 + \rho_{21}^2 + 2\rho_{12}\rho_{21}\lambda + 2\delta(\rho_{12}\rho_{21})^2(1-\lambda^2)] / [2\delta - 4\rho_{12}\rho_{21}\lambda - 2\delta(\rho_{12}\rho_{21})^2(1-\lambda^2)]\}. \quad (6.8)$$

Fig. 2 compares the semiexact worst-case performance (6.8) to the majorant Lyapunov equation bound (6.7). To efficiently illustrate the results the data are specialized to the case $\rho_{12} = \rho_{21}$. Note that the semiexact performance is plotted for several values of δ because of the explicit dependence of (6.8) on δ via δ .

ACKNOWLEDGMENT

The authors wish to thank J. Straehla for excellent typing of the original manuscript and B. Bland for executing the numerical calculations.

REFERENCES

- [1] M. G. Safonov and M. Athans, "Gain and phase margin for multiloop LQG regulators," *IEEE Trans. Automat. Contr.*, vol. AC-22, pp. 173-179, 1977.
- [2] M. G. Safonov, *Stability and Robustness of Multivariable Feedback Systems*. Cambridge, MA: M.I.T. Press, 1980.
- [3] N. A. Lehtomaki, N. R. Sandell, Jr., and M. Athans, "Robustness results in linear-quadratic Gaussian based multivariable control designs," *IEEE Trans. Automat. Contr.*, vol. AC-26, pp. 75-92, 1981.
- [4] J. C. Doyle and G. Stein, "Multivariable feedback design: Concepts for a classical/modern synthesis," *IEEE Trans. Automat. Contr.*, vol. AC-26, pp. 4-16, 1981.
- [5] J. C. Doyle, "Analysis of feedback system: with structured uncertainties," *IEE Proc.*, vol. 129, pp. 242-250, 1982.
- [6] J. C. Doyle, J. E. Wall, and G. Stein, "Performance and robustness analysis for structured uncertainty," in *Proc. 21st IEEE Conf. Decision Contr.*, Orlando, FL, Dec. 1982, pp. 629-636.
- [7] G. Zames, "Feedback and optimal sensitivity: Model reference transformations, multiplicative seminorms, and approximate inverses," *IEEE Trans. Automat. Contr.*, vol. AC-26, pp. 301-320, 1981.
- [8] G. Zames and B. A. Francis, "Feedback, minimax sensitivity, and optimal robustness," *IEEE Trans. Automat. Contr.*, vol. AC-28, pp. 585-601, 1983.
- [9] R. R. E. de Gaston and M. G. Safonov, "A homotopy method for nonconservative stability robustness analysis," in *Proc. 24th IEEE Conf. Decision Contr.*, Fort Lauderdale, FL, Dec. 1985, pp. 1294-1301.
- [10] M. K. H. Fan and A. L. Tits, "Characterization and efficient computation of the structured singular value," *IEEE Trans. Automat. Contr.*, vol. AC-31, pp. 734-743, 1986.
- [11] O. D. I. Nwokah, "The quantitative design of robust multivariable control systems," in *Proc. IEEE Conf. Decision Contr.*, Athens, Greece, Dec. 1986, pp. 16-24.
- [12] I. R. Petersen and C. V. Hollot, "A Riccati equation approach to the stabilization of uncertain systems," *Automatica*, vol. 22, pp. 397-411, 1986.
- [13] R. K. Yedavalli, S. S. Banda, and D. B. Ridgely, "Time-domain stability robustness measures for linear regulators," *J. Guidance Contr. Dyn.*, vol. 8, pp. 520-524, 1985.
- [14] R. K. Yedavalli, "Perturbation bounds for robust stability in linear state space models," *Int. J. Contr.*, vol. 42, pp. 1507-1517, 1985.
- [15] ———, "Improved measures of stability robustness for linear state space models," *IEEE Trans. Automat. Contr.*, vol. AC-30, pp. 577-579, 1985.
- [16] A. R. Galimidi and B. R. Barmish, "The constrained Lyapunov problem and its application to robust output feedback stabilization," *IEEE Trans. Automat. Contr.*, vol. AC-31, pp. 410-419, 1986.
- [17] D. S. Bernstein and S. W. Greeley, "Robust output-feedback stabilization: Deterministic and stochastic perspectives," in *Proc. Amer. Contr. Conf.*, Seattle, WA, June 1986, pp. 1818-1826.
- [18] D. S. Bernstein, "Robust static and dynamic output-feedback stabilization: Deterministic and stochastic perspectives," *IEEE Trans. Automat. Contr.*, to be published.
- [19] D. S. Bernstein and D. C. Hyland, "Optimal projection for uncertain systems (OPUS): A unified theory of reduced-order, robust control design," in *Large Space Structures: Dynamics and Control*, S. N. Atluri and A. K. Amos, Eds. New York: Springer-Verlag, 1987.
- [20] W. M. Haddad, "Robust optimal projection control-system synthesis," Ph.D. dissertation, Dep. Mechanical Eng., Florida Inst. Technol., Melbourne, FL, Mar. 1987.
- [21] A. M. Ostrowski, "On some metrical properties of operator matrices and matrices partitioned into blocks," *J. Math. Anal. Appl.*, vol. 2, pp. 161-209, 1961.
- [22] T. Strom, "On the practical application of majorants for nonlinear matrix iterations," *J. Math. Anal. Appl.*, vol. 41, pp. 137-147, 1973.
- [23] G. Dahlquist, "On matrix majorants and minorants, with applications to differential equations," *Lin. Alg. Appl.*, vol. 52/53, pp. 199-216, 1983.
- [24] S. Barnett and C. Storey, *Matrix Methods in Stability Theory*. New York: Barnes and Noble, 1976.
- [25] J. W. Brewer, "Kronecker products and matrix calculus in system theory," *IEEE Trans. Circuits Syst.*, vol. CAS-25, pp. 772-781, 1978.
- [26] A. Graham, *Kronecker Products and Matrix Calculus*. Chichester: Ellis Horwood, 1981.
- [27] C. R. Rao and S. K. Mitra, *Generalized Inverse of Matrices and Its Applications*. New York: Wiley, 1971.
- [28] G. P. H. Styan, "Hadamard products and multivariate statistical analysis," *Lin. Alg. Appl.*, vol. 6, pp. 217-240, 1973.
- [29] A. Berman and R. J. Plemmons, *Nonnegative Matrices in the Mathematical Sciences*. New York: Academic, 1979.
- [30] D. D. Siljak, *Large-Scale Dynamic Systems*. Amsterdam, The Netherlands: Elsevier/North-Holland, 1978.
- [31] M. Ikeda and D. D. Siljak, "Generalized decomposition of dynamic systems and vector Lyapunov functions," *IEEE Trans. Automat. Contr.*, vol. AC-26, pp. 1118-1125, 1981.
- [32] M. Djordjevic, "Stability analysis of interconnected systems with possibly unstable subsystems," *Syst. Contr. Lett.*, vol. 3, pp. 165-169, 1983.
- [33] A. A. Martynyuk, "The Lyapunov matrix-function," *Nonlinear Anal. Theory, Methods, and Appl.*, vol. 8, pp. 1223-1226, 1984.
- [34] G. H. Golub and C. F. Van Loan, *Matrix Computations*. Baltimore, MD: Johns Hopkins Press, 1983.
- [35] T. Kato, *Perturbation Theory for Linear Operators*. New York: Springer-Verlag, 1980.
- [36] R. K. Mehra, "Optimization of measurement schedules and sensor designs for linear dynamic systems," *IEEE Trans. Automat. Contr.*, vol. AC-21, pp. 55-64, 1976.
- [37] W. M. Wonham, *Linear Multivariable Control: A Geometric Approach*. New York: Springer-Verlag, 1974.
- [38] G. J. Butler, C. R. Johnson, and H. Wolkowicz, "Nonnegative solutions of a quadratic matrix equation arising from comparison theorems in ordinary differential equations," *SIAM J. Alg. Disc. Meth.*, vol. 6, pp. 47-53, 1985.
- [39] H. D. Victory, Jr., "On nonnegative solutions of matrix equations," *SIAM J. Alg. Discrete Meth.*, vol. 6, pp. 406-412, 1985.



David C. Hyland received the B.S., M.S., and Sc.D. degrees in aeronautics from the Massachusetts Institute of Technology, Cambridge, in 1969, 1971, and 1973, respectively.

After serving as a vibration specialist in a Cambridge-based acoustics consulting firm, in 1974 he joined the staff at Lincoln Laboratory, Massachusetts Institute of Technology, Cambridge. His work at Lincoln Laboratory included reentry vehicle dynamics, multibody spacecraft dynamics simulation, and spacecraft attitude control. In 1983

he joined the Government Aerospace Systems Division, Harris Corporation, Melbourne, FL, where he leads the Control Systems Analysis and Synthesis Group. His current research interests include robustness analysis for control-system design with application to vibration suppression in large flexible space structures.



Dennis S. Bernstein (M'82) received the Sc.B. degree in applied mathematics from Brown University, Providence, RI, and the M.S.E. and Ph.D. degrees from the Computer, Information and Control Engineering Program at the University of Michigan, Ann Arbor.

After spending two years at Lincoln Laboratory, Massachusetts Institute of Technology, Lexington, he joined the Controls Analysis and Synthesis Group of the Government Aerospace Systems Division, Harris Corporation, Melbourne, FL. His current research interests include extending the optimal projection control-design approach to a variety of settings including robust, sampled-data, and decentralized control.

APPENDIX C

**Improved Robust Performance Bounds
in Covariance Majorant Analysis**

**Improved Robust Performance Bounds
in Covariance Majorant Analysis**

by

**Emmanuel G. Collins, Jr.
and
David C. Hyland**

**Harris Corporation
Government Aerospace Systems Division
MS 22/4848
Melbourne, FL 32902**

ABSTRACT

Over the past decade a considerable amount of attention has been devoted to the subject of robustness analysis. However, the current literature on robustness analysis concentrates largely on the qualitative issue of robust *stability*. To date, very few results have been developed for the quantitative issue of robust *performance*. An exception to this is the recent work of Hyland and Bernstein in covariance majorant analysis. This work developed bounds on cost functions which can represent the variances of selected system variables. This paper presents improvements in covariance majorant analysis. Specifically, less conservative (i.e., smaller) upper bounds are developed for the cost functions. Lower cost bounds are also developed.

Supported in part by the Air Force Office of Scientific Research under contract F49620-86-C-0038.

1. Introduction

Recent technologies have required the modeling and control of increasingly complex systems such as flexible space structures, electric power systems, large scale manufacturing systems, and flexible manipulators. Correspondingly, there is an obvious need for analysis tools which can qualitatively and quantitatively describe the behavior of these systems in the face of uncertainties in the representative mathematical models. Thus, over the past decade there have been considerable interest among the systems research community in robustness analysis for multivariable systems. (See for example [14,15]).

However, although significant attention has been given to the issue of robustness analysis, the current literature concentrates largely on the qualitative issue of robust *stability*. To date very little work has been published on the quantitative issue of robust *performance*. One notable exception is the application of the μ function [2] to performance analysis. In [2] performance is measured in terms of the L_∞ norm of a specified performance matrix, such as the output or input sensitivity matrix. However, this is only one possible performance measure. For example, one is often interested in time-domain performance measures which are expressed in terms of the transient or steady state behavior of selected system variables (e.g., inputs and outputs) when the system is subjected to specified signals and disturbances. Covariance majorant analysis [1] another recent development in robustness analysis does measure system performance in terms of steady state behavior.

Specifically, covariance majorant analysis considers linear interconnected systems which have structured parametric uncertainty and are subject to white noise disturbances. The analysis of [1] then develops a robust stability condition and upper bounds on the variances of selected system variables. In the present paper it is shown how covariance majorant analysis leads to both lower and upper robust performance bounds. The upper bounds developed here are less conservative (i.e., smaller) than those of [1].

The paper is organized as follows. Section 2 briefly reviews the developments of [1] and presents results which are needed in the analysis of the next section. Section 3 then develops the new bounds. The reduced conservatism of the new bounds is illustrated by the example of Section 4. Section 5 then presents concluding remarks.

Before proceeding some notation and definitions are presented.

I_p	$p \times p$ identity matrix
z_{ij} or $Z_{(i,j)}$	(i, j) element of matrix Z
Z_{ij}	(i, j) matrix block of partitioned matrix Z
$\text{diag}(z_1, \dots, z_m)$	diagonal matrix with listed diagonal elements
block-diag (Z_1, \dots, Z_M)	block-diagonal matrix with listed diagonal blocks
$Y * Z$	$[y_{ij}z_{ij}]$, Hadamard product of matrices Y, Z of equal dimensions [12-13]
Z^{HI}	$[1/z_{ij}]$, Hadamard inverse of square matrix Z
$\text{col}_i(Z)$	i^{th} column of matrix Z
$\text{vec}(z)$	$\begin{bmatrix} \text{col}_1(z) \\ \vdots \\ \text{col}_p(z) \end{bmatrix} \quad z \in \mathbb{R}^{m \times p}$
$Y \otimes Z$	$[y_{ij}Z]$, Kronecker product of matrices Y and Z [10-11]
$Y \oplus Z$	$Y \otimes I_p + I_m \otimes Z$, Kronecker sum of matrices $Y \in \mathbb{R}^{m \times m}$ and $Z \in \mathbb{R}^{p \times p}$ [10-11]
$Y \leq Z$	$Y_{ij} \leq Z_{ij}$ for each i and j
nonnegative matrix	matrix with nonnegative elements ($Z \geq 0$)
$\text{tr } Z$	trace of matrix Z
$\sigma_{\min}(Z), \sigma_{\max}(Z)$	smallest and largest singular values of matrix Z
$\ Z\ _S$	spectral norm of matrix Z ($= \sigma_{\max}(Z)$)
$\ Z\ _F$	Frobenius norm of matrix Z ($\ Z\ _F^2 = \sum_i \sum_j z_{ij}^2 $)
$\ Z\ _A$	absolute norm of matrix Z ($= \max_{i,j} z_{ij} $)

Let Z be the $n \times n$ block-partitioned matrix

$$Z = [Z_{ij}]_{(i,j=1,\dots,r)} \quad (1.1)$$

where $Z_{ij} \in \mathbb{R}^{n_i \times n_j}$ and $\sum_{i=1}^r n_i = n$. The *block norm matrix* [7,3] of Z with respect to the matrix norm $\|\cdot\|_\theta$ (which is also called the " θ block norm") is the $r \times r$ nonnegative matrix

$$\bar{Z}_\theta = [\bar{Z}]_\theta \triangleq [\|Z_{ij}\|_\theta]_{(i,j=1,\dots,r)} \quad (1.2)$$

Thus, \bar{Z}_S and \bar{Z}_F represent respectively the block norm matrices of Z with respect to the spectral and Frobenius norms.

Majorants [8] are essentially upper bounds for block norm matrices. Precisely, $\hat{Z} \in \mathbb{R}^{r \times r}$ is a majorant of Z (with respect to the norm $\|\cdot\|_0$) if

$$\bar{Z}_0 \leq \hat{Z}. \quad (1.3)$$

A matrix $P \in \mathbb{R}^{p \times p}$ is an *M-matrix* [4-6] if it has nonpositive off diagonal elements [i.e., $p_{ij} \leq 0$ for $i \neq j$] and positive principal minors. There are many equivalent definitions for an M-matrix. (See [4]-[6]).

2. Preliminaries

Consider the system

$$\dot{x}(t) = (A + G)x(t) + w(t) \quad (2.1)$$

where $x \in \mathbb{R}^n$ and w is a white noise process with intensity V . It is assumed that the system (2.1) represents r ($r \leq n$) nominally stable subsystems described by A with uncertain interactions and dynamics described by G . Specifically,

$$A = \text{block-diag}\{A_i\}_{i=1}^r \quad (2.2)$$

where $A_i \in \mathbb{R}^{n_i \times n_i}$ is asymptotically stable and $\sum_{i=1}^r n_i = n$. The matrices $G, V \in \mathbb{R}^{n \times n}$ are partitioned conformably so that

$$G = [G_{ij}]_{(i,j=1,\dots,r)} \quad (2.3a)$$

$$V = [V_{ij}]_{(i,j=1,\dots,r)} \quad (2.3b)$$

where $G_{ij}, V_{ij} \in \mathbb{R}^{n_i \times n_j}$. In addition,

$$G \in \mathbf{G} \quad (2.4)$$

where

$$\mathbf{G} = \{G \in \mathbb{R}^{n \times n} : \bar{G}_0 \leq \hat{G}\}. \quad (2.5)$$

That is the spectral norm of each block G_{ij} of the uncertainty matrix G is bounded above by the corresponding (i, j) element of the nonnegative matrix $\hat{G} \in \mathbb{R}^{r \times r}$. Thus \hat{G} is a majorant of each admissible G .

If $A + G$ is asymptotically stable, then the state covariance Q is the unique solution of the Lyapunov equation

$$0 = (A + G)Q + Q(A + G)^T + V. \quad (2.6)$$

Q is partitioned conformably with A, G and V so that

$$Q = [Q_{ij}]_{(i,j=1,\dots,r)} \quad (2.7)$$

where $Q_{ij} \in \mathbb{R}^{n_i \times n_j}$.

Now define the positive matrix $\tilde{A} \in \mathbb{R}^{r \times r}$ by

$$\tilde{a}_{ij} \triangleq \sigma_{\min}(A_j \oplus A_i), \quad i, j = 1, \dots, r. \quad (2.8)$$

Also, define $A \in \mathbb{R}^{r^2 \times r^2}$ as

$$A \triangleq [\text{diag}(\text{vec} \tilde{A})] - \hat{G} \oplus \hat{G}. \quad (2.9)$$

These matrices appear in the following lemma which presents the covariance Frobenius block norm inequality initially proved in [1]. An alternative proof based on the block Kronecker product is found in [3].

Lemma 2.1. Consider $G \in \mathcal{G}$ such that $A+G$ is asymptotically stable and let Q be the solution of (2.6). Then \bar{Q}_F satisfies the matrix inequality,

$$\tilde{A} * \bar{Q}_F \leq \hat{G} \bar{Q}_F + \bar{Q}_F \hat{G}^T + \bar{V}_F \quad (2.10)$$

which is equivalent to the vector inequality

$$A \text{vec} \bar{Q}_F \leq \text{vec} \bar{V}_F. \quad (2.11)$$

Definition 2.1. The pair (\tilde{A}, \hat{G}) is *stable* if A defined by (2.9) is an M-matrix.

If (2.10) is interpreted as an equality, one obtains the Lyapunov-like equation

$$\tilde{A} * \hat{Q} = \hat{G} \hat{Q} + \hat{Q} \hat{G}^T + \bar{V}_F. \quad (2.12)$$

or equivalently

$$A \text{vec} \hat{Q} = \text{vec} \bar{V}_F. \quad (2.13)$$

Since A is an N-matrix [5] (i.e., it has nonpositive off-diagonal elements), it is invertible with $A^{-1} \geq 0$ if and only if it is an M-matrix [4-6]. The following result then follows immediately from the equivalence of (2.12) and (2.13).

Lemma 2.2. The pair (\tilde{A}, \hat{G}) is stable if and only if for any $\bar{V}_F \geq 0$, there exists a unique (nonnegative) solution of \hat{Q} of (2.12).

Remark 2.1. \hat{Q} may be computed by inverting the $r^2 \times r^2$ matrix A in (2.13). Alternatively, it is shown in [1], that $\hat{Q} = \lim_{i \rightarrow \infty} \hat{Q}^{(i)}$ where $\hat{Q}^{(0)} \geq 0$ and the monotonically increasing sequence $\{\hat{Q}^{(i)}\}_{i=1}^{\infty}$ is generated by

$$\begin{aligned} \tilde{A} * \hat{Q}^{i+1} - (I_r * \hat{G})\hat{Q}^{(i+1)} - \hat{Q}^{(i+1)}(I_r * G) \\ = (\hat{G} - I_r * G)\hat{Q}^{(i)} + \hat{Q}^{(i)}(\hat{G} - I_r * G)^T + \bar{V}_F, \quad i = 0, 1, \dots \end{aligned} \quad (2.14)$$

or equivalently

$$\hat{Q}^{(i+1)} = (\tilde{A} - \tilde{G} - \tilde{G}^T)^{HI} * [(\hat{G} - I_r * G)\hat{Q}^{(i)} + \hat{Q}^{(i)}(\hat{G} - I_r * G)^T + \bar{V}_F], \quad i = 0, 1, \dots \quad (2.15)$$

where $\tilde{G} \in \mathbb{R}^{r \times r}$ is defined by

$$\tilde{g}_{ij} \triangleq \hat{g}_{ii}, \quad i, j = 1, \dots, r. \quad (2.16)$$

The following comparison result shows that \hat{Q} is actually a majorant of the state covariance Q . A proof of this result is presented in [1]. A simplified proof is given here.

Lemma 2.3. Suppose (\tilde{A}, \hat{G}) is stable and let \hat{Q} be the solution of (2.12). Then, for each $G \in \mathbf{G}$ such that $A + G$ is asymptotically stable, the solution Q of (2.6) satisfies

$$\bar{Q}_F \leq \hat{Q}. \quad (2.17)$$

Proof. Since \bar{Q}_F satisfies (2.10), it follows that for some nonnegative $U \in \mathbb{R}^{r \times r}$

$$\tilde{A} * \bar{Q}_F = \hat{G}\bar{Q}_F + \bar{Q}_F\hat{G}^T + \bar{V}_F - U. \quad (2.18)$$

Subtracting (2.18) from (2.12) yields

$$\tilde{A} * (\hat{Q} - \bar{Q}_F) = \hat{G}(\hat{Q} - \bar{Q}_F) + (\hat{Q} - \bar{Q}_F)\hat{G}^T + U. \quad (2.19)$$

It then follows from Lemma 2.2 that

$$\hat{Q} - \bar{Q}_F \geq 0. \quad (2.20)$$

The proof of the next result on stability robustness is based on Lemma 2.3 and is presented in [1].

Theorem 2.1. Consider the system described by (2.1)-(2.5) and assume (\tilde{A}, \hat{G}) is stable. Then for each $G \in \mathbf{G}$ the plant matrix $A + G$ is asymptotically stable.

Although Theorem 2.1 is a useful result in covariance majorant analysis, an equally important result is that the majorant analysis allows one to obtain an upper bound on the variances of selected system variables. Thus, in what follows the cost function

$$J(G) = \text{tr } QR, \quad R = R^T \geq 0 \quad (2.21)$$

is considered where R has the partitioned form

$$R = [R_{ij}]_{(i,j=1,\dots,r)} \quad (2.22)$$

and $R_{ij} \in \mathbb{R}^{n_i \times n_j}$. This cost function can represent the variance of one of the system variables. For example if s given by

$$s = c^T x, \quad c \in \mathbb{R}^n \quad (2.23)$$

is a system variable of interest, then

$$R = cc^T \Rightarrow J(G) = E(s^2). \quad (2.24)$$

Now define

$$J_{\min} \triangleq \min_{G \in \mathcal{G}} J(G) \quad (2.25)$$

$$J_{\max} \triangleq \max_{G \in \mathcal{G}} J(G). \quad (2.26)$$

Definition 2.2. If for the system described by (2.1)–(2.5), $J_{\min} \geq \alpha$ and $J_{\max} \leq \beta$, then α is a lower performance bound and β is an upper performance bound.

In [1] majorant analysis was used to develop an upper performance bound β_1 for the special case in which R is block-diagonal (i.e., $R_{ij} \triangleq 0$ for $i \neq j$). This result is presented below in Theorem 2.2.

Before presenting this theorem define the nominal state covariance $Q^\circ \in \mathbb{R}^{n \times n}$ to be the unique, nonnegative definite solution of the Lyapunov equation

$$0 = AQ^\circ + Q^\circ A^T + V. \quad (2.27)$$

Q° has the partitioned form

$$Q^\circ = [Q_{ij}^\circ]_{(i,j=1,\dots,r)} \quad (2.28)$$

where $Q_{ij}^\circ \in \mathbb{R}^{n_i \times n_j}$. Also, for $i = 1, \dots, r$ define $P_i^\circ \in \mathbb{R}^{n_i \times n_i}$ to be the unique nonnegative definite solution of

$$0 = A_i^T P_i^\circ + P_i^\circ A_i + R_{ii}. \quad (2.29)$$

Theorem 2.2. Assume (\tilde{A}, \hat{G}) is stable. Then for each $G \in \mathbf{G}$, $A+G$ is asymptotically stable. In addition, if R is block-diagonal then the system described by (2.1)–(2.5) has the upper performance bound

$$\beta_1 = \text{tr } Q^\circ R + 2 \sum_{i=1}^r (\text{tr } P_i^\circ) (\hat{G} \hat{Q})_{(i,i)} \quad (2.30)$$

where \hat{Q} , Q° and P_i° are the respective solutions of (2.12), (2.27) and (2.29).

3. Improved Performance Analysis

The upper performance bound β_1 presented in Theorem 2.2 is based upon developing a majorant \hat{Q} of the state covariance Q by beginning with (2.6), the Lyapunov equation in Q . In this section Q is expressed as

$$Q = Q^\circ + \Delta Q \quad (3.1)$$

where Q° is the solution of (2.27). Subtracting (2.27) from (2.6) and using (3.1) yields

$$0 = (A + G)\Delta Q + \Delta Q(A + G)^T + GQ^\circ + Q^\circ G^T. \quad (3.2)$$

The perturbation ΔQ has the partitioned form

$$\Delta Q = [\Delta Q_{ij}]_{(i,j=1,\dots,r)} \quad (3.3)$$

where $\Delta Q_{ij} \in \mathbb{R}^{n_i \times n_j}$. In what follows it is shown that by using (3.2) to develop a majorant $\Delta \hat{Q}$ of ΔQ , it is possible to develop a less conservative (i.e. smaller) upper performance bound than that of Theorem 2.2. In addition, the analysis of this section develops a lower performance bound which has no counterpart in [1].

Consider any two matrices $M, N \in \mathbb{R}^{n \times n}$ partitioned identically. Then as shown in [3],

$$[\overline{M + N}]_F \leq \overline{M}_F + \overline{N}_F \quad (3.4a)$$

$$[\overline{MN}]_F \leq \overline{M}_S \overline{N}_F \quad (3.4b)$$

$$[\overline{MN}]_F \leq \overline{M}_F \overline{N}_S. \quad (3.4c)$$

Using (3.4) it follows that for each $G \in \mathbf{G}$,

$$\begin{aligned} \overline{[GQ^\circ + Q^\circ G^T]}_F &\leq \overline{[GQ^\circ]}_F + \overline{[Q^\circ G^T]}_F \\ &\leq \overline{G}_S \overline{Q^\circ}_F + \overline{Q^\circ}_F \overline{G}_S^T \\ &\leq \hat{G} \overline{Q^\circ}_F + \overline{Q^\circ}_F \hat{G}^T. \end{aligned} \quad (3.5)$$

Lemma 3.1 which presents Frobenius block norm inequalities for Q° and ΔQ is now an immediate result of Lemma 2.1 and (3.5).

Lemma 3.1. Consider $G \in \mathbf{G}$ such that $A + G$ is asymptotically stable and let Q° and ΔQ be the unique solutions of (2.27) and (3.2). Then \overline{Q}_F° and $\overline{\Delta Q}_F$ satisfy

$$\tilde{A} * \overline{Q}_F^\circ \leq \overline{V}_F \quad (3.6a)$$

$$\tilde{A} * \overline{\Delta Q}_F \leq \hat{G} \overline{\Delta Q}_F + \overline{\Delta Q}_F \hat{G}^T + \hat{G} \overline{Q}_F^\circ + \overline{Q}_F^\circ \hat{G}^T. \quad (3.6b)$$

Now interpret (3.6) as equalities to obtain

$$\tilde{A} * \hat{Q}^\circ = \overline{V}_F \quad (3.7a)$$

$$\tilde{A} * \Delta \hat{Q} = \hat{G} \Delta \hat{Q} + \Delta \hat{Q} \hat{G}^T + \hat{G} \overline{Q}_F^\circ + \overline{Q}_F^\circ \hat{G}^T. \quad (3.7b)$$

Lemma 3.2 which shows that \hat{Q}° and $\Delta \hat{Q}$ are majorants of Q° and ΔQ follows immediately from Lemma 2.3.

Lemma 3.2. Suppose (\tilde{A}, \hat{G}) is stable and let \hat{Q}° and $\Delta \hat{Q}$ be the (unique, nonnegative) solutions of (3.7). Then for each $G \in \mathbf{G}$ such that $A + G$ is asymptotically stable, Q° and ΔQ , the respective solutions of (2.27) and (3.2) satisfy

$$\overline{Q}_F^\circ \leq \hat{Q}^\circ \quad (3.8a)$$

$$\overline{\Delta Q}_F \leq \Delta \hat{Q}. \quad (3.8b)$$

An important result is now presented. This result reveals that the sum $\overline{Q}_F^\circ + \Delta \hat{Q}$ is a smaller majorant of the covariance Q than is \hat{Q} . This result is subsequently used to develop lower and upper performance bounds α_2 and β_2 and to demonstrate the reduced conservatism of β_2 compared to the performance bound β_1 described in Theorem 2.1.

Lemma 3.3. Suppose (\tilde{A}, \hat{G}) is stable and let \hat{Q} and $\Delta \hat{Q}$ be the (unique, nonnegative) solutions respectively of (2.12) and (3.7b). Then for each $G \in \mathbf{G}$, Q and Q° the solutions respectively of (2.6) and (2.27) satisfy

$$\overline{Q}_F \leq \overline{Q}_F^\circ + \Delta \hat{Q} \leq \hat{Q}. \quad (3.9)$$

Proof. It follows from (3.1), (3.4a) and (3.8a) that

$$\overline{Q}_F = \overline{[Q^\circ + \Delta Q]}_F \leq \overline{Q}_F^\circ + \overline{\Delta Q}_F \leq \overline{Q}_F^\circ + \Delta \hat{Q} \quad (3.10)$$

which proves the left hand inequality in (3.9).

Now, let \hat{Q} be the (unique nonnegative) solution of

$$\tilde{A} * \Delta \hat{Q} = \hat{G} \Delta \hat{Q} + \Delta \hat{Q} \hat{G}^T + \hat{G} \hat{Q}^\circ + \hat{Q}^\circ \hat{G}^T. \quad (3.11)$$

Subtracting (3.7b) from (3.11) yields

$$\tilde{A} * (\Delta \hat{Q} - \Delta \hat{Q}) = \hat{G}(\Delta \hat{Q} - \Delta \hat{Q}) + (\Delta \hat{Q} - \Delta \hat{Q}) \hat{G}^T + \hat{G}(\hat{Q}^\circ - \bar{Q}_F^\circ) + (\hat{Q}^\circ - \bar{Q}_F^\circ) \hat{G}^T. \quad (3.12)$$

Since $\hat{Q}^\circ \geq \bar{Q}_F^\circ$,

$$\hat{G}(\hat{Q}^\circ - \bar{Q}_F^\circ) + (\hat{Q}^\circ - \bar{Q}_F^\circ) \hat{G}^T \geq 0. \quad (3.13)$$

It then follows from (3.12), (3.13) and Lemma 2.2 that

$$\Delta \hat{Q} \leq \Delta \hat{Q}. \quad (3.14)$$

Adding (3.7a) and (3.11) yields

$$\tilde{A} * (\hat{Q}^\circ + \Delta \hat{Q}) = \hat{G}(\hat{Q}^\circ + \Delta \hat{Q}) + (\hat{Q}^\circ + \Delta \hat{Q}) \hat{G}^T + \bar{V}_F. \quad (3.15)$$

Comparing (3.15) and (2.12) reveals that

$$\hat{Q}^\circ + \Delta \hat{Q} = \hat{Q}. \quad (3.16)$$

Thus, using (3.8a), (3.14) and (3.16) yields

$$\bar{Q}_F^\circ + \Delta \hat{Q} \leq \hat{Q}^\circ + \Delta \hat{Q} \leq \hat{Q}^\circ + \Delta \hat{Q} = \hat{Q} \quad (3.17)$$

which proves the right hand inequality in (3.9).

Notice that substituting (3.1) into (2.21) yields

$$J(G) = J^\circ + \Delta J(G) \quad (3.18)$$

where

$$J^\circ \triangleq \text{tr } Q^\circ R \quad (3.19)$$

$$\Delta J(G) \triangleq \text{tr } \Delta Q R. \quad (3.20)$$

Substituting into (3.20) the partitioned forms of R and ΔQ given respectively by (2.22) and (3.3) gives

$$\Delta J(G) = \sum_{i=1}^r \text{tr } \Delta Q_{ii} R_{ii} + \sum_{i=1}^r \sum_{\substack{j=1 \\ j \neq i}}^r \text{tr } \Delta Q_{ij} R_{ji}. \quad (3.21)$$

An alternative expression for the first summation in (3.21) is presented below in Lemma 3.4.

Lemma 3.4. Consider the system described by (2.1)–(2.5) and assume $A+G$ is asymptotically stable. Then $\Delta J(G)$ given by (3.21) can be expressed as

$$\Delta J(G) = \sum_{i=1}^r \sum_{j=1}^r \text{tr } P_i^o (G_{ij} Q_{ji} + Q_{ij} G_{ij}^T) + \sum_{i=1}^r \sum_{\substack{j=1 \\ j \neq i}}^r \text{tr } \Delta Q_{ij} R_{ji}. \quad (3.22)$$

Proof. The perturbation ΔQ solves (3.2) which by using (3.1) can be expressed as

$$0 = A\Delta Q + \Delta Q A^T + GQ + QG^T. \quad (3.23)$$

Using the partitioned forms of the matrices and considering the (i, i) block of (3.23) gives

$$0 = A_i \Delta Q_{ii} + \Delta Q_{ii} A_i^T + \sum_{j=1}^r (G_{ij} Q_{ji} + Q_{ij} G_{ij}^T). \quad (3.24)$$

Then by using the appropriate Kronecker product identities [10–11] (3.24) can be expressed as

$$\text{vec } \Delta Q_{ii} = -(A_i \oplus A_i)^{-1} \sum_{j=1}^r \text{vec} (G_{ij} Q_{ji} + Q_{ij} G_{ij}^T). \quad (3.25)$$

Recognize that for any two square matrices Y and Z

$$\text{tr } YZ = (\text{vec } Y)^T \text{vec } Z. \quad (3.26)$$

Then using (3.25) and (3.26) gives

$$\text{tr } \Delta Q_{ii} R_{ii} = - \sum_{j=1}^r [\text{vec} (G_{ij} Q_{ji} + Q_{ij} G_{ij}^T)]^T (A_i \oplus A_i)^{-T} \text{vec } R_{ii}. \quad (3.27)$$

But it follows from (2.29) that

$$\text{vec } P_i^o = (A_i \oplus A_i)^{-T} \text{vec } R_{ii} \quad (3.28)$$

and so

$$\text{tr } \Delta Q_{ii} R_{ii} = - \sum_{j=1}^r [\text{vec} (G_{ij} Q_{ji} + Q_{ij} G_{ij}^T)]^T \text{vec } P_i^o \quad (3.29)$$

which by using (3.26) can be expressed as

$$\text{tr } \Delta Q_{ii} R_{ii} = \text{tr } P_i^o (G_{ij} Q_{ji} + Q_{ij} G_{ij}^T). \quad (3.30)$$

The proof is completed by substituting (3.30) into (3.21).

The main results of this paper are given below as Theorem 3.1 and Corollaries 3.1 and 3.2. Before presenting this result two important trace inequalities are given. First, for $P \in \mathbb{R}^{q \times p}$ define the matrix I norm by

$$\|P\|_I \triangleq \sum_{i=1}^q \sum_{j=1}^p |p_{ij}|. \quad (3.31)$$

Proposition 3.1. For each $M \in \mathbb{R}^{p \times q}$ and $P \in \mathbb{R}^{q \times p}$,

$$|\text{tr } MP| \leq \|M\|_A \|P\|_I. \quad (3.32)$$

Proof.

$$\begin{aligned} |\text{tr } MP| &= \left| \sum_{i=1}^p \sum_{j=1}^q m_{ij} p_{ji} \right| \\ &\leq \sum_{i=1}^p \sum_{j=1}^q |m_{ij}| |p_{ji}| \\ &\leq \|M\|_A \|P\|_I. \end{aligned}$$

If certain structures of M and P are known, a much less conservative upper bound on $|\text{tr } MP|$ may be given. The next result is derived in [9].

Proposition 3.2. Consider $M, P \in \mathbb{R}^{p \times p}$ such that $M = M^T \geq 0$. Then

$$|\text{tr } MP| \leq (\text{tr } M) \|P\|_s. \quad (3.33)$$

Now the main results of this paper are presented.

Theorem 3.1. Suppose (\tilde{A}, \hat{G}) is stable. Then $A + G$ is asymptotically stable for each $G \in \mathcal{G}$ and

$$\max_{G \in \mathcal{G}} |\Delta J(G)| \leq \Delta \hat{J} \quad (3.34)$$

where

$$\Delta \hat{J} = 2 \sum_{i=1}^r (\text{tr } P_i^o) \left(\hat{G}(\bar{Q}_F^o + \Delta \hat{Q}) \right)_{(i,i)} + \sum_{i=1}^r \sum_{\substack{j=1 \\ j \neq i}}^r \Delta \hat{Q}_{i,j} \|R_{ji}\|_I \quad (3.35)$$

Proof. The asymptotic stability of $A + G$ is simply a restatement of Theorem 2.1. So for each $G \in \mathbf{G}$ consider the cost perturbation $\Delta J(G)$ described by (3.22) and recognize that

$$|\Delta J(G)| \leq |\Delta J_A(G)| + |\Delta J_B(G)| \quad (3.36)$$

where

$$|\Delta J_A(G)| \leq \sum_{i=1}^r \sum_{j=1}^r |\operatorname{tr} P_i^o (G_{ij} Q_{ji} + Q_{ij} G_{ij}^T)| \quad (3.37a)$$

$$|\Delta J_B(G)| \leq \sum_{i=1}^r \sum_{\substack{j=1 \\ j \neq i}}^r |\operatorname{tr} \Delta Q_{ij} R_{ji}| \quad (3.37b)$$

Using (3.33) and (3.9) it follows that for each $G \in \mathbf{G}$

$$\begin{aligned} |\operatorname{tr} P_i^o (G_{ij} Q_{ji} + Q_{ij} G_{ij}^T)| &\leq (\operatorname{tr} P_i^o) \|G_{ij} Q_{ji} + Q_{ij} G_{ij}^T\| \\ &\leq 2(\operatorname{tr} P_i^o) \|G_{ij}\|_s \|Q_{ji}\|_s \\ &\leq 2(\operatorname{tr} P_i^o) \|G_{ij}\|_s \|Q_{ji}\|_F \\ &\leq 2(\operatorname{tr} P_i^o) \hat{G}_{(i,j)} \left[(\bar{Q}_F^o)_{(j,i)} + (\Delta \hat{Q})_{(j,i)} \right] \end{aligned}$$

which substituting into (3.37a) gives

$$|\Delta J_A(G)| \leq 2 \sum_{i=1}^r (\operatorname{tr} P_i^o) \left(\hat{G} (\bar{Q}_F^o + \Delta \hat{Q}) \right)_{(i,i)}. \quad (3.38)$$

Also, using (3.32) and (3.8b) it follows that

$$\begin{aligned} |\operatorname{tr} \Delta Q_{ij} R_{ji}| &\leq \|\Delta Q_{ij}\|_A \|R_{ji}\|_I \\ &\leq \|\Delta Q_{ij}\|_F \|R_{ji}\|_I \\ &\leq \Delta \hat{Q}_{(i,j)} \|R_{ji}\|_I \end{aligned}$$

which substituting into (3.37b) gives

$$|\Delta J_B(G)| \leq \sum_{i=1}^r \sum_{\substack{j=1 \\ j \neq i}}^r \Delta \hat{Q}_{(i,j)} \|R_{ji}\|_I. \quad (3.39)$$

The proof follows from (3.36), (3.38) and (3.39).

Remark 3.1. One may be tempted to apply the inequalities (3.8b), (3.32) and (3.33) to the expression for $\Delta J(G)$ given by (3.21). This yields

$$\max_{G \in \mathbf{G}} |\Delta J(G)| \leq \Delta \hat{J} \quad (3.40)$$

where

$$\Delta \hat{J} = \sum_{i=1}^r (\text{tr } R_{ii}) \Delta \hat{Q}_{(i,i)} + \sum_{i=1}^r \sum_{\substack{j=1 \\ j \neq i}}^r \|R_{ji}\|_I \Delta \hat{Q}_{(i,j)}. \quad (3.41)$$

However, it can be shown that

$$\Delta \hat{J} \geq \Delta J \quad (3.42)$$

such that $\Delta \hat{J}$ is a more conservative bound for the magnitude of the cost perturbation than is ΔJ .

It is easily seen from (3.18) that

$$J^o - |\Delta J(G)| \leq J(G) \leq J^o + |\Delta J(G)| \quad (3.43)$$

where J^o is given by (3.19). The following corollary is then immediate.

Corollary 3.1. Under the conditions of Theorem 3.1 the system described by (2.1)–(2.5) has the lower performance bound α_2 and the upper performance bound β_2 given by

$$\alpha_2 = \text{tr } (Q^o R) - \Delta \hat{J} \quad (3.44)$$

$$\beta_2 = \text{tr } (Q^o R) + \Delta \hat{J} \quad (3.45)$$

where $\Delta \hat{J}$ is given by (3.35).

Remark 3.2. It is important to recognize that the results of Theorem 3.1 and Corollary 3.1 actually allow multiple objective analysis. For example if the analyst is interested in m costs

$$J_i(G) = \text{tr } QR^{(i)}, \quad i = 1, \dots, m \quad (3.46)$$

representing say the variances of m system variables then Corollary 3.1 yields lower and upper bounds $\alpha^{(i)}$ and $\beta^{(i)}$ such that for each $G \in \mathbf{G}$,

$$\alpha^{(i)} \leq J_i(G) \leq \beta^{(i)}, \quad i = 1, \dots, m. \quad (3.47)$$

The next corollary compares the upper performance bounds of Theorem 2.2 and Corollary 3.1 for the case in which R is block-diagonal.

Corollary 3.2. Assume that R is block-diagonal. Then under the conditions of Theorem 3.1 the upper performance bounds β_1 and β_2 given respectively by (2.30) and (3.45) satisfy

$$\beta_2 \leq \beta_1. \quad (3.48)$$

In addition, if

$$\hat{Q}^\circ = \overline{Q}_F^\circ \quad (3.49)$$

then

$$\beta_2 = \beta_1. \quad (3.50)$$

Proof. Subtracting (2.30) from (3.45) yields

$$\beta_2 - \beta_1 = 2 \sum_{i=1}^r (\text{tr } P_i^\circ) \left(\hat{G}(\overline{Q}_F^\circ + \Delta\hat{Q} - \hat{Q}) \right)_{(i,i)}. \quad (3.51)$$

It then follows from (3.9) that

$$\overline{Q}_F^\circ + \Delta\hat{Q} - \hat{Q} \leq 0 \quad (3.52)$$

which implies that

$$\beta_2 - \beta_1 \leq 0. \quad (3.53)$$

Now assume (3.49) holds. It then follows from (3.12) that

$$\Delta\hat{Q} = \Delta\hat{Q}. \quad (3.54)$$

Using (3.49), (3.54) and (3.16) gives

$$\overline{Q}_F^\circ + \Delta\hat{Q} = \hat{Q}^\circ + \Delta\hat{Q} = \hat{Q}^\circ + \Delta\hat{Q} = \hat{Q} \quad (3.55)$$

which substituting into (3.51) reveals

$$\beta_2 - \beta_1 = 0. \quad (3.56)$$

4. An Example

This example considers the robustness of a pair of nominally uncoupled oscillators with respect to uncertain coupling. Specifically, consider the system described by (2.1)–(2.5) with

$$n = 4, \quad r = 2, \quad n_1 = n_2 = 2 \quad (4.1)$$

$$A_1 = \begin{bmatrix} -.1 & 1 \\ -1 & -.1 \end{bmatrix}, \quad \begin{bmatrix} -.2 & 2 \\ -2 & -.2 \end{bmatrix} \quad (4.2)$$

$$V = \text{block-diag} \left(\begin{bmatrix} 1 & .8 \\ .8 & 1 \end{bmatrix}, \quad \begin{bmatrix} 1 & .8 \\ .8 & 1 \end{bmatrix} \right) \quad (4.3)$$

$$\hat{G} = \begin{bmatrix} 0 & .1 \\ .1 & 0 \end{bmatrix}. \quad (4.4)$$

Notice that the eigenvalues of A_1 and A_2 are given by

$$[\lambda(A_1)]_{1,2} = -.1 \pm j \quad (4.5)$$

$$[\lambda(A_2)]_{1,2} = -.2 \pm j2. \quad (4.6)$$

The matrix A defined by (2.9) is an M-matrix and thus the system is stable for each G that satisfies

$$\bar{G}_s \leq \hat{G}. \quad (4.7)$$

Now consider the quadratic performance $J(G)$ defined by (2.1) with

$$R = I_4. \quad (4.8)$$

The results of the robust performance analysis are presented in Table 4.1. The values J_L and J_S were obtained by generating a set G_R of 10,000 random G matrices satisfying

$$\bar{G}_s = \tilde{G} \quad (4.9)$$

and letting

$$J_L = \max_{G \in G_R} J(G) \quad (4.10a)$$

$$J_S = \min_{G \in G_R} J(G). \quad (4.10b)$$

Obviously,

$$J_L \leq J_{\max} \triangleq \max_{G \in G} J(G) \quad (4.11a)$$

$$J_S \geq J_{\min} \triangleq \min_{G \in G} J(G). \quad (4.11b)$$

It is conjectured that

$$J_L \cong J_{\max} \quad (4.12a)$$

$$J_S \cong J_{\min} \quad (4.12b)$$

and thus J_L are useful indicators of the conservatism inherent in the performance bounds β_1, β_2 and α_2 .

The parameter J_L predicts that J_{\max} is 6.81% greater than the nominal performance J^0 . The performance bounds β_1 and β_2 respectively indicate that J_{\max} may be as much as 30.4% or 23.8%

greater than the nominal value. Thus in this example, the new upper performance bound β_2 is significantly less conservative than the original upper bound β_1 .

Table 4.1

nominal performance, J^o	15.0000
upper performance bound, β_2	18.5704
upper performance bound, β_1	19.5579
largest random performance, J_L	16.0208
lower performance bound, α_2	11.4296
smallest random performance, J_S	14.6103

Acknowledgements. We thank Larry Davis and Dennis Bernstein for fruitful discussions which inspired many of these results. Dr. Bernstein was particularly helpful in the development of Remark 3.1. We also wish to thank Jill Straehla for typing the original manuscript and Allen Daubendiek for performing the numerical calculations.

References

1. D. C. Hyland and D. S. Bernstein, "The Majorant Lyapunov Equation: A Nonnegative Matrix Equation for Robust Stability and Performance of Large Scale Systems," *IEEE Trans. Autom. Control*, Vol. AC-32, pp. 1005-1013, 1987.
2. J. Doyle, J. E. Wall and G. Stein, "Performance and Robustness Analysis for Structured Uncertainty," *Proc. 21st IEEE Conf. Decis. Control*, Orlando, FL, pp. 629-636, 1982.
3. D. C. Hyland and E. G. Collins, Jr., "Block Kronecker Products and Block Norm Matrices in Large Scale Systems Analysis," submitted for publication.
4. M. Fiedler and V. Ptak, "On Matrices with Non-Positive Off-Diagonal Elements and Positive Principal Minors," *Czechoslovakian Mathematical Journal*, Vol. 12, pp. 382-400.
5. D. D. Siljak, *Large-Scale Dynamics Systems*, North Holland, New York, 1978.
6. A. Berman and R. J. Plemmons, *Nonnegative Matrices in the Mathematical Sciences*, Academic Press, New York, 1979.
7. A. M. Ostrowski, "On Some Metrical Properties of Operator Matrices and Matrices Partitioned into Blocks," *J. Math. Anal. Appl.*, Vol. 41, pp. 137-147, 1973.
8. G. Dahlquist, "On Matrix Majorants and Minorants with Applications to Differential Equations," *Linear Algebra Appl.*, Vol. 52/53, pp. 199-216, 1983.
9. J. M. Saniuk and I. B. Rhodes, "A Matrix Inequality Associated with Bounds on Solutions of Algebraic Riccati and Lyapunov Equations," *IEEE Trans. Autom. Control*, Vol. AC-32, pp. 739-740, 1987.
10. J. W. Brewer, "Kronecker Products and Matrix Calculus in Systems Theory," *IEEE Trans. Circ. Syst.*, Vol. CAS-25, pp. 772-781, 1978.
11. P. Lancaster and M. Tismenetsky, *The Theory of Matrices*, Academic Press, New York, 1985.
12. G. P. H. Styan, "Hadamard Products and Multivariable Statistical Analysis" *Linear Alg. Appl.*, Vol. 6, pp. 217-240, 1973.
13. C. R. Rao and S. K. Mitra, *Generalized Inverse of Matrices and Its Applications*, Wiley and Sons, New York, 1971.
14. Special issue on "Linear Multivariable Control Systems," *IEEE Trans. Autom. Control*, Vol. AC-26, Feb. 1981.
15. Special issue on "Sensitivity and Robustness in Control Systems Theory and Design," *IEE Proc.*, Vol. 129, Pt.D, Nov. 1982.

APPENDIX D

**Block Kronecker Products and Block Norm Matrices
in Large Scale Systems Analysis**

Block Kronecker Products and Block Norm Matrices
in Large Scale Systems Analysis

by

David C. Hyland and Emmanuel G. Collins, Jr.

Harris Corporation
Government Aerospace Systems Division
MS 22/4848
Melbourne, FL 32902

Abstract

Complex and large scale systems are often viewed as collections of interacting subsystems. Properties of the overall system are then deduced from the properties of the individual subsystems and their interconnections. This analysis process for large scale systems usually requires manipulating the matrix subblocks of block-partitioned matrices. Two tools which have found use in linear systems analysis are the Kronecker product and the matrix modulus ($|a_{ij}|$). However, these tools are designed for matrices partitioned into their scalar elements. Thus, this paper defines and presents properties of the block Kronecker product and block norm matrix, generalizations of the Kronecker product and matrix modulus to block-partitioned matrices. The utility of the results is illustrated by deriving in simplified fashion a recent result in robustness analysis.

1. Introduction

In the analysis of complex and large scale dynamic systems it is often advantageous to regard the overall system as a collection of interacting subsystems. Properties of the aggregate system can then be deduced from the properties of the individual subsystems and their interconnections. (See e.g. [6,7,11,14] for a small sample of the numerous published results which take this approach.) For linear systems this type of analysis often involves manipulating the matrix subblocks of block-partitioned matrices.

Some tools that have been useful in systems analysis are the Kronecker product and the matrix modulus. The Kronecker product, for example, has found use in the solution of linear matrix equations [1,4,10,17], the development of matrix calculus [4,9,13,16] and dynamic sensitivity analysis [3,4]. However, the Kronecker product was designed for matrices partitioned into their scalar elements. For example if A, Q, and B are matrices, then the Kronecker product allows one to write

$$\text{vec}(AQB) = (B^T \otimes A)\text{vec}(Q) \quad (1.1)$$

where $\text{vec}(\cdot)$ is the vector valued operator which stacks the columns of a matrix in a vector. However, suppose Q were partitioned into matrix subblocks. Then the operation (1.1) destroys this structure.

The matrix modulus of the matrix Q is the matrix $|q_{ij}|$ and has been used to develop robust stability conditions for dynamic linear systems [11,18]. However, if Q is partitioned into matrix subblocks, the matrix modulus is too fine in that it is based on a property (the absolute value) of the scalar elements of a matrix. Conversely, a norm $\|Q\|_0$ of the matrix Q is too coarse in that it totally ignores the block-partitioned structure of the matrix.

What are obviously needed are tools designed specifically for block-partitioned matrices. One such collection of tools has been based on matrix

majorants and minorants [5]. The purpose of this paper is to develop additional results based on the block Kronecker product and the block norm matrix, generalizations respectively of the Kronecker product and modulus matrix to block-partitioned matrices.

The paper proceeds as follows. In Section 2 the block Kronecker product is introduced and some of its algebraic properties are presented. Then, in Section 3 the block norm matrix is defined and some related equalities and inequalities are given. Next, Section 4 presents results on block-diagonal and diagonal matrix structures. These results are useful in Section 5, which uses results developed in the previous sections to derive in a simplified fashion the covariance block norm inequality of [7, Proposition 4.2].

Before proceeding we present some notation. It is assumed that the matrices are in general complex.

I_p	$p \times p$ identity matrix
*	Hadamard product [15]
\otimes, \oplus	Kronecker product, Kronecker sum [4,8]
$\text{col}_i(Z)$	i th column of matrix Z
$\text{vec}(Z)$	$\begin{bmatrix} \text{col}_1(Z) \\ \text{col}_2(Z) \\ \vdots \\ \text{col}_q(Z) \end{bmatrix}$, Z is a $p \times q$ matrix
Z^T	transpose of matrix Z
Z^H	conjugate transpose of matrix Z
z_{ij}	(i,j) element of matrix Z
$Z \leq \hat{Z}$	$z_{ij} \leq \hat{z}_{ij}$ for all i and j
nonnegative matrix	matrix with nonnegative elements ($Z \geq 0$)
$\text{tr}(Z)$	trace of matrix Z

$\lambda_{\min}(Z), \lambda_{\max}(Z)$	minimum and maximum eigenvalues of Hermitian matrix Z
$\sigma_i(Z)$	singular value of matrix Z
$\sigma_{\min}(Z), \sigma_{\max}(Z)$	smallest and largest singular values of matrix Z
$\ Z\ _{\theta}$	any norm of matrix Z (not necessarily induced by a vector norm)
$\ Z\ _{\theta}$	any norm of matrix Z induced by a vector norm $\ \cdot\ _{\alpha}$ ($\ Z\ _{\theta} = \max_{\ y\ _{\alpha}=1} \ Zy\ _{\alpha}$)
$\ y\ _2$	Euclidean norm of vector y
$\ Z\ _s$	Spectral norm of matrix Z, induced by the Euclidean norm $\ \cdot\ _2$
$\ Z\ _F$	Frobenius norm of matrix Z ($\ Z\ _F^2 = \sum_i \sum_j z_{ij} ^2$)

2. Block Kronecker Products

This section introduces the block Kronecker product and a related vector valued function $\text{vecb}(\cdot)$. The algebra associated with the block Kronecker product is also presented (in Table A). The reader familiar with the standard Kronecker algebra will quickly recognize that the block Kronecker algebra is almost identical. This is essentially due to property (A.3) of Table A.

It should be recognized that below the primary consideration is the special case of square matrices with square diagonal blocks. This restriction is to avoid notational complexity and confusion. However, most of the results extend to more general partitions. The extensions require a clear definition of how various matrices are partitioned (such as when multiplying rectangular matrices A and B).

Consider the $n \times n$ partitioned matrices

$$A = [A_{ij}] \quad (i, j = 1, \dots, r) \quad (2.1a)$$

$$B = [B_{ij}] \quad (i, j = 1, \dots, r) \quad (2.1b)$$

where A_{ij} and B_{ij} are $n_i \times n_j$ and $\sum_{i=1}^r n_i = n$. The $n^2 \times 1$ vector $\text{vecb}(A)$ is defined by

$$\text{vecb}(A) \triangleq \begin{bmatrix} \text{vec}(A_{11}) \\ \vdots \\ \text{vec}(A_{r1}) \\ \hline \text{vec}(A_{12}) \\ \vdots \\ \text{vec}(A_{r2}) \\ \hline \vdots \\ \hline \text{vec}(A_{1r}) \\ \vdots \\ \text{vec}(A_{rr}) \end{bmatrix} \quad (2.2)$$

Notice that $\text{vecb}(\cdot)$ is a linear operator.

It is desired to define an operation $A \bar{\otimes} B$ such that for an $n \times n$ matrix D partitioned identically to A and B

$$\text{vecb}(BDA^T) = (A \bar{\otimes} B)\text{vecb}(D). \quad (2.3)$$

This motivates the definition of the block Kronecker product of A and B , denoted by $A \bar{\otimes} B$. $A \bar{\otimes} B$ is the $n^2 \times n^2$ matrix defined by

$$A \bar{\otimes} B \triangleq \begin{bmatrix} A_{11} \otimes B & A_{12} \otimes B & \dots & A_{1r} \otimes B \\ A_{21} \otimes B & A_{22} \otimes B & \dots & A_{2r} \otimes B \\ \vdots & \vdots & \ddots & \vdots \\ A_{r1} \otimes B & A_{r2} \otimes B & \dots & A_{rr} \otimes B \end{bmatrix} \quad (2.4)$$

where the $n_i \times n_j$ matrix product $A_{ij} \otimes B$ is defined by

$$A_{ij} \otimes B \triangleq \begin{bmatrix} A_{ij} \otimes B_{11} & A_{ij} \otimes B_{12} & \dots & A_{ij} \otimes B_{1r} \\ A_{ij} \otimes B_{21} & A_{ij} \otimes B_{22} & \dots & A_{ij} \otimes B_{2r} \\ \vdots & \vdots & \ddots & \vdots \\ A_{ij} \otimes B_{r1} & A_{ij} \otimes B_{r2} & \dots & A_{ij} \otimes B_{rr} \end{bmatrix}. \quad (2.5)$$

The block Kronecker sum of A and B is denoted by $A \bar{\oplus} B$ and is defined by

$$A \bar{\oplus} B = A \bar{\oplus} I_n + I_n \bar{\oplus} B. \quad (2.6)$$

Recognize that if the matrices A, B and I_n are partitioned into their scalar elements (i.e., $r=n$) then $A \bar{\oplus} B = A \oplus B$ and $A \bar{\oplus} B = A \oplus B$, such that the block Kronecker product and block Kronecker sum reduce respectively to the Kronecker product and Kronecker sum.

Some of the basic algebraic properties of the block Kronecker product and block Kronecker sum are presented in Table A. In this table it is assumed that A and B are $n \times n$ matrices partitioned as in (2.1) and C and D are $n \times n$ matrices partitioned identically to A and B. Also, $f(\cdot)$ denotes an analytic function. The eigenvalues of A are denoted by $\lambda^{(i)}$ ($i=1, \dots, n$) and $\alpha^{(i)}$ denotes the corresponding eigenvectors. Similarly, the eigenvalues of B are denoted by $\mu^{(i)}$, and $\beta^{(i)}$ denotes the corresponding eigenvectors. Recognize that if A or B have redundant eigenvalues then it is possible to have $\alpha^{(j)} = \alpha^{(k)}$ or $\beta^{(j)} = \beta^{(k)}$ for $j \neq k$. Thus statements (A.15)-(A.17) in Table A are not redundant.

To understand (A.17) it is necessary to define the block Kronecker product of two vectors. So consider the n dimensional partitioned vectors

$$x^T = [x_1^T, x_2^T, \dots, x_r^T] \quad (2.7a)$$

$$y^T = [y_1^T, y_2^T, \dots, y_r^T] \quad (2.7b)$$

where x_i and y_i are n_i vectors and $\sum_{i=1}^r n_i = n$. Then, the $n^2 \times 1$ vector $x \bar{\otimes} y$ is defined by

$$x \bar{\otimes} y \triangleq \begin{bmatrix} x_i \otimes y_1 \\ x_i \otimes y_2 \\ \vdots \\ x_i \otimes y_r \end{bmatrix} \quad (2.8)$$

where

$$x \bar{\otimes} y \triangleq \begin{bmatrix} x_1 \otimes y \\ x_2 \otimes y \\ \vdots \\ x_r \otimes y \end{bmatrix} \quad (2.9)$$

Table A
Algebra of Block Kronecker Products

- (A.1) $\text{vecb}(ADB) = (B^T \bar{\otimes} A) \text{vecb}(D)$
(A.2) $\text{vecb}(AD+DB) = (B^T \bar{\otimes} A) \text{vecb}(D)$
(A.3) $A \bar{\otimes} B = P^T (A \otimes B) D$ for some permutation matrix P
(A.4) $(A+B) \bar{\otimes} C = A \bar{\otimes} C + B \bar{\otimes} C$
(A.5) $A \bar{\otimes} (B+C) = A \bar{\otimes} B + A \bar{\otimes} C$
(A.6) $(A \bar{\otimes} B)^T = A^T \bar{\otimes} B^T$
(A.7) $(A \bar{\otimes} B)(C \bar{\otimes} D) = (AC) \bar{\otimes} (BD)$
(A.8) $(A \bar{\otimes} B)^{-1} = A^{-1} \bar{\otimes} B^{-1}$
(A.9) $B \bar{\otimes} A = Q(A \bar{\otimes} B)Q$ for some permutation matrix Q
(A.10) $\det(A \bar{\otimes} B) = [\det(A)\det(B)]^n$
(A.11) $\text{tr}(A \bar{\otimes} B) = \text{tr}(A)\text{tr}(B)$

- (A.12) $f(I_n \bar{\otimes} A) = I_n \bar{\otimes} f(A)$
- (A.13) $f(A \bar{\otimes} I_n) = f(A) \bar{\otimes} I_n$
- (A.14) $\exp(A \bar{\otimes} B) = \exp(A) \bar{\otimes} \exp(B)$
- (A.15) The eigenvalues of $(A \bar{\otimes} B)$ are the n^2 numbers $\lambda^{(i)} \mu^{(j)}$ ($i, j=1, 2, \dots, n$)
- (A.16) The eigenvalues of $(A \bar{\otimes} B)$ are the n^2 numbers $\lambda^{(i)} \mu^{(j)}$ ($i, j=1, 2, \dots, n$)
- (A.17) $\alpha^{(i)} \bar{\otimes} \beta^{(j)}$ is an eigenvector of $A \bar{\otimes} B$ with eigenvalue $\lambda^{(i)} \mu^{(j)}$ and is also an eigenvector of $A \bar{\otimes} B$ with eigenvalue $\lambda^{(i)} \mu^{(j)}$.

The proofs of most of the properties presented in Table A are easy once the validity of (A.1) and (A.3) is established. Thus the proofs of these two statements are presented and then the proofs of the remaining results are discussed with the exception of property (A.17) whose proof is presented in detail

Proof of (A.1). By definition

$$\text{vecb}(ADB) = \begin{bmatrix} \text{vec}((ADB)_{11}) \\ \vdots \\ \text{vec}((ADB)_{r1}) \\ \hline \text{vec}((ADB)_{12}) \\ \vdots \\ \text{vec}((ADB)_{r2}) \\ \hline \vdots \\ \hline \text{vec}((ADB)_{1r}) \\ \vdots \\ \text{vec}((ADB)_{rr}) \end{bmatrix} \quad (2.10)$$

The (p,q) block of (ADB) is given by

$$(ADB)_{pq} = \sum_{i=1}^r \sum_{i=1}^r A_{pj} D_{ji} B_{iq}. \quad (2.11)$$

Also,

$$\text{vec}(A_{pj} D_{ji} B_{iq}) = (B_{iq}^T \otimes A_{pj}) \text{vec}(D_{ji}). \quad (2.12)$$

Substituting (2.10) and (2.11) into (2.9) shows that $\text{vecb}(ADB)$ may be expressed as an $r \times r$ block matrix where the (p,q) block has dimension $n_{pq} \times n_{pq}$ and is given by

$$[\text{vecb}(ADB)]_{pq} = \begin{bmatrix} \sum_j (B_{qp}^T \otimes A_{1j}) \text{vec}(D_{jq}) \\ \sum_j (B_{qp}^T \otimes A_{2j}) \text{vec}(D_{jq}) \\ \vdots \\ \sum_j (B_{qp}^T \otimes A_{rj}) \text{vec}(D_{jq}) \end{bmatrix} \quad (2.13)$$

or equivalently,

$$[\text{vecb}(ADB)]_{pq} = (B_{qp}^T \otimes A) \begin{bmatrix} \text{vec}(D_{1q}) \\ \text{vec}(D_{2q}) \\ \vdots \\ \text{vec}(D_{rq}) \end{bmatrix}. \quad (2.14)$$

(A.1) follows from (2.14). \square

Proof of (A.3). Consider the equation

$$ADB^T = C \quad (2.15)$$

which is equivalent to

$$(A \otimes B)\text{vec}(D) = \text{vec}(C). \quad (2.16)$$

Applying (A.1) to (2.15) yields

$$(A \bar{\otimes} B)\text{vecb}(D) = \text{vecb}(C). \quad (2.17)$$

Now, there exists a permutation matrix P such that

$$\text{vecb}(C) = P\text{vec}(C) \quad (2.18a)$$

$$\text{vecb}(D) = P\text{vec}(D). \quad (2.18b)$$

Substituting (2.18) into (2.17), premultiplying by P^T and using $P^T P = I_n$ yields

$$P^T(A \bar{\otimes} B)P\text{vec}(D) = \text{vec}(C). \quad (2.19)$$

Subtracting (2.16) from (2.19) yields

$$[P^T(A \bar{\otimes} B)P - (A \otimes B)]\text{vec}(D) = 0. \quad (2.20)$$

Since (2.20) is valid for all choices of D it follows that the expression in [] is identically zero. \square

(A.2) now follows from (A.1). (A.3) implies that

$$A \otimes B = P(A \bar{\otimes} B)P^T. \quad (2.21)$$

The proofs of (A.4)-(A.9) are then obtained by substituting (2.21) into the equivalent expressions for the standard Kronecker product and Kronecker sum [4,8]. For example, substituting (2.21) into

$$(A \otimes B)(C \otimes D) = (AC) \otimes (BD) \quad (2.22)$$

yields

$$P(A \oplus B)P^T P(C \oplus D)P^T = P(AC) \oplus (BD)P^T. \quad (2.23)$$

Pre- and post-multiplying (2.23) respectively by P^T and P yields (A.7).

The proofs of (A.10)-(A.11) and (A.15)-(A.16) follow from the equivalent results for the Kronecker product and Kronecker sum [4,8], the property (A.3) and the fact that the determinant, trace and eigenvalues of a matrix are invariant under similarity transformation.

Since $f(\cdot)$ is analytic, there exists a scalar sequence $\{f_i\}_{i=0}^{\infty}$ such that

$$f(\lambda) = \sum_{n=0}^{\infty} f_n \lambda^n. \quad (2.24)$$

Also, from (A.7) it follows that

$$(I_n \oplus A)^i = I_n \oplus A^i \quad (2.25a)$$

$$(A \oplus I_n)^i = A^i \oplus I_n. \quad (2.25b)$$

The proofs of (A.12) and (A.13) follow from (2.24) and (2.25). (A.14) is a direct result of (A.12) and (A.13).

Finally, the proof of (A.17) is presented.

Proof of (A.17). Let $\text{col}_1(M)$ denote the first column of the matrix M and let the $n \times n$ matrices E and F satisfy

$$\text{col}_1(E) = \alpha^{(i)} \quad (2.26a)$$

$$\text{col}_1(F) = \beta^{(j)}. \quad (2.26b)$$

Then,

$$\text{col}_1(AE) = \lambda^{(i)} \alpha^{(i)} \quad (2.27a)$$

$$\text{col}_1(BF) = \beta^{(j)} \mu^{(j)}. \quad (2.27b)$$

Using (A.7) one may write

$$(A \bar{\oplus} B)(E \bar{\oplus} F) = AE \bar{\oplus} BF \quad (2.28)$$

and thus

$$(A \bar{\oplus} B)\text{col}_1(E \bar{\oplus} F) = AE \bar{\oplus} BF. \quad (2.29)$$

Recognize that for any nxn matrices M and N

$$\text{col}_1(M \bar{\oplus} N) = \text{col}_1(M) \bar{\oplus} \text{col}_1(N). \quad (2.30)$$

The proof is completed by using (2.30) and substituting (2.26) into (2.27) to obtain

$$(A \bar{\oplus} B)(\alpha^{(i)} \bar{\oplus} \beta^{(j)}) = \lambda^{(i)} \beta^{(j)} (\alpha^{(i)} \bar{\oplus} \beta^{(j)}). \quad (2.31)$$

3. Block Norm Matrices

This section defines the block norm matrix and block comparison matrix of a given matrix. Then some basic properties of the block norm matrix are presented.

Consider the pxq partitioned matrix

$$N = [N_{ij}] \quad (i=1, \dots, u; j=1, \dots, v) \quad (3.1)$$

where N_{ij} is $p_i \times q_j$. $\sum_i^u p_i = p$ and $\sum_i^v q_i = q$. Then for any matrix norm $\|\cdot\|_\theta$ define the uxv block norm matrix \bar{N}_θ [12] by

$$\bar{N}_\theta = [\bar{N}]_\theta \triangleq [\|N_{ij}\|_\theta] \quad (i=1, \dots, p; j=1, \dots, q). \quad (3.2)$$

The nonnegative matrix \bar{N}_θ is a generalization of the modulus matrix $(\|N_{ij}\|)$ for scalar partitioned matrices

Also, consider the pxp partitioned matrix

$$M = [M_{ij}] \quad (i, j=1, \dots, u) \quad (3.3)$$

where M_{ij} is $p_i \times p_j$. Let $\|\cdot\|_\phi$ denote a matrix norm induced by the vector norm $\|\cdot\|_\alpha$ and define the uxu block comparison matrix \underline{M}_ϕ [12] by

$$\underline{M}_\phi = [\underline{M}]_\phi \triangleq [\underline{m}_{ij}] \quad (i, j=1, \dots, u) \quad (3.4a)$$

where

$$\underline{m}_{ii} = \|M_{ii}^{-1}\|_\phi^{-1} \quad (3.4b)$$

$$\underline{m}_{ij} = -\|M_{ij}\|_\phi \quad \text{for } i \neq j. \quad (3.4c)$$

Here it is assumed that if M_{ii} is singular, then $\|M_{ii}^{-1}\|_\phi^{-1} = 0$. \underline{M}_ϕ is a generalization of the comparison matrix [2] for scalar partitioned matrices

Some of the properties of block norm and block comparison matrices are presented in Table B. However, before discussing and proving these properties we state the following results on matrix norms.

Proposition 3.1. Let U be an $m \times n$ matrix and V an $n \times p$ matrix. Then

$$\sigma_{\min}(U) \|V\|_F \leq \|UV\|_F \leq \sigma_{\max}(U) \|V\|_F \quad (3.5a)$$

$$\|U\|_F \sigma_{\min}(V) \leq \|UV\|_F \leq \|U\|_F \sigma_{\max}(V). \quad (3.5b)$$

Proof. Express $\|UV\|_F^2$ as

$$\|UV\|_F^2 = \text{tr}(V^H U^H UV). \quad (3.6)$$

But $U^H U$ has the modal composition

$$U^H U = E^H \Omega E \quad (3.7)$$

where E is unitary and

$$\Omega = \text{diag}\{\sigma_i^2(U)\}_{i=1}^n. \quad (3.8)$$

Thus,

$$\|UV\|_F^2 = \text{tr}(V^H E^H \Omega E V) = \text{tr}(\Omega E V V^H E^H). \quad (3.9)$$

It follows that

$$\sigma_{\min}^2(U) \text{tr}(E V V^H E) \leq \|UV\|_F^2 \leq \sigma_{\max}^2(U) \text{tr}(E V V^H E). \quad (3.10)$$

(3.5a) then follows since

$$\text{tr}(E V V^H E) = \text{tr}(V V^H) = \|V\|_F^2. \quad (3.11)$$

(3.5b) is proved similarly by using

$$\|UV\|_F^2 = \text{tr}(U V V^H U^H). \quad (3.12)$$

Proposition 3.2. Let U and V be arbitrary matrices. Then,

$$\sigma_{\max}(U \otimes V) = \sigma_{\max}(U)\sigma_{\max}(V). \quad (3.13)$$

Proof.

$$\sigma_{\max}^2(U \otimes V) = \lambda_{\max}((U \otimes V)(U \otimes V)^H). \quad (3.14)$$

Using known properties of the Kronecker product [4,8] it follows that

$$\begin{aligned} \sigma_{\max}^2(U \otimes V) &= \lambda_{\max}(UU^H \otimes VV^H) \\ &= \lambda_{\max}(UU^H)\lambda_{\max}(VV^H) \\ &= \sigma_{\max}^2(U)\sigma_{\max}^2(V). \quad \square \end{aligned} \quad (3.15)$$

Proposition 3.3. Let U be an arbitrary matrix. Then,

$$\|\text{vec}(U)\|_F = \|U\|_F. \quad (3.16)$$

Proof. The result follows from the definition of the Frobenius norm $\|\cdot\|_F$. \square

In Table B, c denotes a scalar, M is a $p \times p$ matrix partitioned as in (3.3), N and R are $p \times q$ matrices partitioned as in (3.1) and P is an $s \times p$ matrix partitioned compatibly with M and N . A , B and D are $n \times n$ matrices partitioned identically in the form (2.1). The partitions of $\text{vec}(D)$ are assumed to be the vectors $\text{vec}(D_{ij})$ and the partitions of $(A \otimes B)$ are chosen compatibly (i.e. the partitions are all of the form $A_{ij} \otimes B_{kl}$).

Table B
Block Norm Matrix Properties

- (B.1) $[\overline{CN}]_{\theta} = |C| \overline{N}_{\theta}$
- (B.2) $[\overline{N+R}]_{\theta} \ll \overline{N}_{\theta} + \overline{R}_{\theta}$
- (B.3) $[\overline{PN}]_{\phi} \ll \overline{P}_{\phi} \overline{N}_{\phi}$
- (B.4) $[\overline{PN}]_F \ll \overline{P}_s \overline{N}_F$
- (B.5) $[\overline{PN}]_F \ll \overline{P}_F \overline{N}_s$
- (B.6) $[\overline{MN}]_F \gg \underline{M}_s \overline{N}_F$
- (B.7) $[\overline{A \oplus B}]_s = \overline{A}_s \oplus \overline{B}_s$
- (B.8) $[\overline{A \oplus B}]_s \ll \overline{A}_s \oplus \overline{B}_s$
- (B.9) $[\overline{\text{vecb}(D)}]_F = \text{vec}(\overline{D}_F)$

(B.1) and (B.2) follow immediately from the norm properties $\|cN\|_{\theta} = |c| \|N\|_{\theta}$ and the triangle inequality, $\|N+R\|_{\theta} \leq \|N\|_{\theta} + \|R\|_{\theta}$. (B.3) is a result of the triangle inequality and the induced norm property $\|PN\|_{\phi} \leq \|P\|_{\phi} \|N\|_{\phi}$.

Before considering the remaining results, recognize that

$$\sigma_{\max}(N_{ij}) = \|N_{ij}\|_s \quad (3.17a)$$

$$\sigma_{\min}(M_{ii}) = \|M_{ii}^{-1}\|_s^{-1}. \quad (3.17b)$$

(B.4) and (B.5) then follow respectively from the triangle inequality and the right hand side inequalities of (3.5a) and (3.5b).

Proof of (B.6).

$$\|(MN)_{ij}\|_F = \|M_{ii}N_{ij} + \sum_{\substack{k=1 \\ k \neq i}}^u M_{ik}N_{kj}\|_F. \quad (3.18)$$

It then follows from $\|N+R\| \geq \|N\| - \|R\|$ and (3.5a) that

$$\|(MN)_{ij}\|_F \geq \sigma_{\min}(M_{ii})\|N_{ij}\|_F - \left\| \sum_{\substack{k=1 \\ k \neq i}}^u M_{ik}N_{kj} \right\|_F. \quad (3.19)$$

But since

$$\left\| \sum_{\substack{k=1 \\ k \neq i}}^u M_{ik}N_{kj} \right\|_F \leq \sum_{\substack{k=1 \\ k \neq i}}^u \|M_{ik}\|_F \|N_{kj}\|_F, \quad (3.20)$$

it follows that

$$\|(MN)_{ij}\|_F \geq \sigma_{\min}(M_{ii})\|N_{ij}\|_F + \sum_{\substack{k=1 \\ k \neq i}}^u (-\|M_{ik}\|_F) \|N_{kj}\|_F \quad (3.21)$$

which is equivalent to

$$\|(MN)_{ij}\|_F \geq \sum_{k=1}^u (\underline{M}_{ik}) (\bar{N}_{kj}). \quad (3.22)$$

(B.6) follows from (3.22). \square

Proof of (B.7).

$$(A \bar{\otimes} B) = [A_{ij} \bar{\otimes} B]_{(i,j=1,\dots,r)} \quad (3.23)$$

where

$$A_{ij} \otimes B = \begin{bmatrix} A_{ij} \otimes B_{11} & A_{ij} \otimes B_{12} & \dots & A_{ij} \otimes B_{1r} \\ A_{ij} \otimes B_{21} & A_{ij} \otimes B_{22} & \dots & A_{ij} \otimes B_{2r} \\ \vdots & \vdots & \ddots & \vdots \\ A_{ij} \otimes B_{r1} & A_{ij} \otimes B_{r2} & \dots & A_{ij} \otimes B_{rr} \end{bmatrix}. \quad (3.24)$$

It follows that

$$\overline{(A \otimes B)}_s = \overline{[(A_{ij} \otimes B)]_s} \quad (i, j=1, \dots, r). \quad (3.25)$$

Using (3.13), write

$$\|A_{ij} \otimes B_{kl}\|_s = \|A_{ij}\|_s \|B_{kl}\|_s. \quad (3.26)$$

Substituting (3.26) into (3.24) yields

$$\overline{[A_{ij} \otimes B]}_s = [\bar{A}]_s \bar{B}_s. \quad (3.27)$$

(B.7) follows from (3.25) and (3.27). \square

(B.8) now follows from (B.2) and (B.7). (B.9) is a result of (3.16).

4. Diagonal Structures

In this section results concerning block-diagonal and diagonal matrices are presented. These results are used in the example of the next section.

Assume that A and B are nxn matrices of the form

$$A = \text{block-diag}\{A_i\}_{i=1}^r \quad (4.1a)$$

$$B = \text{block-diag}\{B_i\}_{i=1}^r \quad (4.1b)$$

where A_i and B_i are $n_i \times n_i$ and $\sum_{i=1}^r n_i = n$. Then $A \bar{\otimes} B$ is the $n^2 \times n^2$ matrix

$$A \bar{\otimes} B = \text{block-diag}\{C_i\}_{i=1}^r \quad (4.2a)$$

where C_i is the $n_i \times n_i$ block-diagonal matrix,

$$C_i = \begin{bmatrix} A_i \otimes B_1 & & 0 \\ & A_i \otimes B_2 & \\ 0 & & \dots & A_i \otimes B_r \end{bmatrix}. \quad (4.2a)$$

Thus $A \bar{\otimes} B$ is block-diagonal with diagonal subblocks of the form $A_i \otimes B_j$.

It follows that $A \bar{\otimes} B$ is the $n^2 \times n^2$ matrix

$$A \bar{\otimes} B = \text{block-diag}\{D_i\}_{i=1}^r \quad (4.3a)$$

where D_i is the $n_i \times n_i$ block diagonal matrix,

$$D_i = \begin{bmatrix} A_i \oplus B_1 & & 0 \\ & A_i \oplus B_2 & \\ 0 & & \dots & A_i \oplus B_r \end{bmatrix}. \quad (4.3b)$$

Thus $A \bar{\otimes} B$ is block-diagonal with diagonal subblocks of the form $A_i \oplus B_j$.

Now suppose v is an r^2 vector and E is an $r^2 \times r^2$ diagonal matrix. Express E as

$$E = \text{block-diag}\{E_i\}_{i=1}^r \quad (4.4a)$$

where the $r \times r$ diagonal matrix E_i is given by

$$\dot{E}_i = \text{diag}\{\tilde{e}_{ij}\}. \quad (4.4b)$$

Then

$$\text{vec}^{-1}(Ev) = \tilde{E} * \text{vec}^{-1}(v). \quad (4.5)$$

where "*" denotes the Hadamard product and

$$\tilde{E} = [\tilde{e}_{ij}] \quad (i, j=1, \dots, r). \quad (4.6)$$

5. An Illustrative Example

We now use results from Sections 2, 3 and 4 to derive the covariance block norm inequality found in [7, Proposition 4.2].

Consider the nth order system

$$\dot{x}(t) = (A+G)x(t) + w(t) \quad (5.1)$$

where $w(t)$ is white noise with intensity V . It is assumed that the nxn matrix A is a stability matrix of the form

$$A = \text{block-diag}\{A_i\}_{i=1}^r \quad (5.2)$$

where A_i is $n_i \times n_i$ ($\sum_{i=1}^r n_i = n$) and represents the dynamics of the i th

subsystem. G is an nxn matrix partitioned compatibly with A . The off-diagonal blocks of G represent the uncertain interactions among the various subsystems. It is assumed that for some nonnegative rxr matrix \hat{G} ,

$$\bar{G}_s \ll \hat{G}. \quad (5.3)$$

Notice that \hat{G} is a matrix majorant of G [5].

Assuming $(A+G)$ is a stability matrix, the asymptotic state covariance Q satisfies the Lyapunov equation,

$$0 = (A+G)Q + Q(A+G)^T + V. \quad (5.4)$$

Assume that all matrices in (5.4) are partitioned compatibly. Then operating on (5.4) with $\text{vecb}(\cdot)$ and using (A.2) yields

$$-(A \oplus A)\text{vecb}(Q) = (G \oplus G)\text{vecb}(Q) + \text{vecb}(V). \quad (5.5)$$

and thus

$$\overline{[-(A \oplus A)\text{vecb}(Q)]}_F = \overline{[(G \oplus G)\text{vecb}(Q) + \text{vecb}(V)]}_F. \quad (5.6)$$

Considering the right hand side of (5.6) and using (B.2), (B.4), (B.8), (B.9) and (5.3) consecutively, yields

$$\begin{aligned} & \overline{[(G \oplus G)\text{vecb}(Q) + \text{vecb}(V)]}_F \\ & \ll \overline{[(G \oplus G)\text{vecb}(Q)]}_F + \overline{[\text{vecb}(V)]}_F \\ & \ll \overline{[G \oplus G]_s \overline{[\text{vecb}(Q)]}_F + \overline{[\text{vecb}(V)]}_F} \\ & \ll (\bar{G}_s \oplus \bar{G}_s) \text{vecb}(\bar{Q}_F) + \text{vec}(\bar{V}_F) \\ & \ll (\hat{G} \oplus \hat{G}) \text{vec}(\bar{Q}_F) + \text{vec}(\bar{V}_F). \end{aligned} \quad (5.7)$$

Similarly, considering the left hand side of (5.6) and using (B.1), (B.6) and (B.9) yields

$$\overline{[-(A \oplus A)\text{vecb}(Q)]}_F \gg \overline{[A \oplus A]_s \text{vecb}(\bar{Q}_F)}. \quad (5.8)$$

Thus, from (5.6)-(5.8)

$$(\underline{A} + \bar{A})_s \text{vec}(\bar{Q}_F) \ll (\hat{G} + \bar{G})\text{vec}(\bar{Q}_F) + \text{vec}(\bar{V}_F). \quad (5.9)$$

It follows from (4.3) that $(\underline{A} \oplus \bar{A})_s$ is the $r^2 \times r^2$ diagonal matrix

$$(\underline{A} \oplus \bar{A})_s = \text{block-diag}\{[D_i]_s\}_{i=1}^r \quad (5.10a)$$

where $[D_i]_s$ is the $r \times r$ diagonal matrix

$$[D_i]_s = \text{diag}\{\sigma_{\min}(A_i \oplus \bar{A}_j)\}_{j=1}^r. \quad (5.10b)$$

Define the $n \times n$ matrix \bar{A} by

$$\bar{A} = [\sigma_{\min}(A_i \oplus \bar{A}_j)]_{(i,j=1,\dots,r)}. \quad (5.11)$$

Then using (5.10) and (4.5) and operating with $\text{vec}^{-1}(\cdot)$ on both sides of (5.9) yields

$$\bar{A} * \bar{Q}_F \ll \hat{G} \bar{Q}_F + \bar{Q}_F \hat{G}^T + \bar{V}_F \quad (5.12)$$

which is the covariance block norm inequality of [7, Proposition 4.2].

References

1. S. Barnett, Matrix differential equations and Kronecker products, SIAM J. Appl. Math., 24 (1973), pp. 1-5.
2. A. Berman and R. J. Plemmons, Nonnegative Matrices in the Mathematical Sciences, Academic Press, New York, 1979.
3. J. W. Brewer, Matrix calculus and the sensitivity analysis of linear dynamic systems," IEEE Trans. Autom. Control, AC-23 (1978), pp. 748-751.
4. J. W. Brewer, Kronecker products and matrix calculus in systems theory, IEEE Trans. Circuits Systems, CAS-25 (1978), pp. 772-781. (Also, Correction to "Kronecker products and matrix calculus in systems theory," IEEE Trans. Circuits Systems, CAS-26 (1979), p. 360.)
5. G. Dahlquist, On matrix majorants and minorants with applications to differential equations, Linear Algebra and Applications, 52/53 (1983), pp. 199-216.
6. Y. S. Hung and D. J. N. Limebeer, Robust stability of additively perturbed interconnected systems, IEEE Trans. Autom. Control, AC-29 (1984), pp. 1069-1075.
7. D. C. Hyland and D. S. Bernstein, The majorant Lyapunov equation: A nonnegative matrix equation for robust stability and performance of large scale systems, IEEE Trans. Autom. Control, to appear. (Also in Proc. 1987 American Control Conf., Minneapolis, MN, pp. 910-918.)
8. P. Lancaster and M. Tismenetsky, The Theory of Matrices, Academic Press, New York, 1985.
9. H. Neudecker, Some theorems on matrix differentiation with special reference to Kronecker matrix products, J. Amer. Stat. Assoc., 64 (1969), pp. 953-963.
10. H. Neudecker, A note on Kronecker matrix products and matrix equation systems, SIAM J. Appl. Math, 17 (1969), pp. 603-606.
11. O. D. I. Nwokah, The robust decentralized stabilization of complex feedback systems, IEE Proceedings, 134, Pt. D (1987), pp. 43-47.
12. A. M. Ostrowski, On some metrical properties of operator matrices and matrices partitioned into blocks, 2 (1961), pp. 161-209.
13. D. S. G. Pollock, Tensor products and matrix differential calculus, Linear Algebra Appl., 67 (1985), pp. 169-193.

14. D. D. Siljak, Large Scale Dynamic Systems: Stability and Structure, Elsevier North Holland, New York, 1978.
15. G. P. H. Styan, Hadamard products and multivariate statistical analysis, Linear Algebra Appl., 6 (1973), pp. 217-240.
16. W. J. Vetter, Matrix calculus operations and Taylor expansions, SIAM Review, 15 (1973), pp. 352-369.
17. W. J. Vetter, Vector structures and solutions of linear matrix equations, Linear Algebra Appl., 10 (1975), pp. 181-188.
18. R. K. Yedavalli, Perturbation bounds for robust stability in linear state space models, Int. J. Control, 42 (1985), pp. 1507-1517.

APPENDIX E

**An M-Matrix and Majorant Approach to
Robust Stability and Performance Analysis
for Systems with Structured Uncertainty**

**An M -Matrix and Majorant Approach to
Robust Stability and Performance Analysis
for Systems with Structured Uncertainty**

by

David C. Hyland

and

Emmanuel G. Collins, Jr.

Harris Corporation
Government Aerospace Systems Division
MS 22/4848
Melbourne, FL 32902

Abstract

This work considers uncertain multi-input multi-output systems described in the frequency domain. The theory of nonnegative matrices and M -matrices is used along with majorant bounding techniques to develop robust stability and performance results for two types of uncertainty. The first type is uncertainty with norm bounded subblocks (i.e., $\|Q_{ij}(j\omega)\|_S \leq \hat{q}_{ij}(j\omega)$). The second type is uncertainty that has subblocks with known patterns but unknown gains (i.e., $Q_{ij}(j\omega) \in \{\beta_{ij}(j\omega)W_{ij}(j\omega) : |\beta_{ij}(j\omega)| \leq \hat{q}_{ij}(j\omega)\}$). For uncertainties of this type a recursive analysis methodology is developed which yields increasingly nonconservative results. Throughout this paper performance is measured in terms of the deviations of the outputs from their nominal values. The results are illustrated by a numerical example.

1. Introduction

A central problem in feedback control is to achieve acceptable performance in the presence of uncertain plant dynamics and disturbances. This necessitates the development of analysis tools capable of determining the behavior of a given feedback system in the presence of uncertainty. Thus, over the past decade considerable attention has been given to the issue of robustness analysis.

In the frequency domain setting initial attention was given to unstructured uncertainty, that is, norm bounded uncertainty. This focus led to the development of singular value analysis [1-5] which is particularly useful for systems with unmodeled high frequency dynamics. However, when the uncertainty has structure, it is well known that singular value analysis can yield very conservative results.

This conservatism has led to the investigation of analysis tools applicable to systems with uncertainty which is more structured. References [6-18] present analysis methodologies for a variety of forms of structured uncertainty. These methodologies generally depend upon one or more of the following tools:

- (i) non- L_2 (i.e., L_1 or L_∞) matrix norms [7,10]
- (ii) weighted matrix norms or system transformation [6,7,10,14-16]
- (iii) the theory of nonnegative and M-matrices [7,8,10-13]
- (iv) mapping theorems [17,18]

A common feature of many of the robustness results to date is that they consider only the *qualitative* issue of *stability*. However, in practice one is also concerned with the *quantitative* issue of *performance* where performance is measured in terms of the effect of certain signals or disturbances on specified system variables. Robustness results which do address the performance problem are found in [15,26-29].

This paper uses the theory of nonnegative matrices and M-matrices along with majorant bounding techniques [24,33] to develop robust stability and performance results for two types of uncertainty. The first type is *block-structured uncertainty* and consists of uncertainty with norm bounded blocks (i.e., $\|Q_{ij}(j\omega)\|_S \leq \hat{q}_{ij}(j\omega)$). The second type is *patterned block-structured uncertainty*. Uncertainty sets of this type have some blocks with known patterns but unknown gains (i.e., $Q_{ij}(j\omega) \in \{\beta_{ij}(j\omega)W_{ij}(j\omega) : |\beta_{ij}(j\omega)| \leq \hat{q}_{ij}(j\omega)\}$).

The paper is organized as follows. Section 2 presents notation and mathematical preliminaries. Section 3 states and formulates the general problem under consideration. Section 4 then presents robustness results for systems with structured uncertainty. It is shown that the robust stability results are nonconservative if the nominal transfer matrix $P(s)$ is block-diagonal. Next, Section 5 considers systems with highly structured uncertainty and develops a recursive methodology to obtain increasingly nonconservative robustness results. Section 6 presents an illustrative example. Finally, Section 7 summarizes and discusses the main results.

2. Notation and Preliminaries

In the following notation the matrices and vectors are in general assumed to be complex.

\mathbb{R} (\mathbb{R}_+)	set of (nonnegative) real numbers
\mathbb{C} (\mathbb{C}_+)	(closed right half) complex plane
I_p	$p \times p$ identity matrix
Z^H	complex conjugate transpose of matrix Z
z_{ij}	(i, j) element of matrix Z
Z_{ij}	(i, j) matrix block of partitioned matrix Z or (i, j) element of Z
block-diag (Z_1, \dots, Z_M)	block-diagonal matrix with listed diagonal blocks
$Y \leq Z$	$y_{ij} \leq z_{ij}$ for each i and j
nonnegative matrix	matrix with nonnegative elements ($Z \geq 0$ or equivalently $Z \in \mathbb{R}_+^{m \times n}$ for some m and n)
$ \alpha $	absolute value of scalar α
$\rho(Z)$	spectral radius of square matrix Z (If $Z \geq 0$, $\rho(Z)$ is the Perron root of Z [31,32].)
$\det(Z)$	determinant of square matrix Z
$\ x\ _2$	Euclidean norm of vector x ($= \sqrt{x^H x}$)
$\sigma_{\max}(Z)$	largest singular value of matrix Z
$\ Z\ _S$	spectral norm of matrix Z ($= \sigma_{\max}(Z)$), subordinate to the Euclidean norm
L_∞^n	the space of all rational n -vector functions bounded on the $j\omega$ -axis (i.e., $\ v(j\omega)\ _2 < \infty$ for all ω).
$S^{n \times n}$	the space of all rational, stable and proper $n \times n$ transfer-function matrices
$\ S\ _\infty$	H_∞ norm of $S(s) \in S^{n \times n}$ ($= \sup_\omega \sigma_{\max}\{S(j\omega)\}$)

Let $A, B \in \mathbb{C}^{n \times n}$ and $x \in \mathbb{C}^n$ have the partitioned forms

$$A = [A_{ij}]_{(i,j=1,\dots,r)} \quad (2.1)$$

$$B = [B_{ij}]_{(i,j=1,\dots,r)} \quad (2.2)$$

$$x^T = [x_1^T, \dots, x_r^T] \quad (2.3)$$

where $A_{ij}, B_{ij} \in \mathbb{C}^{n_i \times n_j}$, $x_i \in \mathbb{C}^{n_i}$ and $\sum_{i=1}^r n_i = n$. The *block norm matrix* [20,31] of A is the $r \times r$ nonnegative matrix

$$\bar{A} \triangleq [\|A_{ij}\|_S]_{(i,j=1,\dots,r)}. \quad (2.4)$$

Similarly, the *block norm vector* of x is the nonnegative vector $\bar{x} \in \mathbb{R}^r$ defined by

$$\bar{x}^T \triangleq [\|x_1\|_2, \dots, \|x_r\|_2]. \quad (2.5)$$

For convenience block norm matrices and vectors will be referred to simply as "block norms". Subsequent analysis will use the following block norm relations [33].

$$(\overline{\alpha A}) = \alpha \bar{A}, \quad \alpha \in \mathbb{R} \quad (2.6)$$

$$\overline{(A+B)} \leq \bar{A} + \bar{B} \quad (2.7)$$

$$\overline{(AB)} \leq \bar{A} \bar{B} \quad (2.8)$$

$$\overline{(Ax)} \leq \bar{A} \bar{x}. \quad (2.9)$$

Majorants [22] are essentially element-by-element upper bounds for block norms. Precisely, nonnegative $\hat{A} \in \mathbb{R}^{r \times r}$ and $\hat{x} \in \mathbb{R}^r$ are *majorants* respectively of A and x if

$$\bar{A} \leq \hat{A} \quad (2.10)$$

$$\bar{x} \leq \hat{x}. \quad (2.11)$$

A matrix $F \in \mathbb{R}^{p \times p}$ is an *M-matrix* [28-30] if it has nonpositive off-diagonal elements [i.e., $p_{ij} \leq 0$ for $i \neq j$] and positive principal minors. There are many equivalent characterizations of M-matrices [28-30]. A particularly useful one for the analysis of this paper is that F is an M-matrix if and only if it has nonpositive off-diagonal elements and a nonnegative inverse (i.e., $F^{-1} \geq 0$). Also, if $D \in \mathbb{R}_+^{m \times m}$, then $I_m - D$ is an M-matrix if and only if $\rho(D) < 1$.

An $n \times n$ rational transfer-function matrix $H(s)$ is *stable* if it has no poles in the closed right hand plane (i.e., it is analytic). A linear time invariant system with input v , output y and transfer representation

$$y(s) = H(s)v(s) \quad (2.12)$$

is *stable* if $H(s)$ is rational, stable and proper (i.e., $H(s) \in \mathbf{S}^{n \times n}$). This definition of system stability is equivalent to bounded-input bounded-output stability.

The H_∞ -norm of $S(s) \in \mathbf{S}^{n \times n} (\|S\|_\infty)$ generates a topology in $\mathbf{S}^{n \times n}$. Given any set $\mathbf{H} \subseteq \mathbf{S}^{n \times n}$ it is possible to define a relative topology in \mathbf{H} [5]. The set \mathbf{H} is *arcwise connected* if given any two elements $H_0(s)$ and $H_1(s)$ in \mathbf{H} , there exists a continuous map $\mathcal{M} : [0, 1] \rightarrow \mathbf{H}$, such that $\mathcal{M}(0) = H_0(s)$ and $\mathcal{M}(1) = H_1(s)$. In more physical terms, if \mathbf{H} is arcwise connected then it is possible to perturb the system from H_0 to H_1 continuously without abrupt changes in the properties of the plant. For example, if H_0 has a open right half plane zero and H_1 has a open left half plane zero then H_0 can be perturbed continuously to H_1 only by having a zero cross the imaginary axis. That is, for any continuous map $\mathcal{M}(\cdot)$ having the properties described above, there exists a $\mu \in (0, 1)$ such that $H'(\mu) = \mathcal{M}(\mu)$ has a zero on the imaginary axis. The reader is referred to [5,16] for further discussion of these results.

3. Problem Statement and Formulation

Consider the linear time invariant systems

$$y(s) = -P(s)Q(s)y(s) + R(s)v(s) \quad (3.1)$$

$$y(s) = -Q(s)P(s)y(s) + R(s)v(s). \quad (3.1)'$$

The input v and output y are in \mathbb{C}^r and have the partitioned forms

$$v^T = [v_1^T, \dots, v_r^T] \quad (3.2)$$

$$y^T = [y_1^T, \dots, y_r^T] \quad (3.3)$$

where $v_i, y_i \in \mathbb{C}^{n_i}$ and $\sum_{i=1}^r n_i = n$. The transfer-function matrices P, Q and R are partitioned conformably with v and y such that

$$P = [P_{ij}]_{(i,j=1,\dots,r)} \quad (3.4)$$

$$Q = [Q_{ij}]_{(i,j=1,\dots,r)} \quad (3.5)$$

$$R = [R_{ij}]_{(i,j=1,\dots,r)} \quad (3.6)$$

where $P_{ij}, Q_{ij}, R_{ij} \in \mathbb{C}^{n_i \times n_j}$. It is assumed that $P(s)$ is a known matrix while $Q(s)$ and $R(s)$ are members of the given uncertainty sets \mathbf{Q} and \mathbf{R} . That is,

$$Q(s) \in \mathbf{Q} \quad (3.7)$$

$$R(s) \in \mathbf{R}. \quad (3.8)$$

Definition 3.1. A system (3.1) or (3.1') is said to be *robustly stable* if it is stable for each $Q(s) \in \mathbf{Q}$ and $R(s) \in \mathbf{R}$.

Many uncertain systems can be represented in the form (3.1) or (3.1'). For example, consider the decentralized control configuration of Figure 3.1 where $\Delta(s)$ is an additive uncertainty representing uncertain subsystem interconnections. The relationship between \tilde{y} and v can be expressed as

$$[I_n + (G(s) + \Delta(s))K(s)]\tilde{y}(s) = [G(s) + \Delta(s)]K(s)v(s). \quad (3.9)$$

Now, (omitting the argument s for convenience) the return difference matrix can be factored as

$$[I_n + (G + \Delta)K] = [I + \Delta K(I_n + GK)^{-1}][I_n + GK]. \quad (3.10)$$

Substituting (3.10) into (3.9) and letting

$$y(s) = [I_n + G(s)\Delta(s)]\tilde{y}(s) \quad (3.11)$$

yields

$$[I_n + Q(s)P(s)]y(s) = R(s)v(s) \quad (3.12)$$

where

$$Q(s) = \Delta(s) \quad (3.13)$$

$$P(s) = K(s)[I_n + G(s)K(s)]^{-1} \quad (3.14)$$

$$R(s) = [G(s) + Q(s)]K(s). \quad (3.15)$$

Notice that equation (3.12) is identical to (3.1'). Also, notice that $P(s)$ is block-diagonal. This motivates the specialization of the robust stability result of Theorem 4.1 (given in the next section) to the case in which $P(s)$ is block-diagonal.

An example of a system which is representable by (3.1) is the block-diagonal perturbation configuration [7,14-15,18] of Figure 3.2 which motivated Doyle to develop the structured singular value [14]. This configuration corresponds to choosing

$$P(s) = M(s) \quad (3.16)$$

$$Q(s) = \Delta(s) \quad (3.17)$$

$$R(s) = P(s) \quad (3.18)$$

in (3.1).

In what follows only the system (3.1) is considered. However, all results are applicable to the system (3.1') by making trivial modifications.

Subsequent analysis also assumes that the input v in (3.1) is known and bounded on the imaginary axis (i.e., $v(s) \in L_\infty^n$). It is desired to obtain sufficient (or necessary and sufficient) conditions for robust stability and to obtain bounds on the performance degradation due to the uncertainty. Performance here is measured in terms of the magnitude of the deviation of the vector partitions of $y(j\omega)$ from their nominal values (i.e., the values of the $y_i(j\omega)$ for $Q(s) = Q^0(s) \in \mathbf{Q}$ and $R(s) = R^0(s) \in \mathbf{R}$). This criterion allows us to look at performance degradation as a function of frequency. The choice of the nominal transfer-function matrices $Q^0(s)$ and $R^0(s)$ is elaborated in subsequent discussion.

Below, it is also assumed that $P(s)$ and each $R(s) \in \mathbf{R}$ are rational, proper and stable (i.e., $P(s) \in \mathbf{S}^{n \times n}$ and $\mathbf{R} \subset \mathbf{S}^{n \times n}$). In addition it is assumed that the uncertainty set \mathbf{Q} is a set of $n \times n$ transfer-function matrices with (at least) the following four properties.

P1. $\mathbf{Q} \subset \mathbf{S}^{n \times n}$.

P2. \mathbf{Q} is arcwise connected.

P3. $0 \in \mathbf{Q}$.

P4. There exists nonzero $Q(s) \in \mathbf{Q}$ such that $P(s)Q(s)$ is nonconstant and

$$\det [I_n + P(s)Q(s)] \neq 0 \text{ for all } s \in \mathbb{C}_+.$$

An example of an uncertainty set satisfying properties P1-P4 is the set of transfer-function matrices in $\mathbf{S}^{n \times n}$ whose matrix blocks have norms which satisfy fixed bounds on the $j\omega$ -axis, (i.e., $\|Q_{ij}(j\omega)\|_s \leq \hat{q}_{ij}(j\omega)$). This case is considered in Section 4.

Since $P(s)$, $Q(s)$ and $R(s)$ are each assumed to be proper and stable, it follows that the system (3.1) is stable if and only if

$$\det [I_n + P(s)Q(s)] \neq 0 \quad \text{for all } s \in \mathbb{C}_+. \quad (3.19)$$

The nominal transfer matrix $Q^0(s)$ is now chosen as

$$Q^0(s) = 0. \quad (3.20)$$

It is not necessary to specify the nominal transfer matrix $R^0(s)$. However, in practice it will generally be chosen to be compatible with $Q^0(s)$. For example, if $R(s)$ is given by (3.15), then one would choose

$$R^0(s) = G(s)K(s). \quad (3.21)$$

Likewise, if $R(s)$ is given by (3.18), then one would choose

$$R^0(s) = P(s). \quad (3.22)$$

Let y^0 denote the output corresponding to the system (3.1) with $Q(s) = Q^0(s) = 0$ and $R(s) = R^0(s)$. Then,

$$y^0(s) = R^0(s)v(s). \quad (3.23)$$

Let e denote the deviation of the output from its nominal value, i.e.,

$$e(s) \triangleq y(s) - y^0(s). \quad (3.24)$$

Then, subtracting (3.23) from (3.1) shows that $e(s)$ satisfies

$$[I_n + P(s)Q(s)]e(s) = x(s) \quad (3.25)$$

where

$$x(s) \triangleq -P(s)Q(s)R^0(s)v(s) + [R(s) - R^0(s)]v(s). \quad (3.26)$$

The input x has the partitioned form

$$x^T = [x_1^T, \dots, x_r^T] \quad (3.27)$$

where $x_i \in \mathbb{C}^{n_i}$.

Definition 3.2. A nonnegative r -vector $\hat{e}(j\omega)$ function is said to be a *performance bound* of a system (3.1) if for each $Q(s) \in \mathbf{Q}$ and $R(s) \in \mathbf{R}$,

$$\bar{e}(j\omega) \leq \hat{e}(j\omega) \text{ for all } \omega. \quad (3.28)$$

The objective of the robust performance analysis is to find a nonconservative performance bound $\hat{e}(j\omega)$.

The following theorem shows that system stability can be determined from behavior on the $j\omega$ -axis. The corollary to this theorem relates the objectives of the stability analysis and performance analysis by showing that the system (3.1) is stable if and only if $\bar{e}(j\omega)$ is bounded.

Theorem 3.1. The system (3.1) is robustly stable if and only if for each $Q(s) \in \mathbf{Q}$

$$\det [I_n + P(j\omega)Q(j\omega)] \neq 0 \quad \text{for all } \omega. \quad (3.29)$$

Proof. Define

$$\mathbf{H} \triangleq \{ [I_n + P(s)Q(s)] : Q(s) \in \mathbf{Q} \}. \quad (3.30)$$

Since for each $Q(s) \in \mathbf{Q}$, $P(s)Q(s)$ is stable and proper, each $H(s) \in \mathbf{H}$ is also stable and proper (i.e., $\mathbf{H} \subset \mathbf{S}^{n \times n}$). Also, the arcwise connectedness of \mathbf{Q} implies that \mathbf{H} is also arcwise connected. Using the stability characterization (3.19) it follows that the system (3.1) is stable for each $Q(s) \in \mathbf{Q}$ and $R(s) \in \mathbf{R}$ if and only if for each $H(s) \in \mathbf{H}$

$$\det [H(s)] \neq 0 \quad \text{for all } s \in \mathbf{C}_+ \quad (3.31)$$

or equivalently, $H(s)$ does not have any left half plane zeros. Now assume that (3.29) is satisfied and there exists an $H_0(s) \in \mathbf{H}$ that has a closed right half plane zero. The proof proceeds by showing that this is a contradiction and thus (3.29) and (3.31) are equivalent.

From property P4 of the set \mathbf{Q} , it follows that there exists an $H''(s) \in \mathbf{H}$ that has a zero in the open left hand plane. However, since \mathbf{H} is arcwise connected there exists an $H'(s) \in \mathbf{H}$ that has a zero on the imaginary axis which (since $H'(s)$ has no poles on the imaginary axis) implies there exists $Q'(s) \in \mathbf{Q}$ and $\omega' \in \mathbf{IR}$ such that

$$\det [I_n + P(j\omega')Q'(j\omega')] = 0. \quad (3.32)$$

This contradicts (3.29) and thus the theorem is proved. \square

Since $P(s)$, $Q(s)$, $R(s)$ and $R^0(s)$ are stable and proper transfer matrices or constant matrices, they are bounded on the $j\omega$ -axis. Thus, $x(s)$ defined by (3.26) is also bounded on the $j\omega$ -axis. The next corollary results from this property of $x(s)$.

Corollary 3.1. The system (3.1) is robustly stable if and only if there exists a nonnegative n -vector function $\hat{e}(j\omega)$ such that for each $Q(s) \in \mathcal{Q}$ and $R(s) \in \mathcal{R}$,

$$\bar{e}(j\omega) \leq \hat{e}(j\omega) \quad \text{for all } \omega. \quad (3.33)$$

Proof. Since $x(j\omega)$ is bounded for all ω (3.25) indicates that (3.29) is satisfied if and only if $e(j\omega)$ is bounded for all ω . \square

As mentioned previously, the objectives are not only to determine conditions for robust stability but also to determine \hat{e} satisfying (3.33). In the next section this problem is considered for a particular uncertainty set \mathcal{Q} .

4. Uncertainty with Norm Bounded Blocks

This section considers the case in which the uncertainty set \mathcal{Q} is given by \mathcal{Q}' where

$$\mathcal{Q}' \triangleq \{Q(s) \in \mathcal{S}^{n \times n} : \bar{Q}(j\omega) \leq \hat{Q}(j\omega)\} \quad (4.1)$$

for some nonnegative $r \times r$ transfer-function matrix $\hat{Q}(j\omega)$. The *block-structured uncertainty* set \mathcal{Q}' satisfies properties P1-P4 of Section 3 and thus the results of the previous section apply. In fact, it should be noted that \mathcal{Q}' is not only arcwise connected but is also convex (which is a stronger condition). This fact is used to facilitate the proof of Theorem 4.1.

Theorem 4.1, the main result of this section, is a multiloop small gain theorem and presents a sufficient condition for robust stability and a performance bound \hat{e} . This result is essentially a frequency domain version of earlier results by Porter, Michel and Lasley [18,19]. If the nominal matrix $P(s)$ is block-diagonal, the first corollary shows that the robust stability condition of Theorem 4.1 is actually nonconservative (i.e., necessary and sufficient). The results are also interpreted in the context of systems with block-diagonal uncertainty matrices $Q(s)$ and are shown to yield an upper bound for the structured singular value.

Theorem 4.1. Suppose $\mathcal{Q} = \mathcal{Q}'$. Then, if

$$\rho[\bar{P}(j\omega)\hat{Q}(j\omega)] < 1 \quad \text{for all } \omega, \quad (4.2)$$

the system (3.1) is robustly stable. In this case a performance bound is given by $\hat{e}^{(-)}(j\omega)$ where

$$\hat{e}^{(-)}(j\omega) \triangleq [I_r - \bar{P}(j\omega)\hat{Q}(j\omega)]^{-1}\hat{x}(j\omega) \quad (4.3)$$

and $\hat{x}(j\omega)$ satisfies

$$\bar{x}(j\omega) \leq \hat{x}(j\omega). \quad (4.4)$$

Proof. See Appendix A. \square

Now, consider the case in which $P(s)$ is block-diagonal (i.e., $P_{ij}(s) = 0$ for $i \neq j$). This restriction on $P(s)$ can correspond to situations in which an interconnected system has well known subsystem dynamics and uncertain interconnections. An example of this is the decentralized control configuration of Figure 3.1. The following corollary shows that the robust stability condition of Theorem 4.1 is actually a necessary and sufficient condition when $P(s)$ is block-diagonal.

Corollary 4.1. Assume that $P(s)$ is block-diagonal. Then the system (3.1) is robustly stable for $Q = Q'$ if and only if (4.2) is satisfied.

Proof. See Appendix B. \square

The next corollary considers the case in which $\hat{Q}(j\omega)$ in (4.1) is given by

$$\hat{Q}(j\omega) = \alpha(j\omega)I_r \quad (4.5)$$

where

$$\alpha(j\omega) \geq 0 \quad \text{for all } \omega. \quad (4.6)$$

The problem of robust stability in this case is the block-diagonal perturbation problem considered in [7,14,15,18] which motivated the development of the structured singular value.

Corollary 4.2. Assume that \hat{Q} in (4.1) is given by (4.5). Then, if

$$\rho[\bar{P}(j\omega)] < \frac{1}{\alpha(j\omega)} \quad \text{for all } \omega, \quad (4.7)$$

the system (3.1) is robustly stable.

Proof. The proof follows by substituting (4.6) into (4.2). \square

Remark 4.1. Recognize that the performance bound (4.4) remains valid under the assumptions of Corollaries 4.1 and 4.2.

Now recall that under the assumption of Corollary 4.2, the "small μ theorem" [15] states that the system (3.1) is robustly stable *if and only if*

$$\mu[P(j\omega)] < \frac{1}{\alpha(j\omega)} \quad \text{for all } \omega \quad (4.8)$$

where $\mu(\cdot)$ denotes the structured singular value [14,15].

An immediate consequence of the above discussion is then the following corollary.

Corollary 4.3. For $\omega_0 \in \mathbb{R}$

$$\mu[P(j\omega_0)] \leq \rho[\bar{P}(j\omega_0)]. \quad (4.9)$$

Remark 4.2. If $r = 2$ and $n_1 = n_2 = 1$, then as mentioned in [17] it can be shown that

$$\mu[P(j\omega_0)] = \rho[\bar{P}(j\omega_0)]. \quad (4.10)$$

Remark 4.3. An alternative proof of Corollary 4.3 is also available [25]. This proof is based on the characterization of $\mu(\cdot)$ found in Theorem 1 of [14]. The proof then follows by using the inequality

$$\rho(P(j\omega_0)) \leq \rho[\bar{P}(j\omega_0)] \quad (4.11)$$

which is presented in Theorem 4 of [20]. (A simpler proof of (4.11) is presented in the Appendix of [20].)

5. A Recursive Refinement of Robustness Results for Highly Structured Uncertainty

This section considers the robust stability of the system (3.1) for an uncertainty set Q'' which is more structured than the uncertainty set Q' of Section 4. Further discussion requires the introduction of some additional notation and definitions.

Let \mathbf{m} be some set of integer pairs

$$\mathbf{m} \subseteq \{(i, j) : 1 \leq i \leq r, \quad i \leq j \leq r\}. \quad (5.1)$$

For each $(i, j) \in \mathbf{m}$ let $W_{ij}(j\omega)$ be an $n_i \times n_j$ transfer-function matrix. Also, for some $r \times r$ nonnegative transfer-function matrix $\hat{Q}(j\omega)$ let

$$Q'' = \{Q(s) \in Q' : \text{for all } \omega \text{ and } (i, j) \in \mathbf{m}, \\ Q_{ij}(j\omega) = \beta_{ij}(j\omega)W_{ij}(j\omega), \quad |\beta_{ij}(j\omega)| \leq \hat{q}_{ij}(j\omega)/\|W_{ij}\|_s\}. \quad (5.2)$$

Notice that

$$Q'' \subseteq Q' \quad (5.3)$$

If \mathfrak{n} is nonempty, Q'' is said to be an uncertainty set containing *patterned block-structured uncertainty*.

The set Q'' satisfies properties P1-P4 of Section 3 and like Q' is convex. Since $Q'' \subseteq Q'$ the robustness results of Theorem 4.1 apply with $Q' = Q''$. However, (if \mathfrak{n} is nonempty) the additional structural information associated with the uncertainty set Q'' allows the development of less conservative results. Below, we develop a recursive methodology to obtain robust stability conditions and performance bounds. Each stage of the recursion yields robustness results which can be significantly less conservative than the results of the previous step and are guaranteed to never be more conservative.

The development of this section begins by showing that the robustness properties of the system (3.1) can be determined by analyzing any one of a sequence of equations. First, for $k \in \{0, 1, 2, \dots\}$ consider the equation

$$(I_n - (-PQ)^{2^k})e^{(k)} = \left[\prod_{m=0}^{k-1} (I_n + (-PQ)^{2^m}) \right] x \quad (5.4)$$

where we use the convention

$$\prod_{m=0}^{-1} (I_n + (-PQ)^{2^m}) \triangleq I_n \quad (5.5)$$

and x is defined by (3.26). Also recognize that

$$\prod_{m=0}^{k-1} (I_n + (-PQ)^{2^m}) = \sum_{m=0}^{2^k-1} (-PQ)^m \quad \text{for } k = 1, 2, \dots \quad (5.6)$$

(Note that the argument s is implicit in (5.4)-(5.6)). An important theorem is now presented.

Theorem 5.1. Let $k \in \{0, 1, 2, \dots\}$. Then the system (3.1) is robustly stable for $Q = Q''$ if and only if for each $Q(s) \in Q''$

$$\det \left[I_n - (-P(j\omega)Q(j\omega))^{2^k} \right] \neq 0 \quad \text{for all } \omega. \quad (5.7)$$

In this case, for each $Q(s) \in Q''$ and $R(s) \in \mathbb{R}$ the error vector $e(j\omega)$ which solves (3.25) is given by

$$e(j\omega) = e^{(k)}(j\omega) \quad (5.8)$$

where $e^{(k)}(j\omega)$ satisfies (5.4) with $x(j\omega)$ given by (3.26).

Proof. The proof is found in Appendix C and uses Lemma C which is also presented in Appendix C. \square

Now for $k \in \{0, 1, 2, \dots\}$ and each $Q(s) \in \mathcal{Q}''$ and $R(s) \in \mathcal{R}$ define

$$T^{(k)}(j\omega) = (-P(j\omega)Q(j\omega))^{2^k} \quad (5.9)$$

$$x^{(k)}(j\omega) = \left[\prod_{m=0}^{k-1} (I_n + T^{(m)}(j\omega)) \right] x(j\omega) \quad (5.10)$$

where $x(j\omega)$ is given by (3.25). $T^{(k)}$ and $x^{(k)}$ have the partitioned forms

$$T^{(k)} = [T_{ij}^{(k)}]_{(i,j=1,\dots,r)} \quad (5.11)$$

$$(x^{(k)})^T = [(x_1^{(k)})^T, \dots, (x_r^{(k)})^T] \quad (5.12)$$

where $T_{ij}^{(k)} \in \mathbb{C}^{n_i \times n_j}$ and $x_i^{(k)} \in \mathbb{C}^{n_i}$. Now choose $r \times r$ $\hat{T}^{(k)}(j\omega)$ and r dimensional $\hat{x}(j\omega)$ such that for each $Q(s) \in \mathcal{Q}''$ and $R(s) \in \mathcal{R}$

$$\overline{T}^{(k)}(j\omega) \leq \hat{T}^{(k)}(j\omega) \quad \text{for all } \omega \quad (5.13)$$

$$\overline{x}^{(k)}(j\omega) \leq \hat{x}^{(k)}(j\omega) \quad \text{for all } \omega. \quad (5.14)$$

Notice that

$$T^{(k+1)}(j\omega) = [T^{(k)}(j\omega)]^2 \quad (5.15)$$

$$x^{(k+1)}(j\omega) = (I_n + T^{(k)}(j\omega))x^{(k)}(j\omega). \quad (5.16)$$

It then follows from (5.19), (5.20) and the block norm inequalities (2.7)–(2.9) that it is always possible to choose sequences $\{\hat{T}^{(k)}(j\omega)\}_{k=0}^{\infty}$ and $\{\hat{x}^{(k)}(j\omega)\}_{k=0}^{\infty}$ such that

$$\hat{T}^{(k+1)}(j\omega) = [\hat{T}^{(k)}(j\omega)]^2 \quad \text{for all } \omega \quad (5.17)$$

$$\hat{x}^{(k+1)}(j\omega) = [I_r + \hat{T}^{(k)}(j\omega)]\hat{x}^{(k)}(j\omega) \quad \text{for all } \omega. \quad (5.18)$$

However, in general it is possible to choose the sequences $\{\hat{T}^{(k)}(j\omega)\}_{k=0}^{\infty}$ and $\{\hat{x}^{(k)}(j\omega)\}_{k=0}^{\infty}$ such that

$$\hat{T}^{(k+1)}(j\omega) \leq [\hat{T}^{(k)}(j\omega)]^2 \quad \text{for all } \omega \quad (5.19)$$

$$\hat{x}^{(k+1)}(j\omega) \leq [I_r + \hat{T}^{(k)}(j\omega)]\hat{x}^{(k)}(j\omega) \quad \text{for all } \omega. \quad (5.20)$$

This fact is illustrated by the following example. This example corresponds to considering a system of the form (3.1) at a fixed frequency ω_0 .

Example 5.1. Suppose

$$P(j\omega_0) = \text{block-diag}\{P_1(j\omega_0), P_2(j\omega_0)\}$$

where

$$P_1(j\omega_0) = \begin{bmatrix} 1 & 0 \\ 0 & 0 \end{bmatrix}, \quad P_2(j\omega_0) = \begin{bmatrix} 0 & 0 \\ 0 & 1 \end{bmatrix},$$

$$W(j\omega_0) = \begin{bmatrix} 0 & W_{12}(j\omega_0) \\ W_{21}(j\omega_0) & 0 \end{bmatrix}$$

where

$$W_{12}(j\omega_0) = \begin{bmatrix} 1 & 0 \\ 0 & 0 \end{bmatrix}, \quad W_{21}(j\omega_0) = \begin{bmatrix} 0 & 0 \\ 0 & 1 \end{bmatrix},$$

$$Q(\omega_0)'' \in \{Q(j\omega_0) \in \mathbb{C}^{4 \times 4} : Q(j\omega_0) = \beta(j\omega_0)W(j\omega_0), |\beta(j\omega_0)| \leq \hat{q}(j\omega_0)\}$$

and

$$x^T(j\omega_0) = [x_1^T(j\omega_0), x_2^T(j\omega_0)].$$

where

$$x_1^T(j\omega_0) = [1, 0], \quad x_2^T(j\omega_0) = [0, 1].$$

Then for each $Q(j\omega_0) \in Q(\omega_0)''$

$$T^{(0)}(j\omega_0) = PQ(j\omega_0) = -\beta(j\omega_0) \begin{bmatrix} 0 & P_1W_{12}(j\omega_0) \\ P_2W_{21}(j\omega_0) & 0 \end{bmatrix}$$

$$T^{(1)}(j\omega_0) = -[PQ(j\omega_0)]^2 = -\beta(j\omega_0)^2 \begin{bmatrix} P_1W_{12}P_2W_{21}(j\omega_0) & 0 \\ 0 & P_2W_{21}P_1W_{12}(j\omega_0) \end{bmatrix}$$

and

$$x^{(0)}(j\omega_0) = x(j\omega_0) = \begin{bmatrix} x_1(j\omega_0) \\ x_2(j\omega_0) \end{bmatrix}$$

$$x^{(1)}(j\omega_0) = [I_4 + T^{(0)}(j\omega_0)]x^{(0)}(j\omega_0) = \begin{bmatrix} x_1(j\omega_0) \\ x_2(j\omega_0) \end{bmatrix} - \beta(j\omega_0) \begin{bmatrix} P_1W_{12}x_2(j\omega_0) \\ P_2W_{21}x_1(j\omega_0) \end{bmatrix}.$$

Choose

$$\hat{T}^{(0)}(j\omega_0) = \hat{q}(j\omega_0) \begin{bmatrix} 0 & 1 \\ 1 & 0 \end{bmatrix}$$

This is the smallest possible choice of $\hat{T}^{(0)}(j\omega_0)$ in the sense that there exists $Q(j\omega_0) \in Q(\omega_0)''$ such that $\bar{T}^{(0)}(j\omega_0) = \hat{T}^{(0)}(j\omega_0)$. Noticing that $W_{12}P_2(j\omega_0) = W_{21}P_1(j\omega_0) = 0$ it is possible to choose

$$\hat{T}^{(1)}(j\omega_0) = 0 \ll [\hat{T}^{(0)}(j\omega_0)] = \hat{q}(j\omega_0)^2 I_2$$

Now choose

$$\hat{x}^{(0)}(j\omega_0) = \begin{bmatrix} 1 \\ 1 \end{bmatrix}$$

This is obviously the smallest possible choice of $\hat{x}^{(0)}(j\omega_0)$ since $\bar{x}^{(0)}(j\omega_0) = \hat{x}^{(0)}(j\omega_0)$. Now notice that $P_1W_{12}x_1(j\omega_0) = P_2W_{21}x_2(j\omega_0) = 0$. Thus it is possible to choose

$$\hat{x}^{(1)}(j\omega_0) = \hat{x}^{(0)}(j\omega_0) \ll (I + \hat{T}^{(0)}(j\omega_0))\hat{x}^{(0)}(j\omega_0) = (1 + \hat{q}(j\omega_0)) \begin{bmatrix} 1 \\ 1 \end{bmatrix}. \quad \square$$

The main results of this section are now presented below in Theorem 5.2 and Corollary 5.1. Theorem 5.2 provides a sufficient condition for robust stability while Corollary 5.1 provides the foundation of a recursive methodology for obtaining less conservative bounds.

Theorem 5.2. Suppose $Q = Q''$ and consider any $k \in \{0, 1, 2, \dots\}$. Then, if

$$\rho[\hat{T}^{(k)}(j\omega)] < 1 \quad \text{for all } \omega, \quad (5.21)$$

the system (3.1) is robustly stable. In this case, a performance bound is given by $\hat{e}^{(k)}(j\omega)$ where

$$\hat{e}^{(k)}(j\omega) \triangleq [I_r - \hat{T}^{(k)}(j\omega)]^{-1} \hat{x}^{(k)}(j\omega). \quad (5.22)$$

Proof. The proof of this theorem depends upon Theorem 5.1 and is essentially identical to the proof of Theorem 4.1 found in Appendix A. \square

Corollary 5.1. Suppose $Q = Q''$ and the sequences $\{\hat{T}^{(k)}(j\omega)\}_{k=0}^{\infty}$ and $\{\hat{x}^{(k)}(j\omega)\}_{k=0}^{\infty}$ satisfy (5.19) and (5.20). Then, if for some $m \in \{0, 1, 2, \dots\}$

$$\rho[\hat{T}^{(m)}(j\omega)] < 1 \quad \text{for all } \omega, \quad (5.23)$$

the system (3.1) is robustly stable. In this case, for any $k \geq m$

$$\rho[\hat{T}^{(k)}(j\omega)] < 1 \quad \text{for all } \omega \quad (5.24)$$

and $\hat{e}^{(k)}(j\omega)$ defined by (5.22) is a performance bound. In addition

$$\hat{e}^{(k+1)}(j\omega) \leq \hat{e}^{(k)}(j\omega) \quad \text{for all } \omega. \quad (5.25)$$

Proof. The inequality (5.24) is a direct consequence of (5.21) and (5.19). That $\hat{e}^{(k)}(j\omega)$ is a performance bound then follows immediately from Theorem 5.2.

Now $\hat{e}^{(k)}(j\omega)$ satisfies

$$[I_r - \hat{T}^{(k)}(j\omega)]\hat{e}^{(k)}(j\omega) = \hat{x}^{(k)}(j\omega). \quad (5.26)$$

Premultiplying (5.26) by the invertible matrix $[I_r + \hat{T}^{(k)}(j\omega)]$ and rearranging gives

$$\hat{e}^{(k)}(j\omega) = [\hat{T}^{(k)}(j\omega)]^2 \hat{e}^{(k)}(j\omega) + [I_r + \hat{T}^{(k)}(j\omega)]\hat{x}^{(k)}(j\omega). \quad (5.27)$$

It then follows from (5.19) and (5.20) that

$$\hat{e}^{(k)}(j\omega) \geq \hat{T}^{(k+1)}(j\omega)\hat{e}^{(k)}(j\omega) + \hat{x}^{(k+1)}(j\omega). \quad (5.28)$$

Thus, there exists $\Theta \in \mathbb{R}_+^r$ such that

$$\hat{e}^{(k)}(j\omega) = \hat{T}^{(k+1)}(j\omega)\hat{e}^{(k)}(j\omega) + \hat{x}^{(k+1)}(j\omega) + \Theta. \quad (5.29)$$

Next notice that

$$\hat{e}^{(k+1)}(j\omega) = \hat{T}^{(k+1)}(j\omega)\hat{e}^{(k+1)}(j\omega) + \hat{x}^{(k+1)}(j\omega). \quad (5.30)$$

Subtracting (5.30) from (5.29) and rearranging yields

$$[\hat{e}^{(k)}(j\omega) - \hat{e}^{(k+1)}(j\omega)] = [I_r - \hat{T}^{(k+1)}(j\omega)]^{-1}\Theta. \quad (5.31)$$

It follows from (5.24) that $[I_r - \hat{T}^{(k+1)}(j\omega)]$ is an M-matrix and thus

$$[I_r - \hat{T}^{(k+1)}(j\omega)]^{-1} \geq 0 \quad \text{for all } \omega. \quad (5.32)$$

The inequality (5.25) follows from (5.31) and (5.32). \square

Remark 5.1. If (5.23) is satisfied, then since the sequence $\{\hat{e}^{(k)}(j\omega)\}_{k=m}^{\infty}$ is bounded below by the zero vector and is monotonically nonincreasing (i.e., it satisfies (5.25)), it is guaranteed to converge.

Remark 5.2. Recognize that the calculation of successive members of the sequences $\{\hat{T}^{(k)}(j\omega)\}_{k=0}^{\infty}$ and $\{\hat{x}^{(k)}(j\omega)\}_{k=0}^{\infty}$ is increasingly complex.

Remark 5.3. It is always possible to choose $\hat{T}^{(0)}(j\omega)$ and $\hat{x}^{(0)}(j\omega)$ such that

$$\hat{e}^{(0)}(j\omega) \leq \hat{e}^{(-)}(j\omega) \quad \text{for all } \omega \quad (5.33)$$

where $\hat{e}^{(-)}(j\omega)$ is the bound defined by (4.4).

Corollary 5.1 is the basis of the following recursive algorithm for the analysis of robust stability and performance.

Recursive Algorithm for Robustness Analysis

This algorithm assumes that for some $p \in \{0, 1, 2, \dots\}$ the sequence $\{\hat{T}^{(k)}(j\omega)\}$ satisfies (5.21) for $k \geq p$.

Step 1: Initialize $m = 0$.

Step 2: Determine if $\hat{T}^{(m)}(j\omega)$ satisfies (5.28).

Step 3: If $\hat{T}^{(m)}(j\omega)$ satisfies (5.28) go to Step 4. If $\hat{T}^{(m)}(j\omega)$ does not satisfy (5.28) and $m < p$, then let $m \leftarrow m + 1$ and go to Step 2. If $\hat{T}^{(m)}(j\omega)$ does not satisfy (5.28) and $m = p$ then stability cannot be guaranteed and the algorithm stops.

Step 4: Let $k = m$.

Step 5: Compute the performance bound $\hat{e}^{(k)}(j\omega)$. If the bound is close (or equal) to the limit of the sequence $\{\hat{e}^{(k)}(j\omega)\}_{k=m}^{\infty}$ or is satisfactory in some other sense considered by the analyst, then stop. Otherwise go to Step 6.

Step 6: Let $k \leftarrow k + 1$ and go to Step 5.

6. An Illustrative Example

Consider the configuration of Figure 6.1 which describes two oscillators with uncertain coupling. This system can be described by (3.1) with

$$y^T(s) = [y_1^T(s), y_2^T(s)] \quad (6.1)$$

$$v_s^T = [v_1^T(s), v_2^T(s)] \quad (6.2)$$

$$R(s) = P(s) = \begin{bmatrix} P_1(s) & 0 \\ 0 & P_s(s) \end{bmatrix} \quad (6.3)$$

$$Q(s) = \begin{bmatrix} 0 & Q_{12}(s) \\ Q_{21}(s) & 0 \end{bmatrix}. \quad (6.4)$$

Notice also that

$$P_i(s) = \frac{1}{(s + \nu_i)^2 + \Omega_i^2} \begin{bmatrix} s + \nu_i & \Omega_i \\ -\Omega_i & s + \nu_i \end{bmatrix}. \quad (6.5)$$

The nominal output y^o (corresponding to $Q^0(s) = 0$) is given by

$$y^o(s) = P(s)v(s). \quad (6.6)$$

In addition, the error vector

$$e(s) \triangleq y(s) - y^o(s) \quad (6.7)$$

is given by

$$[I_4 + P(s)Q(s)]e(s) = x(s) \quad (6.8)$$

where

$$x(s) = -P(s)Q(s)P(s)v(s) \quad (6.9)$$

or equivalently

$$x(s) = \begin{bmatrix} x_1(s) \\ x_2(s) \end{bmatrix} = - \begin{bmatrix} P_1(s)Q_{12}(s)P_2(s)v_2(s) \\ P_2(s)Q_{21}(s)P_1(s)v_1(s) \end{bmatrix}. \quad (6.10)$$

Now let

$$\hat{Q}(j\omega) = \begin{bmatrix} 0 & \hat{q}_{12}(\omega) \\ \hat{q}_{21}(\omega) & 0 \end{bmatrix} \quad (6.11)$$

where

$$\hat{q}_{12}(\omega) = \sigma \left(1 - \frac{\Omega_A}{\sqrt{\omega^2 + \Omega_A^2}} \right) \quad (6.12)$$

$$\hat{q}_{21}(\omega) = \sigma \left(\frac{\Omega_S}{\sqrt{\omega^2 + \Omega_S^2}} \right). \quad (6.13)$$

Also, let Q be given by Q'_E where

$$Q'_E = \{Q(s) \in S^{4 \times 4} : \bar{Q}(j\omega) \leq \hat{Q}(j\omega)\}. \quad (6.14)$$

Subsequent results consider the case

$$\nu_1 = \nu_2 = 0.005 \quad (6.15)$$

$$\Omega_1 = 1.0, \quad \Omega_2 = 10.0 \quad (6.16)$$

$$\Omega_A = \Omega_S = 5.0 \quad (6.17)$$

$$v_1^T(j\omega) = v_2^T(j\omega) = [0 \quad 1]. \quad (6.18)$$

Standard singular value analysis assures stability if

$$\bar{\sigma}(P(j\omega))L(\omega) < 1 \quad \text{for all } \omega \quad (6.19)$$

where

$$L(\omega) = \max \{ \hat{q}_{12}(\omega), \hat{q}_{21}(\omega) \}. \quad (6.20)$$

For the case under consideration the condition (6.19) is satisfied only for

$$\sigma < 0.0051. \quad (6.21)$$

However, the stability condition of Corollary 4.1 shows that the system is actually stable if and only if

$$\sigma < 0.428. \quad (6.22)$$

comparing (6.21) and (6.22) demonstrates the conservatism sometimes inherent in singular value analysis.

Figure 6.2 shows a plot of $\|y_1^0(j\omega)\|_2$ and $\|y_2^0(j\omega)\|_2$ versus ω . For $\sigma = 0.3$ Figures 6.3 and 6.4 show plots of $\hat{e}_1^{(-)}(j\omega)$ and $\hat{e}_2^{(-)}(j\omega)$ respectively versus ω , computed using (4.3) with

$$\hat{x}^T(j\omega) = [\hat{x}_1^T(j\omega), \hat{x}_2^T(j\omega)] \quad (6.23)$$

where

$$\hat{x}_1(j\omega) = \|P_1(j\omega)\|_S \hat{q}_{12}(\omega) \|P_2(j\omega)v_2\|_2 \quad (6.24)$$

$$\hat{x}_2(j\omega) = \|P_2(j\omega)\|_S \hat{q}_{21}(\omega) \|P_1(j\omega)v_1\|_2. \quad (6.25)$$

The latter plots shows the possible performance degradation in the outputs y_1 and y_2 due to the system uncertainty.

Now assume that the patterns of the subblocks of $Q(s)$ are known in addition to bounds on the norms of the subblocks. In particular let W_{12} and W_{21} be the constant matrices

$$W_{12} = \frac{1}{2} \begin{bmatrix} 1 & j \\ -j & 1 \end{bmatrix} \quad (6.26)$$

$$W_{21} = \frac{1}{2} \begin{bmatrix} 1 & -j \\ j & 1 \end{bmatrix} \quad (6.27)$$

and notice that

$$\|W_{12}\|_* = \|W_{21}\|_* = 1. \quad (6.28)$$

Now, let Q be given by Q_E'' where

$$Q_E'' = \{Q(s) \in Q_E' : \text{for all } \omega, Q_{12}(j\omega) = \beta_{12}(\omega)W_{12}, \quad (6.29)$$

$$Q_{21}(j\omega) = \beta_{21}(\omega)W_{21}, |\beta_{12}(\omega)| \leq \hat{q}_{12}(\omega), |\beta_{21}(\omega)| \leq \hat{q}_{21}(\omega)\},$$

and $\hat{q}_{12}(\omega)$ and $\hat{q}_{21}(\omega)$ are defined by (6.12) and (6.13).

Now, notice that

$$T^{(0)}(j\omega) = -P(j\omega)Q(j\omega) = - \begin{bmatrix} 0 & P_1 Q_{12} \\ P_2 Q_{21} & 0 \end{bmatrix} (j\omega), \quad (6.30)$$

$$T^{(1)}(j\omega) = (-P(j\omega)Q(j\omega))^2 = \begin{bmatrix} P_1 Q_{12} P_2 Q_{21} & 0 \\ 0 & P_2 Q_{21} P_1 Q_{12} \end{bmatrix} (j\omega), \quad (6.31)$$

$$x^{(0)}(j\omega) = x(j\omega),$$

$$x^{(1)}(j\omega) = [I + T^{(0)}(j\omega)]x(j\omega) = x(j\omega) + \begin{bmatrix} P_2 Q_{21} P_1 Q_{12} P_2 v_2 \\ P_1 Q_{12} P_2 Q_{21} P_1 v_1 \end{bmatrix} (j\omega). \quad (6.32)$$

Choose $\hat{T}^{(0)}(j\omega)$, $\hat{T}^{(1)}(j\omega)$, $\hat{x}^{(0)}(j\omega)$, $\hat{x}^{(1)}(j\omega)$ as

$$\hat{T}^{(0)}(j\omega) = \begin{bmatrix} 0 & \hat{t}_{12}^{(0)}(j\omega) \\ \hat{t}_{21}^{(0)}(j\omega) & 0 \end{bmatrix} \quad (6.33)$$

where

$$\hat{t}_{12}^{(0)}(j\omega) = \hat{q}_{12}(\omega) \|P_1 W_{12}\|_s(j\omega) \quad (6.34)$$

$$\hat{t}_{21}^{(0)}(j\omega) = \hat{q}_{21}(\omega) \|P_2 W_{21}\|_s(j\omega); \quad (6.35)$$

$$\hat{T}^{(1)}(j\omega) = \begin{bmatrix} \hat{t}_{11}^{(1)}(j\omega) & 0 \\ 0 & \hat{t}_{22}^{(1)}(j\omega) \end{bmatrix} \quad (6.36)$$

where

$$\hat{t}_{11}^{(1)}(j\omega) = \hat{q}_{12} \hat{q}_{21}(\omega) \|P_1 W_{12} P_2 W_{21}\|_s(j\omega) \quad (6.37)$$

$$\hat{t}_{22}^{(1)}(j\omega) = \hat{q}_{21} \hat{q}_{12}(\omega) \|P_2 W_{21} P_1 W_{12}\|_s(j\omega); \quad (6.38)$$

$$\hat{x}^{(0)}(j\omega) = \begin{bmatrix} \hat{x}_1^{(0)}(j\omega) \\ \hat{x}_2^{(0)}(j\omega) \end{bmatrix} \quad (6.39)$$

where

$$\hat{x}_1^{(0)}(j\omega) = \hat{q}_{12}(\omega) \|P_1 W_{12} P_2 v_2\|_2(j\omega) \quad (6.40)$$

$$\hat{x}_2^{(0)}(j\omega) = \hat{q}_{21}(\omega) \|P_2 W_{21} P_1 v_1\|_2(j\omega); \quad (6.41)$$

$$\hat{x}^{(1)}(j\omega) = \begin{bmatrix} \hat{x}_1^{(1)}(j\omega) \\ \hat{x}_2^{(1)}(j\omega) \end{bmatrix} \quad (6.42)$$

where

$$\hat{x}_1^{(1)}(j\omega) = \hat{x}_1^{(0)}(j\omega) + \hat{q}_{21} \hat{q}_{12}(\omega) \|P_2 W_{21} P_1 W_{12} P_2 v_2\|_2(j\omega) \quad (6.43)$$

$$\hat{x}_2^{(1)}(j\omega) = \hat{x}_2^{(0)}(j\omega) + \hat{q}_{12} \hat{q}_{21}(\omega) \|P_1 Q_{12} P_2 W_{21} P_1 v_1\|_2(j\omega). \quad (6.44)$$

For $k = 0$, the robust stability condition of Theorem 5.2 shows that the system is stable for

$$\sigma < 0.470 \quad (6.45)$$

which describes a larger stability region than (6.22). For $k = 1$, the robust stability condition of Theorem 5.2 shows that the system is stable for

$$\sigma < 1.5 \times 10^5 \quad (6.46)$$

which is a much less conservative result! Since for this example for $k \in \{2, 3, \dots\}$ one must choose

$$\hat{T}^{(k)}(j\omega) \geq [\hat{T}^{(1)}(j\omega)]^{2^{(k-1)}} \text{ for all } \omega,$$

(6.46) describes the largest stability region which can be obtained by the recursive algorithm of Section 5.

Figure 6.3 shows plots of $\hat{e}_1^{(0)}(j\omega)$ and $\hat{e}_1^{(1)}(j\omega)$ vs. ω , computed using (5.27) with $k = 0$. Likewise, Figure 6.4 shows plots of $\hat{e}_2^{(0)}(j\omega)$ and $\hat{e}_2^{(1)}(j\omega)$ vs. ω , computed using (5.27) with $k = 1$. As insured by the theory

$$\hat{e}_1^{(1)}(j\omega) \leq \hat{e}_1^{(0)}(j\omega) \quad \text{for all } \omega \quad (6.47)$$

$$\hat{e}_2^{(1)}(j\omega) \leq \hat{e}_2^{(0)}(j\omega) \quad \text{for all } \omega. \quad (6.48)$$

Summary

This paper has used the theory of nonnegative and M-matrices to develop robust stability and performance results for two types of uncertainty characterizations. Performance was measured in terms of the deviations of the system outputs from their nominal values. For uncertainty with norm bounded subblocks the development led to a frequency dependent multi-loop small gain theorem. The stability result was shown to be *necessary and sufficient* when the nominal transfer matrix $P(s)$ is block-diagonal. For uncertainty that has subblocks with known patterns the developments led to a recursive methodology which is guaranteed to yield increasingly nonconservative results.

The results were illustrated by considering two oscillators with uncertain couplings. The frequency dependent multi-loop small gain theorem was shown to yield much less conservative results than standard singular value analysis. However, for a given case in which the patterns of the uncertain coupling blocks were assumed to be known the recursive analysis methodology yielded a stability region over 5 orders of magnitude greater than that obtained by using the multiloop small gain theorem. The recursive methodology also yielded better (i.e., smaller) bounds on the output perturbations, a result guaranteed by the theory.

Acknowledgements. We wish to thank Jill Straehla for the excellent typing of the original manuscript, Allen Daubendiek for performing the numerical computations, Dennis Bernstein for several helpful comments, and Teresa Rhodes for assisting in the preparation of the figures.

Appendix A

Proof of Theorem 4.1. First recognize that since $Q = Q'$,

$$(\overline{PQ}) \leq \overline{P\hat{Q}} \quad \text{for all } \omega. \quad (\text{A.1})$$

(Here the block norm inequality (2.8) has been used.) Now assume that the system (3.1) is robustly stable for some $Q \in Q'$. Then the corresponding output perturbation e_Q is bounded on the imaginary axis and satisfies

$$e_Q = PQe_Q + z \quad \text{for all } \omega. \quad (\text{A.2})$$

It follows by using (A.1), (4.4) and the block norm inequalities (2.8) and (2.9) that

$$\bar{e}_Q \leq \overline{P\hat{Q}}\bar{e}_Q + \hat{z} \quad \text{for all } \omega \quad (\text{A.3})$$

or equivalently

$$(I_r - \overline{P\hat{Q}})\bar{e}_Q \leq \hat{z} \quad \text{for all } \omega. \quad (\text{A.4})$$

If $\rho(\overline{P\hat{Q}}) < 1$ (i.e., $I_r - \overline{P\hat{Q}}$ is an M-matrix) for all ω , then $(I_r - \overline{P\hat{Q}})^{-1} \in \mathbb{R}_+^{r \times r}$ for all ω . Premultiplying (A.4) by $(I_r - \overline{P\hat{Q}})^{-1}$ then gives

$$\bar{e}_Q \leq \hat{e} \quad \text{for all } \omega \quad (\text{A.5})$$

where \hat{e} is the solution of

$$\hat{e} = (I_r - \overline{P\hat{Q}})^{-1}\hat{z}. \quad (\text{A.6})$$

Next assume that $(I_r - \overline{P\hat{Q}})$ is an M-matrix for all ω and that the system (3.1) is *not* robustly stable. Recognize that for $\omega_o \in \mathbb{R}$ $|\det[I_r + P(j\omega_o)Q(j\omega_o)]|$ is a continuous function of Q . Define

$$f(Q) \triangleq \inf_{\omega} |\det(I_r + PQ)|. \quad (\text{A.7})$$

The function $f(Q)$ is also continuous in Q . In addition, the system (3.1) is stable for $Q \in Q'$ if and only if $f(Q) > 0$. Now there always exist a neighborhood in Q' of $Q = 0$ such that for each Q in the neighborhood, $f(Q) > 0$. Since Q' is convex, there exist $Q_o \in Q'$ such that $f(\mu Q_o) > 0$ for $\mu \in [0, 1)$ and $f(Q_o) = 0$. It follows that for $\mu \in [0, 1)$

$$\bar{e}_{\mu Q_o} \leq \hat{e} \quad \text{for all } \omega \quad (\text{A.8})$$

and there exists $\omega_o \in \mathbb{R}$ such that

$$\lim_{\mu \rightarrow 1} \left| \det [I_r + \mu P(j\omega_o)Q(j\omega_o)] \right| = 0. \quad (\text{A.9})$$

The limit (A.9) implies that

$$\lim_{\mu \rightarrow 1} \|e_{\mu Q_o}(j\omega_o)\| = \infty \quad (\text{A.10})$$

which implies there exists $\mu_o \in [0, 1)$ such that

$$\|\bar{e}_{\mu_o Q_o}(j\omega_o)\| \geq \|\bar{e}(j\omega_o)\|. \quad (\text{A.11})$$

This contradicts (A.8) and ends the proof. \square

Appendix B

Proof of Corollary 4.1. The sufficiency of (4.2) for robust stability is guaranteed by Theorem 4.1. So assume that for some $\omega_0 \in \mathbb{R}$

$$\rho[\bar{P}(j\omega_0)] = \alpha \geq 1. \quad (\text{B.1})$$

It will be shown that there exist $Q(s) \in \mathcal{Q}'$ such that

$$\rho[P(j\omega_0)Q(j\omega_0)] = 1. \quad (\text{B.2})$$

First recognize that since (B.2) implies that

$$\det [I - P(j\omega_0)\tilde{Q}(j\omega_0)] = 0, \quad (\text{B.3})$$

it also implies that the system (3.1) is unstable for $Q(s) = \tilde{Q}(s)$.

Now let

$$\mathcal{P} = P(j\omega_0) \quad (\text{B.4})$$

$$\hat{\Omega} = \hat{Q}(j\omega_0) \quad (\text{B.5})$$

$$\Omega = \{\Omega \in \mathbb{C}^{n \times n} : \bar{\Omega} \leq \hat{\Omega}\}. \quad (\text{B.6})$$

Here it is assumed that each $\Omega \in \Omega$ has the partitioned form

$$\Omega = [\Omega_{ij}]_{(i,j=1,\dots,r)} \quad (\text{B.7})$$

where $\Omega_{ij} \in \mathbb{C}^{n_i \times n_j}$. Since $P(s)$ is block-diagonal,

$$\mathcal{P} = \text{block-diag}\{\mathcal{P}_1, \dots, \mathcal{P}_r\} \quad (\text{B.8})$$

where $\mathcal{P}_i \in \mathbb{C}^{n_i \times n_i}$. Also, in the new notation (B.2) is equivalent to

$$\rho[\bar{\mathcal{P}}\hat{\Omega}] = \alpha. \quad (\text{B.9})$$

Now for each $\Omega \in \Omega$ there exist a $Q(s) \in \mathcal{Q}$ such that $Q(j\omega_0) = \Omega$. Thus, it suffices to complete the proof by showing that there exist $\Omega \in \Omega$ such that

$$\rho(\mathcal{P}\Omega) = 1. \quad (\text{B.10})$$

For each $\Omega \in \Omega$, $\mathcal{P}\Omega$ is given by

$$\mathcal{P}\Omega = [(\mathcal{P}\Omega)_{ij}]_{i,j=1,\dots,r} \quad (\text{B.11})$$

where

$$(\mathcal{P}\Omega)_{ij} = \mathcal{P}_i \Omega_{ij}. \quad (\text{B.12})$$

Let the singular value decompositions of the diagonal blocks of \mathcal{P} be given by

$$\mathcal{P}_i = E_i \Sigma_i F_i^H, \quad i = 1, \dots, r \quad (\text{B.13})$$

where

$$(\Sigma_i)_{11} = \|\mathcal{P}_i\|_s. \quad (\text{B.14})$$

Now choose Ω such that its block partitions have the singular value decompositions

$$\Omega_{ij} = F_i \Lambda_{ij} E_j^H, \quad i, j = 1, \dots, r \quad (\text{B.15})$$

where

$$(\Lambda_{ij})_{11} = \hat{\Omega}_{11}. \quad (\text{B.16})$$

Clearly, $\Omega \in \Omega$ and

$$\bar{\Omega} = \hat{\Omega} \quad (\text{B.17})$$

In addition,

$$(\mathcal{P}\Omega)_{ij} = E_i \bar{\Sigma} \Lambda_{ij} E_j^H, \quad i, j = 1, \dots, r \quad (\text{B.18})$$

which implies

$$(\overline{\mathcal{P}\Omega}) = \bar{\mathcal{P}} \hat{\Omega} \quad (\text{B.19})$$

Next, let

$$\Omega = \frac{1}{\alpha} \bar{\Omega}. \quad (\text{B.20})$$

Recognize that $\Omega \in \Omega$ and the block partitions of $\mathcal{P}\Omega$ have the singular value decompositions

$$(\mathcal{P}\Omega)_{ij} = E_i \Lambda_{ij} E_j^H, \quad i, j = 1, \dots, r \quad (\text{B.21})$$

where

$$(\Lambda_{ij})_{11} = \bar{\mathcal{P}}_{11} \bar{\Omega}_{ij}. \quad (\text{B.22})$$

It follows that

$$(\overline{\mathcal{P}\Omega}) = \overline{\mathcal{P}\Omega} = \frac{1}{\alpha} \overline{\mathcal{P}\hat{\Omega}}. \quad (\text{B.23})$$

It is easily seen from (B.9) and (B.23) that

$$\rho(\overline{\mathcal{P}\Omega}) = 1 \quad (\text{B.24})$$

Define the unitary matrix $U \in \mathbb{C}^{n \times n}$ by

$$U = \text{block-diag}\{E_1, \dots, E_r\} \quad (\text{B.25})$$

and let \mathcal{W} be given by

$$\mathcal{W} = U^H (\mathcal{P}\Omega) U. \quad (\text{B.26})$$

Note that \mathcal{W} is an $n \times n$ nonnegative matrix and has the partitioned form

$$\mathcal{W} = [A_{ij}]_{(i,j=1,\dots,r)}. \quad (\text{B.27})$$

In addition,

$$\overline{\mathcal{W}} = \overline{\mathcal{P}\Omega} \quad (\text{B.28})$$

and thus

$$\rho(\overline{\mathcal{W}}) = 1. \quad (\text{B.29})$$

Let $u \in \mathbb{R}_+^r$ be the eigenvector of $\overline{\mathcal{W}}$ corresponding to the Perron root ($\rho(\overline{\mathcal{W}}) = 1$). Then,

$$\overline{\mathcal{W}}u = u. \quad (\text{B.30})$$

Now define $\mu \in \mathbb{R}_+^n$ by

$$\mu^T = [\mu_1^T, \dots, \mu_r^T] \quad (\text{B.31})$$

where $\mu_i \in \mathbb{R}_+^{n_i}$ is given by

$$\mu_i^T = [u_i \ 0 \dots 0]. \quad (\text{B.32})$$

(Here u_i is the i th element of u). Then,

$$\mathcal{W}\mu = \mu. \quad (\text{B.33})$$

To see this, recall that \mathcal{W} is given by (B.27) and notice that:

(i) If $n_i \leq n_j$,

$$A_{ij} = [A_{ij}^0 \ 0] \quad (\text{B.34})$$

where $\Lambda_{ij}^0 \in \mathbb{R}_+^{n_i \times n_i}$ is diagonal and

$$(\Lambda_{ij}^0)_{11} = \overline{\mathcal{W}}_{ij}. \quad (\text{B.35})$$

(ii) If $n_i > n_j$,

$$\Lambda_{ij} = \begin{bmatrix} \Lambda_{ij}^0 \\ 0 \end{bmatrix} \quad (\text{B.36})$$

where $\Lambda_{ij}^0 \in \mathbb{R}_+^{n_j \times n_j}$ is diagonal and

$$(\Lambda_{ij}^0)_{11} = \overline{\mathcal{W}}_{ij}. \quad (\text{B.37})$$

It follows from (B.26) and (B.33) that

$$\rho(\mathcal{P}\Omega) = \rho(\mathcal{W}) = 1. \quad (\text{B.38})$$

Thus, the corollary is proved. \square

Appendix C

This Appendix presents and proves Lemma C and then presents a proof of Theorem 5.1.

Lemma C. Consider any $k \in \{1, 2, 3, \dots\}$. Then, the system (3.1) is robustly stable for $Q = Q''$ if and only if for each $Q(s) \in Q''$

$$\rho[(P(j\omega)Q(j\omega))^k] < 1 \quad \text{for all } \omega. \quad (\text{C.1})$$

Proof. Suppose (C.1) holds for each $Q(s) \in Q''$. Then

$$\rho[P(j\omega)Q(j\omega)] < 1 \quad \text{for all } \omega \quad (\text{C.2})$$

which implies that

$$\det[I + P(j\omega)Q(j\omega)] \neq 0 \quad \text{for all } \omega. \quad (\text{C.3})$$

Theorem 3.1 then guarantees that the system is robustly stable.

Now suppose that for some $\omega \in \mathbb{R}$ and $Q(s) \in Q''$

$$\rho[(P(j\omega)Q(j\omega))^k] = \alpha^k \geq 1. \quad (\text{C.4})$$

This implies that for some $\theta \in \mathbb{R}$ an eigenvalue of $P(j\omega)Q(j\omega)$ is given by

$$\lambda[P(j\omega)Q(j\omega)] = \alpha \exp(\theta) \quad (\text{C.5})$$

where $\alpha > 1$.

Next define

$$\tilde{Q}(s) = -\frac{1}{\alpha} \exp(-\theta)Q(s). \quad (\text{C.6})$$

Clearly, $\tilde{Q}(s) \in Q''$ and there exist an eigenvalue of $P(j\omega)\tilde{Q}(j\omega)$ given by

$$\lambda[P(j\omega)\tilde{Q}(j\omega)] = -1. \quad (\text{C.7})$$

Thus,

$$\det[I + P(j\omega)\tilde{Q}(j\omega)] = 0 \quad (\text{C.8})$$

and by Theorem 3.1 the system is *not* robustly stable. \square

Proof of Theorem 5.1. First it is shown that for each $Q(s) \in \mathcal{Q}''$

$$\det [I_n - (-P(j\omega)Q(j\omega))^{2^k}] \neq 0 \quad \text{for all } \omega \quad (\text{C.9})$$

if and only if for each $Q(s) \in \mathcal{Q}''$

$$\rho[(P(j\omega)Q(j\omega))^{2^k}] < 1 \quad \text{for all } \omega \quad (\text{C.10})$$

which by Lemma C is a necessary and sufficient condition for robust stability.

It is obvious that if (C.10) is satisfied for each $Q(s) \in \mathcal{Q}''$, then (C.9) is satisfied for each $Q(s) \in \mathcal{Q}''$. So assume that there exist $Q^0(s) \in \mathcal{Q}''$ and $\omega_0 \in \mathbb{R}$ such that

$$\rho[(P(j\omega_0)Q^0(j\omega_0))^{2^k}] = \alpha \geq 1. \quad (\text{C.11})$$

Then for some $\theta \in \mathbb{R}$ an eigenvalue of $(P(j\omega_0)Q^0(j\omega_0))^{2^k}$ is given by

$$\lambda[(P(j\omega_0)Q^0(j\omega_0))^{2^k}] = \alpha \exp(\theta). \quad (\text{C.12})$$

Now, let

$$\tilde{Q}(s) = (-1)^{2^k} \frac{1}{\alpha} \exp(-\theta) Q(s). \quad (\text{C.13})$$

Clearly, $\tilde{Q}(s) \in \mathcal{Q}$ and there exist an eigenvalue of $(P(j\omega_0)\tilde{Q}(j\omega_0))^{2^k}$ given by

$$\lambda[(P(j\omega_0)\tilde{Q}(j\omega_0))^{2^k}] = (-1)^{2^k} \quad (\text{C.14})$$

which implies

$$\det [I_n - (-P(j\omega_0)\tilde{Q}(j\omega_0))^{2^k}] = 0. \quad (\text{C.15})$$

The proof is completed by showing that if the system is robustly stable, then for each $Q(s) \in \mathcal{Q}$ and $R(s) \in \mathcal{R}$

$$e(j\omega) = e^{(k)}(j\omega). \quad (\text{C.16})$$

So assume that the system (3.1) is robustly stable and consider $Q(s) \in \mathcal{Q}''$ and $R(s) \in \mathcal{R}$. Then $e(j\omega)$ is the unique solution

$$[I_n + P(j\omega)Q(j\omega)]e(j\omega) = x(j\omega) \quad (\text{C.17})$$

where $x(j\omega)$ is obtained from (3.26). Also, let

$$\Theta_Q(j\omega) = \prod_{m=0}^{k-1} (I_n + (-P(j\omega)Q(j\omega))^{2^m}) \quad (\text{C.18})$$

$$\Gamma_Q(j\omega) = \Theta_Q(j\omega) [-I_n + P(j\omega)Q(j\omega)]. \quad (\text{C.19})$$

It is easily shown by induction that

$$\Gamma_Q(j\omega) = I_n - (-P(j\omega)Q(j\omega))^{2^k}. \quad (\text{C.20})$$

Since the system is robustly stable, (C.9) insures that

$$\det [\Theta_Q(j\omega)] \neq 0 \quad \text{for all } \omega. \quad (\text{C.21})$$

Then, premultiplying (C.18) by $\Theta_Q(j\omega)$ and using (C.17) by $\Theta_Q(j\omega)$ and using (C.19) shows that

$$\Gamma_Q(j\omega)e(j\omega) = \Theta_Q(j\omega)x(j\omega). \quad (\text{C.22})$$

Finally, using (C.18) and (C.19) and comparing (C.22) and (5.8) shows that (C.16) holds. \square

References

1. J. C. Doyle and G. Stein, "Multivariable Feedback Design: Concepts for a Classical/Modern Synthesis," *IEEE Trans. Autom. Control*, Vol. AC-26, pp. 4-16.
2. I. Postlethwaite, J. M. Edmunds and A. G. J. MacFarlane, "Principal Gains and Principal Phases in the Analysis of Linear Multivariable Systems," *IEEE Trans. Autom. Control*, Vol. AC-26, pp. 32-46, 1981.
3. M. G. Safanov, A. J. Laub and G. L. Hartmann, "Feedback Properties of Multivariable Systems: The Role and Use of the Return Difference Matrix," *IEEE Trans. Autom. Control*, Vol. AC-26, pp. 47-65, 1981.
4. N. A. Lehtomaki, Nils R. Sandell, Jr. and J. Athans, "Robustness Results in Linear-Quadratic Gaussian Based Multivariable Control Designs," *IEEE Trans. Autom. Control*, Vol. AC-26, pp. 75-93, 1981.
5. I. Postlethwaite and Y. K. Foo, "Robustness with Simultaneous Pole and Zero Movement across the $j\omega$ -Axis," *Automatica*, Vol. 21, pp. 433-443, 1985.
6. M. F. Barrett, "Conservatism with Robustness Tests for Linear Feedback Control Systems," *Proc. 19th IEEE Conf. Decis. Control*, pp. 885-890, 1980.
7. M. G. Safanov, "Stability Margins of Diagonally Perturbed Multivariable Feedback Systems," *IEE Proc.*, Vol. 129, Pt.D., pp. 251-256, 1982.
8. D. H. Owens and A. Chotai, "On Eigenvalues, Eigenvectors and Singular Values in Robust Stability Analysis," *Int. J. Control*, Vol. 40, pp. 285-296, 1984.
9. N. A. Lehtomaki, D. A. Castanon, B. C. Levy, G. Stein, Nils R. Sandell, Jr. and M. Athans, "Robustness and Modeling Error Characterization," *IEEE Trans. Autom. Control*, Vol. AC-29, pp. 212-220, 1984.
10. H-H Yen, S. S. Banda and D. B. Ridgely, "Stability Robustness Measures Utilizing Structural Information," *Int. J. Control*, Vol. 41, pp. 365-387, 1985.
11. O. D. I. Nwokah, "On Nonsingular Value Based Design of Controllers for Robust Stability," *IEE Proc.*, Vol. 133, Pt.D., pp. 57-64, 1986.
12. J. C. Kantor and R. P. Andres, "Characterization of 'Allowable Perturbations' for Robust Stability," *IEEE Trans. Autom. Control*, Vol. AC-28, pp. 107-109, 1983.
13. J. C. Kantor, "Spectral Radius Design for Robust Multivariable Control," *Proc. 1986 Amer. Control. Conf.*, Seattle, WA, pp. 7-10, 1986.
14. J. Doyle, "Analysis of Feedback Systems with Structured Uncertainty," *IEE Proc.*, Vol. 129, Pt.D., pp. 242-250, 1982.
15. J. C. Doyle, J. E. Wall and G. Stein, "Performance and Robustness Analysis for Structured Uncertainty," *Proc. 21st IEEE Conf. Decis. Control*, Orlando, FL, pp. 629-636, 1982.
16. Y. K. Foo and I. Postlethwaite, "Extensions of the Small- μ Test for Robust Stability," *IEEE Trans. Autom. Control*, Vol. 33, pp. 172-176, 1988.
17. M. Saeki, "A Method of Robust Stability Analysis with Highly Structured Uncertainties," *IEEE Trans. Autom. Control*, Vol. AC-31, pp. 935-940, 1986.
18. R. R. E. DeGaston and M. G. Safonov, "Exact Calculation of the Multiloop Stability Margin," *IEEE Trans. Autom. Control*, Vol. 33, pp. 156-171, 1988.
19. P. Grosdidier and M. Morari, "Interaction Measures for Systems Under Decentralized Control," *Automatica*, Vol. 22, pp. 309-319, 1986.

20. D. W. Porter and A. N. Michel, "Input-Output Stability of Time-Varying Nonlinear Multiloop Feedback Systems," *IEEE Trans. Autom. Control*, Vol. AC-19, pp. 422-427, 1974.
21. E. L. Lasley and A. N. Michel, "Input-Output Stability of Interconnected Systems," *IEEE Trans. Autom. Control*, pp. 84-89, Feb. 1976.
22. A. M. Ostrowski, "On Some Metrical Properties of Operator Matrices and Matrices Partitioned Into Blocks," *J. Math. Anal. Appl.*, Vol. 2, pp. 161-209, 1961.
23. P. A. Cook, "Estimates for the Inverse of a Matrix," *Lin. Alg. Appl.*, Vol. 10, pp. 41-53, 1975.
24. G. Dahlquist, "On Matrix Majorants and Minorants with Applications to Differential Equations," *Lin. Alg. Appl.*, Vol. 52/53, pp. 199-216, 1983.
25. Carl N. Nett, private communication.
26. R. K. Yedavalli, "Time Domain Robust Control Design for Linear Quadratic Regulators by Perturbation Bound Analysis," *Proc. IFAC Workshop on Model Error Concepts and Compensation*, R. E. Skelton and D. H. Owens, eds., pp. 129-135, June 1985, Boston, MA.
27. D. C. Hyland and D. S. Bernstein, "The Majorant Lyapunov Equation: A Nonnegative Matrix Equation for Robust Stability and Performance of Large Scale Systems," *IEEE Trans. Autom. Control*, Vol. AC-32, pp. 1005-1013, 1987.
28. E. G. Collins, Jr. and D. C. Hyland, "Improved Robust Performance Bounds in Covariance Majorant Analysis," submitted for publication.
29. D. S. Bernstein and W. M. Haddad, "Robust Stability and Performance Analysis for Linear Dynamic Systems with Unstructured Uncertainty via Quadratic Lyapunov Bounds," submitted for publication.
30. M. Fiedler and V. Ptak, "On Matrices with Non-Positive Off-Diagonal Elements and Positive Principal Minors," *Czechoslovakian Mathematical Journal*, Vol. 12, pp. 382-400, 1962.
31. E. Seneta, *Non-Negative Matrices*, Wiley, New York, 1973.
32. A. Berman and R. J. Plemmons, *Nonnegative Matrices in the Mathematical Sciences*, Academic Press, New York, 1979.
33. D. C. Hyland and E. G. Collins, Jr., "Block Kronecker Products and Block Norm Matrices in Large Scale Systems Analysis," submitted for publication.

APPENDIX F

**Reduced-Order Compensation:
LQG Reduction Versus Optimal Projection**

Reduced-Order Compensation:
LQG Reduction Versus Optimal Projection*

S. W. Greeley** and D. C. Hyland†
Government Aerospace Systems Division
MS 22/2406
Harris Corporation
Melbourne, Florida 32902

Abstract

Six methods for design of reduced-order compensation are compared using an example problem given by Enns. The methods considered comprise five LQG reduction techniques, reviewed in a recent paper by Liu and Anderson, and the Optimal Projection theory as implemented via a simple homotopy solution algorithm. Design results obtained by the different methods for forty-two different design cases are compared with respect to closed-loop stability and transient response characteristics. Of the LQG-reduction procedures two are found to offer distinctly superior performance. However, only the Optimal Projection method provided stable designs in all cases. Further details are given on the performance of the numerical algorithms for solving the optimal projection equations and the corresponding design results.

1. Introduction

The design of reduced-order dynamic controllers for high-order systems is of considerable importance for applications involving large spacecraft and flexible flight systems. Hence it is not surprising that extensive research has been devoted to this area. A recent paper by Liu and Anderson [1] subjected five reduced-order controller design methods to both theoretical and numerical comparison. The computational comparison was based upon an example problem considered by Enns [2]. The five methods compared in [1] are:

1. Method of Enns [2]: This method is a frequency-weighted, balanced realization technique applicable to either model or controller reduction
2. Method of Glover [3]: This method utilizes the theory of Hankel norm optimal approximation for controller reduction
3. Davis and Skelton [4]: This is a modification of compensator reduction via balancing which covers the case of unstable controllers

*This research was supported in part by the Air Force Office Of Scientific Research, contract AFOSR F49620-84-C-0038.

**Technical Staff, Control Systems Engineering Group

†Leader, Control Systems Engineering Group

4. Youseff and Skelton [5]: This is a further modification of balancing for handling stable or unstable controllers
5. Liu and Anderson [1]: In place of using a balanced approximation of the compensator transfer function directly, this method approximates the component parts of a fractional representation of the compensator.

All of the above methods proceed by first obtaining the full-order LQG compensator design for a high-order state-space model and then reducing the dimension of this LQG compensator.

The present paper complements the results of Liu and Anderson by giving a numerical comparison (again using Enns' example) of methods 1-5 with a sixth method:

6. Optimal Projection (OP) equations [6]: Reduced-order compensator design by direct solution of the necessary conditions for quadratically optimal fixed-order dynamic compensation.

Method (6), like methods (1-5), has been shown to have intimate connections with balancing ideas [7]. Moreover, the first step in one iterative method for solution of the OP equations is almost identical to method (4). Method (6) differs from the other methods, however in that it does not reduce the order of a previously obtained LQG design but rather directly characterizes the quadratically optimal compensator of a given fixed-order. The OP equations constitute four coupled modified Riccati and Lyapunov equations wherein the steps of regulator design, observer design and order reduction are completely and inseparably intermingled.

The organization of this paper is as follows. In section 2, we state the problem considered and review the OP design equations. Section 3 gives the computational algorithm used herein for OP design synthesis. Finally, section 4 sets forth the example problem of Enns and compares the results of all six methods obtained for this example.

2. Problem Statement and Review of OP Design Equations

Here we consider the linear, finite-dimensional, time-invariant system:

$$\begin{aligned} \dot{x} &= Ax + Bu + w_1; & x &\in R^N, \\ y &= Cx + w_2; & y &\in R^P \end{aligned} \quad (1)$$

where x is the plant state, A is the plant dynamics matrix and B and C are control input and sensor output matrices, respectively. w_1 is a white disturbance noise with intensity matrix $V_1 \geq 0$ and w_2 is observation noise with nonsingular intensity $V_2 > 0$.

The reduced-order compensation problem consists in designing a constant gain dynamic compensator of order $N_c < N$:

$$\begin{aligned} u &= -Kq, & u &\in R^d \\ \dot{q} &= A_c q + Fy; & q &\in R^{N_c} \end{aligned} \quad (2)$$

Obviously, the heart of the design problem is the selection of the constant matrices K , F and A_c .

Methods 1-6 all associate with the closed-loop system (1,2) a steady-state quadratic performance index, J :

$$\begin{aligned} J &\triangleq \lim_{t_1 - t_0 \rightarrow \infty} \bar{J} / |t_1 - t_0| \\ \bar{J} &\triangleq \int_{t_0}^{t_1} dt E[x^T R_1 x + u^T R_2 u] \\ R_1 &\geq 0, \quad R_2 > 0 \end{aligned} \quad (3)$$

Methods 1-5 first design an LQG compensator (select K , F , A_c to minimize J_g) and then reduce the order of the resulting N state compensator. Thus, in methods 1-5, the quadratic performance (3) is brought into play in the initial LQG design step, but a variety of balancing and Hankel norm approximation ideas are utilized for the subsequent compensator-order reduction step. In contrast, method 6 selects, K , F , A_c by addressing the quadratically optimal, fixed-order compensation problem i.e., for N_c fixed (and $< N$), choose K , F , A_c to minimize J_g . The OP design methodology proceeds by solving the first-order necessary conditions for this optimization problem using the new forms for the necessary conditions given in [6]. The basic OP design equations reduce to four modified Lyapunov and Riccati equations all coupled by a projection of rank N_c . In general these design equations produce compensators that cannot be obtained by reduction of an LQG compensator [7].

Methods 1-5 have been reviewed extensively in [1-5], and will not be discussed in detail. Here we shall merely review the OP design equations to the extent needed to illustrate the solution algorithm used for this study.

To do this, a few preliminary results and notational conventions must be given. First, we have Lemma 1, [7]:

Lemma 1. Suppose $\hat{Q} \in R^{N \times N}$ and $\hat{P} \in R^{N \times N}$ are nonnegative definite and $\text{rank}(\hat{Q}) = \text{rank}(\hat{P}) = \text{rank}(\hat{Q}\hat{P})$. Then the product $\hat{Q}\hat{P}$ is semisimple (all Jordan blocks are of order unity) with real, non-negative eigenvalues. Moreover, there exists a nonsingular $\Psi[\hat{Q}, \hat{P}]$ such that:

$$\Psi^{-1}[\hat{Q}, \hat{P}] \hat{Q} \hat{P} \Psi[\hat{Q}, \hat{P}] = \Lambda^2 \quad (4a)$$

$$\Psi^T[\hat{Q}, \hat{P}] \hat{P} \Psi[\hat{Q}, \hat{P}] = \Lambda \quad (4b)$$

$$\Psi^{-1}[\hat{Q}, \hat{P}] \hat{Q} \Psi^{-T}[\hat{Q}, \hat{P}] = \Lambda \quad (4c)$$

where

$$\Lambda = \text{diag} \{ \lambda_k \}_{k=1 \dots N} \quad (5)$$

is the positive diagonal matrix of the square roots of the eigenvalues of $\hat{Q}\hat{P}$.

When for a given pair \hat{Q} and \hat{P} , a $\Psi[\hat{Q}, \hat{P}]$ exists such that (4) hold, \hat{Q} and \hat{P} are said to be contragradiently diagonalizable and balanced [9] and $\Psi[\hat{Q}, \hat{P}]$ constitutes a simultaneous contragradient transformation. Determination of such a transformation is the fundamental mathematical operation of balancing.

Furthermore, it is clear that the quantities:

$$\Pi_k[\hat{Q}, \hat{P}] \triangleq \Psi[\hat{Q}, \hat{P}] E^{(k)} \Psi^{-1}[\hat{Q}, \hat{P}] \quad (6)$$

$$E_{mn}^{(k)} = \begin{cases} 1; & m=n=k \\ 0; & \text{otherwise} \end{cases}$$

form a set of mutually disjoint unit rank projections i.e.:

$$\Pi_k[\hat{Q}, \hat{P}] \Pi_j[\hat{Q}, \hat{P}] = \Pi_k[\hat{Q}, \hat{P}] \delta_{kj} \quad (7)$$

Thus the sum of r distinct Π_k 's is itself a projection of rank r . Also $\hat{Q}\hat{P}$ can be alternatively expressed as:

$$\hat{Q}\hat{P} = \sum_{k=1}^n \Pi_k[\hat{Q}, \hat{P}] \Lambda_k^2 \quad (8)$$

By virtue of (8) and the usage in [10], we term $\Pi_k[\hat{Q}, \hat{P}]$ the eigen-projection of $\hat{Q}\hat{P}$ associated with the k^{th} eigenvalue.

The above results and conventions, together with the notations:

$$\Sigma = B R_2^{-1} B^T \quad (9a)$$

$$\bar{\Sigma} = C^T V_2^{-1} C \quad (9b)$$

$$\tau_1 = I_n - \tau \quad (9c)$$

allow us to state the main result [6-8] upon which the OP reduced-order compensator design method is based:

Theorem 1. Consider the quadratically optimal, fixed-order compensation problem with $N_c \leq N$ fixed.

Let nonnegative definite $Q, P, \hat{Q}, \hat{P} \in R^{N \times N}$ be determined as solutions to the following equations:

$$0 = A\hat{Q} + \hat{Q}A^T + \hat{V}_1 - \hat{Q}\bar{\Sigma}\hat{Q} + \tau\hat{Q}\bar{\Sigma}Q\tau^T \quad (10a)$$

$$0 = A^T\hat{P} + \hat{P}A + \hat{R}_1 - \hat{P}\bar{\Sigma}\hat{P} + \tau^T\hat{P}\bar{\Sigma}P\tau \quad (10b)$$

$$0 = (A - \bar{\Sigma}P)\hat{Q} + \hat{Q}(A - \bar{\Sigma}P)^T + \hat{Q}\bar{\Sigma}Q - \tau\hat{Q}\bar{\Sigma}Q\tau^T \quad (10c)$$

$$0 = (A - \bar{\Sigma}P)^T\hat{P} + \hat{P}(A - \bar{\Sigma}P) + \hat{P}\bar{\Sigma}P - \tau^T\hat{P}\bar{\Sigma}P\tau \quad (10d)$$

$$\tau = \sum_{K=1}^{N_c} \Pi_K[\hat{Q}\hat{P}] \quad (10e)$$

Then with $\Gamma, G \in R^{N_c \times N}$ given by:

$$\Gamma = [I_{N_c} \ 0] \Psi^{-1}[\hat{Q}, \hat{P}] \quad (11)$$

$$G = [I_{N_c} \ 0] \Psi^T[\hat{Q}, \hat{P}]$$

the gains:

$$K = R_2^{-1} B^T P G^T$$

$$F = \Gamma Q C^T V_2^{-1} \quad (12)$$

$$A_c = \Gamma(A - \bar{\Sigma}P - \bar{\Sigma}P)G^T$$

determine an extremal of the performance index J .

As has been remarked in [8], the value of the performance index is unchanged by any transformation of the compensator state basis - in other words, for any nonsingular $S \in R^{N_c \times N_c}$:

$$J(K, F, A_c) = J(KS, S^{-1}F, S^{-1}A_c S) \quad (13)$$

Furthermore, when $N_c = N$, τ is a rank N projection on R^N by virtue of (10e). Hence $\tau = I_N$ and $\tau_1 = 0$ and equations (10a), (10b) become uncoupled Riccati equations for determination of \hat{Q} and \hat{P} . Also Γ and G become $\Psi^{-1}[\hat{Q}, \hat{P}]$ and $\Psi^T[\hat{Q}, \hat{P}]$. Finally, setting $S = \Psi^{-1}$ and using (13) and (12), extremalizing gains are given by:

$$K = R_2^{-1} B^T P$$

$$F = Q C^T V_2^{-1} \quad (14)$$

$$A_c = A - Q \bar{\Sigma} - \bar{\Sigma} P$$

with Q and P given as solutions to the independent Riccati equations, (10a, 10b), with $\tau_1 = 0$. Hence when $N_c = N$, the design equations (10), (11) and (12) immediately reduce to the LQG design for a full-order compensator.

However for $N_c < N$, equations (10) are first-order necessary conditions and generally possess multiple solutions corresponding to multiple extremals that can exist. This matter was explored in [11] relative to the related quadratically optimal model reduction problem. Basically, equation (10e) tells us that the rank N_c projection, τ , which defines the geometry of the fixed-order compensator, is the sum of N_c out of N eigenprojections of $\hat{Q}\hat{P}$. However, the necessary conditions do not tell us which N_c out of N eigenprojections are to be selected to secure a global minimum of J . Indeed for any possible selection of N_c eigenprojections out of N ,

equations (10) may possess a solution corresponding to a local extremal. By virtue of (10e) and the notational conventions of (4) and (8), the selection of N_c eigenprojections is defined (generically) by the manner in which the eigenvalues, Λ_k , are ordered. Recently, Richter

[12] has applied topological degree theory to investigate the possible solution branches and the character of the associated extrema and has devised a homotopy solution algorithm which selects the Λ -ordering which homotopically converges to the global minimum.

For the example considered in this paper, we adopt the ordering convention:

$$\Lambda_1 \geq \Lambda_2 \geq \dots \geq \Lambda_N \quad (15)$$

in constructing $\Psi[\hat{Q}, \hat{P}]$. (15) together with (10e) imply that τ is taken to be the sum of the N_c eigenprojections corresponding to the N_c largest

eigenvalues of $\hat{Q}\hat{P}$. Generically, this choice leads to an unequivocal choice of one solution branch of (10) corresponding to a particular extremal.

Thus, the OP design method investigated here consists in solving (10) with convention (15) and then evaluating the gains according to (12). We apply a simple homotopy solution algorithm, described in the next section, to the example problem of Enns specified in Section 4 and compare results with methods 1-5. A more advanced and efficient homotopy algorithm is given in [12].

3. An Algorithm for Solution of the OP Design Equations

As stated, the OP design method is to solve (10) (with stipulation (15)) for P, Q, \hat{P}, \hat{Q} , and then evaluate the gains using (11), (12). A logically distinct issue is precisely how equations (10) are to be solved. Here we present an algorithm that has been used for some time and requires only a standard LQG software package for its implementation. For convenience this same algorithm was employed to obtain the numerical results for method 6 presented in the next section.

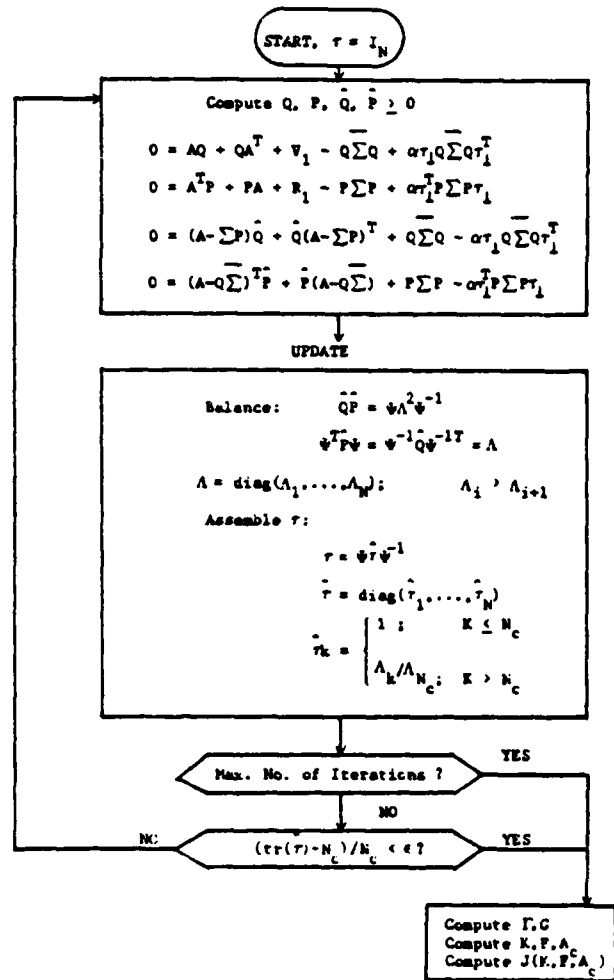
The basic motivation of this algorithm is the observation that the four main equations (10a)-(10d) are coupled only via the terms involving τ_1 on the right hand sides. If these τ_1 terms were deleted, then all five equations can be solved sequentially - moreover (10a), (10b) reduce to ordinary Riccati equations and (10a), (10b) are Lyapunov equations. Likewise under conditions in which $Q\Sigma Q$ and $P\Sigma P$ are "small" relative to the remaining terms (e.g., sufficiently small state-weighting and disturbance noise intensity and/or sufficiently large control weighting and observation noise intensity) the τ_1 terms are typically found to have little effect. In this situation the artifact of fixing an initial τ_1 , and then solving (10) as ordinary Riccati and Lyapunov equations is likely to give a reasonable approximation to the true solution.

Since only the τ_1 terms on the right of (10a-10d) occasion most of the difficulties, it is necessary to somehow bring these terms into play gradually. There are two principal ways to do this. The first is an iterative relaxation approach, i.e., fix τ_1 , solve (10a)-(10d) sequentially, then update τ using (10e) and repeat until convergence, in some sense, is achieved. The second method is a homotopy approach, i.e., multiply the τ_1 terms by a scalar parameter, $\alpha \in [0,1]$, then starting with $\alpha = 0$ and gradually increasing α , solve (10) repeatedly until $\alpha = 1$.

The algorithm used here consists of two iterative loops. The inner loop uses the relaxation approach and is embedded within an outer loop which implements the simple homotopy approach.

The inner loop follows the earlier computational scheme discussed in [7] and is illustrated in Figure 1. Note that the parameter $\alpha \in [0,1]$ multiplies the τ_1 terms but is held fixed within the inner loop and is only incremented on the outer loop. As Figure 1 shows, one first fixes τ equal to the previous iterate (or set $\tau = I_N$ when starting) and then solves (10a)-(10d). Once new iterates for Q, P, \hat{Q}, \hat{P} are obtained, τ is updated by determining the balancing transformation $\Psi(Q, P)$. To enhance convergence of the modified Riccati equations, the updated τ is taken to be the weighted sum of all N eigenprojections - the first N_c eigenprojections are given unity weight while the r^{th} ($r > N_c$)

Figure 1: Inner Loop of OP Solution Algorithm



eigenprojection is weighted by $\Lambda_r / \Lambda_{N_c} < 1$. As convergence proceeds, $\Lambda_r / \Lambda_{N_c}$ approaches zero for all $r > N_c$ and the numerical rank of τ approaches N_c . The indicated convergence check tests the relative excess of the numerical rank of τ over N_c and terminates the inner loop iterations when this "rank excess" falls below tolerance ϵ . In these studies $\epsilon = 0.1$ is used. The inner loop is terminated when either this tolerance is achieved or when the prescribed number of iterations is exceeded.

When the convergence criterion is satisfied, the gains, K, F, A_c are computed using (11) and (12) and the steady-state performance, J , is evaluated. Performance evaluation invokes no assumptions regarding the convergence and optimality of the solutions to (10). Specifically, the values of K, F, A_c resulting from application of (12) are accepted as they stand and are used to construct the system matrices of the augmented system with state vector $X^T = [x^T, q^T]$. Next the $(N+N_c) \times (N+N_c)$ Lyapunov

equation for the second moment matrix of the augmented, closed-loop system is solved. Finally, J is evaluated as a linear function of various sub-blocks of the augmented system second moment matrix.

The outer loop, depicted in Figure 2, implements the homotopy approach by incrementing α and controlling the increment step size. Only at the start is the inner loop initialized by $\tau = I_N$. Otherwise, when α is incremented, the inner loop is initialized using P, Q, \hat{P}, \hat{Q} , and τ as obtained with the previous value of α . α is taken to be 0 at the start and is subsequently incremented by Δ . The default value of Δ is 0.1 although other desired values may be input. However, whenever the inner loop is terminated without achieving the convergence tolerance ϵ , the homotopy parameter increment, Δ , is halved. This provides simple control over the homotopy step size. The entire algorithm terminates when $\alpha = 1.0$. Alternatively, at the user's option, the algorithm can be terminated when the change of the performance index, J , over two successive outer loop iterations is sufficiently small - thus indicating acceptable convergence with respect to quadratic performance.

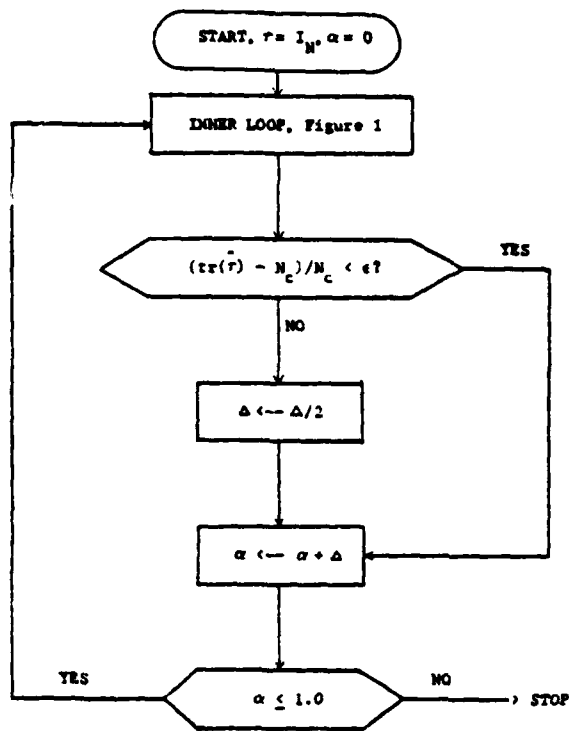


Figure 2: Outer (Homotopy) Loop of OP Solution Algorithm

4. A Design Example and Comparison of Results

We use the example problem given by Enns' [2] to compare methods 1-6. Results on this example obtained by use of methods 1-5 are discussed in [1]. Here, we augment these results by considering method 6 and undertake an overall comparison.

The plant to be controlled in this example is a four-disk system and is linear, time-invariant, SISO, neutrally stable (with a double pole at the origin) and non-minimum phase and of eighth order. Numerical values of the matrices $A, B, C, R_1, R_2, V_1, V_2$ defining this problem are given in Table 1.

$$A = \begin{bmatrix} -0.161 & 1 & 0 & 0 & 0 & 0 & 0 & 0 \\ -6.004 & 0 & 1 & 0 & 0 & 0 & 0 & 0 \\ -0.5822 & 0 & 0 & 1 & 0 & 0 & 0 & 0 \\ -9.9835 & 0 & 0 & 0 & 1 & 0 & 0 & 0 \\ -0.4073 & 0 & 0 & 0 & 0 & 1 & 0 & 0 \\ -3.982 & 0 & 0 & 0 & 0 & 0 & 1 & 0 \\ 0 & 0 & 0 & 0 & 0 & 0 & 0 & 1 \\ 0 & 0 & 0 & 0 & 0 & 0 & 0 & 0 \end{bmatrix}$$

$$B^T = [0, 0, 0.0064, .00235, 0.0713, 1.0002, 0.1045, 0.9955]$$

$$C = [1, 0, 0, 0, 0, 0, 0, 0]$$

$$R = (1.0 \times 10^{-6}) I^T; \quad N = [0, 0, 0, 0, 0.55, 11, 1.32, 18.0]$$

$$R_2 = 1$$

$$V_1 = q_2 B B^T \quad (q_2 = [0.01, 2000.0])$$

$$V_2 = 1$$

Table 1: Data Matrices for the Example Problem of Enns [2]

For each of the methods 1-6, controllers of different reduced orders (from seventh to second order) were obtained for seven different values of the disturbance noise intensity parameter, q_2 :

$$q_2 = 0.01, 0.1, 1.0, 10, 100, 1000, 2000$$

Thus each method was used to obtain results on 42 different design cases.

Each of the six methods was originally devised according to a wide variety of different criterion for adequate performance of a reduced-order compensator design. Despite this wide disparity among the different aims and motivations of the several methods there are at least three criteria that may be reasonably applied to judge the success of a reduced-order design:

1. Closed-loop stability
2. Extent to which the reduced-order compensator impulse and step response match the full-order, LQG, compensator response
3. The closed-loop quadratic cost

However, item 3 will not be considered since costs for methods 1-5 were not provided [1]. The comparison in item 2 examines the output $y(t)$ in response to an input $v(t)$ injected in the loop as indicated in Figure 3.

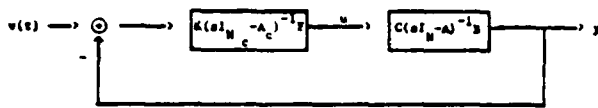


Figure 3. Comparison of unit step or impulse response
 $v(t)$ = Unit step or impulse
 (K, F, A_c) = full-order LQG or reduced-order compensator gains

Figure 3. Comparison of unit step or impulse response

First, Table 2 summarizes the closed-loop stability properties of all design methods in all 42 cases. Generally, it is seen that all methods achieve a high rate of success in achieving closed-loop stability for the larger N_c values and small q_2 . On the other hand, methods 1-5 experience greater difficulties for low values of N_c and, particularly, for large q_2 . With respect to stability, the only qualitative distinction among the methods is that method 6 (optimal projection) produces stable design in all 42 design cases.

The trend toward increasing difficulty of the design with increasing disturbance noise intensity is highlighted by Table 3 which shows the percentage of closed-loop stable designs given by the different methods for the different values of q_2 and in total. That the fraction of stable designs declines with increasing q_2 is to be expected since larger disturbance noise intensity increases Q , thereby increasing observer gains to produce faster observers that are more sensitive to order reduction.

Overall, for this example problem, method 4 exhibits the smallest fraction of stable designs (with 24 unstable designs) and does not achieve any order reduction for $q_2 = 100, 1000, 2000$. Of the LQG reduction methods (1-5), methods 1 and 5 fare best - with only 4 unstable designs out of 42. As noted, optimal projection (method 6) yields stable designs in all cases.

To permit independent corroboration by interested readers of the OP design capabilities we give numerical values of the compensator gains obtained by method 6 for a selection of the more difficult cases* - namely:

* See Reference [13] for a complete listing of all 42 cases

Table 2. Stability of the Reduced-Order Controller by Different Methods

Method	$\frac{q_2}{N_c}$	0.01	0.1	1	10	100	1000	2000
Kane (1)	7	S	S	S	S	S	S	S
	6	S	S	S	S	S	S	S
	5	S	S	S	S	S	S	S
	4	S	S	S	S	S	S	S
	3	S	S	S	S	S	S	S
	2	S	S	S	S	S	S	S
Glover (2)	7	S	S	S	S	S	U	S
	6	S	S	S	S	U	U	U
	5	S	S	S	S	U	U	U
	4	S	S	S	S	U	U	U
	3	S	S	U	S	U	U	U
	2	S	U	S	L	S	U	U
Davis & Shelton (3)	7	S	U	U	S	S	S	S
	6	S	S	S	S	S	S	S
	5	S	U	S	S	S	U	U
	4	S	S	U	S	S	U	U
	3	U	U	U	U	U	U	U
	2	S	U	S	U	U	U	U
Yousuff & Shelton (4)	7	S	S	S	S	U	U	U
	6	S	S	S	S	U	U	U
	5	S	S	S	U	U	U	U
	4	S	S	S	U	U	U	U
	3	S	U	U	U	U	U	U
	2	S	S	S	U	U	U	U
Liu & Anderson (5)	7	S	S	S	S	S	S	U
	6	S	S	S	S	S	S	U
	5	S	S	S	S	S	S	U
	4	S	S	S	S	S	S	S
	3	S	S	S	S	S	S	U
	2	S	S	S	S	S	S	S
Optimal Projection (6)	7	S	S	S	S	S	S	S
	6	S	S	S	S	S	S	S
	5	S	S	S	S	S	S	S
	4	S	S	S	S	S	S	S
	3	S	S	S	S	S	S	S
	2	S	S	S	S	S	S	S

S - The closed-loop system is stable
 U - Unstable

Table 3. Percentage of Stable Designs Given by the Different Methods

Method	0.01	0.1	1	10	100	1000	2000	Total % for All Cases
Kane (1)	100	100	100	100	83.3	83.3	66.7	90.5
Glover (2)	100	83.3	83.3	83.3	33.3	0	16.7	57.1
Davis & Shelton (3)	83.3	33.3	50.0	66.7	66.7	33.3	33.3	52.4
Yousuff & Shelton (4)	100	83.3	83.3	33.3	0	0	0	42.9
Liu & Anderson (5)	100	100	100	100	100	83.3	50.0	90.5
Optimal Projection (6)	100	100	100	100	100	100	100	100.0

$$q_2 = 2000. N_c = 2, 3, 4, 5, 6, 7$$

$$N_c = 2. q_2 = 0.01, 0.1, 1.0, 10, 100, 1000, 2000$$

Next, consider the accuracy with the step and impulse responses (see Figure 3) of the various reduced-order compensator designs track the corresponding response of the full-order LQG design. These characteristics exhibit similar trends as noted with respect to closed-loop stability. For example, Figure 4 shows a comparison of unit step responses for second-order compensator designs with a small value of

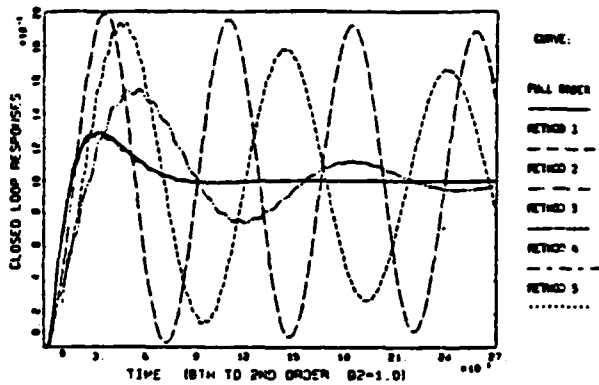


Figure 4.a - Comparison of unit step responses of second-order compensators given by methods 1-5 with full-order design (small q_2)

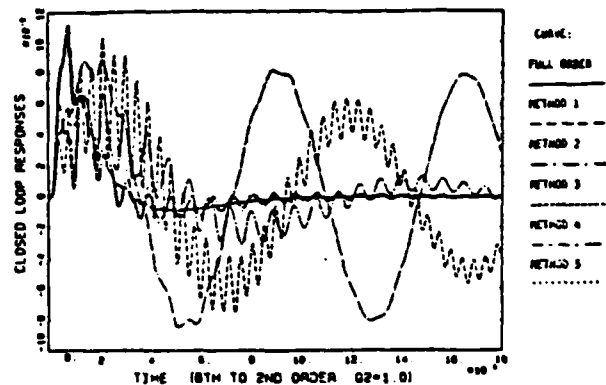


Figure 5.a - Comparison of impulse responses of second-order compensators given by methods 1-5 with full-order design (small q_2)

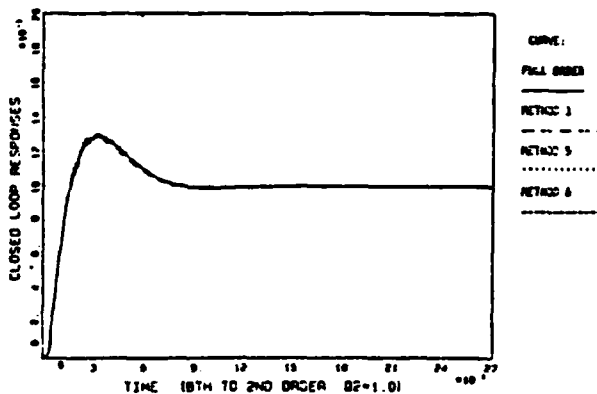


Figure 4.b - Comparison of unit step responses of second-order compensators given by methods 1, 5, and 6 with full-order design (small q_2)

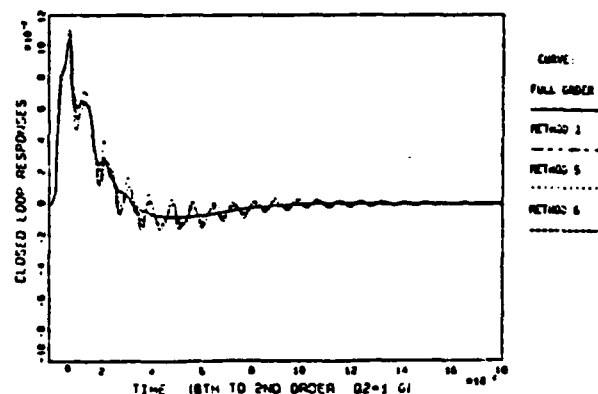


Figure 5.b - Comparison of impulse responses of second-order compensators given by methods 1, 5, and 6 with full-order design (small q_2)

$q_2 (= 1.0)$. In this case, all methods exhibit stability and reasonable agreement with full order design. However, as the comparison of methods 1-5 in Figure 4.a shows, methods 1 and 5 show distinctly superior tracking accuracy. For clarity, methods 1 and 5 are compared with method 6 in Figure 4.b. Here it is clear that method 5 is somewhat closer to the LQG response than method 1 while method 6 is closest of all.

Similar trends are seen in the comparisons of the impulse responses (for the same design case) in Figure 5. Once again, of the LQG reduction methods (compared in Figure 5.a), methods 1 and 5 display significantly better agreement with the LQG response. This agreement is slightly exceeded by method 6 (Figure 5.b), but on the whole, methods 1, 5 and 6 show excellent performance.

On the other hand, for a fairly large value of q_2 , both stability and agreement with LQG response is degraded somewhat for several methods. Figures 6 and 7 show comparisons of unit step and impulse responses for the case $N_c = 5$, $q_2 = 100$. In this case, only methods 1, 3, 5 and 6 yield stable designs and are thus compared. Of the LQG

reduction methods, method 5 exhibits distinctly better agreement with the LQG responses. Once again, it is found (Figures 6.b and 7.b) that method 6 somewhat excels in the accuracy with which it's transient responses track the full-order design.

Thus, for the 42 design cases studied in this example problem, methods 1 and 5 demonstrate good success in achieving stable closed-loop designs while method 5 achieves stable designs in all cases.

Also, in the cases examined, methods 1 and 5 offer good transient response characteristics while method 6 tracks the full-order compensator responses the closest.

In view of the good performance exhibited by method 6, we present, in the remainder of this section, additional details on the OP design results and the performance of the solution algorithm described in Section 3.

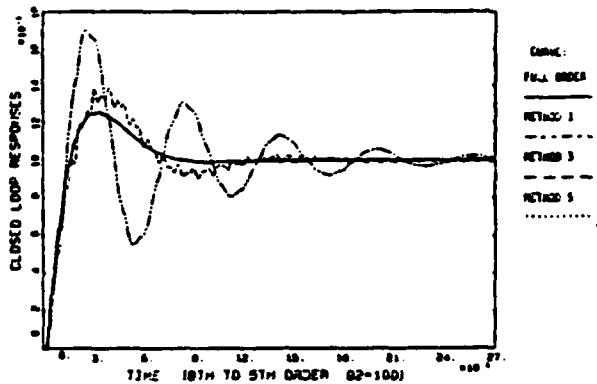


Figure 6.a - Comparison of unit step responses of fifth-order compensators given by methods 1, 3, and 5 with full-order design (large q_2)

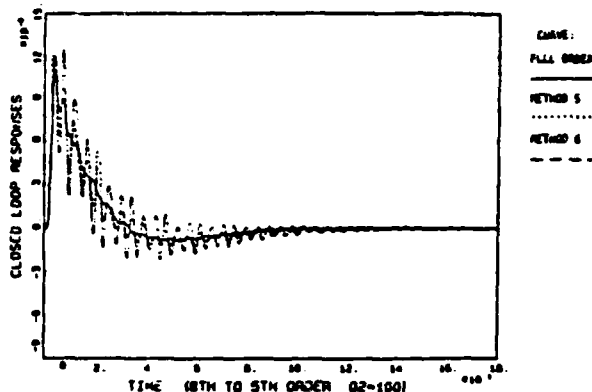


Figure 7.b - Comparison of unit step responses of fifth-order compensators given by methods 5 and 6 with full-order design (large q_2)

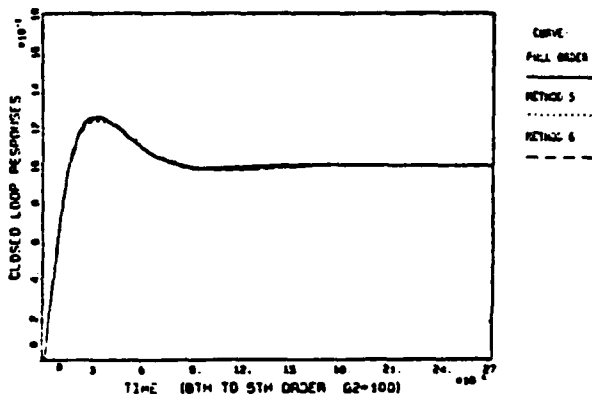


Figure 6.b - Comparison of unit step responses of fifth-order compensators given by methods 5 and 6 with full-order design (large q_2)

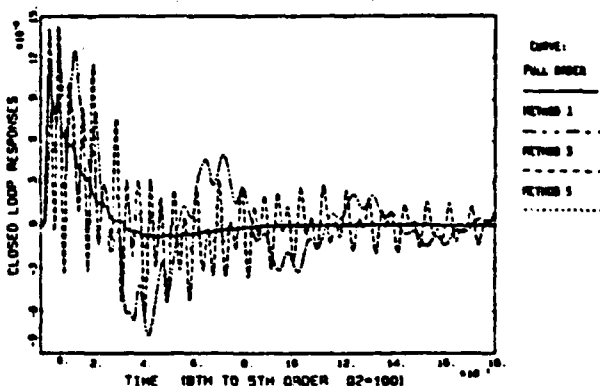


Figure 7.a - Comparison of impulse responses of fifth-order compensators given by methods 1, 3, and 5 with full-order design (large q_2)

First, as noted, the OP design philosophy focuses on the steady state quadratic performance index, J , (defined in (3)) as the "figure of merit" for a reduced-order compensator design. Thus, we appropriately display, in Figure 8, several plots of the performance index J (normalized by q_2) versus compensator order for all 7 values of q_2 . Note that apart from minor variations that are likely due to the benign convergence tolerance used in the solution algorithm, J generally decreases monotonically with increasing N_c . These graphs thus illustrate the basic tradeoff between performance and controller complexity.

Note that for small q_2 (Figure 8.a), performance is not much affected by order reduction. This is to be expected since small disturbance noise intensity, in this problem, leads to low observer gains and to small values for the terms involving τ_1 in equations (10). Since the τ_1 terms in equations (10) have little effect, the OP designs are approximated by balanced projections of the LQG design. This might also help to explain the relatively successful performance of all methods for small q_2 .

For large (Figure 8.b) and for very large (Figure 8.c) values of q_2 , however, the degradation of performance with reduction in order is increasingly steep. For example, while for $q_2 = 1.0$, the 2nd order performance is only 2.5% above the LQG performance, for $q_2 = 2000$, the second-order performance is 270% above the LQG value. Thus, order reduction under large disturbance noise does appear to be a more delicate matter.

While increasing difficulties with q_2 are not clearly manifested in the stability or transient response properties of the OP designs, these are reflected in the computation required to arrive at the final designs.

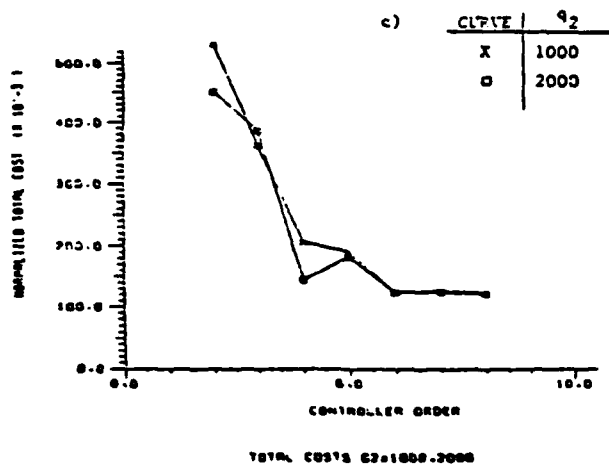
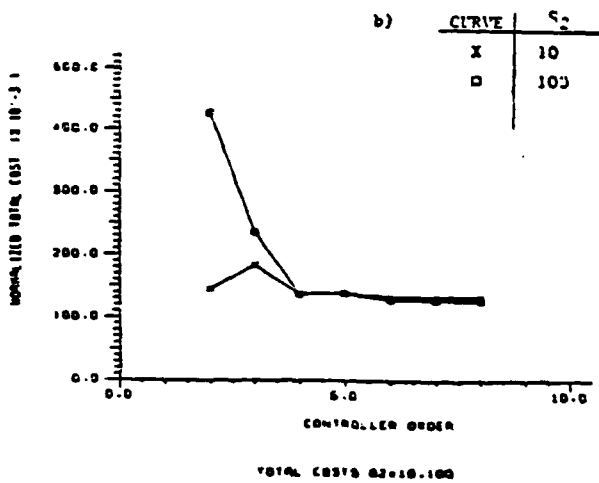
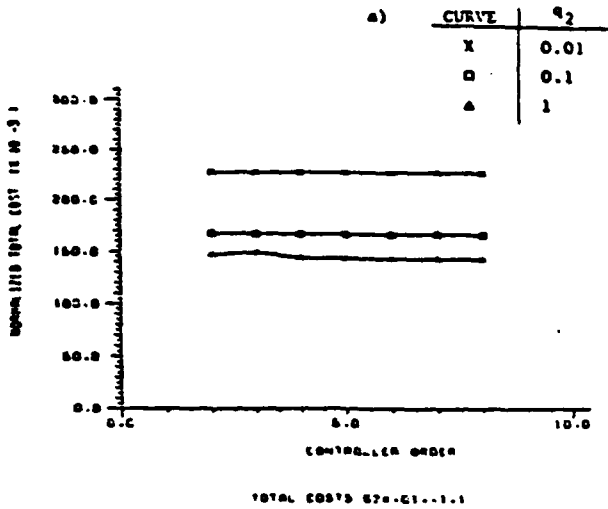


Figure 8 - Steady-state quadratic performance of OP designs versus compensator order for all values of q_2 .

To explain this we now describe the specific design steps taken and the performance of the solution algorithms. Each design case was treated using the OP solution algorithm shown in Figures 1 and 2 and a maximum homotopy step size of 1.0 was input. Furthermore, for each design case, the algorithm was started "cold" - i.e., without being initialized with gain values obtained in previous cases. On initial application of the algorithm, the OP design results presented here were obtained after using the numbers of inner loop iterations given for each case in Table 4.

Table 4. Number of Inner-Loop Iterations Used in OP Solution Algorithm - Initial Design Computations

q_2 / Order, N_c	0.01	0.1	1	10	100	1000	2000
7	2	2	2	4	5	8	10
6	2	2	2	6	4	8	10
5	2	2	2	6	5	5	7
4	2	2	2	8	9	6	10
3	4	4	4	8	9	7	8
2	4	4	4	8	9	9	10

Note that with $\Delta = 1.0$, the logic of the outer loop (Figure 2) implies a minimum of two inner-loop iterations. Inspection of the results obtained in some of the benign cases suggested the possibility that only one inner loop iteration was needed. Consequently we re-examined the cases comprising $q_2 = 0.01, 0.1, 1.0$ and $N_c = 5, 6, 7$, by revising the outer loop logic to output gain values after only one pass through the inner loop. It was found that this produced acceptable accuracy in the cases $q_2 = 0.01; N_c = 5, 6, 7$, $q_2 = 0.1, N_c = 6, 7$ and $q_2 = 1.0, N_c = 7$. Thus, the revised results are as given in Table 4'. Since the gains are essentially unchanged, the design results obtained on the first application are the ones presented here.

Table 4'. Number of Inner-Loop Iterations Used in OP Solution Algorithm - Revised after Reconsideration of cases $q_2 = 0.01, 0.1, 1.0; N_c = 5, 6, 7$

q_2 / Order, N_c	0.01	0.1	1	10	100	1000	2000
7	1	1	1	4	5	8	10
6	1	1	2	6	4	8	10
5	1	2	2	6	5	5	7
4	2	2	2	8	9	6	10
3	4	4	4	8	9	7	8
2	4	4	4	8	9	9	10

As Table 4' shows, relatively few iterations were required in the benign, small q_2 , cases. In particular, only one inner loop iteration was needed in most of the cases comprising $q_2 = 0.01$, 0.1, 1.0 and $N_c = 5, 6, 7$. However, for large q_2 , up to 10 iterations were required. Thus it is clear that all methods run up against a fundamental source of difficulty when disturbance noise is large.

At the time of writing, full compilation of the computation times required for all methods on the same machine is not available. All OP calculations were performed on a Harris H800 minicomputer. However, as a rough estimate, it is fair to say that in the benign cases, the OP computation is comparable to the burden incurred by methods 1-5. For the difficult, large q_2 cases the OP computational burden is clearly in excess of methods 1-5 (although certainly not excessive from a practical point of view). However, it is precisely in these cases that the LQG reduction methods experience the greatest difficulties in producing closed-loop stable designs. Thus a meaningful comparison of relative computational burden in these cases cannot be performed.

Finally it should be noted that the computational burden associated with OP for the designs presented here is also an artifact of the solution algorithm depicted in Figures 1 and 2 and is not solely the result of the design equations themselves. This algorithm was convenient to use, and was the first implemented since it requires only standard LQG software. On the other hand, the algorithm discussed in section 3 takes no particular advantage of the special structure of the fundamental design equations, (10). Its principal draw-back is that it involves the iterative solution of four $N \times N$, nonlinear matrix equations. To remedy this, Richter [12] has developed a step-wise homotopy algorithm which requires, at each homotopy step, the solution of four $N \times N$ linear equations. Clearly, for small N_c , this offers the potential for computing an OP design with less computational burden than is required for a full-order LQG design. It is anticipated that the future utilization of Richter's algorithm will permit a more accurate and definitive comparison between the computational cost of the LQG-reduction techniques and the Optimal Projection formulation.

5. Concluding Remarks

In this paper, we have used the example problem of Enns [2] to perform a computational comparison of six methods for reduced-order dynamic compensator design. Methods 1-5 are based upon LQG-reduction procedures while method 6 is based upon the Optimal Projection (OP) formulation.

Of the LQG-reduction methods, the methods of Enns [2] and of Liu and Anderson [1] exhibited particularly good stability and transient response properties. However, in the cases examined, the OP method gave somewhat better transient response characteristics and, unlike the LQG-reduction procedures, produced closed-loop stable designs for all the 42 design cases.

A precise comparison of the computational burdens incurred by the various methods is not possible at present. However, as a rough comparison, it is fair to say that the OP method entailed comparable computation in the relatively benign design cases and more computation in the difficult cases. However in this case LQG reduction methods often produce unstable designs. Thus the OP method exhibits a tradeoff between computational burden and corresponding design reliability. Present developments are directed toward implementation of advanced homotopy techniques which take particular advantage of the structure of the basic OP design equations to markedly improve design computation speed.

Appendix 1

In the following, numerical values of the reduced-order compensator gains, K , F and A_c obtained via the OP solution algorithm discussed in section 3 are given for the design cases:

$$q_2 = 2000, \quad N_c = 2, 3, 4, 5, 6, 7$$

and

$$N_c = 2, \quad q_2 = 0.01, 0.1, 1.0, 10, 100, 1000, 2000$$

CASE: $q_2 = 0.01, \quad N_c = 2$

$$A_c = \begin{bmatrix} 0.1357E-01 & -0.1398 \\ 0.3985 & -0.3430 \end{bmatrix}$$

$$F^T = [0.3451E-02 \quad 0.9371E-01]$$

$$K = [-0.3045E-01 \quad 0.1421]$$

CASE: $q_2 = 0.1, \quad N_c = 2$

$$A_c = \begin{bmatrix} 0.9915E-02 & -0.1578 \\ 0.7650 & -0.5093 \end{bmatrix}$$

$$F^T = [0.1695E-02 \quad 0.1266]$$

$$K = [-0.5729E-01 \quad 0.2733]$$

CASE: $q_2 = 1, \quad N_c = 2$

$$A_c = \begin{bmatrix} 0.7832E-02 & -0.1812 \\ 1.269 & -0.7143 \end{bmatrix}$$

$$F^T = [0.8516E-03 \quad 0.1356]$$

$$K = [-0.1003 \quad 0.5206]$$

CASE: $q_2 = 10$, $N_c = 2$

$$A_c = \begin{bmatrix} 0.7474E-02 & 0.1970 \\ -1.699 & -0.8276 \end{bmatrix}$$

$$F^T = [0.4814E-03 \quad -0.1081]$$

$$K = [-0.1740 \quad -0.9190]$$

CASE: $q_2 = 100$, $N_c = 2$

$$A_c = \begin{bmatrix} 0.2742E-02 & 0.4216 \\ -2.396 & -0.2274E-01 \end{bmatrix}$$

$$F^T = [-0.1538E-03 \quad 0.1303]$$

$$K = [0.2351 \quad 0.4178]$$

CASE: $q_2 = 1000$, $N_c = 2$

$$A_c = \begin{bmatrix} 0.1745E-02 & 0.4039 \\ -2.129 & -0.7569E-02 \end{bmatrix}$$

$$F^T = [-0.6242E-04 \quad 0.7341E-01]$$

$$K = [0.3753 \quad 0.5049]$$

CASE: $q_2 = 2000$, $N_c = 2$

$$A_c = \begin{bmatrix} -0.8376E-03 & -0.4671 \\ 2.047 & -0.1095E-01 \end{bmatrix}$$

$$F^T = [0.3272E-04 \quad -0.7625E-01]$$

$$K = [0.3807 \quad -0.6411]$$

CASE: $q_2 = 2000$, $N_c = 3$

$$A_c = \begin{bmatrix} 0.2351E-02 & 0.1516 & 0.1492 \\ -1.447 & -0.9385E-01 & 0.6597 \\ -1.592 & -0.7041 & -0.1027E-02 \end{bmatrix}$$

$$F^T = [0.5944E-04 \quad -0.3619E-01 \quad -0.3990E-01]$$

$$K = [-0.5372 \quad -1.410 \quad 0.1033]$$

CASE: $q_2 = 2000$, $N_c = 4$

$$A_c = \begin{bmatrix} 0.3225E-02 & -0.3717 & 0.1238E-01 & -0.5735E-01 \\ 2.170 & -0.3860E-02 & -0.3623 & -0.1829E-01 \\ -0.1140 & 0.5365 & -0.2564E-01 & -0.2749 \\ 1.176 & -0.1297 & 0.3488 & -0.4452 \end{bmatrix}$$

$$F^T = [0.9245E-04 \quad 0.6044E-01 \quad -0.3234E-02 \quad 0.3370E-01]$$

$$K = [-0.4871 \quad 0.5626 \quad 0.6852 \quad 2.540]$$

CASE: $q_2 = 2000$, $N_c = 5$

$$A_c = \begin{bmatrix} 0.1335E-02 & -0.3220 & 0.5462E-02 & 0.4440E-01 & -0.1963 \\ 2.226 & -0.3920E-02 & -0.4659 & -0.3941E-01 & 0.4951E-02 \\ -0.5418E-01 & 0.6432 & -0.1099E-01 & 0.2117 & -0.4355 \\ -0.8042 & 0.2011 & -0.2791 & -0.1891 & -1.488 \\ 6.046 & -0.1203E-01 & 1.376 & 2.351 & -0.6778E-03 \end{bmatrix}$$

$$F^T = [0.4018E-04 \quad 0.6557E-01 \quad -0.1614E-02 \quad -0.2413E-01 \quad 0.1817]$$

$$K = [-0.4697 \quad 0.5101 \quad 0.4346 \quad -1.795 \quad -0.4017E-01]$$

CASE: $q_2 = 2000$, $N_c = 6$

$$A_c = \begin{bmatrix} 0.8190E-03 & 0.3031 & 0.8960E-03 & 0.7075E-01 & 0.3110 & 0.2265 \\ -2.356 & -0.2845E-02 & 0.5058 & 0.1198E-01 & 0.3847E-02 & -0.4306E-01 \\ -0.7592E-02 & -0.6887 & -0.1431E-02 & 0.2356 & 0.7586 & 0.5132 \\ -1.358 & -0.9398E-01 & -0.3875 & -0.1281 & 1.265 & -0.8882E-01 \\ -8.168 & -0.1105E-01 & -1.861 & -1.709 & 0.1190E-02 & 0.1426 \\ -16.17 & -0.4290E-01 & -3.152 & -1.545 & -0.3782 & -1.799 \end{bmatrix}$$

$$F^T = [0.2713E-04 \quad -0.7675E-01 \quad -0.2492E-03 \quad -0.4487E-01 \quad -0.2702 \quad -0.5356]$$

$$K = [-0.4324 \quad -0.5140 \quad 0.1322 \quad -1.545 \quad -0.1364 \quad -3.524]$$

CASE: $q_2 = 2000$, $N_c = 7$

$$A_c = \begin{bmatrix} 0.8683E-03 & -0.3085 & -0.1180E-02 & 0.6098E-01 & -0.2844 & -0.2619 & -0.9244E-03 \\ 2.329 & -0.2821E-02 & 0.4921 & -0.1784E-01 & 0.4468E-02 & -0.4780E-01 & -0.1950E-02 \\ 0.1041E-01 & -0.6794 & -0.2057E-02 & -0.2171 & 0.6977 & 0.6175 & 0.4106E-02 \\ -1.169 & 0.1132 & 0.3505 & -0.1381 & -1.303 & -0.1929E-01 & 0.2136E-01 \\ 7.940 & -0.1091E-01 & -1.846 & 1.851 & 0.9687E-03 & 0.1872 & 0.7926E-02 \\ 19.90 & -0.4695E-01 & -4.056 & 2.398 & -0.4123 & -2.407 & -0.7051E-01 \\ 0.1906 & -0.4634E-02 & -0.3824E-01 & 0.2680E-01 & -0.5793E-01 & -0.3975 & -0.1242E-01 \end{bmatrix}$$

$$F^T = [0.2832E-04 \quad 0.7462E-01 \quad 0.3362E-03 \quad -0.3801E-01 \quad 0.2586 \quad 0.6490 \quad 0.6217E-02]$$

$$K = [-0.4387 \quad 0.5134 \quad -0.1642 \quad -1.591 \quad 0.7063E-01 \quad 3.924 \quad 0.1567]$$

References

1. Y. Liu and B. D. O. Anderson, "Controller Reduction Via Stable Factorization and Balancing," Int. J. Contr., Vol. 44, No. 2, 507-531, 1986.
2. D. Enns, "Model Reduction for Control System Design," Ph.D. Thesis, Dept. of Electrical Engineering, Stanford University, 1984.
3. H. Glover, "All Optimal Hankel-Norm Approximations of Linear Multivariable Systems and Their L₂-Error Bounds," Int. J. Contr., Vol. 39, 1115, 1984.
4. J. A. Davis and R. E. Skelton, "Another Balanced Controller Reduction Algorithm," System Control Lett., Vol. 4, 79, 1984.
5. A. Yousuff and R. E. Skelton, "A Note on Balanced Controller Reduction," IEEE Trans. Autom. Contr., Vol. 29, 254, 1984.
6. D. C. Hyland and D. S. Bernstein, "The Optimal Projection Equations for Fixed-Order Dynamic Compensation," IEEE Trans. Autom. Contr., Vol. AC-29, pp. 1034-1037, 1984.
7. D. C. Hyland, "Comparison of Various Controller-Reduction Methods: Suboptimal Versus Optimal Projection," Proc. AIAA Dynamics Specialists Conf., pp. 381-389, Palm Springs, CA, May 1984.
8. D. S. Bernstein and D. C. Hyland, "The Optimal Projection Equations for Finite-Dimensional Fixed-Order Dynamic Compensation of Infinite-Dimensional Systems," SIAM J. Contr. Optim., Vol. 24, pp. 122-151, 1986.
9. C. R. Rao and S. K. Mitra, Generalized Inverse of Matrices and Its Applications, John Wiley and Sons, New York, 1971.
10. T. Kato, Perturbation Theory for Linear Operators, Springer-Verlag, New York, 1966.
11. D. C. Hyland and D. S. Bernstein, "The Optimal Projection Equations for Model Reduction and the Relationships Among the Methods of Wilson, Skelton and Moore," IEEE Trans. Autom. Contr., Vol. AC-30, pp. 1201-1211, 1985.
12. S. Richter, "A Homotopy Algorithm for Solving the Optimal Projection Equations for Fixed-Order Dynamic Compensation: Existence, Convergence and Global Optimality," Amer. Contr. Conf., Minneapolis, MN, June 1987.
13. S. Greeley and D. Hyland, "Optimal Projection Controller Gains for an Example of Enns," Harris GASD TR-87-1, January, 1987.

APPENDIX G

**Reduced-Order Control Design via the
Optimal Projection Approach:
A Homotopy Algorithm for Global Optimality**

Reduced-Order Control Design
via the
Optimal Projection Approach:
A Homotopy Algorithm for Global Optimality

Stephen Richter

Harris Corporation
Government Aerospace Systems Division
MS 22/4848
Melbourne, FL 32902

ABSTRACT

The purpose of this paper is to present a homotopy algorithm for solving the Optimal Projection Equations. Questions of existence and the number of solutions will also be examined. It will be shown that the number of stabilizing solutions to the given Optimal Projection Equations can be determined and that all solutions can be computed via a homotopic continuation from a simple problem. For an important special case, where the number of inputs or the number of outputs to the system is less than or equal to the dimension of the compensator, there is only one solution to the OPE, thus guaranteeing that globally optimum reduced order controller can be computed.

1. Introduction

Despite significant advances in the cost and performance of digital computers over the last decade, there remains a need in several technological areas for low-order, high-performance controllers. In particular, this paper is motivated by the problem of vibration suppression in large flexible space structures. Such systems are infinite-dimensional (distributed parameter) in nature and hence any finite-dimensional controller is necessarily of reduced order. The need for low-order controllers is further driven by severe constraints on cost, weight and power in space systems, not to mention the restriction to space-qualified computational hardware.

A wide variety of approaches have been proposed to obtaining reduced-order controllers. A comparison of several approaches to controller reduction is given in [1]. These methods operate by first designing a high-order LQG controller and then obtaining a suitable low-order controller by means of controller reduction.

A more direct approach to designing reduced-order controllers involves optimizing the quadratic performance functional over the class of controllers of fixed order. The controller order may be determined by implementation constraints or can be varied for performance/throughput tradeoff studies.

Supported in part by the Air Force Office of Scientific Research under contract F49620-86-C-0038.

An interesting reformulation of the parameter optimization approach was given recently in [2]. By setting the gradients to zero, the authors showed that the first order necessary conditions can be transformed to yield explicit gain expressions for extremal fixed-order controllers. An appealing aspect of this formulation is the recasting of the necessary conditions in a form which generalizes the classical (full-order) LQG solution. Specifically, instead of a pair of separated Riccati equations, the necessary conditions for fixed-order dynamic compensation comprise a system of two modified Riccati equations and two modified Lyapunov equations coupled by an oblique projection whose rank is precisely equal to the order of the compensator. When specialized to the full-order case, the projection becomes the identity, the modified Lyapunov equations drop out, and the modified Riccati equations simplify to the classical Riccati equations. Hence this approach appears to be a natural and fundamental generalization of LQG.

Regardless of how appealing the optimal projection formulation may appear to be and in spite of the empirical advantages claimed in [2-10], its contribution is vacuous unless certain serious questions can be resolved. These include:

1. Under what conditions on the problem data can the optimal projection equations be guaranteed a priori to possess a solution?
2. Given problem data, exactly how many solutions do the equations possess?
3. Of the possible solutions, what are their stability properties, what is their performance, and which is the global optimum?
4. How can numerical algorithms be constructed which can be guaranteed to converge to any desired solution especially the global minimum?

It seems clear that any attempt to address the above issues must utilize mathematical methods which are global in nature. To this end we have applied degree theory and associated homotopic continuation methods ([13-24]) to analyze the solutions to the optimal projection equations and to construct convergent, implementable algorithms for their computation. The purpose of this paper is to report significant results in this regard.

2. Homotopic Continuation and Degree Theory

2.1 Homotopic Continuation. A homotopic continuation method for solving a problem is to first solve an easy "similar" problem, and then to continuously deform the easy problem into the original problem and to follow the path of solutions as the easy problem is deformed into the original problem. This is shown conceptually in Figure 1.

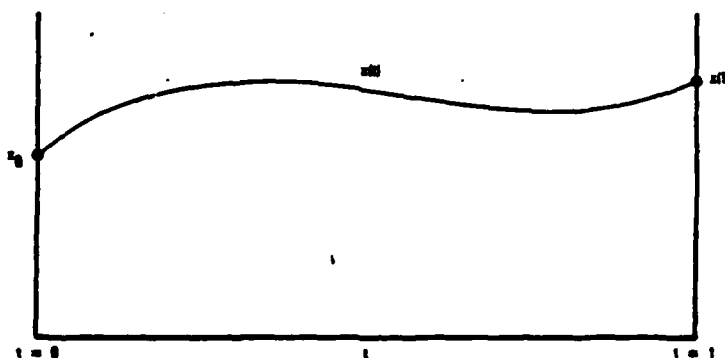


Figure 1

The problem then becomes to follow the path of solutions $x(t)$ of $F(t, x(t))=0$ from $t=0$ to $t=1$. Differentiating $F(t, x(t))=0$ with respect to t one obtains the Daudenko differential equation

$$F_x(t, x(t)) \frac{dx}{dt} + F_t(t, x(t)) = 0, \text{ or}$$

$$\frac{dx}{dt} = -F_x^{-1}(t, x(t)) F_t(t, x(t)), \quad x(0) = x_0$$

Integration of this initial value problem yields $x(1)$, the solution to $F(x)=0$.

Example 1. Consider calculating the roots of a polynomial

$$F(Z) = Z^n + a_1 Z^{n-1} + a_2 Z^{n-2} \dots + a_n = 0.$$

Let the easy problem be $F_0(Z) = Z^n - 1 = 0$ and deform F_0 to F

$$F(Z, t) = Z^n + t(a_1 Z^{n-1} + a_2 Z^{n-2} \dots a_n) - 1 + t.$$

At $t=0$, $F(Z, 0)=F_0(Z)$ and $F(Z, 1)=F(Z)$.

The solutions $Z_k(t)$ which satisfy $F(Z_k, t)=0$ are found by differentiating $F(Z_k(t), t)=0$ to obtain

$$\frac{dZ_k}{dt} = - \frac{a_1 Z_k^{n-1} + a_2 Z_k^{n-2} \dots a_n - 1}{nZ_k^{n-1} + t(a_1(n-1)Z_k^{n-2} \dots a_{n-1})}$$

This differential equation can be integrated from the n initial values

$$z_k(0) = e^{-\frac{i2\pi}{n}k}$$

to the n solutions at $t=1$.

2.2 Degree Theory. The main theoretical question which must be answered when using a continuation method to solve a given problem is: Is there in fact a continuous path of solutions connecting $F(0,x)=0$ with $F(1,x)=0$, and if so, how many paths are there?

Topological degree theory can be used to answer this question.

Definition 1: Given a function f mapping D in R^N into V in R^K a regular value of f is an element p in V such that the $N \times K$ matrix of partial derivatives of f , $f_x(x)$, has full rank for each x in $f^{-1}(p)$. Note that if $N=K$ then $f_x(x)$ having full rank is equivalent to $\det(f_x(x)) \neq 0$.

Definition 2: Given a function f mapping an open set D in R^N with boundary \bar{D} into V in R^K and a point p in V , the degree of f for domain D and point p (written $\text{Deg}(f,D,p)$) is defined and is an integer if there is no x in the boundary \bar{D} of D such that $f(x)=p$. If p is a regular point of f then the degree is the sum of the signs of the determinant of the Jacobians of f evaluated at all x such that $f(x)=p$, i.e.,

$$\text{deg}(f,D,p) = \sum \text{Sign}(\text{Det}(f_x(x_p)))$$

$$\text{where } f(x_p) = p$$

The degree has the following properties:

- 1) If $\text{deg}(f,D,p) \neq 0$ then $f(x)=p$ has at least one solution in D
- 2) Let $f(x,t) : R^N$ to R^K for each t in $[0,1]$ with f continuous. If for each t , $f(x,t)=p$ has no solutions for x in \bar{D} , then $\text{deg}(f,D,p)$ is constant for t in $[0,1]$.
- 3) If f is as in (2) and $\text{deg}(f,D,p) \neq 0$, then at least one solution of $f(x,0)=p$ connects with a solution of $f(x,1)=p$.

Example 2. Every polynomial has at least one root (over the complex numbers)

$$\text{Let } f(z) = z^n + a_1 z^{n-2} + \dots + a_n$$

We wish to show that $\deg(f, D, 0) \neq 0$.

$$\text{Let } f(z, t) = z^n + t(a_1 z^{n-1} + a_2 z^{n-2} + \dots + a_n) - 1 + t$$

Let $D = \{z \mid |z| < R\}$, where R is some large number.

For z on \bar{D} ($|z|=R$) z^n is much larger than $t a_1 z^{n-1}$ so $f(z, t) \neq 0$ for z in \bar{D} , thus $\deg(f, D, 0)$ is constant for t in $[0, 1]$.

For $t=0$, $f(z, 0) = z^n - 1$ and writing $f(r, \theta) = x + iy$ we have that the solutions to $f(r, \theta, 0) = 0$ are $r=1$, $\theta = k\pi/2n$ for $k=0, 1, \dots, n$

$$f(z, 0) = \begin{matrix} r^n \cos(n\theta) + 1.0 \\ r^n \sin(n\theta) \end{matrix}$$

The Jacobian of f is

$$f_{r, \theta} = \begin{bmatrix} nr^{n-1} \cos(n\theta), & -nr^n \sin(n\theta) \\ nr^{n-1} \sin(n\theta), & nr^n \cos(n\theta) \end{bmatrix}$$

$$\text{Det}(f_{r, \theta}) = n^2 r^{2n-1}$$

The sign of the Jacobian is always $+1$, thus $\deg(f, D, 0) = n$

3. Homotopy for the Optimal Projection Equations

The object is to find P, Q, \hat{P}, \hat{Q} , which solve

$$0 = A Q + Q A^T + V_1 - Q \bar{\Sigma} Q + \tau \begin{matrix} Q \bar{\Sigma} Q \\ \perp \end{matrix} \tau \begin{matrix} \perp \\ \perp \end{matrix}$$

$$0 = A^T P + P A + R_1 - P E P + \tau \begin{matrix} \perp \\ \perp \end{matrix} P E P \tau \begin{matrix} \perp \\ \perp \end{matrix}$$

$$0 = (A - \Sigma P) \hat{Q} + \hat{Q} (A - \Sigma P)^T + Q \bar{\Sigma} Q - \tau \begin{matrix} Q \bar{\Sigma} Q \\ \perp \end{matrix} \tau \begin{matrix} \perp \\ \perp \end{matrix}$$

$$0 = (A - Q \bar{\Sigma})^T \hat{P} + \hat{P} (A - Q \bar{\Sigma}) + P E P - \tau \begin{matrix} \perp \\ \perp \end{matrix} P E P \tau \begin{matrix} \perp \\ \perp \end{matrix}$$

$\tau = G^T$, where

$$\hat{Q}\hat{P} = G^T M \Gamma, \quad \Gamma G^T = I_{n_c}$$

given $\Sigma, \bar{\Sigma}, R_1, V_1, n_c, A$. To do this let

$$A(\tau) = \begin{bmatrix} D_1 & & \\ & D_2 & \\ & & \ddots \\ & & & D_n \end{bmatrix} (1-\tau) + \tau A$$

$$R_1(\tau) = I(1-\tau) + \tau R_1, \quad V_1(\tau) = I(1-\tau) + \tau V_1$$

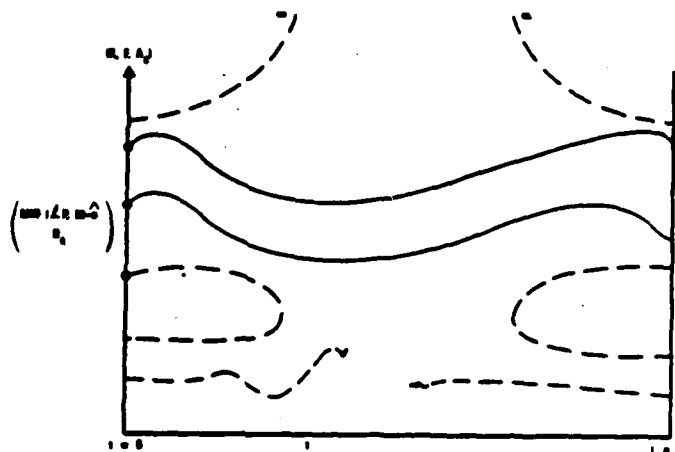
$$\Sigma(\tau) = \begin{bmatrix} \Sigma_0 & 0 \\ 0 & 0 \end{bmatrix} (1-\tau) + \tau \Sigma$$

$$\bar{\Sigma}(\tau) = \begin{bmatrix} \bar{\Sigma} & 0 & 0 \\ 0 & 0 & 0 \end{bmatrix} (1-\tau) + \tau \bar{\Sigma}$$

For $\tau=0$ the solution is easy to find. The object is to follow the path or paths of solutions $P(\tau), Q(\tau), \hat{P}(\tau), \hat{Q}(\tau)$ from $\tau=0$ to $\tau=1$. Note that if $n_c > \min\{l, n\} - n_u$ then there is only one solution at $\tau=0$. If

$n_c < \min\{l, n\} - n_u$ then there are $\binom{\min\{l, n\} - n_u}{n_c - n_u}$ solutions at $\tau=0$.

In following these initial solutions from $\tau=0$ to $\tau=1$ there are several situations which could occur (see figure 2).



Topological degree theory \Rightarrow The dashed paths do not exist
 if $n_c \geq \min\{l, n\} - n_u$, there is only one solution (\Rightarrow global minimum)

Figure 2

It can be shown using degree theory that the situations shown in dashed lines cannot occur. That is, the only solutions to the OPE at $t=1$ (or for $0 < t < 1$) are those which are continuously derived from the solutions at $t=0$.

Thus we have the following result. Let n_u denote the dimension of the unstable subspace of A .

Main Theorem. Assume that the plant is stabilizable and detectable, $V_1 > 0$, $R_1 > 0$ and $n_u < n_c$. Then, in the class of nonnegative-definite solutions Q, P, \hat{Q}, \hat{P} with

$$\text{rank } \hat{Q} = \text{rank } \hat{P} = \text{rank } \hat{Q}\hat{P} = n_c,$$

the optimal projection equations possess at most

$$\begin{pmatrix} \min(n, m, l) - n_u \\ n_c - n_u \end{pmatrix}, \quad n_c \leq \min(n, m, l),$$

1 . otherwise,

stabilizing solutions. Each such solution is reachable via a homotopic path with starting point corresponding to diagonal initial data. Furthermore, if the plant is stabilizable by means of an n_c th-order dynamic compensator, then there exists at least one solution.

Remark 3.1. As shown in [26], stabilizing controllers of arbitrary reduced order may not always exist.

The proof of the main theorem is lengthy and technically complex and beyond the scope of this paper. Rather than proving the main theorem for the optimal projection equations, the full order Riccati equation will be examined using degree theory to obtain some well known results for the Riccati equation. The proof of the main theorem follows the same method as will be used for the full order Riccati equation.

Full Riccati Equation:

We will now use degree theory to examine the full order Riccati equation

$$(1) \quad A^T P + PA - PSP + V = 0$$

Where A is an $n \times n$ matrix and S and V are $n \times n$ symmetric matrices with $V > 0$. Denote $|P| = \max |P_{ij}|$ and restrict P to be symmetric. Define

$F(x, t)$ to map R^N into R^N ($N = n(n+1)/2$) for each t in $[0, 1]$ by

$$(2) \quad F(P, t) = A^T(t)P + PA(t) - PS(t)P + V(t)$$

where $A(t)$, $S(t)$ and $V(t)$ are continuous and $S(t)$, $V(t)$ are symmetric with $V(t) > 0$. Let D be the set of all P such that $|P| < R$ and $P > 0$. This is an open set in R^N . The object is to show that $\text{Deg}(F, D, 0)$ is constant and $\neq 0$ for t in $[0, 1]$.

Lemma 1. There exists $R > 0$ such that for all t in $[0, 1]$, if P satisfies (2) and $(A(t), B(t))$ is stabilizable, then $|P| < R$. Note $S = BB^T$.

Proof: Suppose that the lemma is not true, then there must exist t_i and P_i such that $F(P_i, t_i) = 0$, and $|P_i| \rightarrow \infty$. We will show that this cannot occur.

Let $\bar{P}_i = P_i / |P_i|$ so $|P_i| \bar{P}_i = P_i$. Then

$$A^T(t_i) \bar{P}_i + \bar{P}_i A(t_i) - |P_i| \bar{P}_i S(t_i) \bar{P}_i + V(t_i) / |P_i| = 0$$

Write $\bar{P}_i = P_i^1 + P_i^2$, where $P_i^1 B = 0$ and P_i^2 is in the range of B . Then

$$A^T(P_i^1 + P_i^2) + (P_i^1 + P_i^2) A - |P_i| P_i^2 BB^T P_i^2 + V / |P_i| = 0$$

Since P_i^1 and P_i^2 are bounded and A and V are bounded, and $|P_i| \rightarrow \infty$, $P_i^2 \rightarrow 0$. Thus

$$A^T P_i^1 + A P_i^1 - |P_i| P_i^2 BB^T P_i^2 = O(1/|P_i|)$$

Multiplying on the left by B^T and on the right by B yields

$$|P_i| B^T P_i^2 BB^T P_i^2 B = O(1/|P_i|).$$

Thus $B^T P_i BB^T P_i B$ is bounded, note that this does not imply that $P_i BB^T P_i$ is bounded, but it does imply that $P_i^{1/2} B$ is bounded. Let $SG = \lim P_i^{1/2} BB^T P_i^{1/2}$ and \bar{P} be limit \bar{P}_i , then

$$A^T \bar{P} + \bar{P} A - \bar{P}^{1/2} SG \bar{P}^{1/2} = 0.$$

Note also that \bar{P} the subspace spanned by \bar{P} is an A invariant subspace, i.e. $A \bar{P}$ is contained in \bar{P} . Let \bar{A} be the operator A restricted to \bar{P} . Since \bar{P} is an invariant subspace, eigenvalues of \bar{A} are eigenvalues of A . \bar{A} and \bar{P} satisfy

$$(-A^*)\bar{P} + \bar{P}(-A) + \bar{P}^{1/2}SGP^{-1/2} = 0$$

Since $P > 0$ and $\bar{P}^{1/2}SGP^{-1/2} > 0$ we have $(-A^*)$ is neutrally stable.

Since $\bar{P}B=0$ we finally have that there exists eigenvectors of A say E , such that $BE=0$ and the eigenvalue of AE is non-negative, or that A, B is not stabilizable. Thus $|P_i| \rightarrow \infty$ implies that A, B is not stabilizable, so A, B stabilizable implies $|P_i|$ bounded. QED

Lemma 2. $F(P, t) \neq 0$ for P in \bar{D} . Proof: \bar{D} consists of all symmetric P such that either $|P|=R$ and $P > 0$ or $|P| < R$ and $P > 0$ with P singular. Lemma 1 has shown that $F(P, t) \neq 0$ for $|P|=R$. Suppose there exists a P which is singular with $F(P, t)=0$. Then there exists a vector u such that $Pu=0$ and $u^T P=0$. Multiplying (2) on the left by u^T and on the right by u yields $u^T V(t)u=0$, which contradicts $V(t) > 0$. Q.E.D.

We now have that $\text{Deg}(F, D, 0) = \text{const}$ for all t in $[0, 1]$.

Lemma 3. $\text{Deg}(F, D, 0) = 1$. Proof: Let $A(0)$, $S(0)$, and $V(0)$ be diagonal. There is only one positive definite solution to (2) for this A, S, V , and this solution has Jacobian non-zero, thus the $\text{Deg}(F, D, 0) = \underline{+1}$.

The above analysis shows that there is always at least one solution to $F(x, t)=0$ and that the solution set at $t=0$ (consisting of just one point) connects with the solution set at $t=1$, but the solution set at $t=1$ may consist of more than one point so that the desired solution is not obtained from the homotopy. We will now show that this is not the case, i.e., for the full Riccati equation, there is one and only one positive solution at each point on the homotopy path.

Proof: Let $F: C^{n \times n} \rightarrow C^{n \times n}$ by

$$F(P, t) = A^T P + P A^T - P S(t) P + V(t)$$

where $A(t), S(t)$, and $V(t)$ are as above and P is an $n \times n$ complex matrix.

Let D be all P such that $|P| < R$, and real part of eigenvalues of P are positive.

D is open domain in $C^{n \times n}$. By the same argument as in the real case, $F(P, t) \neq 0$ for $|P|=R$. Also, it can be shown that only solutions to $F(P, t)=0$ are Hermitian, so the eigenvalue of P are real. Thus

$F(P, t)=0$ and P in \bar{D} is for $|P|=R$ (which cannot occur) or for P to be singular and $F(P, T)=0$ which also cannot occur. Thus the $\text{deg}(F, D, 0) = \text{const}$ for t in $[0, 1]$, and by using $A(0), V(0)$, and $S(0)$ diagonal, we get that $\text{deg}(F, D, 0) = 1$.

We also know that an analytic map from C^k into C^k preserves orientation, that is the Jacobians always have the same sign, thus we have that the number of solutions (at a regular value) is equal to the degree and is always less than or equal to the degree. Thus we have that there is one and only one complex solution to (2), and since there is at least one real solution, there is one and only one real positive solution to (2).

4. Algorithm Description and Numerical Results

In a homotopy path following algorithm one follows the path of solutions of $F(x(t), t)$ by integrating the initial value problem

$$\frac{dx}{dt} = F_x(x(t)) \frac{dF}{dt}(x(t), t); \quad x(0) = x_0.$$

For the optimal projections equations the solution P, \hat{P}, Q, \hat{Q} can be easily determined once τ is known so the $P(t)=P(\tau(t)), Q(t)=Q(\tau(t))$ etc. Thus the derivatives of P, Q, \hat{P}, \hat{Q} can be written in terms of derivatives of G^T and Γ . Thus we obtain

$$\text{vec} \begin{bmatrix} \Gamma' \\ G^{T'} \end{bmatrix} = \begin{bmatrix} M \end{bmatrix} \text{vec } f(\Gamma, G^T).$$

which gives $2n_c n$ equation for Γ' and $G^{T'}$. P', Q', \hat{P}' and \hat{Q}' are then calculated from Γ' and $G^{T'}$ and finally $\Gamma(t+\Delta t)$ is updated by

$$\Gamma(t+\Delta t) = \Gamma(t) + \Gamma' \times \Delta t$$

and likewise for G, P, Q, \hat{P} and \hat{Q} .

Figure 3 summarizes the results reported in [1] for LQG reduction methods along with results obtained using the homotopy method for solving the optimal projection equations. Here q_2 is a scale factor for the plant disturbance noise affecting controller authority. Clearly, LQG reduction methods experience increasing difficulty as authority increases, i.e., as the τ_1 terms become increasingly more important in coupling the control and reduction operations.

One of the main goals of the development effort was to extend the range of disturbance intensity or, equivalently, observer bandwidth, out beyond $q_2=2000$. To this end, second-order ($n_c=2$) controllers were obtained with relatively little computation for $q_2=10,000, 100,000, 1,000,000$. The performance of these results is summarized in Figure 4.

Method	$\frac{G_1}{s}$	0.01	0.1	1	10	100	1000	2000
Enns	7	S	S	S	S	S	S	S
	6	S	S	S	S	S	S	S
	5	S	S	S	S	S	S	S
	4	S	S	S	S	S	S	S
	3	S	S	S	S	S	S	S
Glover	7	S	S	S	S	S	U	S
	6	S	S	S	S	U	U	U
	5	S	S	S	S	U	U	U
	4	S	S	S	S	U	U	U
	3	S	S	S	U	U	U	U
Davis & Shelton	7	S	U	U	S	S	S	S
	6	S	U	U	S	S	S	S
	5	S	U	U	S	S	S	S
	4	S	U	U	U	S	S	S
	3	U	U	U	U	U	U	U
Yousoff & Shelton	7	S	S	S	S	U	U	U
	6	S	S	S	S	U	U	U
	5	S	S	S	S	U	U	U
	4	S	S	S	S	U	U	U
	3	S	S	S	S	U	U	U
Lin & Anderson	7	S	S	S	S	S	S	U
	6	S	S	S	S	S	S	S
	5	S	S	S	S	S	S	S
	4	S	S	S	S	S	S	S
	3	S	S	S	S	S	S	S
Optimal Projection	7	S	S	S	S	S	S	S
	6	S	S	S	S	S	S	S
	5	S	S	S	S	S	S	S
	4	S	S	S	S	S	S	S
	3	S	S	S	S	S	S	S

S - The closed-loop system is stable
 U - The closed-loop system is unstable

Figure 3. The Optimal Projection Approach Was Compared to Several LQG Reduction Techniques Over a Range of Controller Authorities for an Example of Enns

OP VIA HOMOTOPY ALGORITHM
 ENN'S EXAMPLE

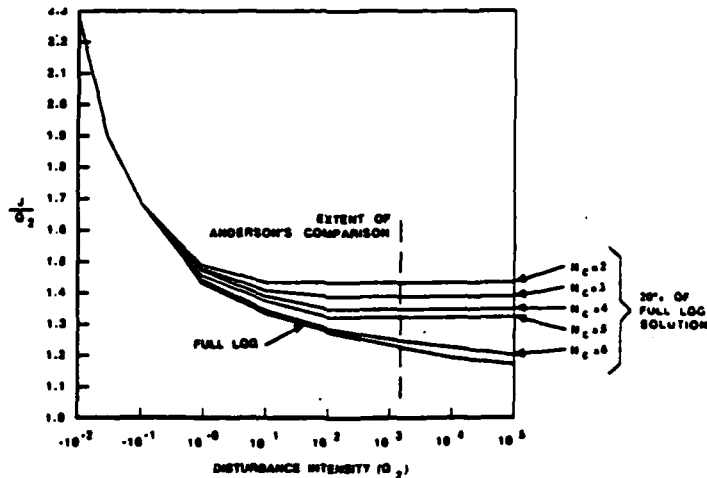


Figure 4

References

1. Y. Liu and B. D. O. Anderson, "Controller Reduction via Stable Factorization and Balancing," Int. J. Contr., Vol. 44, pp. 507-531, 1986.
2. D. C. Hyland and D. S. Bernstein, "The Optimal Projection Equations for Fixed-Order Dynamic Compensation," IEEE Trans. Autom. Contr., Vol. AC-29, pp. 1034-1037, 1984.
3. D. C. Hyland and D. S. Bernstein, "The Optimal Projection Equations for Model Reduction and the Relationships Among the Methods of Wilson, Skelton and Moore," IEEE Trans. Autom. Contr., Vol. AC-30, pp. 1201-1211, 1985.
4. D. C. Hyland, "The Optimal Projection Approach to Fixed-Order Compensation: Numerical Methods and Illustrative Results," AIAA 21st Aerospace Sciences Meeting, paper 83-0303, Reno, NV, January 1983.
5. D. C. Hyland, "Comparison of Various Controller-Reduction Methods: Suboptimal Versus Optimal Projection," Proc. AIAA Dynamics Specialists Conf., pp. 381-389, Palm Springs, CA, May 1984.
6. D. S. Bernstein, L. D. Davis and D. C. Hyland, "The Optimal Projection Equations for Reduced-Order, Discrete-Time Modelling, Estimation and Control," J. Guid. Contr. Dyn., Vol. 9, pp. 288-293, 1986.
7. D. S. Bernstein and D. C. Hyland, "The Optimal Projection/Maximum Entropy Approach to Designing Low-Order, Robust Controllers for Flexible Structures," Proc. 24th IEEE Conf. Dec. Contr., pp. 745-752, Fort Lauderdale, FL, December 1985.
8. D. S. Bernstein, L. D. Davis, S. W. Greeley and D. C. Hyland, "Numerical Solution of the Optimal Projection/Maximum Entropy Design Equations for Low-Order, Robust Controller Design," Proc. 24th IEEE Conf. Dec. Contr., pp. 1795-1798, Fort Lauderdale, FL, December 1985.
9. D. S. Bernstein and S. W. Greeley, "Robust Controller Synthesis Using the Maximum Entropy Design Equations," IEEE Trans. Autom. Contr., Vol. AC-31, pp. 362-364, 1986.
10. D. C. Hyland, D. S. Bernstein, L. D. Davis, S. W. Greeley and S. Richter, "MEOP: Maximum Entropy/Optimal Projection Stochastic Modelling and Reduced-Order Design Synthesis," Final Report, Air Force of Scientific Research, Bolling AFB, Washington, DC, April 1986.
11. A. Gruzen and W. E. Vander Velde, "Robust Reduced-Order Control of Flexible Structure Using the Optimal Projection/Maximum Entropy Design Methodology," AIAA Guid. Nav. Contr. Conf., Williamsburg, VA, August 1986.
12. A. Gruzen, "Robust Reduced Order Control of Flexible Structures," C. S. Draper Laboratory Report #CSDL-T-900, April 1986.

13. E. Wasserstrom, "Numerical Solutions by the Continuation Method," SIAM Review, Vol. 15, pp. 89-119, 1973.
14. J. H. Avila, "The Feasibility of Continuation Methods for Nonlinear Equations," SIAM J. Numer. Anal., Vol. 11, pp. 102-122, 1974.
15. H. Wacker, Continuation Methods, Academic Press, New York, 1978.
16. N. G. Lloyd, Degree Theory, Cambridge University Press, London, 1978.
17. J. C. Alexander and J. A. Yorke, "The Homotopy Continuation Method: Numerically Implementable Procedures," Trans. Amer. Math. Soc., Vol. 242, pp. 271-284, 1978.
18. B. C. Eaves, F. J. Gould, H. O. Peitgen, and M. J. Todd, Homotopy Methods and Global Convergence, Plenum Press, New York, 1983.
19. M. Mariton and R. Bertrand, "A Homotopy Algorithm for Solving Coupled Riccati Equations," Optim. Contr. Appl. Meth., Vol. 6, pp. 351-357, 1985.
20. S. Richter and R. DeCarlo, "Continuation Methods: Theory and Applications," IEEE Trans. Autom. Contr., Vol. 28, pp. 660-665, 1983.
21. S. Richter and R. DeCarlo, "A Homotopy Method for Eigenvalue Assignment Using Decentralized State Feedback," IEEE Trans. Autom. Contr., Vol. AC-29, pp. 148-155, 1984.
22. S. Lefebvre, S. Richter and R. DeCarlo, "A Continuation Algorithm for Eigenvalue Assignment by Decentralized Constant-Output Feedback," Int. J. Contr., Vol. 41, pp. 1273-1292, 1985.
23. D. R. Sebok, S. Richter and R. DeCarlo, "Feedback Gain Optimization in Decentralized Eigenvalue Assignment," Automatica, Vol. 22, pp. 433-447, 1986.
24. P. T. Kabamba, R. W. Longman and S. Jian-Guo, "A Homotopy Approach to the Feedback Stabilization of Linear Systems," preprint.
25. R. de Gaston and M. Safonov, "A Homotopy Method for Nonconservative Stability Robustness Analysis," Proc. 24th IEEE Conf. Dec. Contr., pp. 1294-1301, Fort Lauderdale, FL, December, 1985.
26. Malcolm C. Smith, "On Minimal Order Stabilization of Single Loop Plants," Sys. Contr. Lett., Vol. 7, pp. 39-40, 1986.

APPENDIX H

Sequential Design of Decentralized Dynamic Compensators Using the Optimal Projection Equations

Sequential design of decentralized dynamic compensators using the optimal projection equations

DENNIS S. BERNSTEIN†

The optimal projection equations for quadratically optimal centralized fixed-order dynamic compensation are generalized to the case in which the dynamic compensator has, in addition, a fixed decentralized structure. Under a stabilizability assumption for the particular feedback configuration, the resulting optimality conditions explicitly characterize each subcontroller in terms of the plant and remaining subcontrollers. This characterization associates an oblique projection with each subcontroller and suggests an iterative sequential design algorithm. The results are applied to an interconnected flexible beam example.

1. Introduction

The purpose of this note is to consider the problem of designing decentralized dynamic feedback controllers using recently obtained results on quadratically optimal fixed-order dynamic compensation (Hyland and Bernstein 1984). As in Bernussou and Titli (1982), Looze *et al.* (1978), and Singh (1981), the overall approach is to fix the structure (information pattern and order) of the linear controller and optimize the steady-state regulation cost with respect to the controller parameters. The underlying philosophy is that the ability to carry out such an optimization procedure permits the evaluation of a particular decentralized configuration which may be dictated by implementation constraints. If there is some flexibility in designing the decentralized architecture, then these results can be used to evaluate the optimal performance of each permissible configuration, and hence to determine preferable structures. Since the present paper is confined to the question of optimal regulation, trade-offs with regard to robustness in the presence of plant variations are not considered. Such trade-offs can be included, however, by utilizing the Stratonovich multiplicative white noise approach developed by Bernstein and Hyland (1985).

To further motivate our approach, consider the problem of controlling an n th-order plant \mathcal{P} by means of a decentralized dynamic compensator consisting of subcontrollers \mathcal{C}_1 and \mathcal{C}_2 . A straightforward design technique that immediately comes to mind is that of *sequential optimization* (Davison and Gesing 1979, Jamshidi 1983). To begin, ignore \mathcal{C}_2 and design \mathcal{C}_1 as a centralized controller for \mathcal{P} . Next, regard the closed-loop system consisting of \mathcal{P} and \mathcal{C}_1 as an augmented system \mathcal{P}' and design \mathcal{C}_2 as a centralized controller for \mathcal{P}' . Now *redesign* \mathcal{C}_1 to be a centralized controller for the augmented closed-loop system composed of \mathcal{P} and \mathcal{C}_2 , and so forth. One difficulty with this scheme, however, is that of *dimension*. If, for example, one were to employ LQG at each step of this algorithm, then on the first iteration \mathcal{C}_1 would have dimension n and thus \mathcal{C}_2 would have dimension $2n$. On the second iteration, \mathcal{C}_1 would require dimension $3n$ and \mathcal{C}_2 would have order $4n$, and so forth. Such

Received 15 December 1986.

† Harris Corporation, Government Aerospace Systems Division, P.O. Box 94000, Melbourne, Florida 32902, U.S.A.

difficulties can be avoided by setting $n = 0$, which essentially corresponds to static output feedback. Although easier to implement, static output feedback lacks filtering abilities such as are inherent in LQG controllers, which are purely dynamic (i.e. strictly proper).

As discussed by Sandell *et al.* (1978), p. 119, the explanation for this difficulty is provided by the 'second-guessing' phenomenon: when LQG is used, each subcontroller must consist of linear feedback, not only of estimates of the plant states but also of *estimates of the other subcontrollers' estimates*. Hence the 'optimal' controller is given by an irrational transfer function, i.e. a distributed parameter (infinite-dimensional) system. Such controllers, of course, must be ruled out since their design and implementation (except in special cases) violate physical realizability (see, for example, Bernstein and Hyland 1986).

Having thus ruled out zeroth-order and infinite-order decentralized controllers, we focus on the problem of designing purely dynamic decentralized compensators. Moreover, by invoking the constraint of fixed subcontroller order, we overcome the *second-guessing phenomenon*. Utilizing the parameter optimization approach thus leads to a generalization of the result obtained by Hyland and Bernstein (1984) for centralized control. In brief, it was shown in Hyland and Bernstein (1984) that the unwieldy first-order necessary conditions for fixed-order dynamic compensation can be simplified by exploiting the presence of a previously unrecognized *oblique projection*. The resulting *optimal projection equations*, which consist of a pair of modified Riccati equations and a pair of modified Lyapunov equations coupled by the optimal projection, yield insight into the structure of the optimal dynamic compensator and emphasize the breakdown of the separation principle for reduced-order controller design. For example, the optimal compensator is the projection of a full-order dynamic controller which is generally different from the LQG design. Furthermore, this full-order controller and the oblique projection are intricately related since they are simultaneously determined by the coupled design equations. An immediate consequence is the observation that stepwise schemes employing either model reduction followed by LQG or LQG followed by model reduction are generally suboptimal. For computational purposes, the optimal projection equations permit the development of novel numerical methods which operate through successive iteration of the oblique projection (Hyland and Bernstein 1985). Such algorithms are thus philosophically and operationally distinct from gradient search methods.

The generalization of the optimal projection equations to the decentralized case is straightforward and immediate. In the optimization process each subcontroller is viewed as a centralized controller for an augmented 'plant' consisting of the *actual plant* and all other subcontrollers. It need only be observed that the necessary conditions for optimality for the decentralized problem must consist of the collection of necessary conditions obtained by optimizing over each subcontroller separately while keeping the other subcontrollers fixed. More precisely, this statement corresponds to the fact that setting the Frechet derivative to zero is equivalent to setting the individual partial derivatives to zero. Hence it is not surprising that the optimal projection equations for the decentralized problem involve multiple oblique projections, one associated with each subcontroller. Furthermore, each subcontroller incorporates an internal model (in the sense of an oblique projection of full-order dynamics) not only of the plant but also of all other subcontrollers. The structure of the equations suggests a sequential design algorithm such as that proposed in this work.

The simplicity with which this result is obtained should not belie its relevance to the decentralized control problem. Specifically, our approach is distinct from subsystem-decomposition techniques (Ikeda and Siljak 1980, 1981, Ikeda *et al.* 1981, 1984, Lindner 1985, Linnemann 1984, Ozguner 1979, Ramakrishna and Viswanadham 1982, Saeks 1979, Sezer and Huseyin 1984, Siljak 1978, 1983) and model-reduction methods since the optimal projection equations retain the full, interconnected plant at all times. For the proposed algorithm, decomposition techniques which exploit subsystem-interconnection data can play a role by providing a starting point for subsequent iterative refinement and optimization. Decomposition methods may also play a role when very high dimensionality precludes direct solution of the optimal projection equations. These are areas for future research.

With regard to the role of the oblique projection, it should be noted that such transformations do not, in general, preserve plant characteristics such as poles, zeros, subspaces, etc. Indeed, since the oblique projection arises as a consequence of optimality, approaches that seek to retain system invariants (e.g. Uskokovic and Medanic 1985) are generally suboptimal. In addition, the complex coupling among the plant and subcontrollers via multiple oblique projections provides an additional measure for evaluating the suboptimality of the methods proposed.

The plan of the paper is as follows. The fixed-structure decentralized dynamic-compensation problem is stated in § 2 along with the generalization of the optimal projection equations. In § 3 we propose a sequential design algorithm for solving these equations and state conditions under which convergence is guaranteed. Finally, in § 4 the algorithm is applied to the 8th-order model of a pair of simply supported beams connected by a spring. For this example, we obtain a two-channel decentralized design which is 4th-order in each channel and compare its performance with the (8th-order) centralized LQG design.

2. Problem statement and main theorem

Given the controlled system

$$\dot{x}(t) = Ax(t) + \sum_{i=1}^p B_i u_i(t) + w_0(t) \quad (2.1)$$

$$y_i(t) = C_i x(t) + w_i(t), \quad i = 1, \dots, p \quad (2.2)$$

design a fixed-structure decentralized dynamic compensator

$$\dot{x}_{ci}(t) = A_{ci} x_{ci}(t) + B_{ci} y_i(t), \quad i = 1, \dots, p \quad (2.3)$$

$$u_i(t) = C_{ci} x_{ci}(t), \quad i = 1, \dots, p \quad (2.4)$$

which minimizes the steady-state performance criterion

$$J(A_{c1}, B_{c1}, C_{c1}, \dots, A_{cp}, B_{cp}, C_{cp}) \triangleq \lim_{t \rightarrow \infty} E \left[x(t)^T R_0 x(t) + \sum_{i=1}^p u_i(t)^T R_i u_i(t) \right] \quad (2.5)$$

where, for $i = 1, \dots, p$: $x \in \mathbb{R}^n$, $u_i \in \mathbb{R}^{m_i}$, $y_i \in \mathbb{R}^{l_i}$, $c_{ci} \in \mathbb{R}^{n_{ci}}$, $n_c \triangleq \sum_{i=1}^p n_{ci}$, $n_{ci} \leq n + n_c - n_{ci}$, A , B_i , C_i , A_{ci} , B_{ci} , C_{ci} , R_0 and R_i are matrices of appropriate dimension with R_0 (symmetric) non-negative definite and R_i (symmetric) positive definite; w_0 is white disturbance noise with $n \times n$ non-negative-definite intensity V_0 , and w_i is white

observation noise with $l_i \times l_i$ positive-definite intensity V_i , where w_0, w_1, \dots, w_p are mutually uncorrelated and have zero mean. E denotes expectation and superscript T indicates transpose.

To guarantee that J is finite and independent of initial conditions we restrict our attention to the set of admissible stabilizing compensators

$$\mathcal{A} \triangleq \{(A_{c1}, B_{c1}, C_{c1}, \dots, A_{cp}, B_{cp}, C_{cp}) : \tilde{A} \text{ is asymptotically stable}\}$$

where the closed-loop dynamics matrix \tilde{A} is given by

$$\tilde{A} \triangleq \begin{bmatrix} A & \tilde{B}C_c \\ B_c \tilde{C} & A_c \end{bmatrix}$$

where

$$\tilde{B} \triangleq [B_1 \quad \dots \quad B_p], \quad \tilde{C} \triangleq \begin{bmatrix} C_1 \\ \vdots \\ C_p \end{bmatrix}$$

$$A_c \triangleq \text{block-diagonal}(A_{c1}, \dots, A_{cp})$$

$$B_c \triangleq \text{block-diagonal}(B_{c1}, \dots, B_{cp})$$

$$C_c \triangleq \text{block-diagonal}(C_{c1}, \dots, C_{cp})$$

(For possibly non-square matrices S_1, S_2 , block-diagonal (S_1, S_2) denotes the matrix $\begin{bmatrix} S_1 & 0 \\ 0 & S_2 \end{bmatrix}$.)

It is possible that for certain decentralized structures the system is not stabilizable, i.e. \mathcal{A} is empty (Wang and Davison 1973, Seraji 1982, Sezer and Siljak 1981). Our approach, however, is to assume that \mathcal{A} is not empty and characterize the optimal decentralized controller over the stabilizing class. Since the value of J is independent of the internal realization of each subcompensator, without loss of generality we can further restrict our attention to

$$\mathcal{A}_+ \triangleq \{(A_{c1}, B_{c1}, C_{c1}, \dots, A_{cp}, B_{cp}, C_{cp}) \in \mathcal{A} : (A_{ci}, B_{ci}) \text{ is controllable and } (C_{ci}, A_{ci}) \text{ is observable, } i = 1, \dots, p\}$$

The following lemma is an immediate consequence of Theorem 6.2.5, p. 123 of Rao and Mitra (1971). Let I_r denote the $r \times r$ identity matrix.

Lemma 2.1

Suppose $\hat{Q}, \hat{P} \in \mathbb{R}^{q \times q}$ are non-negative definite and $\text{rank } \hat{Q}\hat{P} = r$. Then there exist $G, \Gamma \in \mathbb{R}^{r \times q}$ and invertible $M \in \mathbb{R}^{r \times r}$ such that

$$\hat{Q}\hat{P} = G^T M \Gamma \quad (2.6)$$

$$\Gamma G^T = I_r \quad (2.7)$$

For convenience in stating the main theorem, call (G, M, Γ) satisfying (2.6), (2.7) a

projective factorization of $\hat{Q}\hat{P}$. Such a factorization is unique modulo an arbitrary change in basis in \mathbb{R}^r , which corresponds to nothing more than a change of basis for the internal representation of the compensator (or subcompensators in the present context).

We shall also require the following notation. Let \tilde{A}_i denote \tilde{A} with the rows and columns containing A_{ci} deleted. Similarly, let \tilde{R}_i be obtained by deleting the rows and columns corresponding to $C_{ci}^T R_i C_{ci}$ in the matrix

$$\tilde{R} \triangleq \text{block-diagonal} (R_0, C_{c1}^T R_1 C_{c1}, \dots, C_{cp}^T R_p C_{cp})$$

And furthermore, \tilde{V}_i is obtained by deleting the rows and columns containing $B_{ci} V_i B_{ci}^T$ in

$$\tilde{V} \triangleq \text{block-diagonal} (V_0, B_{c1} V_1 B_{c1}^T, \dots, B_{cp} V_p B_{cp}^T)$$

Also define

$$\tilde{B}_i \triangleq \begin{bmatrix} B_i \\ 0_{(n_c - n_{ci}) \times m_i} \end{bmatrix}, \quad \tilde{C}_i \triangleq [C_i \quad 0_{1 \times (n_c - n_{ci})}]$$

where $0_{r \times s}$ denotes the $r \times s$ zero matrix. Note that \tilde{A}_i , \tilde{B}_i , \tilde{C}_i , \tilde{R}_i and \tilde{V}_i essentially represent the closed-loop system minus the i th subcontroller as controlled by the latter. Finally, define

$$\Sigma_i \triangleq \tilde{B}_i R_i^{-1} \tilde{B}_i^T, \quad \tilde{\Sigma}_i \triangleq \tilde{C}_i^T V_i^{-1} \tilde{C}_i$$

and, for $\tau \in \mathbb{R}^{r \times r}$, let

$$\tau_{\perp} \triangleq I_r - \tau$$

Main theorem

Suppose $(A_{c1}, B_{c1}, C_{c1}, \dots, A_{cp}, B_{cp}, C_{cp}) \in \mathcal{A}_+$ solves the steady-state fixed-structure decentralized dynamic-compensation problem. Then for $i = 1, \dots, p$ there exist $(n + n_c - n_{ci}) \times (n + n_c - n_{ci})$ non-negative-definite matrices Q_i , P_i , \hat{Q}_i and \hat{P}_i such that A_{ci} , B_{ci} and C_{ci} are given by

$$A_{ci} = \Gamma_i (\tilde{A}_i - Q_i \Sigma_i - \Sigma_i P_i) G_i^T \quad (2.8)$$

$$B_{ci} = \Gamma_i Q_i \tilde{C}_i^T V_i^{-1} \quad (2.9)$$

$$C_{ci} = -R_i^{-1} \tilde{B}_i^T P_i G_i^T \quad (2.10)$$

for some projective factorization G_i , M_i , Γ_i of $\hat{Q}_i \hat{P}_i$, and such that, with $\tau_i = G_i^T \Gamma_i$, the following conditions are satisfied:

$$0 = \tilde{A}_i Q_i + Q_i \tilde{A}_i^T + \tilde{V}_i - Q_i \Sigma_i Q_i + \tau_{i\perp} Q_i \Sigma_i Q_i \tau_{i\perp}^T \quad (2.11)$$

$$0 = \tilde{A}_i^T P_i + P_i \tilde{A}_i + \tilde{R}_i - P_i \Sigma_i P_i + \tau_{i\perp}^T P_i \Sigma_i P_i \tau_{i\perp} \quad (2.12)$$

$$0 = (\tilde{A}_i - \Sigma_i P_i) \hat{Q}_i + \hat{Q}_i (\tilde{A}_i - \Sigma_i P_i)^T + Q_i \Sigma_i Q_i - \tau_{i\perp} Q_i \Sigma_i Q_i \tau_{i\perp}^T \quad (2.13)$$

$$0 = (\tilde{A}_i - Q_i \Sigma_i)^T \hat{P}_i + \hat{P}_i (\tilde{A}_i - Q_i \Sigma_i) + P_i \Sigma_i P_i - \tau_{i\perp}^T P_i \Sigma_i P_i \tau_{i\perp} \quad (2.14)$$

$$\text{rank } \hat{Q}_i = \text{rank } \hat{P}_i = \text{rank } \hat{Q}_i \hat{P}_i = n_{ci} \quad (2.15)$$

Remark 2.1

Because of (2.7) the matrix τ_i is idempotent, i.e. $\tau_i^2 = \tau_i$. This projection corresponding to the i th subcontroller is an *oblique* projection (as opposed to an orthogonal projection) since it is not necessarily symmetric. Furthermore, τ_i is given in closed form by

$$\tau_i = \hat{Q}_i \hat{P}_i (\hat{Q}_i \hat{P}_i)^{\#}$$

where $(\)^{\#}$ denotes the (Drazin) group generalized inverse (see, for example, Campbell and Meyer, 1979, p. 124).

3. Proposed algorithm*Sequential design algorithm*

- Step 1.** Choose a starting point consisting of initial subcontroller designs;
- Step 2.** For a sequence $\{i_k\}_{k=1}^{\infty}$, where $i_k \in \{1, \dots, p\}$, $k = 1, 2, \dots$, redesign subcontroller i_k as an optimal fixed-order centralized controller for the plant and remaining subcontrollers;
- Step 3.** Compute the cost J_k of the current design and check $J_k - J_{k-1}$ for convergence.

Note that the first two steps of the algorithm consist of (i) bringing suboptimal subcontrollers 'on line' and (ii) iteratively refining each subcontroller. As discussed in § 1, the choice of a starting design for Step 1 can be obtained by a variety of existing methods such as subsystem decomposition. As for subcontroller refinement, note that each subcontroller redesign procedure is equivalent to replacing a suboptimal subcontroller with a subcontroller which is optimal with respect to the plant and remaining subcontrollers.

Proposition 3.1

For a given starting design and redesign sequence $\{i_k\}_{k=1}^{\infty}$ suppose that the optimal projection equations can be solved for each k to yield the global minimum. Then $\{J_k\}_{k=1}^{\infty}$ is monotonically non-increasing and hence convergent.

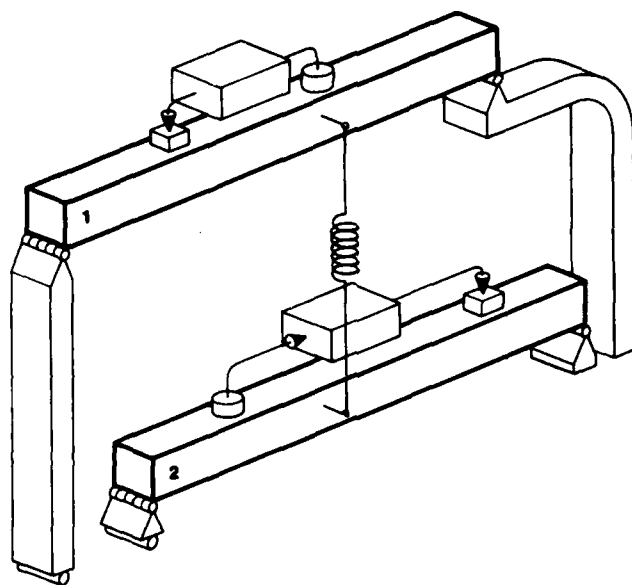
Determining both a suitable starting point and redesign sequence for solvability and attaining the decentralized global minimum remain areas for future research. With regard to algorithms for solving the optimal projection equations for each subcontroller redesign procedure, details of proposed algorithms can be found in the works of Hyland (1983, 1984) and Hyland and Bernstein (1985).

4. Application to interconnected flexible beams

To demonstrate the applicability of the main theorem and the sequential design algorithm, we consider a pair of simply supported Euler-Bernoulli flexible beams interconnected by a spring (see the Figure). Each beam possesses one rate sensor and one force actuator. Retaining two vibrational modes in each beam, we obtain the 8th-order interconnected model

$$A = \begin{bmatrix} A_{11} & A_{12} \\ A_{21} & A_{22} \end{bmatrix}, \quad B_1 = \begin{bmatrix} B_{11} \\ 0_{4 \times 1} \end{bmatrix}, \quad B_2 = \begin{bmatrix} 0_{4 \times 1} \\ B_{22} \end{bmatrix}$$

$$C_1 = [C_{11} \quad 0_{1 \times 4}], \quad C_2 = [0_{1 \times 4} \quad C_{22}]$$



where

$$A_{ii} = \begin{bmatrix} 0 & \omega_{1i} & 0 & 0 \\ -\omega_{1i} - (k/\omega_{1i})(\sin \pi c_i)^2 & -2\zeta_i \omega_{1i} & -(k/\omega_{2i})(\sin \pi c_i)(\sin 2\pi c_i) & 0 \\ 0 & 0 & 0 & \omega_{2i} \\ -(k/\omega_{1i})(\sin \pi c_i)(\sin 2\pi c_i) & 0 & -\omega_{2i} - (k/\omega_{2i})(\sin 2\pi c_i)^2 & -2\zeta_i \omega_{2i} \end{bmatrix}$$

$$A_{ij} = \begin{bmatrix} 0 & 0 & 0 & 0 \\ (k/\omega_{1j})(\sin \pi c_i)(\sin \pi c_j) & 0 & (k/\omega_{2j})(\sin \pi c_i)(\sin 2\pi c_j) & 0 \\ 0 & 0 & 0 & 0 \\ (k/\omega_{1j})(\sin \pi c_j)(\sin 2\pi c_i) & 0 & (k/\omega_{2j})(\sin 2\pi c_i)(\sin 2\pi c_j) & 0 \end{bmatrix}$$

$i \neq j$

$$B_{ii} = \begin{bmatrix} 0 \\ -\sin \pi a_i \\ 0 \\ -\sin 2\pi a_i \end{bmatrix}, \quad C_{ii} = [0 \quad \sin \pi s_i \quad 0 \quad \sin 2\pi s_i]$$

$$a_i = \hat{a}_i/L_i, \quad s_i = \hat{s}_i/L_i, \quad c_i = \hat{c}_i/L_i$$

In the above definitions, k is the spring constant, ω_{ji} is the j th modal frequency of the i th beam, ζ_i is the damping ratio of the i th beam, L_i is the length of the i th beam, and \hat{a}_i , \hat{s}_i and \hat{c}_i are, respectively, the actuator, sensor and spring-connection coordinates as measured from the left in the Figure. The chosen values are

$$k = 10$$

$$\omega_{1i} = 1, \quad \omega_{2i} = 4, \quad \zeta_i = 0.005, \quad L_i = 1, \quad i = 1, 2$$

$$\hat{a}_1 = 0.3, \quad \hat{s}_1 = 0.65, \quad \hat{c}_1 = 0.6$$

$$\hat{a}_2 = 0.8, \quad \hat{s}_2 = 0.2, \quad \hat{c}_2 = 0.4$$

In addition, weighting and intensity matrices are chosen to be

$$R_1 = \text{block-diagonal} \left(\begin{bmatrix} 1 & 0 \\ 0 & 1/\omega_{11} \end{bmatrix}, \begin{bmatrix} 1 & 0 \\ 0 & 1/\omega_{21} \end{bmatrix}, \begin{bmatrix} 1 & 0 \\ 0 & 1/\omega_{12} \end{bmatrix}, \begin{bmatrix} 1 & 0 \\ 0 & 1/\omega_{22} \end{bmatrix} \right)$$

$$R_2 = R_3 = 0.1I_2$$

$$V_0 = \text{block-diagonal} \left(\begin{bmatrix} 0 & 0 \\ 0 & 1 \end{bmatrix}, \begin{bmatrix} 0 & 0 \\ 0 & 1 \end{bmatrix}, \begin{bmatrix} 0 & 0 \\ 0 & 1 \end{bmatrix}, \begin{bmatrix} 0 & 0 \\ 0 & 1 \end{bmatrix} \right)$$

$$V_1 = V_2 = 0.1I_2$$

For this problem the open-loop cost was evaluated and the centralized 8th-order LQG design was obtained to provide a baseline. To provide a starting point for the sequential design algorithm, a pair of 4th-order LQG controllers were designed for each beam separately ignoring the interconnection, i.e. setting $k = 0$. The optimal projection equations were then utilized to iteratively refine each subcontroller. The results are summarized in the Table.

Design	Cost
Open loop	163.5
Centralized LQG	
$n_c = 8$	19.99
Suboptimal decentralized	
$n_{c1} = n_{c2} = 4$	59.43
Redesign subcontroller 2	28.19
Redesign subcontroller 1	23.29
Redesign subcontroller 2	23.04
Redesign subcontroller 1	22.25
Redesign subcontroller 2	21.94
Redesign subcontroller 1	21.86
Redesign subcontroller 2	21.81
Redesign subcontroller 1	21.79

ACKNOWLEDGMENTS

This research was supported in part by the Air Force Office of Scientific Research under contracts F49620-86-C-0002 and F49620-86-C-0038.

The author wishes to thank Scott W. Greeley for providing the beam model in § 4 and for carrying out the design computations.

REFERENCES

- BERNSTEIN, D. S., and HYLAND, D. C., 1985, *Proc. 24th I.E.E.E. Conf. Dec. Control*, 745; 1986, *SIAM JI Control Optim.*, **24**, 122.
- BERNUSSOU, J., and TITLI, A., 1982, *Interconnected Dynamical Systems: Stability, Decomposition and Decentralization* (New York: North-Holland).
- CAMPBELL, S. L., and MEYER, C. D., Jr., 1979, *Generalized Inverses of Linear Transformations* (London: Pitman).
- DAVISON, E. J., and GESING, W., 1979, *Automatica*, **15**, 307.
- DE CARLO, R. A., and SAEKS, R., 1981, *Interconnected Dynamical Systems* (New York: Marcel Dekker).
- HYLAND, D. C., 1983, *AIAA 21st Aerospace Sciences Meeting*, paper 83-0303; 1984, *Proc. AIAA Dynamics Specialists Conf.*, 381.
- HYLAND, D. C., and BERNSTEIN, D. S., 1984, *I.E.E.E. Trans. autom. Control*, **29**, 1034; 1985, *Ibid.*, **30**, 1201.
- IKEDA, M., and SILJAK, D. D., 1980, *Large-scale Syst.*, **1**, 29; 1981, *I.E.E.E. Trans. autom. Control*, **26**, 1118.
- IKEDA, M., SILJAK, D. D., and WHITE, D. E., 1981, *J. optim. Theory Applic.*, **34**, 279; 1984, *I.E.E.E. Trans. autom. Control*, **29**, 244.
- JAMSHIDI, M., 1983, *Large-Scale Systems* (New York: North-Holland).
- LINDNER, D. K., 1985, *Syst. Control Lett.*, **6**, 109.
- LINNEMANN, A., 1984, *I.E.E.E. Trans. autom. Control*, **29**, 1052.
- LOOZE, D. P., HOUP, P. K., SANDELL, N. R., and ATHANS, M., 1978, *I.E.E.E. Trans. autom. Control*, **23**, 268.
- OZGUNER, U., 1979, *I.E.E.E. Trans. autom. Control*, **24**, 652.
- RAMAKRISHNA, A., and VISWANADHAM, N., 1982, *I.E.E.E. Trans. autom. Control*, **27**, 159.
- RAO, C. R., and MITRA, S. K., 1971, *Generalized Inverse of Matrices and its Applications* (New York: Wiley).
- SAEKS, R., 1979, *I.E.E.E. Trans. autom. Control*, **24**, 269.
- SANDELL, N., VARAIYA, P., ATHANS, M., and SAFONOV, M. G., 1978, *I.E.E.E. Trans. autom. Control*, **23**, 108.
- SERAJI, H., 1982, *Int. J. Control*, **35**, 775.
- SEZER, M. E., and HUSEYIN, O., 1984, *Automatica*, **16**, 205.
- SEZER, M. E., and SILJAK, D. D., 1981, *Syst. Control Lett.*, **1**, 60.
- SILJAK, D. D., 1978, *Large Scale Dynamic Systems* (New York: North-Holland); 1983, *Large-Scale Syst.*, **4**, 279.
- SINGH, M. G., 1981, *Decentralised Control* (New York: North-Holland).
- USKOKOVIC, Z., and MEDANIC, J., 1985, *Proc. 24th I.E.E.E. Conf. on Decision and Control*, 837.
- WANG, S. H., and DAVISON, E. J., 1973, *I.E.E.E. Trans. autom. Control*, **18**, 473.

APPENDIX I

**Robust Decentralised Optimal Output Feedback:
The Static Controller Case**

February 1987
Revised August 1987

Robust Decentralized Optimal Output Feedback:
The Static Controller Case

by

Dennis S. Bernstein*
Harris Corporation
Government Aerospace Systems
Division
MS 22/4848
Melbourne, FL 32902
(305) 729-2140

and

Wassim M. Haddad
Department of Mechanical
Engineering
Florida Institute of Technology
Melbourne, FL 32901

Abstract

Sufficient conditions are developed for designing robust decentralized static output feedback controllers. The approach involves deriving necessary conditions for minimizing a bound on closed-loop performance over a specified range of uncertain parameters. The effect of plant parameter variations on the closed-loop covariance is overbounded by means of a modified Lyapunov equation whose solutions are guaranteed to provide robust stability and performance.

*Supported in part by the Air Force Office of Scientific Research under contracts F49620-86-C-0002 and F49620-86-C-0038.

Notation For Typesetting

A, J, S Script face type

E, R Open face type

1. Introduction

Because of implementation constraints, cost, and reliability considerations, a decentralized controller architecture is often required for controlling large scale systems. Furthermore, such controllers must be robust to variations in plant parameters. The present paper addresses both of these concerns within the context of a robust decentralized design theory for continuous-time static controllers.

The approach to controller design considered herein involves optimizing closed-loop performance with respect to the feedback gains. This approach to output feedback was studied for centralized controllers in [8,9] and for decentralized controllers in [10]. An interesting feature of [9,10] is the recognition of an oblique projection (idempotent matrix) which allows the necessary conditions to be written in terms of a modified Riccati equation. When the problem is specialized to full-state feedback, the projection becomes the identity and the modified Riccati equation coincides with the standard Riccati equation of LQR theory. It should be pointed out that this oblique projection is distinct from the oblique projection arising in dynamic compensation ([7]). A unified treatment of the static/dynamic (nonstrictly proper) centralized control problem involving both projections is given in [2].

The present paper goes beyond earlier work by deriving sufficient conditions for robust stability and performance with respect to variations in the plant parameters. Although plant disturbances are represented in the usual stochastic manner by means of additive white noise, uncertainty in the plant dynamics is modeled deterministically by means of constant structured parameter variations within bounded sets. Thus, for example, the dynamics

matrix A is replaced by $A + \sum_{k=1}^p \sigma_k A_k$, where σ_k is a constant uncertain

parameter assumed only to lie within the interval $[-\alpha_k, \alpha_k]$ but otherwise unknown, and A_k is a fixed matrix denoting the structure of the uncertain parameter σ_k as it appears in the nominal dynamics matrix A . The system performance is defined to be the worst-case value over the parameter

uncertainties of a quadratic criterion averaged over the disturbance statistics.

Since the closed-loop performance can be written in terms of the second-moment matrix, a performance bound over the class of uncertain parameters can be obtained by bounding the state covariance. The key to bounding the state covariance is to replace the usual Lyapunov equation for the second-moment matrix by a modified Lyapunov equation. In the present paper the modified Lyapunov equation is constructed by adding two additional terms. The first term corresponds to a uniform right shift of the open-loop dynamics. As is well known ([1]), such a shift may arise from an exponential performance weighting and leads to a uniform stability margin for the closed-loop system. In order to obtain robustness with respect to specified structured parameter variations, however, an additional term of the form $A_k Q A_k^T$ is required. Such terms arise naturally in systems with multiplicative white noise; see [4] and the references therein for further details. The exponential cost weighting and multiplicative noise interpretations for the uncertainty bound have no bearing in the present paper, however, since parameter variations are modeled deterministically as constant variations within bounded sets.

Having bounded the state covariance over the class of parameter uncertainties, the performance can thus be bounded in terms of the solution of the modified Lyapunov equation. The performance bound can be viewed as an auxiliary cost and thus leads to the Auxiliary Minimization Problem: Minimize the performance bound while satisfying the modified Lyapunov equation. The nice feature of the auxiliary problem is that necessary conditions for optimality of the performance bound now serve as sufficient conditions for robust performance in the original problem. Thus our approach seeks to rectify one of the principal drawbacks of necessity theory, namely, guarantees of stability and performance. Furthermore, it should be noted that if numerical solution of the optimality conditions yields a local extremal which is not the global optimum, then robust stability and performance are still guaranteed, although the performance of the extremal may not be as good as the performance provided by the global minimum. Philosophically, the overall approach of control design for a

performance bound is related to guaranteed cost control ([6]). We note, however, that the bound utilized in [6] is nondifferentiable, which precludes the approach of the present paper.

A further extension of previous approaches considered in the present paper involves the types of feedback loops considered. Specifically, the usual approach to static output feedback involves nonnoisy measurements and weighted controls, while the dual problem involves feeding back noisy measurements to unweighted controls. This situation leads to an additional projection ([2]) which is dual to the projection discussed in [9,10]. The inclusion of the dual case now leads to a pair of modified Riccati equations coupled by both the uncertainty bounds and the oblique projections.

In addition to the two types of loops discussed above, one may wish to consider the two remaining cases, namely, feeding back noisy measurements to weighted controls and feeding back nonnoisy measurements to unweighted controls. It is easy to show, however, that the former case leads to an undefined (i.e., infinite) value for the performance while the latter case is highly singular and fails to yield explicit gain expressions.

Finally, the scope of the present paper is limited to a rigorous elucidation of sufficient conditions for robust decentralized output feedback. Numerical solution of these equations can be carried out by extending available algorithms for centralized output feedback. Numerical algorithms for solving a single modified Riccati equation in the absence of uncertainty bounds are discussed in [10].

2. Notation and Definitions

$\underline{R}, \underline{R}^{rxs}, \underline{R}^r, \underline{E}$	real numbers, rxs real numbers, \underline{R}^{rx1} , expectation
$I_r, ()^T$	rxr identity, transpose
\oplus, \otimes	Kronecker sum, Kronecker product ([5])
\underline{S}^r	rxr symmetric matrices

$\underline{\underline{N}}^r$	$r \times r$ symmetric nonnegative-definite matrices
$\underline{\underline{P}}^r$	$r \times r$ symmetric positive-definite matrices
$Z_1 < Z_2$	$Z_2 - Z_1 \in \underline{\underline{N}}^r, \quad Z_1, Z_2 \in \underline{\underline{S}}^r$
$Z_1 < Z_2$	$Z_2 - Z_1 \in \underline{\underline{P}}^r, \quad Z_1, Z_2 \in \underline{\underline{S}}^r$
asymptotically stable matrix	matrix with eigenvalues in open left half plane
n, r, s, p	positive integers
i, j, k	indices, $i=1, \dots, r, \quad j=1, \dots, s, \quad k=1, \dots, p$
\hat{m}_i, \hat{l}_i	positive integers, $i=1, \dots, r$
\hat{m}_j, \hat{l}_j	positive integers, $j=1, \dots, s$
x	n -dimensional vector
\hat{u}_i, \hat{y}_i	\hat{m}_i, \hat{l}_i -dimensional vectors, $i=1, \dots, r$
\hat{u}_j, \hat{y}_j	\hat{m}_j, \hat{l}_j -dimensional vectors, $j=1, \dots, s$
$A, \Delta A$	$n \times n$ matrices
$B_i, \Delta B_i; \hat{C}_i$	$n \times \hat{m}_i$ matrices; $\hat{l}_i \times n$ matrices, $i=1, \dots, r$
$\hat{B}_j; C_j, \Delta C_j$	$n \times \hat{m}_j$ matrices; $\hat{l}_j \times n$ matrices, $j=1, \dots, s$
A_k	$n \times n$ matrices, $k=1, \dots, p$
B_{ik}	$n \times \hat{m}_i$ matrices, $i=1, \dots, r, \quad k=1, \dots, p$
C_{jk}	$\hat{l}_j \times n$ matrices, $j=1, \dots, s, \quad k=1, \dots, p$
D_{ci}	$\hat{m}_i \times \hat{l}_i$ matrices, $i=1, \dots, r$
E_{cj}	$\hat{m}_j \times \hat{l}_j$ matrices, $j=1, \dots, s$
α	positive number
A_α	$A + \frac{\alpha}{2} I_n$
α_k	positive number, $k=1, \dots, p$
γ_k	$\alpha_k^2 / \alpha, \quad k=1, \dots, p$
σ_k	real number, $k=1, \dots, p$

$w_o(t), w_j(t)$	n -dimensional, l_j -dimensional white noise, $j=1, \dots, s$
V_o, V_j	intensities of w_o, w_j ; $V_o \in \mathbb{N}^n, V_j \in \mathbb{P}^{l_j}, j=1, \dots, s$
V_{oj}	$n \times l_j$ cross intensity of $w_o, w_j, j=1, \dots, s$
R_o, R_i	state and control weightings; $R_o \in \mathbb{N}^n, R_i \in \mathbb{P}^{m_i}, i=1, \dots, r$
R_{oi}	$n \times m_i$ cross weighting; $R_o - R_{oi} R_i^{-1} R_{oi}^T \geq 0, i=1, \dots, r$
\bar{A}, \bar{A}_α	$A + \sum_{i=1}^r B_i D_{ci} \hat{C}_i + \sum_{j=1}^s \hat{B}_j E_{cj} C_j, \quad \bar{A} + \frac{\alpha}{2} I_n$
$\Delta \bar{A}$	$\Delta A + \sum_{i=1}^r \Delta B_i D_{ci} \hat{C}_i + \sum_{j=1}^s \hat{B}_j E_{cj} \Delta C_j$
$\bar{w}(t)$	$w_o(t) + \sum_{j=1}^s \hat{B}_j E_{cj} w_j(t)$
\bar{R}	$R_o + \sum_{i=1}^r [R_{oi} D_{ci} \hat{C}_i + \hat{C}_i^T D_{ci}^T R_{oi}^T + \hat{C}_i^T D_{ci}^T R_i D_{ci} \hat{C}_i]$
\bar{V}	$V_o + \sum_{j=1}^s [V_{oj} E_{cj}^T \hat{B}_j^T + \hat{B}_j E_{cj} V_{oj}^T + \hat{B}_j E_{cj} V_j E_{cj}^T \hat{B}_j^T]$

For arbitrary $n \times n$ Q, P define:

$$R_{ai} \triangleq R_i + \sum_{k=1}^p \gamma_k B_{ik}^T P B_{ik}, \quad P_{ai} \triangleq B_i^T P + R_{oi}^T + \sum_{k=1}^p \gamma_k B_{ik}^T P A_k, \quad i=1, \dots, r.$$

$$V_{aj} \triangleq V_j + \sum_{k=1}^p \gamma_k C_{jk} Q C_{jk}^T, \quad Q_{aj} \triangleq Q C_j^T + V_{oj} + \sum_{k=1}^p \gamma_k A_k Q C_{jk}^T, \quad j=1, \dots, s.$$

3. Robust Stability and Performance Problem

In this section we state the Robust Stability and Performance Problem along with related notation for later use. Let

$\underline{U} \subset \underline{\mathbb{R}}^{n \times n} \times \underline{\mathbb{R}}^{n \times m_1} \times \dots \times \underline{\mathbb{R}}^{n \times m_r} \times \underline{\mathbb{R}}^{l_1 \times n} \times \dots \times \underline{\mathbb{R}}^{l_s \times n}$ denote the set of uncertain perturbations $(\Delta A, \Delta B_1, \dots, \Delta B_r, \Delta C_1, \dots, \Delta C_s)$ of the nominal system matrices $A, B_1, \dots, B_r, C_1, \dots, C_s$.

Robust Stability and Performance Problem. Determine

$(D_{c1}, \dots, D_{cr}, E_{c1}, \dots, E_{cs})$ such that the closed-loop system consisting of the nth-order controlled and disturbed plant

$$\dot{x}(t) = (A + \Delta A)x(t) + \sum_{i=1}^r (B_i + \Delta B_i)u_i(t) + \sum_{j=1}^s \hat{B}_j \hat{u}_j(t) + w_o(t), \quad t \in [0, \infty), \quad (3.1)$$

nonnoisy and noisy measurements

$$\hat{y}_i(t) = \hat{C}_i x(t), \quad i=1, \dots, r, \quad (3.2)$$

$$y_j(t) = (C_j + \Delta C_j)x(t) + w_j(t), \quad j=1, \dots, s, \quad (3.3)$$

and static output feedback controller

$$u_i(t) = D_{ci} \hat{y}_i(t), \quad i=1, \dots, r, \quad (3.4)$$

$$\hat{u}_j(t) = E_{cj} y_j(t), \quad j=1, \dots, s, \quad (3.5)$$

is asymptotically stable for all variations in \underline{U} and the performance criterion

$$J(D_{c1}, \dots, D_{cr}, E_{c1}, \dots, E_{cs}) \triangleq \quad (3.6)$$

$$\sup_{\underline{U}} \limsup_{t \rightarrow \infty} \mathbb{E} [x^T(t) R_o x(t) + 2 \sum_{i=1}^r x^T(t) R_{oi} u_i(t) + \sum_{i=1}^r u_i^T(t) R_i u_i(t)]$$

is minimized.

For each controller $(D_{c1}, \dots, D_{cr}, E_{c1}, \dots, E_{cs})$ and variation in \underline{U} , the closed-loop system (3.1)-(3.5) is given by

$$\dot{\underline{x}}(t) = (\underline{A} + \Delta \underline{A})\underline{x}(t) + \tilde{w}(t), \quad t \in [0, \infty), \quad (3.7)$$

where $\tilde{w}(t)$ is white noise with intensity $\tilde{V} \in \underline{N}^n$.

Remark 3.1. In the case $\Delta A, \Delta B_i, \Delta C_j = 0$ it is well known that stabilizability is related to the existence of fixed modes ([11]). When plant uncertainties are present the problem is, of course, far more complex. In the present paper sufficient conditions for robust stability are obtained as a consequence of the existence of robust performance bounds.

Remark 3.2. Note that the controller architecture is quite general in that it includes two distinctly different types of decentralized loops. The first type, indexed by $i=1, \dots, r$, involves feeding back nonnoisy measurements to weighted controls. This is the standard setting in the optimal output-feedback literature ([8-10]). In addition, we include the dual situation, indexed by $j=1, \dots, s$, which involves feeding back noisy measurements to unweighted controls. The case in which only one type of loop is present can be formally recovered from our results by ignoring B_i and \hat{C}_i or \hat{B}_j and C_j as required. As noted in Section 1, noisy measurements cannot be fed back to weighted controls via static control, while feeding back nonnoisy measurements to unweighted controls is a highly singular problem.

Remark 3.3. Note that the problem statement is restrictive in the sense that uncertainties in both the control and observation matrices are not permitted within the same feedback loop. Although it is indeed possible to permit such simultaneous uncertainties, the development is considerably more complex and hence is outside the scope of this paper.

Remark 3.4. The cost functional (3.6) is identical to the LQG criterion (usually stated in terms of an averaged integral) with the exception of the supremum for evaluating worst case over \underline{U} .

4. Sufficient Conditions for Robust Stability and Performance

In practice, steady-state performance is only of interest when the closed-loop system (3.7) is stable over \underline{U} . The following result, which expresses the performance in terms of the state covariance, is immediate.

Lemma 4.1. Let $(D_{c1}, \dots, D_{cr}, E_{c1}, \dots, E_{cs})$ be given and suppose the system (3.7) is stable for all variations in \underline{U} . Then

$$J(D_{c1}, \dots, D_{cr}, E_{c1}, \dots, E_{cs}) = \sup_{\underline{U}} \operatorname{tr} Q_{\underline{R}, \underline{\Delta A}} \quad (4.1)$$

where $Q_{\underline{R}, \underline{\Delta A}} \triangleq \lim_{t \rightarrow \infty} \underline{\underline{E}}[x(t)x(t)^T] \in \underline{\underline{N}}^n$ is the unique solution to

$$0 = (\underline{\underline{A}} + \underline{\underline{\Delta A}}) Q_{\underline{R}, \underline{\Delta A}} + Q_{\underline{R}, \underline{\Delta A}} (\underline{\underline{A}} + \underline{\underline{\Delta A}})^T + \underline{\underline{V}}. \quad (4.2)$$

Remark 4.1. When \underline{U} is compact, "sup" in (4.1) can be replaced by "max".

We now seek upper bounds for $J(D_{c1}, \dots, D_{cr}, E_{c1}, \dots, E_{cs})$. Our assumptions allow us to obtain robust stability as a consequence of robust performance.

Theorem 4.1. Let $\underline{\underline{Q}}: \underline{\underline{N}}^n \times \underline{\underline{R}}^{\hat{m}_1 \times \hat{l}_1} \times \dots \times \underline{\underline{R}}^{\hat{m}_r \times \hat{l}_r} \times \underline{\underline{R}}^{\hat{m}_1 \times \hat{l}_1} \times \dots \times \underline{\underline{R}}^{\hat{m}_s \times \hat{l}_s} \rightarrow \underline{\underline{S}}^n$ be such that

$$\underline{\underline{\Delta A}} \underline{\underline{Q}} + \underline{\underline{Q}} \underline{\underline{\Delta A}}^T \leq \underline{\underline{Q}}(Q, D_{c1}, \dots, D_{cr}, E_{c1}, \dots, E_{cs}),$$

$$(\underline{\underline{\Delta A}}, \underline{\underline{\Delta B}}_1, \dots, \underline{\underline{\Delta B}}_r, \underline{\underline{\Delta C}}_1, \dots, \underline{\underline{\Delta C}}_s) \in \underline{\underline{U}}, \quad (4.3)$$

$$(Q, D_{c1}, \dots, D_{cr}, E_{c1}, \dots, E_{cs}) \in \underline{\underline{N}}^n \times \underline{\underline{R}}^{\hat{m}_1 \times \hat{l}_1} \times \dots \times \underline{\underline{R}}^{\hat{m}_r \times \hat{l}_r} \times \underline{\underline{R}}^{\hat{m}_1 \times \hat{l}_1} \times \dots \times \underline{\underline{R}}^{\hat{m}_s \times \hat{l}_s}.$$

Furthermore, for given $(D_{c1}, \dots, D_{cr}, E_{c1}, \dots, E_{cs})$ suppose there exists $Q \in \underline{N}^n$ satisfying

$$0 = \bar{A}Q + Q\bar{A}^T + \Omega(Q, D_{c1}, \dots, D_{cr}, E_{c1}, \dots, E_{cs}) + \bar{V}, \quad (4.4)$$

and suppose the pair $(\bar{V}^{1/2}, \bar{A} + \Delta\bar{A})$ is detectable for all variations in \underline{U} . Then, for all variations in \underline{U} , $\bar{A} + \Delta\bar{A}$ is asymptotically stable,

$$Q_{\Delta\bar{A}} \leq Q, \quad (4.5)$$

where $Q_{\Delta\bar{A}}$ satisfies (4.2), and

$$J(D_{c1}, \dots, D_{cr}, E_{c1}, \dots, E_{cs}) \leq \text{tr } QR. \quad (4.6)$$

Proof. For all variations in \underline{U} , (4.4) is equivalent to

$$0 = (\bar{A} + \Delta\bar{A})Q + Q(\bar{A} + \Delta\bar{A})^T + \Phi(Q, D_{c1}, \dots, D_{cr}, E_{c1}, \dots, E_{cs}, \Delta\bar{A}) + \bar{V}, \quad (4.7)$$

where

$$\Phi(Q, D_{c1}, \dots, D_{cr}, E_{c1}, \dots, E_{cs}, \Delta\bar{A}) \triangleq \Omega(Q, D_{c1}, \dots, D_{cr}, E_{c1}, \dots, E_{cs}) - (\Delta\bar{A}Q + Q\Delta\bar{A}^T).$$

Note that by (4.3), $\Phi(\cdot) \geq 0$ for all variations in \underline{U} . Since $(\bar{V}^{1/2}, \bar{A} + \Delta\bar{A})$ is detectable for all variations in \underline{U} , it follows from Theorem 3.6 of [12] that $([\bar{V} + \Phi(Q, D_{c1}, \dots, D_{cr}, E_{c1}, \dots, E_{cs}, \Delta\bar{A})]^{1/2}, \bar{A} + \Delta\bar{A})$ is detectable for all variations in \underline{U} . Hence Lemma 12.2 of [12] implies $\bar{A} + \Delta\bar{A}$ is asymptotically stable for all variations in \underline{U} . Next, subtracting (4.2) from (4.7) yields

$$0 = (\bar{A} + \Delta\bar{A})(Q - Q_{\Delta\bar{A}}) + (Q - Q_{\Delta\bar{A}})(\bar{A} + \Delta\bar{A})^T + \Phi(Q, D_{c1}, \dots, D_{cr}, E_{c1}, \dots, E_{cs}, \Delta\bar{A}),$$

or, equivalently, (since $\bar{A} + \Delta\bar{A}$ is asymptotically stable)

$$Q - Q_{\Delta\bar{A}} = \int_0^{\infty} e^{(\bar{A} + \Delta\bar{A})t} \Phi(Q, D_{c1}, \dots, D_{cr}, E_{c1}, \dots, E_{cs}, \Delta\bar{A}) e^{(\bar{A} + \Delta\bar{A})^T t} dt \geq 0,$$

which implies (4.5). Finally, (4.5) and (4.1) yield (4.6). \square

Remark 4.2. If \tilde{V} is positive definite then the detectability hypothesis of Theorem 4.1 is automatically satisfied.

5. Uncertainty Structure and the Quadratic Lyapunov Bound

The uncertainty set \underline{U} is assumed to be of the form

$$\underline{U} = \{(\Delta A, \Delta B_1, \dots, \Delta B_r, \Delta C_1, \dots, \Delta C_s) :$$

$$\Delta A = \sum_{k=1}^P \sigma_k A_k, \quad \Delta B_i = \sum_{k=1}^P \sigma_k B_{ik}, \quad i=1, \dots, r, \quad (5.1)$$

$$\Delta C_j = \sum_{k=1}^P \sigma_k C_{jk}, \quad j=1, \dots, s, \quad \left\{ \sum_{k=1}^P \sigma_k^2 / \alpha_k^2 \leq 1 \right\},$$

where, for $k=1, \dots, p$: $(A_k, B_{1k}, \dots, B_{rk}, C_{1k}, \dots, C_{sk})$ are fixed matrices denoting the structure of the parametric uncertainty; α_k is a given uncertainty bound; and σ_k is an uncertain parameter. Note that the uncertain parameters σ_k are assumed to lie in a specified ellipsoidal region in \mathbb{R}^P . The closed-loop system thus has structured uncertainty of the form

$$\Delta \tilde{A} = \sum_{k=1}^P \sigma_k \tilde{A}_k, \quad (5.2)$$

where

$$\tilde{A}_k \triangleq A_k + \sum_{i=1}^r B_{ik} D_{ci} \hat{C}_i + \sum_{j=1}^s \hat{B}_j E_{cj} C_{jk}, \quad k=1, \dots, p. \quad (5.3)$$

To obtain explicit gain expressions for $(D_{c1}, \dots, D_{cr}, E_{c1}, \dots, E_{cs})$ we assume that, for each $k \in \{1, \dots, p\}$, at most one of the matrices $B_{1k}, \dots, B_{rk}, C_{1k}, \dots, C_{sk}$ is nonzero. Note that this assumption does not preclude the treatment of uncertainties in the input and output matrices. It requires only that such uncertainties be modeled as uncorrelated.

Given the structure of \underline{U} defined by (5.1), the bound \mathcal{Q} satisfying (4.3) can now be specified. In the following result Q denotes an arbitrary element of \underline{N}^n , not necessarily a solution of (4.4).

Proposition 5.1. Let α be an arbitrary positive scalar. Then the function

$$\mathcal{Q}(Q, D_{c1}, \dots, D_{cr}, E_{c1}, \dots, E_{cs}) = \alpha Q + \alpha^{-1} \sum_{k=1}^P \alpha_k^2 \tilde{A}_k Q \tilde{A}_k^T \quad (5.4)$$

satisfies (4.3) with \underline{U} given by (5.1).

Proof. Note that

$$\begin{aligned} 0 &\leq \sum_{k=1}^P [(\alpha^{1/2} \sigma_k / \alpha_k) I_n - (\alpha_k / \alpha^{1/2}) \tilde{A}_k] Q [(\alpha^{1/2} \sigma_k / \alpha_k) I_n - (\alpha_k / \alpha^{1/2}) \tilde{A}_k]^T \\ &= \alpha \sum_{k=1}^P (\sigma_k^2 / \alpha_k^2) Q + \alpha^{-1} \sum_{k=1}^P \alpha_k^2 \tilde{A}_k Q \tilde{A}_k^T - \sum_{k=1}^P \sigma_k (\tilde{A}_k Q + Q \tilde{A}_k^T), \end{aligned}$$

which yields (4.3). \square

Remark 5.1. Note that the bound \mathcal{Q} given by (5.4) consists of two distinct terms. The first term αQ can be thought of as arising from an exponential time weighting of the cost, or, equivalently, from a uniform

right shift of the open-loop dynamics ([1]). The second term $\alpha^{-1} \sum_{k=1}^P \alpha_k^2 \tilde{A}_k \tilde{Q} \tilde{A}_k^T$ arises naturally from a multiplicative white noise model ([3,4]). Such interpretations have no bearing on the results obtained here since only the bound \underline{Q} defined by (5.4) is required. Note that the bound is valid for all positive α .

Remark 5.2. The conservatism of the bound (5.4) is difficult to predict for two reasons. First, the overbounding (4.3) holds with respect to the partial ordering of the nonnegative-definite matrices for which no scalar measure of conservatism is available. And, second, the bound (4.3) is required to hold for all nonnegative-definite matrices Q and feedback gains $(D_{c1}, \dots, D_{cr}, E_{c1}, \dots, E_{cs})$. The conservatism will thus depend upon the actual values of $Q, D_{c1}, \dots, D_{cr}, E_{c1}, \dots, E_{cs}$ determined by solving (4.4).

6. The Auxiliary Minimization Problem and Necessary Conditions for Optimality

Rather than minimizing the actual cost (3.6), we shall consider the upper bound (4.6). This leads to the following problem.

Auxiliary Minimization Problem. Determine $(Q, D_{c1}, \dots, D_{cr}, E_{c1}, \dots, E_{cs})$ which minimizes

$$\underline{J}(Q, D_{c1}, \dots, D_{cr}, E_{c1}, \dots, E_{cs}) \triangleq \text{tr } \tilde{Q} \tilde{R} \quad (6.1)$$

subject to

$$Q \in \underline{N}^n, \quad (6.2)$$

$$0 = \tilde{A}_\alpha Q + Q \tilde{A}_\alpha^T + \sum_{k=1}^P \gamma_k \tilde{A}_k \tilde{Q} \tilde{A}_k^T + \tilde{V} \quad (6.3)$$

and

$$(\bar{V}^{1/2}, \bar{A} + \Delta \bar{A}) \text{ is detectable for all variations in } \underline{U}. \quad (6.4)$$

The relationship between the Auxiliary Minimization Problem and the Robust Stability and Performance Problem is straightforward as shown by the following observation.

Proposition 6.1. If $(Q, D_{c1}, \dots, D_{cr}, E_{c1}, \dots, E_{cs})$ satisfies (6.2)-(6.4) then $\bar{A} + \Delta \bar{A}$ is asymptotically stable for all variations in \underline{U} , and

$$J(D_{c1}, \dots, D_{cr}, E_{c1}, \dots, E_{cs}) \leq \underline{J}(Q, D_{c1}, \dots, D_{cr}, E_{c1}, \dots, E_{cs}). \quad (6.5)$$

Proof. With \underline{Q} given by (5.4), Proposition 5.1 implies that (4.3) is satisfied. Since the hypotheses of Theorem 4.1 are satisfied, robust stability with performance bound (4.6) is guaranteed. Note that with definition (6.1), (6.5) is merely a restatement of (4.6). \square

The derivation of the necessary conditions for the Auxiliary Minimization Problem is based upon the Fritz John form of the Lagrange multiplier theorem.* Rigorous application of this technique requires that $(Q, D_{c1}, \dots, D_{cr}, E_{c1}, \dots, E_{cs})$ be restricted to the open set

$$\underline{S} \triangleq \{(Q, D_{c1}, \dots, D_{cr}, E_{c1}, \dots, E_{cs}) : Q \in \underline{P}^n \text{ and } \bar{A} \text{ is asymptotically stable}\},$$

where

$$\bar{A} \triangleq \bar{A}_0 \oplus \bar{A}_\alpha + \sum_{k=1}^P \gamma_k \bar{A}_k \oplus \bar{A}_k.$$

*The Kuhn-Tucker theorem requires a priori verification of a constraint qualification which is impossible to confirm in the present context. The Fritz John version is less restrictive and hence more suitable in the present context.

The requirement $(Q, D_{c1}, \dots, D_{cr}, E_{c1}, \dots, E_{cs}) \in \underline{S}$ implies that Q and its nonnegative-definite dual P are unique solutions of the modified Lyapunov equations (6.3) and

$$0 = \tilde{A}_\alpha^T P + P \tilde{A}_\alpha + \sum_{k=1}^P \gamma_k \tilde{A}_k^T P \tilde{A}_k + \tilde{R}. \quad (6.6)$$

An additional technical requirement is that $(Q, D_{c1}, \dots, D_{cr}, E_{c1}, \dots, E_{cs})$ be confined to the set

$$\underline{S}^+ \triangleq \{(Q, D_{c1}, \dots, D_{cr}, E_{c1}, \dots, E_{cs}) \in \underline{S} : \hat{C}_i Q \hat{C}_i^T > 0, \quad i=1, \dots, r, \\ \text{and } \hat{B}_j^T P \hat{B}_j > 0, \quad j=1, \dots, s\}.$$

The positive definiteness conditions in the definition of \underline{S}^+ hold when \hat{C}_i and \hat{B}_j have full row and column rank, respectively, and Q and P are positive definite. As can be seen from the proof of Theorem 6.1 these conditions imply the existence of the projections τ_i and $\hat{\tau}_j$ corresponding to the two distinct types of feedback loops. Note that \underline{S}^+ is open.

Remark 6.1. As pointed out in Remark 3.1, the set \underline{S} may be empty in which case, of course, our results do not apply. As will be seen, however, our approach does not require explicit verification that \underline{S} is nonempty since robust stability is obtained as a consequence of robust performance.

Remark 6.2. As will be seen, the constraint $(Q, D_{c1}, \dots, D_{cr}, E_{c1}, \dots, E_{cs}) \in \underline{S}$ need not be verified in practice and is not required for either robust stability or robust performance since Proposition 6.1 shows that only (6.2)-(6.4) are needed. Rather, the set \underline{S} constitutes sufficient conditions under which the Lagrange multiplier technique is applicable to the Auxiliary Minimization Problem. Specifically, the condition $Q > 0$ replaces (6.2) by an open set constraint, while the asymptotic stability of \underline{A} serves as a normality condition which further implies that the dual P of Q is nonnegative definite.

Necessary conditions for the Auxiliary Minimization Problem can now be obtained.

Theorem 6.1. If $(Q, D_{c1}, \dots, D_{cr}, E_{c1}, \dots, E_{cs}) \in \underline{S}^+$ solves the Auxiliary Minimization Problem with \underline{U} given by (5.1) then there exists $P \in \underline{N}^n$ such that $D_{c1}, \dots, D_{cr}, E_{c1}, \dots, E_{cs}$ are given by

$$D_{ci} = -R_{ai}^{-1} P_{ai} \hat{Q} C_i^T (\hat{C}_i \hat{Q} C_i^T)^{-1}, \quad i=1, \dots, r, \quad (6.7)$$

$$E_{cj} = -(\hat{B}_j^T P \hat{B}_j)^{-1} \hat{B}_j^T P Q_{aj} V_{aj}^{-1}, \quad j=1, \dots, s, \quad (6.8)$$

and such that Q, P satisfy

$$\begin{aligned} 0 = & (A_{\alpha} - \sum_{i=1}^r B_{ai} R_{ai}^{-1} P_{ai} \tau_i) Q + Q (A_{\alpha} - \sum_{i=1}^r B_{ai} R_{ai}^{-1} P_{ai} \tau_i)^T + V_0 \\ & + \sum_{k=1}^p \gamma_k (A_k - \sum_{i=1}^r B_{ik} R_{ai}^{-1} P_{ai} \tau_i) Q (A_k - \sum_{i=1}^r B_{ik} R_{ai}^{-1} P_{ai} \tau_i)^T \\ & - \sum_{j=1}^s Q_{aj} V_{aj}^{-1} Q_{aj}^T + \sum_{j=1}^s \hat{\tau}_{jl} Q_{aj} V_{aj}^{-1} Q_{aj}^T \hat{\tau}_{jl}^T. \end{aligned} \quad (6.9)$$

$$\begin{aligned} 0 = & (A_{\alpha} - \sum_{j=1}^s \hat{\tau}_j Q_{aj} V_{aj}^{-1} C_j)^T P + P (A_{\alpha} - \sum_{j=1}^s \hat{\tau}_j Q_{aj} V_{aj}^{-1} C_j) + R_0 \\ & + \sum_{k=1}^p \gamma_k (A_k - \sum_{j=1}^s \hat{\tau}_j Q_{aj} V_{aj}^{-1} C_{jk})^T P (A_k - \sum_{j=1}^s \hat{\tau}_j Q_{aj} V_{aj}^{-1} C_{jk}) \\ & - \sum_{i=1}^r P_{ai}^T R_{ai}^{-1} P_{ai} + \sum_{i=1}^r \hat{\tau}_{il}^T P_{ai}^T R_{ai}^{-1} P_{ai} \hat{\tau}_{il}. \end{aligned} \quad (6.10)$$

where

$$\tau_i \triangleq QC_i^T(\hat{C}_i QC_i^T)^{-1} \hat{C}_i, \quad \tau_{i1} \triangleq \tau_i - I_n, \quad i=1, \dots, r, \quad (6.11)$$

$$\hat{\tau}_j \triangleq \hat{B}_j(\hat{B}_j^T \hat{P} \hat{B}_j)^{-1} \hat{B}_j^T P, \quad \hat{\tau}_{j1} \triangleq \hat{\tau}_j - I_n, \quad j=1, \dots, s. \quad (6.12)$$

Furthermore, the auxiliary cost is given by

$$\underline{J}(Q, D_{c1}, \dots, D_{cr}, E_{c1}, \dots, E_{cs}) = \text{tr} \left[Q(R_o + \sum_{i=1}^P \tau_i^T P^T R_{ai}^{-1} R_i R_{ai}^{-1} P \tau_i - 2R_{oi} R_{ai}^{-1} P \tau_i) \right]. \quad (6.13)$$

Conversely, if there exist $Q, P \in \underline{N}^n$ satisfying (6.9) and (6.10) then Q satisfies (6.3) with $(D_{c1}, \dots, D_{cr}, E_{c1}, \dots, E_{cs})$ given by (6.7) and (6.8), and $\underline{J}(Q, D_{c1}, \dots, D_{cr}, E_{c1}, \dots, E_{cs})$ is given by (6.13).

Proof. To optimize (6.1) over the open set $\hat{\underline{S}}$, where

$$\hat{\underline{S}} \triangleq \{(Q, D_{c1}, \dots, D_{cr}, E_{c1}, \dots, E_{cs}) \in \underline{S}^+ : (6.4) \text{ is satisfied}\},$$

subject to the constraint (6.3), form the Lagrangian

$$L(Q, D_{c1}, \dots, D_{cr}, E_{c1}, \dots, E_{cs}) \triangleq \text{tr} [\lambda QR + (\bar{A}Q + Q\bar{A}^T + \sum_{k=1}^P \gamma_k \bar{A}_k Q \bar{A}_k^T + \bar{V})P],$$

where the Lagrange multipliers $\lambda \geq 0$ and $P \in \underline{R}^{n \times n}$ are not both zero. Setting $\partial L / \partial Q = 0$, $\lambda = 0$ implies $P = 0$ since \bar{A} is asymptotically stable. Hence, without loss of generality set $\lambda = 1$. Thus the stationarity conditions are given by

$$\frac{\partial L}{\partial Q} = \bar{A}_\alpha^T P + P \bar{A}_\alpha + \sum_{k=1}^P \gamma_k \bar{A}_k^T P \bar{A}_k + \bar{R} = 0, \quad (6.14)$$

$$\frac{\partial L}{\partial D_{ci}} = R_{ai} D_{ci} \hat{C}_i QC_i^T + P_{ai} QC_i^T = 0, \quad i=1, \dots, r, \quad (6.15)$$

$$\frac{\partial L}{\partial E_{cj}} = \hat{B}_j^T P \hat{B}_j E_{cj} V_{aj} + \hat{B}_j^T P Q_{aj} = 0, \quad j=1, \dots, s. \quad (6.16)$$

Since $(Q, D_{c1}, \dots, D_{cr}, E_{c1}, \dots, E_{cs}) \in \underline{S}^+$, $\hat{C}_i Q C_i^T$ and $B_j^T P B_j$ are invertible and hence (6.15) and (6.16) imply (6.7) and (6.8). Finally, (6.9) and (6.10) are equivalent to (6.3) and (6.6). \square

Remark 6.3. Several special cases can be recovered formally from Theorem 6.1. For example, when the control weighting is nonsingular and the measurement noise is zero, i.e., when \hat{u}_i and y_i are absent for $i=1, \dots, r$, delete (6.8) and set $\hat{\tau}_j = 0$ in (6.9). In this case the last two terms in (6.9) can be deleted. Deleting also the uncertainty terms A_k, B_{ik}, C_{jk} yields the results of [10] with the added features of correlated plant/measurement noise (V_{oj}) and cross weighting (R_{oi}). Furthermore, assuming a centralized structure for the static controller, i.e., $r=1$, yields the usual static output feedback result ([8,9]).

7. Sufficient Conditions for Robust Stability and Performance

We now combine Proposition 6.1 and Theorem 6.1 to obtain sufficient conditions for robust stability and performance.

Theorem 7.1. Suppose there exist $Q, P \in \underline{N}^n$ satisfying (6.9) and (6.10) and suppose that $(\tilde{V}^{1/2}, \tilde{A} + \Delta \tilde{A})$ is detectable for all variations in \underline{U} with $(D_{c1}, \dots, D_{cr}, E_{c1}, \dots, E_{cs})$ given by (6.6) and (6.7) and \underline{U} given by (5.1). Then, with $(D_{c1}, \dots, D_{cr}, E_{c1}, \dots, E_{cs})$ given by (6.6) and (6.7), $\tilde{A} + \Delta \tilde{A}$ is asymptotically stable for all variations in \underline{U} , and the performance of the closed-loop system satisfies the bound

$$J(D_{c1}, \dots, D_{cr}, E_{c1}, \dots, E_{cs}) \leq \text{tr} \left[Q (R_o + \sum_{i=1}^p \tau_i^T P^T R_i^{-1} R_i R_i^{-1} P \tau_i - 2R_{oi} R_i^{-1} P \tau_i) \right]. \quad (7.1)$$

Proof. The converse of Theorem 6.1 shows that Q satisfies (6.3) with $(D_{c1}, \dots, D_{cr}, E_{c1}, \dots, E_{cs})$ given by (6.7) and (6.8). Hence, with the detectability assumption (6.4), Proposition 6.1 implies robust stability and performance. \square

Remark 7.1. The application of Theorem 7.1 in practice requires 1) numerical solution of (6.9) and (6.10), and 2) verification of the detectability hypothesis. No other assumptions need be verified in applying this result.

8. Concluding Remarks

We have developed a theory of robust decentralized output feedback via static control. The development permits the treatment of noisy and nonnoisy measurements, weighted and unweighted controls, and structured real-valued parameter uncertainties in the plant matrices. The theory provides a robustification of results given in [8-10] for both centralized and decentralized optimal output feedback. The theory is constructive in nature rather than existential. Specifically, the main result, Theorem 7.1, involves a coupled pair of modified Riccati equations (6.9), (6.10) whose solutions, when they exist, are used to explicitly construct feedback gains (6.7), (6.8) which are guaranteed to provide both robust stability and performance. Future research is required for evaluating the conservativeness of the theory. The numerical algorithms developed in [10] provide a starting point in this regard.

References

- [1] B. D. O Anderson and J. B. Moore, Linear Optimal Control (Prentice-Hall, Englewood Cliffs, NJ, 1970).
- [2] D. S. Bernstein, The optimal projection equations for static and dynamic output feedback: The singular case, IEEE Trans. Autom. Contr., AC-32, 1987, to appear.
- [3] D. S. Bernstein, Robust static and dynamic output-feedback stabilization: Deterministic and stochastic perspectives, IEEE Trans. Autom. Contr., AC-32, 1987, to appear.
- [4] D. S. Bernstein and D. C. Hyland, The optimal projection equations for reduced-order modelling, estimation and control of linear systems with multiplicative white noise, J. Optim. Thy. Appl., 1987, to appear.
- [5] J. W. Brewer, Kronecker products and matrix calculus in system theory, IEEE Trans. Circ. Sys., CAS-25 (1978) 772-781.
- [6] S. S. L. Chang and T. K. C Peng, Adaptive guaranteed cost control of systems with uncertain parameters, IEEE Trans. Autom. Contr., AC-17 (1972) 474-483.
- [7] D. C. Hyland and D. S. Bernstein, The optimal projection equations for fixed-order dynamic compensation, IEEE Trans. Autom. Contr., AC-29 (1984) 1034-1037.
- [8] W. S. Levine and M. Athans, On the determination of the optimal constant output feedback gains for linear multivariable systems, IEEE Trans. Autom. Contr., AC-15 (1970) 44-48.
- [9] J. Medanic, On stabilization and optimization by output feedback, Proc. Twelfth Asilomar Conf. Circ., Sys. Comp., (1978) 412-416.
- [10] S. Renjen and D. P. Looze, Synthesis of decentralized output/state regulators, Proc. Amer. Contr. Conf., Arlington, VA, (1982) 758-762.
- [11] S. H. Wang and E. J. Davison, On the stabilization of decentralized control systems, IEEE Trans. Autom. Contr., AC-18 (1973) 473-478.
- [12] W. M. Wonham, Linear Multivariable Control: A Geometric Approach (Springer-Verlag, New York, 1979).

END